University of Glasgow | School of Engineering

Geothermal district heating networks: modelling novel operational strategies incorporating heat storage

SOTIRIOS A. KYRIAKIS

Submitted in fulfilment of the requirements for the degree of Doctor of Philosophy at the University of Glasgow

School of Engineering

University of Glasgow

March 2016

Abstract

The value of integrating a heat storage into a geothermal district heating system has been investigated. The behaviour of the system under a novel operational strategy has been simulated focusing on the energetic, economic and environmental effects of the new strategy of incorporation of the heat storage within the system. A typical geothermal district heating system consists of several production wells, a system of pipelines for the transportation of the hot water to end-users, one or more re-injection wells and peak-up devices (usually fossil-fuel boilers). Traditionally in these systems, the production wells change their production rate throughout the day according to heat demand, and if their maximum capacity is exceeded the peak-up devices are used to meet the balance of the heat demand. In this study, it is proposed to maintain a constant geothermal production and add heat storage into the network. Subsequently, hot water will be stored when heat demand is lower than the production and the stored hot water will be released into the system to cover the peak demands (or part of these). It is not intended to totally phase-out the peak-up devices, but to decrease their use, as these will often be installed anyway for back-up purposes. Both the integration of a heat storage in such a system as well as the novel operational strategy are the main novelties of this thesis.

A robust algorithm for the sizing of these systems has been developed. The main inputs are the geothermal production data, the heat demand data throughout one year or more and the topology of the installation. The outputs are the sizing of the whole system, including the necessary number of production wells, the size of the heat storage and the dimensions of the pipelines amongst others. The results provide several useful insights into the initial design considerations for these systems, emphasizing particularly the importance of heat losses. Simulations are carried out for three different cases of sizing of the installation (small, medium and large) to examine the influence of system scale. In the second phase of work, two algorithms are developed which study in detail the operation of the installation throughout a random day and a whole year, respectively. The first algorithm can be a potentially powerful tool for the operators of the installation, who can know *a priori* how to operate the installation on a random day given the heat demand. The second algorithm is used to obtain the amount of electricity used by the pumps as well as the amount of fuel used by the peak-up boilers over a whole year. These comprise the main operational costs of the installation and are among the main inputs of the third part of the study. In the third part of the study, an integrated energetic, economic and environmental analysis of the

studied installation is carried out together with a comparison with the traditional case. The results show that by implementing heat storage under the novel operational strategy, heat is generated more cheaply as all the financial indices improve, more geothermal energy is utilised and less fuel is used in the peak-up boilers, with subsequent environmental benefits, when compared to the traditional case. Furthermore, it is shown that the most attractive case of sizing is the large one, although the addition of the heat storage most greatly impacts the medium case of sizing. In other words, the geothermal component of the installation should be sized as large as possible.

This analysis indicates that the proposed solution is beneficial from energetic, economic, and environmental perspectives. Therefore, it can be stated that the aim of this study is achieved in its full potential. Furthermore, the new models for the sizing, operation and economic/energetic/environmental analyses of these kind of systems can be used with few adaptations for real cases, making the practical applicability of this study evident. Having this study as a starting point, further work could include the integration of these systems with end-user demands, further analysis of component parts of the installation (such as the heat exchangers) and the integration of a heat pump to maximise utilisation of geothermal energy.

Keywords: Geothermal, energy, district, heating, storage, operation, strategy.

Acknowledgments

This thesis denotes the end of my doctoral studies. My sincere gratefulness and appreciation goes to the following people who helped me throughout these years with many different ways:

My supervisor, Professor Paul Younger, for trusting me in this position and giving me the chance to do a Ph.D. which has always been a dream for me. His help and advice throughout my studies have been priceless.

My second and third supervisors, Dr Manosh Paul and Dr Edryd W. Stephens, for their useful comments and supervision. Many thanks also to Dr Zhibin Yu for giving me the chance to assist him with his courses.

Cluff Geothermal Ltd., the Energy Technology Partnership of Scotland (ETP) and the University of Glasgow for funding this research project. A distinct acknowledgment goes to Dr Michael Feliks of Cluff Geothermal, my industrial supervisor, for the many fruitful discussions, the times that he hosted me in his home and the general help and advice that he provided me.

Mr Bert Young from the Estates and Buildings office of the University of Glasgow for providing me with the heat demand data that I used in my thesis, the British Atmospheric Data Centre (BADC) for giving me access to the weather data that I used in a part of my thesis as well as to Dr Richard Coulton for the very useful information on the storage tank costs.

Mrs Elaine McNamara and Mrs Heather Lambie of the University of Glasgow for answering my endless questions and being always willing to help.

My Greek friends from Glasgow- Nikos, Marianna, Andreas, Ignatios and many others- for their wonderful company. Thanks a lot to all my foreign friends that I made in Glasgow- my Spanish friend and ex-flatmate Juan, my Mexican friend Fernando, my Italian friends Alessandro and Nicola- and all the other wonderful people that I have met these 3.5 years.

My friends from Greece- Dimitris, Christos, Kostas, Serafeim, Anna, Stefanos and Thanasis- for suffering me all these years.

Finally, my most sincere gratitude goes to my very own people: My parents- Anastasios and Maria- for their endless support, love and values that they provided me since I was born; My sisters- Eleana and Dimitra- for the very beautiful moments; and the most important person for me- my girlfriend, Athina- for her endless love, support and for believing in me and my capabilities.

This thesis is dedicated to the memory
of my friend, George Apostolou.

Declarations

Part of the work presented in this thesis has been published in the following articles:

Kyriakis, S.A., and Younger, P.L., 2016. Towards the increased utilisation of geothermal energy in a district heating network through the use of a heat storage. Applied Thermal Engineering, 94: 99-110.

Kyriakis, S.A., 2015. Improving the operation of a geothermal district heating network through the use of a heat storage tank. In: *Proceedings of the 14th UK Heat Transfer Conference*, Edinburgh, UK, 7-8 September 2015.

Kyriakis, S.A., 2015. Effect of heat storage in geothermal district heating systems. In: *Proceedings of the 2015 ASME-ATI-UIT Conference*, Naples, Italy, 17-20 May 2015. (ISBN: 978-88-98273-17-1)

Kyriakis, S.A., Younger, P.L., Paul, M.C., and Stephens, W.E., 2014. Matching production and demand in geothermal district heating networks. Poster presentation to the annual ETP Conference, Dundee, UK.

Kyriakis, S.A., Younger, P.L., Paul, M.C., and Stephens, W.E., 2014. Matching production and demand in geothermal district heating networks. In: *Proceedings of the 5th European Geothermal Ph.D. Day*, Darmstadt, Germany, 31 March-2 April 2014, pp.: 49-50.

Kyriakis, S.A., Younger, P.L., Paul, M.C., and Stephens, W.E., 2013. Advanced analysis of geothermal district heating systems. Poster presentation to the annual ETP Conference, Edinburgh, UK.

I declare that, except when explicit reference is made to the contribution of others, this thesis is my own work and it has not been submitted for any other degree at the University of Glasgow or any other institution.

Sotirios Kyriakis
Glasgow, March 2016

Table of Contents

List of Tables

List of Figures

1 INTRODUCTION

Worldwide concerns about the environment grow day by day. The need for change to our energy policy and behaviour seems more necessary than ever as their impacts on the environment worsen. Nowadays, the main concerns in energy policy are sustainability, security of supply, as well as reduction of fossil fuels consumption. So, increasing the share of renewable energy sources on the supply side and improving the efficiency on the demand side are necessary for sustainable growth (Hepbasli, 2010; Parri, 2007).

Over the last two decades, a lot of research has been carried out on renewable energy technologies which can be a crucial solution to the aforementioned problems. Renewable energy sources have many advantages, such as the negligible environmental pollution and the fact that these are an indigenous source, increasing the energy independence from expensive energy imports and providing jobs and growth to the local communities. The importance of energy independence can be seen by the data published in DECC (2015), where it is shown that a big fraction of the fossil resources used for energy production in the U.K. are imported. It is easily understood that this energy import is also dependent on the political relations between the involved countries. This fact becomes even more important when taking into account the fragile contemporary political scene, which highly endangers the relationships between countries that can stop the fossil fuel supply to each other at any time. This scenario could potentially be catastrophic for a big importer, like the U.K. Therefore, the need for local, indigenous and, if possibly, environmentally-friendly energy resources is even more necessary. All these criteria are fulfilled by the renewable energy sources, such as wind, solar, geothermal, and biomass energy amongst others.

A basic disadvantage of the majority of renewable energy sources is their intermittent production which leads to unstable production. The latter together with the intermittent, and often unpredictable, pattern of energy demand (heat, electricity, and transportation) poses a clear problem for matching supply and demand. This problem can be solved by geothermal energy, which is the only renewable energy source other than biomass which offers constant production and reaches availability factors close to 100%. Geothermal energy also has the previously mentioned advantages of the other renewable energy sources.

In general, heating accounts for a large proportion of our energy demands. More specifically, in the U.K. the use of heat accounts for 48% of the total end energy use as can be seen in Fig. 1.1. This means that almost half of the energy produced is used in the final form of heat and thus heating is a big contributor to overall carbon emissions. This indicates that using renewable energy sources for heating applications should be prioritised. In this point a paradox arises, as the majority of the funding and the research is focused on the increased use of renewable energy sources for electricity production (mainly wind and solar energy). This paradox is highlighted even more by the fact that with current technology (mainly in the electrical networks), there is a huge gap to achieve 100% penetration of renewable energy sources in electricity consumption. Furthermore, even if this is achieved sometime, for several countries it is quite difficult to fulfil their energy targets only by decarbonising electricity. All these facts point out the necessity of developing or improving existing technologies that can support heat provision by renewables. This thesis intends to show that decarbonising the heating sector by means of geothermal energy is not only possible, but can also be very effective and attractive.

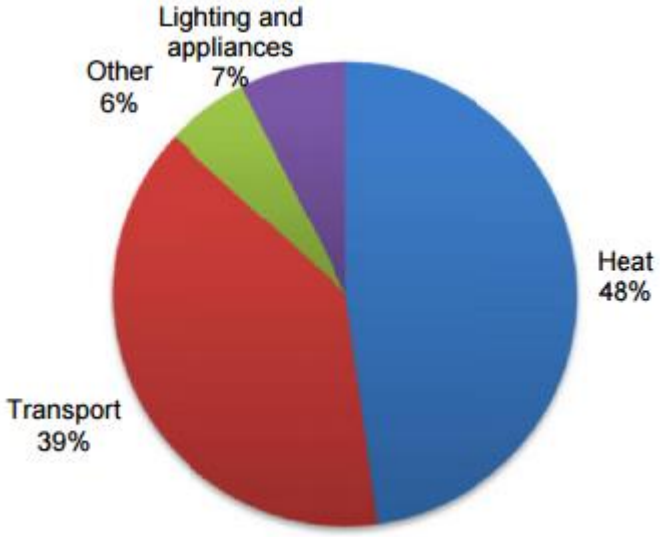

Figure 1.1 *Total U.K. end energy use in 2013 (DECC, 2014)*

Our focus in this study will be on heat provision in domestic buildings, but the methods and the results can be applied in any case of heating if the temperature level of the source is adequate for the end-user needs. The focus is on domestic buildings as the typical range of temperatures needed is physically close to that of geothermal energy, as will be seen later. Typically, heating is provided in buildings by two different means. Firstly, it can be provided by local boilers, stoves, electric heating and, in general, by equipment which produces heat within the building. A second option is to be provided by a district heating

system, in which the heat is produced in a central plant and distributed to the end-users by means of a pipeline network. As will be seen in the literature review, district heating systems are generally cheaper, more efficient and more environmentally friendly than local heating systems. Additionally, geothermal energy (apart from ground-source heat pumps) is usually produced at scales larger than those of a single building and a single well can provide heat to numerous buildings. For these two reasons, this study is focused on geothermal district heating systems for heat provision in buildings.

A point that should be mentioned here is that it is assumed that the studied systems are heat-only production units and not CHP units. Usually, in the latter the heat production is a by-product of the electricity production and, therefore, it is strongly coupled with it. A heat-only production unit is obviously more flexible as its production is independent of any electricity production. This is true for many geothermal systems, as outside of volcanic regions their temperatures in the majority of the cases are not high enough for efficient electricity production using current technology, but it is high enough for heating provision. So, in the studied systems it is assumed that the pumped geothermal water is utilised directly for heating purposes.

Geothermal district heating, which is the topic of this research, addresses all of the above aspects of energy policy as it is a green and indigenous energy resource, which decreases the use of fossil-fuels and can be a pioneering technology for sustainable growth.

1.1 Motivation, aim, objectives and novelties of this thesis

As mentioned before, the topic of this thesis is the study of geothermal district heating systems (GDHSs) as these combine the advantages of geothermal energy and district heating systems and can provide an affordable, efficient and environmentally-friendly solution for heating purposes and can be a potential solution to the energetic problem. In the next Chapter, an exhaustive literature review has been carried out on GDHSs and it will be observed that the main gap is on their operation. To the author's knowledge, there has been no published research which studies in detail the operation of GDHSs. For that purpose, this thesis will be focused on the operation of GDHSs.

Firstly, a brief explanation of a GDHS should be given. A typical geothermal district heating system can be seen in Fig. 1.2. In these systems, the geothermal water is pumped

from the underground through one or more production wells. The geothermal water is usually corrosive and in order to minimise these effects and the possible scaling due to its dissolved minerals, its heat is transferred to fresh water through a geothermal heat exchanger. It should be mentioned that a geothermal heat exchanger is a typical heat exchanger (usually plate heat exchanger), but the word “geothermal” is used to distinguish it from any other heat exchangers that might exist in the installation, such as in the substation or in the end-users. Subsequently, the heated fresh water is distributed to the end-users through a system of pipelines which typically includes a transmission and distribution network. The connection between the transmission and distribution network often happens with a substation. After the heated water provides its heat to the end-users, it returns to the geothermal heat exchanger in order to be re-heated and continue the cycle. At the same time, the cooled geothermal water is either re-injected to the underground or used in other purposes (such as agriculture) which require lower temperatures. These are the so-called indirect GDHSs and these will be studied throughout this thesis as the case of direct GDHSs is quite rare.

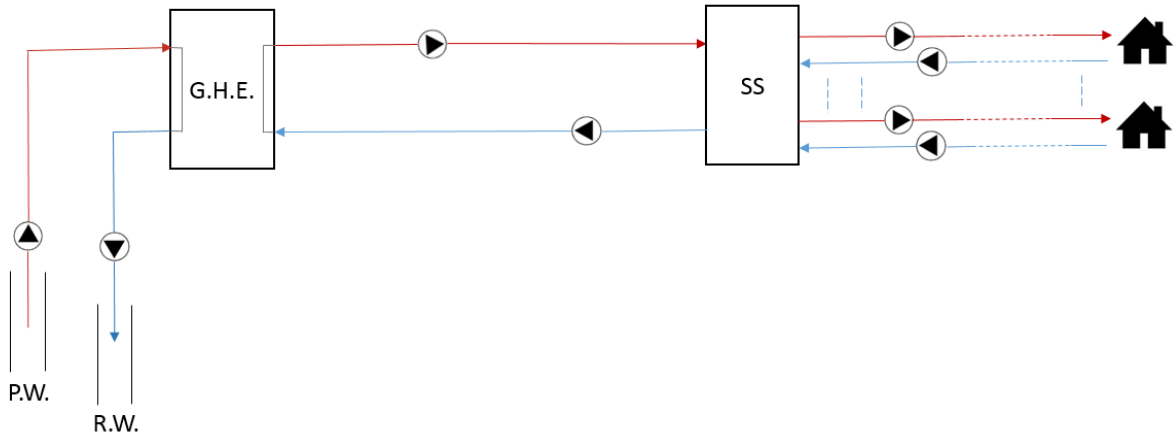

Figure 1.2 *Typical layout of a Geothermal District Heating System (P.W. = Production Well, R.W. = Re-injection Well, G.H.E. = Geothermal Heat Exchanger, SS = Substation)*

In practise, a GDHS is sized so that it can cover up to a specific amount of heat demand which is equal to its capacity and its typical operation is as follows: The mass flow rate from the geothermal wells is fluctuating throughout the day, according to heat demand, up to its maximum capacity and if the heat demand cannot be covered by geothermal energy solely, peak-up devices (usually fossil-fired boilers) are used to cover the excess heat demand. On the other hand, the heat demand throughout the day is usually far from constant and fluctuates a lot throughout the day. As an indicator, Figure 1.3 shows the fluctuation of the heat demand for a set of houses that was used in another study. This

figure shows the average heat demand and its deviation throughout the day for a set of 10 and 100 houses. It should be noted that the values of this figure have no relation with this thesis and this figure is only used to depict the fluctuation of the heat demand.

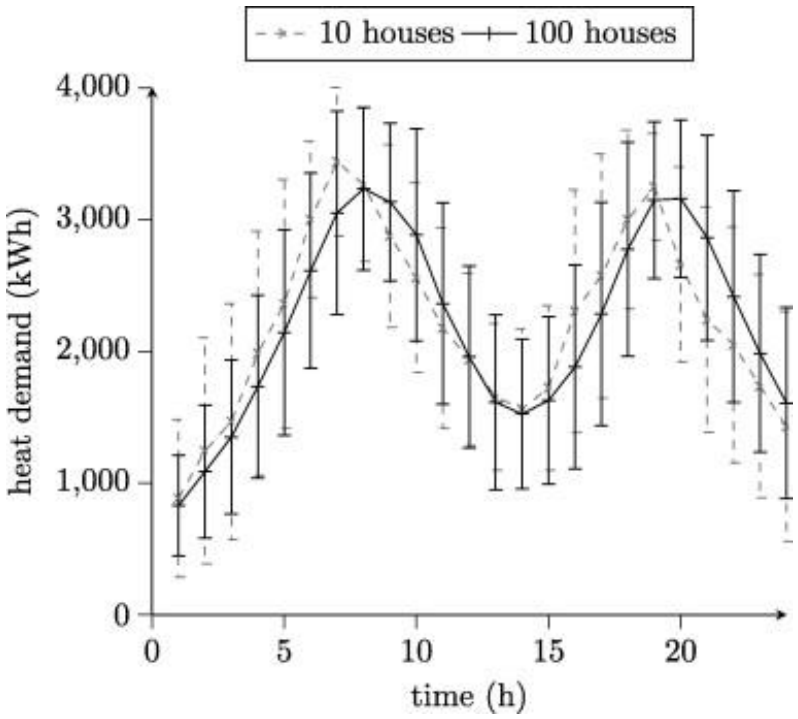

Figure 1.3 *Fluctuation of the heat demand for a set of houses (Bosman et al., 2012)*

It can be easily understood that according to the fluctuation of the heat demand and the capacity of the GDHS, the geothermal field can be under-utilised several times (i.e. producing less geothermal energy than the available one), while at other times it might not be enough to cover the heat demand. In the latter case, expensive and polluting peak-up boilers are used. Furthermore, in renewable energy sources it is desirable to maximise their utilisation and to produce as much energy from these sources as possible. Intuitively, the basis of the main idea of this study arises, which is to the increase geothermal production when the field is under-utilised in order to use this energy later when needed.

The latter together with the lack of published research on the operation of geothermal district heating systems gave rise to the main idea explored in this thesis, as follows:

- Instead of changing its production throughout the day the geothermal system will operate at a constant production rate. More details on how to calculate this constant production rate will be given in Chapter 3. Furthermore, the

installation will be planned to operate on a daily basis, so each day may have a different constant production.

- When the geothermal production is higher than the heat demand, the excess geothermal energy will be stored in a heat storage.
- On the other hand, the stored energy will be released to the network when the geothermal production is not enough to cover the heat demand, thus smoothing the overall operation of the installation and decreasing the use of the peak-up boilers.

The layout of the proposed system can be seen in Fig. 1.4. It should be noted in this point that it is not intended to totally phase-out the use of the peak-up boilers, as this would probably lead to over-dimensioning of the geothermal installation which would likely render the investment unfeasible, but to minimise their use. After all, there will always be some peak-up boilers in this kind of installations for back-up purposes, so phasing them out would not remove their capital cost in reality.

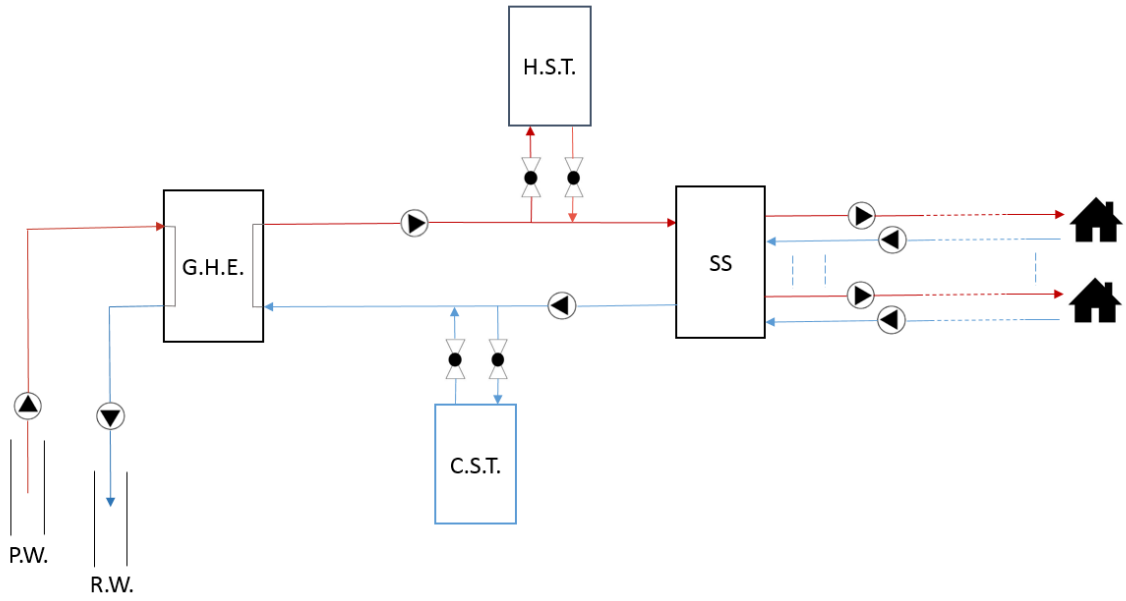

Figure 1.4 *Layout of the proposed system (H.S.T. = Hot Water Storage Tank, C.S.T. = Cold Water Storage Tank, the other abbreviations are as in Fig. 1.2)*

So, the **aim** of this thesis is to study the effect of including a heat storage in a GDHS under the proposed novel operational strategy. In other words, this thesis will examine whether it is beneficial to include a heat storage under the proposed strategy in a GDHS from energetic, environmental and economic perspectives. This is achieved by developing the following three core models which are the **objectives** of this thesis:

- **Model for the sizing of a GDHS.** This is a robust model for the sizing of a GDHS that operates under the proposed strategy. The results of this model will also provide useful insights about the operation of the principal components of a GDHS and identify where improvements can be made.
- **Model for the operation of a GDHS.** This model will involve two sub-models, where the first will study the operational strategy of the installation over a random day with a given heat demand and the second will simulate the annual operation of the installation. The first sub-model will be a useful tool for the operators of the installation as they will know in advance how to schedule the operation of the installation. The second sub-model will simulate how the installation operates over an annual cycle and will use this to identify the basic operational costs of it.
- **Model for the energetic, economic and environmental analysis of a GDHS.** In this model, the main energetic, economic and environmental indices of the installation will be calculated and a comparison with the traditional case, i.e. the geothermal district heating system that operates without a heat storage and as mentioned in the beginning of this section, will be carried out. By doing this comparison, the main question which is posed in the end of this section will be answered and the aim of this thesis will have been achieved.

The first two of the above models are necessary for the third model as this is a novel operation of a GDHS so both its sizing and detailed operation should be fully understandable. Both of these models are quite practically-oriented as will be seen in the correspondent Chapters, and can be used in real installations as tools for their corresponding use. So, these models are also an important outcome of this thesis and can be a powerful tool for geothermal companies and planners.

The main novelty of this study is not only the inclusion of the heat storage in the system, but also the operation in a novel way. Another novelty of this thesis is the approach to the modelling of the heat storage. Usually in district heating systems, stratified hot water storage tanks are used as the heat storage. More details on this are given in Chapter 2. In this case, as there is no published research on this aspect too in a GDHS and by taking into account that the flow rates are quite big in these systems (as will be shown in Chapter 3), it is considered difficult to maintain the stratification within the tank and, therefore, fully mixed storage tanks will be used. Furthermore, there will be no single

storage tank for the hot and cold streams, but, two different storage tanks, one to store hot water and one to store cold water. The proposed configuration can be seen in Fig. 3.1. In contrast with the stratified tanks which are always full with water (only the proportion of hot and cold water changes throughout the day), in our case both tanks will operate in a "fill-release" mode. This means that the amount of water that is stored in each tank will change throughout the day and it will depend on the mass balance of the whole system. All these will be more understandable in Chapter 3 of the thesis.

In the proposed approach, the mass flow rate to the left of the hot water storage tank (see Fig. 3.1) will be constant throughout the day, while the flow rate to the right of the storage tank will change according to the heat demand. It is assumed that the hot water storage tank will be placed as close as possible to the substation in order to obtain a quicker response in the change of the heat demand. The cold water storage tank will ensure that the flow rate to the geothermal heat exchanger will remain constant and can be placed anywhere between the heat exchanger and the substation. The important component that has to be modelled is the hot water storage tank as this is the main regulator between the production and the demand. The mass fluxes between this tank and the network as well as its heat losses will be studied in detail. As will be seen in Chapter 3, the heat losses of the hot storage tank will be negligible, so the heat losses of the cold storage tank will be even smaller as the temperature gradient between the environment and the tank will be smaller. Therefore, the cold water storage tank will not be studied further as its operation can be ensured by the use of a control-valve and this is out of the scope of this thesis. So, in the following, the word "tank" will refer to the hot water storage tank unless otherwise stated.

This thesis intends to study mainly if for a given installation, the inclusion of the heat storage and the novel operation can cover economically a higher fraction of the heat demand with geothermal energy. From another point of view, this could indicate the possible downsizing of the installation for the same heat demand coverage by geothermal energy.

In conclusion, the aim of this thesis is to study the effect of including a heat storage in a GDHS under a novel operational strategy from an energetic, economic and environmental point of view. The main question that will be addressed is the following: "Is it worthwhile including a heat store within the proposed operation of a geothermal district heating system or not?"

1.2 Structure of the thesis

In this Chapter, a brief introduction in GDHSs, which are the topic of this thesis was given. Through a clear logical path it was explained why these systems are worth to study and what these can offer to a sustainable future society. Furthermore, the main idea of this study was explained briefly and the objectives were clearly defined.

In Chapter 2, the literature review of this topic is provided. More specifically, the literature review commences with several details on geothermal energy and district heating, their advantages and disadvantages, several historical data on them as well as some limits on their expansion. Then, an exhaustive review of geothermal district heating systems follows with the majority of the review concerning the design aspects of the systems and their energetic as well as their economic analysis. Through this review the gap that was explained above and set the objectives of this thesis is identified. Finally, some details are presented on the use of heat storage in district heating systems, in general, an in geothermal district heating systems in specific.

In Chapter 3, a model for the integrated and robust sizing of a GDHS is developed. The mathematical model is explained in detail accompanied by all the governing equations of the involved phenomena, such as mass conservation equations, heat and friction losses etc. The whole study is carried out for three different cases of sizing which are also explained in detail, while the only data that are real data are the heat demand data. The rest of the data are arbitrary realistic inputs selected by the author to make the whole model as realistic as possible. This is the case for the other Chapters too. Thereafter, the results of this model are presented which provide many useful conclusions, through an extensive discussion, on the design of GDHSs and will be quite useful during the preliminary design of these systems.

In Chapter 4, the outcome of the previous model (i.e. the sized installation) is used as input in order to study the operation of this installation in detail. Theoretically, the installation which is the result of Chapter 3 will have been built and the model of this Chapter will be used to study its operation. Initially, a model that provides the operational strategy of the installation over a random day with a known (or predicted) heat demand is presented. By “operational strategy” is meant the complete knowledge of the operation of the installation, i.e. the necessary geothermal flow rate, when and by how much should the

storage tank be charged or discharged etc. In reality, this model could be a powerful tool for the operators of the installation as they would know *a priori* how to operate the installation when the heat demand is known. Then, this model is extended for the study of the operation of the installation over a whole year. Although this model uses the daily model as a basis, it has quite different outputs. Its outputs are the main operational costs of the installation which are among the main inputs of the next Chapter. The results of the first model are shown for different random days with various daily heat demands which provide useful knowledge on the operation of the installation for a range of heat demands. Finally, the results of the annual operation are also presented followed by an extensive discussion for both models.

In Chapter 5, the operational costs of the installation as well as the other outputs of the second part of Chapter 4 are used as inputs together with the capital costs of the installation in order to carry out a comprehensive economic, energetic and environmental analysis of the studied case. More specifically, several financial indices are calculated and the cash flows are presented for the investment, while two energetic indices are used for the energetic analysis together with the calculation of the emissions of the installation for the environmental part. All these calculations are carried out both for the studied as well as for the traditional case of operation of a GDHS. Through the analysis of the results and the comparison of the two cases, a clear answer is given to the most important question of this thesis on whether the inclusion of a heat storage in a GDHS is eventually beneficial or not.

Finally, in Chapter 6 a synopsis of the main findings of the thesis is provided together with its contributions to the field. The thesis ends with some propositions about further work that could be carried out on the basis of this study and for different approaches that could be potentially used to maximise the use of geothermal energy in the future energy system.

2 LITERATURE REVIEW

2.1 District heating

In general, district heating refers to the production of heat in a central plant and its distribution to the consumers via a network of pipelines. An important factor for the early development of district heating was the availability of industrial waste heat, especially from power plants (Cassito, 1990). District heating can use many heat sources, such as combined heat and power plants (CHP; coal-, gas- or biomass-fired), which is the most common source; conventional boilers; waste incinerators; industrial waste heat sources; solar collectors; heat pumps and geothermal energy (Lund and Lienau, 2009). The main advantages of district heating, as opposed to private heating provision in each building, are well summarised by Rosada (1988) and Rezaie and Rosen (2012) as: the higher efficiency of the whole procedure, with subsequent reduction of emissions; the facility of waste-heat recovery; the ability to utilize heat sources which would be difficult to utilize in single-dwelling installations, such as heat from waste; the high level of reliability etc. The economic viability of district heating depends a lot on the heat demand density of the examined area. As the heat demand density increases, the viability of district heating increases (see Dalla Rosa *et al.*, 2012, amongst others).

The advantage of reliability was studied by Lauenburg *et al.* (2010). More specifically, those authors examined what happens in a district heating network in the case of power failure. They found that usually natural circulation occurs, so heat is still being provided to houses (usually about 80% of the nominal heat) despite the power failure. A basic prerequisite for that is the maintenance of district heating production, i.e. the heat production must not be interrupted by the power failure as would happen for example with heat pumps.

District heating also has some disadvantages, mainly from an economic point of view. Usually it is not viable in areas of low population density and it is necessary to provide some incentives. District heating also has high capital costs, so most of the time subsidies are necessary. In addition, due to the high capital costs, it usually becomes the monopoly of the owner, which is counter to the desire to have liberalisation of energy markets (Grohnheit and Mortensen, 2003). Furthermore, it is difficult to retrofit existing buildings from a technical and an economical point of view. Finally, district heating is usually

produced in CHP stations, and the heat production is coupled with, or limited by, the electricity production. The latter reduces the flexibility of the heating installation.

The development of district heating was faster in countries with cold climates, such as Iceland, Germany, Finland, Sweden (Gustavsson, 1994a, b; amongst others), Denmark (Moller and Lund, 2010, amongst others), Latvia (Lund *et al.*, 1999), Lithuania (Rezaie and Rosen, 2012), Belgium, Romania (Iacobescu and Badescu, 2011), Poland (Zgoda, 1986) etc. In the UK, the penetration of district heating is still quite low, about 1%, apparently due to short/mid-term high risks and regulatory uncertainties (Kelly and Pollitt, 2010). However, the UK together with Germany and France hosts 50% of the short-term market expansion potential for district heating within the European Union (Persson and Werner, 2011).

In the last 20 years, a lot of research has been carried out on various aspects of district heating. A few examples are given below for the interested reader. Gustavsson (1994a, b) analysed possible energy conservation measures for buildings. The results showed that with typical conservation measures a decrease of 30-50% in building energy consumption can be achieved. Dalla Rosa and Christensen (2011) studied the concept of low energy district heating for buildings. This concept is based on low-temperature operation of the installation. In any case, the lowest possible return temperature is needed for maximum utilization of thermal energy. Noro and Lazzarin (2006) compared local heating by natural gas with district heating. Concerning emissions and energy efficiency, the modern local heating systems turn out to be more efficient than district heating. In contrast, this is not the case from an economic point of view. The latter depends a lot on the taxation of the fuel in local and district heating systems.

Torchio *et al.* (2009) undertook environmental research into district heating systems, finding that district heating is advantageous concerning CO_2 emissions, but concerning the other pollutants the positive effect of district heating is not always so clear. The authors also mention that a distinction between global and local emissions should always be made. Moller and Lund (2010) examined the potential expansion of district heating in areas previously supplied by domestic boilers in the Danish district heating system. The results showed that it is worth expanding the existing network around cities and towns and replacing natural gas boilers. In more remote areas, individual heat pumps seem to be the optimum solution.

Dotzauer (2003) applied an optimization algorithm to a district heating network which included the energy production unit, energy storage and energy sinks. The objective was to minimize the operational cost and to find the optimum production plan, satisfying the condition of fulfilling the heat demand on the mid-term horizon, i.e. 10-30 days. Verda *et al.* (2012) studied another optimization problem, which examined which users in an urban area should be connected to the district heating network and which ones should not, in favour of being served with a ground-source heat-pump system.

Concluding, it can be said that he future of district heating depends mainly on the prices of alternatives, the price of electricity and the distance from the nearest network. In high heat density areas district heating seems a better solution, while as heat density decreases, heat pumps become more favorable. Of course, clear and precise legislation is necessary for the construction, adoption and expansion of district heating networks. In some cases, the change of the legislative framework might also be necessary.

2.2 Geothermal Energy

Geothermal energy is the energy contained in the Earth's crust as heat and its origin is mainly from the processes that occur in Earth's interior and heat conduction taking place to the upper layers. This energy can be used for electricity production and / or for direct uses. Typically, temperatures above 15^{o}C can be utilized and even lower if heat pumps are used (Banks, 2012). More details on the use of heat pumps for geothermal applications can be found in the work of Underwood (2014). Depending on the temperature of the source, different utilizations of geothermal energy can be achieved. Temperatures above 150^{o}C are usually used for electricity generation, but in recent years the development of new technologies, i.e. binary cycles, has made it possible to produce electricity from water with temperatures of only 120^{o}C. Lower temperatures still are used for direct uses, such as space heating, district heating, agriculture, aquaculture, balneology, drying, snow melting, industrial processes, heating of pools and spa, distillation etc. (e.g. Kecebas, 2011, amongst many others).

Geothermal wells are categorised into: hydrothermal wells, which are the most common wells; geo-pressured wells; shallow wells; and enhanced geothermal systems (EGS) or hot dry rocks (Di Pippo, 2007). The latter are an emerging technology which are believed to increase geothermal potential by a large factor, compared to the currently

proven potential. For example, the potential of EGS systems is estimated to be ten times higher than the potential of hydrothermal systems. In EGS systems, reservoir properties are developed in deep strata by means of physical stimulation processes, and then water is injected through a first well, heated in the enhanced reservoir, and pumped to surface by a second well (Thorsteinsson and Tester, 2010, amongst many others).

Historically, the expansion of geothermal energy has been slow compared to other renewable energy sources, such as wind energy, for many reasons, such as the low fossil-fuel prices, the historic lack of ecological concerns and the high upfront capital expenditure requirements, particularly those considered risky in the early years of development of a given geothermal field. For example as stated by Rybach (2014), the average annual geothermal growth between 1995 and 2013 is around 5%, while for wind and solar PV systems the growth rate exceeds 25-30% from 2004 onwards. Nowadays, this situation has changed and new, cleaner, more efficient local energy sources are enthusiastically investigated. Another important reason for the delay of development of geothermal energy was that local authorities and societies were, and might still be in some cases, unaware of geothermal energy and its benefits, since it was perceived as a complex and risky energy source. So, education is necessary for the benefits of geothermal energy, as well as for the other renewable energy sources, to be fully realised. Finally, a lack of the necessary knowledge to develop geothermal systems, especially geothermal district heating systems, was an important reason for this delay (Thorsteinsson and Tester, 2010).

According to Lund *et al.* (2005), 71 countries reported geothermal energy utilization for direct uses in 2005, showing a significant rise over the corresponding values in 2000 (i.e. 58) and 1995 (i.e. 28). These direct uses comprised: 20% for direct space heating, 33% for space heating using heat pumps, 29% for bathing and swimming, 7.5% for greenhouse uses, 4% for aquaculture, 1% for agricultural uses etc. District heating accounts for 75-77% of space heating from geothermal energy. Kecebas (2013) states that in 2013 at least 76 countries were using geothermal energy for direct use purposes, with 24 countries producing electricity. The USA, Philippines, Mexico, Italy, Indonesia, Japan and New Zealand are the leading countries in electricity production, while Iceland, Turkey, Japan, China and France are the leaders in heat production from geothermal energy. Iceland, Turkey, China and France are the leaders in geothermal district heating, while Russia, Japan, Italy and USA are the leaders in individual home heating by geothermal energy (Lund *et al.*, 2005).

2.3 Geothermal district heating

2.3.1 General

Geothermal district heating systems are a combination of geothermal energy with district heating systems. More specifically, heat is extracted from the ground using one or more wells and is distributed (either directly or via a secondary working fluid) through a district heating network to many consumers, such as individual and commercial buildings or industries. The subsurface formation in which heat is stored is called a reservoir. Depending on the combination of pressure and temperature within the reservoir, heat can be extracted either in the form of hot water or as a steam-water mixture, or even in the form of saturated or dry steam. Most common are the wells that produce hot water (Kanoglu and Cengel, 1999).

A geothermal district heating system mainly consists of a heat production unit, a transmission-distribution system and the in-building equipment. More specifically, heat is extracted from the production wells, then is distributed to the consumers and finally is re-injected in another well, called a re-injection well or otherwise disposed of into the environment. Often, the geothermal fluid has corrosive properties, so a primary heat exchanger is used to extract heat from the geothermal fluid, and a secondary fluid distributes the heat to the consumers through a transmission and distribution network. Additionally, there are usually conventional boilers, which operate as back-up units and for the coverage of peak load. In some occasions, storage tanks are implemented for the same purpose. A simplified scheme of a geothermal district heating system is shown on Fig. 2.1.

It should be mentioned that a geothermal source can have multiple uses. In general, maximisation of the temperature drop of the geothermal fluid across the user infrastructure is desirable in order to extract the maximum amount of thermal energy. So, if there is more than one use for the geothermal fluid , they will be implemented simultaneously or in series (so-called ‘cascading use’, with each process using water cooler than the last) in order to achieve maximum efficiency. For example, in Iceland, the geothermal fluid is first used for electricity and heat production, and subsequently is used for snow melting, achieving high utilization efficiencies (Bjornsson, 2010).

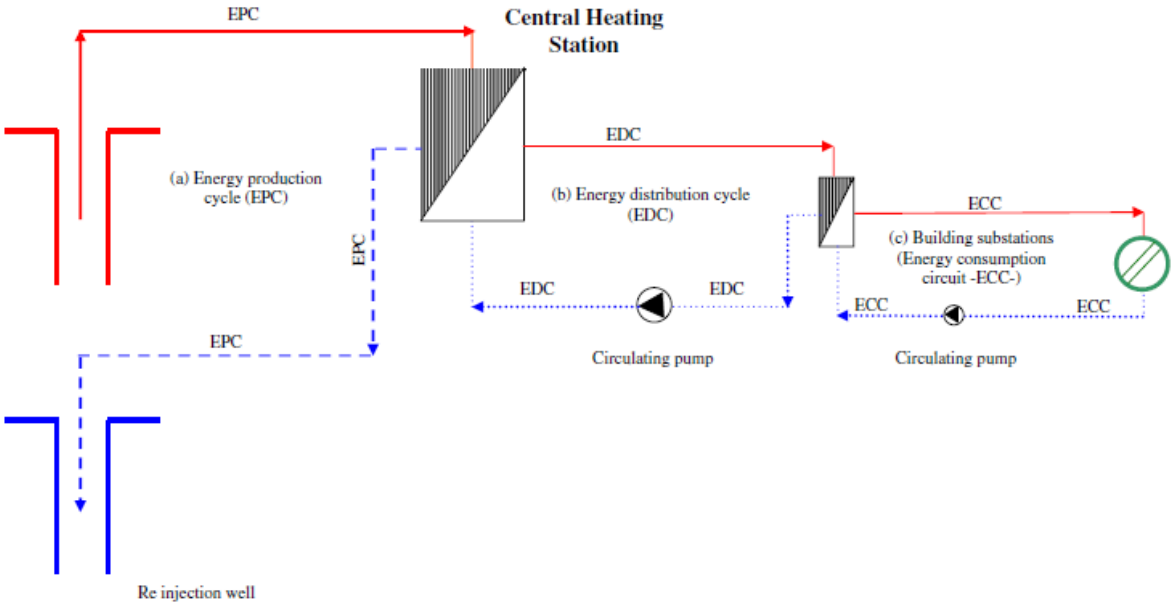

Figure 2.1 *Simplified schematic flow-chart for a geothermal district heating energy system (from Hepbasli, 2010)*

Another example of integrated use of geothermal energy is given by Bellache *et al.* (2000), where the heat extracted from the geothermal fluid is used in order to heat hotels and a spa. Arslan and Kose (2010) studied the integrated use of geothermal energy in Kutahya, Turkey. In this region, geothermal energy was used for multiple purposes, but not in an integrated way. A more complex system is proposed to achieve higher utilization. More specifically, it is proposed to build a binary cycle for electricity production, with the waste heat of the electricity plant then being used for district heating, and subsequently for greenhouse heating and spa heating.

The basic services that can be provided by geothermal district heating are the same as in any other district heating scheme, i.e. space heating, domestic hot water delivery, agriculture, balneology, industrial uses, etc. Indeed, the integration with industrial uses is very desirable in a geothermal district heating system because the demand profile is quite stable in the latter, so the fluctuation of the total heat demand is flattened a lot. The importance of the penetration of industrial uses in district heating systems is highlighted in the work of Difs *et al.* (2009). In general, the fluctuation of the heat demand in dwellings throughout the day is quite large. Hence, flattening of the demand is highly beneficial for the installation. Additionally, the industrial users usually have a stable demand throughout the year, making the installation more feasible to operate all year round.

A new, emerging technology is district cooling. In this technology, the heat is provided to an absorption chiller, which operates usually with a LiBr/water mixture and provides cooling. A basic disadvantage of these installations is that they need slightly higher temperatures than heating systems in order to operate, i.e. at least 80-90ºC (Nicol, 2009) for single stage absorption chillers. But, with the implementation of this technology, the annual demand rises a lot. It can be said that the reduction of heat demand during the summer can go hand in hand with the increase of the cooling demand over the same period. So, in that way the total demand will be much more constant throughout the year, while previously in summer the demand decreased a lot, since it comprised solely of the hot water preparation load, which usually was not enough to make the installation feasible for this period. The importance of the development of district cooling is obvious (Bloomquist, 2003; Hederman and Cohen, 1981).

The ability to provide a continuous and adequate flow at the required temperature is a basic prerequisite for a geothermal heating system (Ozgener *et al.*, 2006a). Other prerequisites are an area with high heat demand density, and a high load factor (i.e. the proportion of the total hours in a year over which the system is used).

Geothermal district heating systems provide numerous advantages both to individual customers and the society, such as (Lund and Lienau, 2009):

- Reduced fossil fuel consumption, since fuel is needed only for the peak demands. Consequently, a major reduction in emissions is achieved.
- Reduced heating cost: geothermal energy usually provides heating at lower cost than conventional fuels.
- Reduced fire hazard in buildings, because no combustion takes place in them.
- Possibility of “cogeneration”, i.e. utilization of the geothermal fluid for multiple uses.
- Provision of continuous base load, in contrast with the other renewable energy sources. Indeed, geothermal energy has a high capacity factor, due to high availability.
- Simple, safe and adaptable systems and electromechanical equipment.
- A geothermal resource usually has a lifetime of 30-50 years, but in some cases can be maintained even for 100-300 years. But, in order to do that a proper management of the reservoir has to be implemented in order to avoid depletion.

In most cases, re-injection of the geothermal fluid is necessary. So, geothermal energy can be considered as a sustainable energy source.

- Geothermal energy has huge potential. As stated by Li *et al.* (2011), in China alone the geothermal energy that is stored in the subsurface (within 2000m) of the sedimentary basins is equivalent to 250 million tons of standard coal.
- Geothermal energy does not depend on weather conditions (Kecebas *et al.* 2011).
- Low operating costs.
- Geothermal energy will probably have a stable price in the future, in contrast with combustible fuel prices.
- Because low-grade geothermal energy is widespread, it is invariably a domestic source of energy, thus contributing to security of supply and energy independence, as well as enhancement of local economies. Concerning the latter, many new jobs are also created (Hepbasli and Canakci, 2003).
- In purely heat production stations, the heat production is independent of any electricity production. As was mentioned before, concerning CHP plants, the dependence of heat production on electricity production was a big disadvantage.
- Very weak dependence on electricity prices, since the only electricity needed is for the pump systems

According to Lund *et al.* (2005), up to 2005 the usage of 25.4 million tonnes of fuel-oil had been avoided due to geothermal energy use. The environmental impact of geothermal energy is quite low, since the emissions of a geothermal plant are just a fraction of the emissions of fossil fuel plants, and of the same magnitude as the other renewable energy sources. During the construction and the decommissioning of the plant, there are some emissions, but the life-cycle emissions of a geothermal installation still remain quite low. Indeed, the emissions from low temperature resources are even smaller. If careful re-injection of the geothermal fluid takes place and the leaks are prevented, then pollution is minimised.

A study which highlights the advantages of geothermal energy for local economies was carried out by Karytsas *et al.* (2003). More specifically, a socio-economic study was carried out about the utilization of low enthalpy geothermal resources in a region in north Greece. The geothermal fluid would be utilized in a district heating network as well as for greenhouses uses. The benefits for the local society would be numerous, such as: reduction

in annual fuel consumption of up to 2325 tonnes of oil equivalent; subsequent reduction in CO_2 emissions of up to 7440 tonnes per year; annual savings of up to US$1,250,000; and 60 new jobs in the region. A governmental subsidy would definitely enhance the feasibility of the investment.

Inevitably geothermal energy, and subsequently geothermal district heating, has some disadvantages. Geothermal energy is site dependent, i.e. geothermal energy of higher enthalpies cannot be found everywhere. Additionally, in the case of district heating the production plant must be relatively near to the consumers in order to be feasible, whereas geothermal fields may exist in areas far away from inhabited districts (Sommer *et al.*, 2003). A specific heat load density is also necessary, as has been previously mentioned for district heating in general. So, it is beneficial to find consumers with constant and high loads throughout the year, such as industries, hotels, hospitals etc., which are also close to the production area. Initial capital costs are quite high for these instalments, for this reason a large part of them are of public ownership. Finally, it must be highlighted that the drilling of the geothermal wells is quite risky, because there is always an uncertainty about the temperature, the flow rate and the pressures of the underground water, at least during the early stages of field development. Taking into account that geothermal district heating networks are a capital intensive investment, it is obvious that initial engineering decisions are crucial both from a technical and an economical point of view. A wrong initial decision in the technical design of the system can lead to high financial losses as shown by Kristmannsdottir and Bjornsson (2012).

It can be concluded that geothermal district heating seems a potential solution for many current energy and environmental problems and that it can play an important role in the future energy target in the built environment sector. As noted by Ostergaard and Lund (2011), the integrated use of renewable energy sources, such as geothermal energy, waste incineration, heat pumps etc., can enhance the way to a sustainable future. In the latter study, the role of low temperature geothermal energy in a 100% renewable energy system was also analysed. The case of a small town in Denmark was examined, and the results showed that low temperature geothermal energy, combined with an absorption heat pump, could cover more than 40% of the total heat needs.

2.3.2 Examples of geothermal district heating systems

In this section, a few examples of geothermal district heating systems in several areas (from specific systems up to whole countries) will be given in order to highlight their difference in size and operation as well as their potential. For example, in Paris 100,000 residences are provided with heat by geothermal energy, while in Iceland, 22 geothermal district heating systems have been constructed. The system in Reykjavik which is one of the biggest in the world has a total installed capacity of 1,070MW_{th}. Almost 90% of the space heating in Iceland is provided by geothermal energy. The huge development of geothermal energy in Iceland has occurred mainly due to the rich physical resources of the country, as well as the positive attitude of people towards geothermal energy, which is seen as a reliable and clean source that has improved quality of life. It is worth mentioning that the fuel saved between 1970-2000 through switching to geothermal energy had a value of some £8.2M, i.e. three times the 2000 budget of the country (Loftsdottir and Thorarinsdottir, 2006; Bjornsson, 2010).

Turkey, on the other hand, has around 12% of the worldwide geothermal potential, but 95% is suitable for direct uses only. More specifically, direct use potential is estimated to be 31,500MW_{th}, but by the turn of the Millennium only 2-3% of this potential had been utilized (Hepbasli and Canakci, 2003, amongst many others). In the USA, 18 geothermal district heating networks have been constructed, but the identified potential is capable of providing heat to more than 271 cities (Sommer *et al.*, 2003). Finally, as stated by the European Geothermal Energy Association, 216 geothermal district heating systems existed in Europe by 2012, with a total installed capacity of 4900MW_{th} ,and 157 of these systems exist in the EU27 states. Figure 2.2 indicates the installed capacity of geothermal district heating systems at the end of 2012 (GeoDH, 2013).

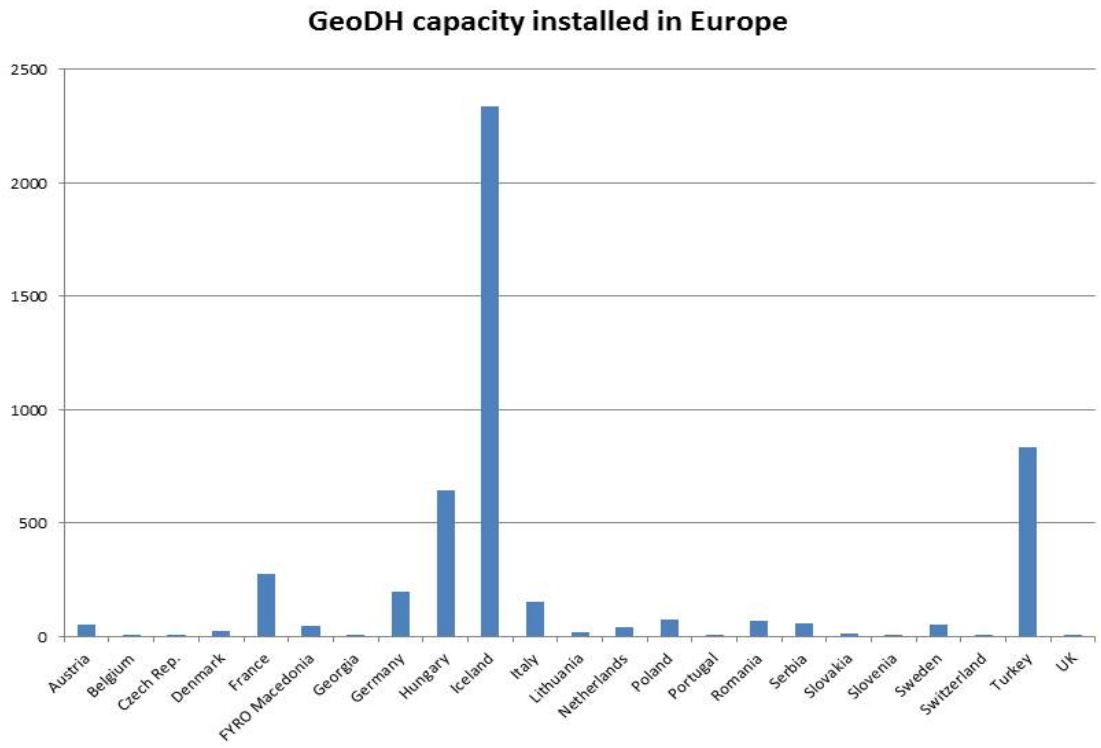

Figure 2.2 *Installed geothermal direct-use capacity in MW_{th} in European countries at the end of 2012 (GeoDH, 2013)*

The first geothermal district heating installation was constructed at Chaudes-Aigues Cantal, France, in the 14th century. The first municipal installations were constructed in Boise, Idaho, USA in 1893 and in Reykjavik in 1930 (Little and Bissell, 1980).

Geothermal district heating systems can differ greatly in size: for instance, the system in Reykjavik provides heat to 150,000 houses, with over 60 million cubic meters of geothermal fluid used annually. At the other end of the range, in Klamath Falls, Oregon, USA, a mini district heating system is used to heat 11 buildings on a University campus as mentioned in the work of Thorsteinsson and Tester (2010).

Harrison (1994) highlights the range of different operational strategies of geothermal district heating networks, through two extremely different examples. In Iceland, the hot springs of Deildartunga heat the nearby town of Akranes. The water is produced from a shallow depth almost free of pumping costs, at a high flow rate of almost 180kg/s, and is transported over a distance of 62km to the town of Akranes. The water is potable, so it is used directly to heat the houses. After heating the houses the water is discharged to the sea. In this case, even the peaks are met by those springs. In Beauvais, France, the water is produced from great depths and at smaller flow rates. The water is saline, so a heat

exchanger is used to extract heat from the geothermal fluid. The geothermal fluid is then re-injected into the reservoir to prevent head depletion and pollution of the environment. In this case, the heat production is much lower than in the case of Akranes.

In some extreme cases, such as Akranes, geothermal energy provides almost all the necessary heat. But, this is usually not economically viable, because the district heating network is oversized for most of the time and the field is underutilized. Hence geothermal energy usually provides base load, and the peaks are covered by auxiliary boilers or storage tanks. It must be emphasised that Iceland is a country with unusually high potential for geothermal energy, which can be produced at a very cheap price, and the danger of depletion of the wells is almost non-existent. Hence re-injection does not always take place there.

2.3.3 Design aspects

In this section, the basic design principles of a geothermal district heating system will be analysed. More specifically, details will be provided about the basic configuration of the network, the heat load estimation, the selection and the design of the appropriate heat exchangers, the basic aspects of the pipeline system and the in-house system, and finally a few details will be provided on the necessity of having a re-injection system.

Depending on the quality of the underground water, a geothermal district heating system can be a direct cycle (as in Reykjavik), with the geothermal fluid being circulated directly to the end-users, or an indirect cycle, providing the geothermal heat to a secondary fluid which is then distributed to the consumers. Indirect systems are more common, although they contain three extra costs compared to direct systems, i.e. the cost of a heat exchanger, the cost of circulating pumps and the cost of heat losses in the heat exchanger. Obviously, direct systems are cheaper than indirect systems, mainly because of avoiding the cost of the heat exchanger. Indirect cycles are used in order to minimize the corrosive action of the geothermal fluid and they are the most common case. Further information about corrosion problems in geothermal systems can be found in the work of Richter *et al.* (2006). However, injection of anti-corrosive as well as anti-freezing additives may take place in the distribution network (Chuanshan, 1997). An extra reason which may lead to the adaptation of indirect systems is the scaling problem which may occur due to the dissolved salts in the geothermal water. As stated by Kristmannsdottir and Bjornsson

(2012) scaling and corrosion can cause big problems in the operation of the system. So, careful research about the composition of geothermal water must be carried out during the preliminary study of the installation.

Design components for geothermal district heating systems are generally simple, safe and adaptable electromechanical devices. However, careful design is necessary due to the large scale of the investment. In general, it is found that the pipeline network, the heat exchanger and the re-injection system need the most careful design (Kecebas, 2011, amongst others). Finally, if the temperature of the geothermal fluid is not adequate for heating purposes, integration with a heat pump may be implemented (Harrison, 1994).

In the preliminary research of a new well, the sustainable flow rate, the temperature and the quality of the water have to be identified (as noted by Lund and Lienau, 2009, amongst many others). Of course, the final verification will be based on drilling tests. Available areas with geothermal potential can be identified by constructing isotherms for different depths. Additionally, in the preliminary design, if there is more than one production well, a lot of attention has to be paid to the minimization of the interaction between these wells.

To summarise, a geothermal district heating system consists of (Kanoglu and Cengel 1999):

- The production system, i.e. the production wells, the well pumps and the primary heat exchanger.
- The transmission-distribution system, which comprises of the pipeline system and the circulating pumps.
- The end-user systems. A secondary heat exchanger may be used in the buildings circuit, in order to avoid high values of pressure in the distribution network (Harrison, 1987). In many cases, two heat exchangers are used in each building, one for space heating and one for domestic hot water preparation.
- Disposal and re-injection system.
- Peaking and back-up systems, such as boilers or storage tanks.

Of course, at many points in the network, there are various meters and valves to ensure the correct operation of the network (Bloomquist, 2003). Additionally, it is shown in

numerous studies that automatic control will reduce the human involvement and increase the efficiency of the system.

A crucial initial factor for the proper design of a district heating network is an adequate estimation of the heat load. Domestic heat load consists mainly of the space heating load and the load of domestic hot water. The latter is quite stable throughout the year and can be easily estimated (see Oktay *et al.*, 2008). However, it is not usually sufficient to justify the investment feasible for the summer period, so additional loads, such as district cooling, industrial processes, pool heating are usually necessary in order to enhance the economic viability of the system (Popovski *et al.*, 2000). The most common method to estimate the space heating demand is the degree-day or degree-hour method which is summarised in the work of Heller (2002). In this method, the amount of observations where the ambient temperature is lower than a specific threshold are metered. The extent of the observation is usually an hour or a day as the aforementioned names indicate. This process is done for a normal or representative day for which the heat load is also known. Then for any other day or hour, the degree-days or hours are calculated based on the predicted meteorological data and the heat demand is then calculated as:

$$\frac{HL}{HL_n} = \frac{DD}{DD_n} \tag{2.1}$$

Where:

HL = Heat load (W)

HL_n = Nominal heat load (W)

DD = Degree-day or hour (Dimensionless)

DD_n = Nominal degree-day or hour (Dimensionless)

Yetemen and Yalcin (2009) proposed a prediction model, which predicts the demand the next day when knowing the weather conditions on the present day plus the consumption the previous day. It is considered to be a reliable model, since weather prediction for the next day is quite reliable. Of course, the heat load duration curve is of huge importance in order to estimate the optimum size of the geothermal plant and the integration of peak-up devices. The interested reader can find further information about heat load prediction in the works of Barelli *et al.* (2006), Nielsen and Madsen (2006) and Popescu *et al.* (2009).

Gelegenis (2005) proposed an algorithm for the quick estimation of the coverage of total heat load in a district heating system by geothermal energy. Geothermal systems of all kinds were examined, i.e. direct system; primary heat exchange system; heat pump assisted system; heat pump only system. In general, it was concluded that maximum supply temperature and minimum return temperature in the distribution network are desirable, in order to maximize the coverage achieved by geothermal energy. The proposed algorithm shows very good agreement with actual data.

According to Milanovic *et al.* (2004), the overall heat transfer coefficient of the building can be considered stable throughout the heating season. So, if the heat load is known for a specific set of indoor and outdoor temperature, then the heat load for any other set of these temperatures can be calculated using the following equation:

$$\frac{HL}{HL_n} = \frac{T_{ind} - T_{outd}}{T_{ind,n} - T_{outd.n}} \tag{2.2}$$

Where:

T_{ind}, T_{outd} = Indoor and outdoor temperatures, respectively (K)

$T_{ind,n}$, $T_{outd,n}$ = Nominal indoor and outdoor temperatures, respectively (K)

The above equation is very similar to Eq. (2.1) and the index nominal also refers to a representative case of indoor and outdoor temperatures for which the heat load is known.

Usually, each system is designed for a set of inlet and outlet temperatures and the demand fluctuations are met by variations in flow rate. The supply temperature of the geothermal network is usually constant, while the supply temperature of the secondary network is usually also kept constant because certain services, such as domestic hot water, need particular temperatures. The primary design of the network is made in such a way that the re-injection temperature of the geothermal fluid is minimised, i.e. maximum thermal energy is extracted. So, by varying the flow rate, the fluctuation of heat demand is met. In order to meet very high demands, usually peak-up boilers or storage tanks are used.

Harrison (1987) studied the basic design principles of indirect geothermal district heating systems. A fundamental principle is that the flow rate of the distribution network has to be higher than the flow rate of the geothermal fluid in order to obtain optimum heat

transfer and maximum utilization of the geothermal heat. The location of the peak-up boilers can be either centrally, after the primary heat exchanger, or individually in each building. It has been found that the latter approach is worthwhile only in buildings that previously had an individual boiler. Storage tanks operate to meet peaks and keep the flow constant through the heat exchanger. This means that for the small variations of the load through the day the flow rate in each building changes to meet the demand and peak-up boilers or storage tanks are used for the peak demands. However, the total flow rate through the primary heat exchanger does not usually change with the fluctuation of demand. A change in the return temperature of the distribution network, and consequently in the return temperature of the geothermal fluid may occur due to the demand variation. The viability of heat storage depends a lot on the fluctuation of the heat demand.

In most geothermal district heating networks usually counter-flow plate heat exchangers are used. According to Ozisik (1985), plate type heat exchangers have better corrosion resistance, require less space, are cheaper and can cope better with the changes of the heat demand than can shell-and-tube heat exchangers.

Coated carbon steel heat exchangers seem a good solution to meet corrosion problems of geothermal fluids (Chuanshan, 1997), while in some cases titanium plates are also used, though those are much more expensive. Obviously, the latter is an extreme situation used at very high corrosivity rates. In the primary heat exchanger the minimum difference between the hot temperatures of the two flows is desirable in order to maximize the efficiency of the heat exchanger.

The heat extracted from the geothermal fluid is given by the following equation:

$$\dot{Q}_G = \dot{m}_G \cdot Cp_G \cdot \left(T_{G,h} - T_{G,c}\right) \tag{2.3}$$

Where:

$\dot{Q}_G$ = Heat extracted from the geothermal fluid (W)

$\dot{m}_G$ = Mass flow rate of the geothermal fluid ($\frac{kg}{s}$)

Cp_G = Specific heat capacity of the geothermal fluid ($\frac{J}{kg \cdot K}$)

$T_{G,h}$, $T_{G,c}$ = Hot and cold temperature of the geothermal fluid, respectively (K)

The heat provided to the secondary flow is given by the following equation:

$$\dot{Q}_{sf} = \dot{m}_{sf} \cdot Cp_{sf} \cdot \left(T_{sf,h} - T_{sf,c}\right) \tag{2.4}$$

All the terms are defined as for equation (2.3), though here referring to the secondary fluid instead of the geothermal fluid. The suffix w denotes the secondary working fluid, which flows through the transmission and distribution network.

The equation of heat exchange between the two flows is as follows:

$$\dot{Q}_{trans} = A_{HE} \cdot K_t \cdot \Delta T_{lm} = A_{HE} \cdot K_t \cdot \frac{\left(T_{G,h} - T_{sf,h}\right) - \left(T_{G,c} - T_{sf,c}\right)}{ln\frac{T_{G,h} - T_{sf,h}}{T_{G,c} - T_{sf,c}}} \tag{2.5}$$

Where:

A_{HE} = Active surface area of the heat exchanger (m^2)

In the above equation K_t ($\frac{W}{m^2 \cdot K}$) the overall heat transfer coefficient of the heat exchanger given by the following equation (Jialing and Wei, 2003, amongst many others):

$$K_t = \frac{1}{\frac{1}{h_{c,h}} + R_{f,h} + \frac{\delta_{plate}}{k_{plate}} + R_{f,c} + \frac{1}{h_{c,c}}} \tag{2.6}$$

Where:

K_t = Overall heat transfer coefficient ($\frac{W}{m^2 \cdot K}$)

$h_{c,h}$, $h_{c,c}$ = Convective heat transfer coefficient of the hot (geothermal) and cold (distribution network) water stream, respectively ($\frac{W}{m^2 \cdot K}$)

$R_{f,h}$, $R_{f,c}$ = Fouling factor of the hot and cold water stream, respectively ($\frac{m^2 \cdot K}{W}$)

δ_{plate} = Thickness of each plate of the heat exchanger (m)

k_{plate} = Conductive heat transfer coefficient of each plate of the heat exchanger ($\frac{W}{m \cdot K}$)

The convective heat transfer (h) coefficient for both sides can be calculated by the following equation:

$$h_c = \frac{Nu \cdot k_f}{d_h} \tag{2.7}$$

Where:

Nu = Nusselt number (Dimensionless)

k_f = Conductive heat transfer coefficient of the corresponding fluid ($\frac{W}{m \cdot K}$)

d_h = Hydraulic diameter (m)

In the above equation, the Nusselt number can be calculated using the appropriate equation according to the prevalent conditions.

Additionally, the fouling factor can be considered equal for both the hot and the cold sides, as $R_{f,h}=R_{f,c}=0.0002$. The conductive heat transfer coefficient of the plate can be considered to be equal to $50\frac{W}{m^2 \cdot K}$, while the thickness of the plate can be considered to be equal to 0.0005m (Arslan *et al.*, 2009). Of course, all these values are just indicative.

Usually, the properties of the geothermal fluid are considered to be those of pure water, since the effects of salts and non-condensable gases are considered negligible (Kanoglu, 2002). So, in the rest of the study there will be no distinction between the properties of the geothermal fluid and those of pure water and the index w (water) will be used for that purpose.

On the other hand, during the heat exchange process some heat losses will occur, which have to be taken into account. In an ideal analysis, the above heat transfer rates (Eqs. (2.3)-(2.5)) are considered equal to each other. Further analysis of counter flow heat exchangers can be found in the work of Dagdas (2007), who states that an optimum heat exchange surface area of the heat exchanger can be found, taking into account the investment cost of the heat exchanger as an expenditure, as well as the fuel saving due to geothermal energy as an income.

According to Stoecker (1989) amongst many others, the effectiveness of a plate type heat exchanger, assuming no losses, is equal to the ratio of the heat transferred to the maximum available heat, and can be calculated by the following equation:

$$\eta_{HE} = \frac{\dot{Q}_{trans}}{\dot{Q}_{max}} = \frac{\dot{m}_{sf} \cdot Cp_w \cdot (T_{sf,h} - T_{sf,c})}{\dot{m}_G \cdot Cp_w \cdot (T_{G,h} - T_{sf,c})} \quad (2.8)$$

Where all the terms are defined as previously.

In the transmission and distribution networks, pre-insulated pipes are usually used. Kanoglu and Cengel (1999), amongst others, mentioned that a temperature drop of about 1^{o}C occurs in every 3-4 km of pipeline. The most important steps in the design of the pipeline system are the selection of the proper material and the determination of target pressure losses. Carbon steel pipes are 13-35% cheaper than composite pipes, but they are not usually suitable for geothermal loops, because of the corrosive effects. So, carbon steel pipes are usually used in secondary loops, and composite materials are used for geothermal loops. According to Bloomquist (2003), jacketed welded steel pipes can also be used, and in the return lines plastic pipes can also been used.

The pipes are usually buried underground in order to minimize heat losses and to avoid visual disturbance. Usually, they are buried directly into the soil because it is cheaper, but the construction of an underground tunnel can provide other advantages, such as easy access for maintenance, easier future expansion and an available corridor for other uses. However, the cost of the latter is typically double that of the direct burying of pipes and is thus usually not preferred.

Typically, in order to determine the optimum diameter of the pipes two aspects must be taken into account. These are the cost of material of the pipeline and the pressure losses. Obviously, the smaller the diameter, the lower the material costs of the pipeline. However, the smaller the diameter, the higher are the pressure (i.e. frictional head) losses, which leads to increased power consumption by the pumps, which consequently means higher electrical energy costs. So, an optimum diameter of the pipelines exists and has to be determined.

Furthermore, great attention has to be paid to any leakage from the pipeline system, since this is an energy loss, and as will be made clear in the following section, it can be a

huge component of loss (Kecebas, 2013, amongst many others). Finally, Brown (2006) stated that great attention has to be paid in the moisture on the external surface of the pipelines, which can also lead to corrosion. Consequently, he proposes that sometimes a concrete tunnel with a ventilation system might be necessary.

Chuanshan (1997) provides a summary of the basic equations for the heat exchange process within a building. The heat needed to maintain a stable indoor temperature T_{ind} when the outdoor temperature is T_{outd} can be calculated by the following equation:

$$\dot{Q}_1 = C_{q,b} \cdot V_b \cdot (T_{ind} - T_{outd}) \tag{2.9}$$

Where:

$C_{q,b}$ = Specific volumetric heat load capacity of the building ($\frac{W}{m^3 \cdot K}$)

V_b = Internal volume of the building (m^3)

The same amount of heat can also be estimated by the following equation according to Yildirim *et al.* (2005):

$$\dot{Q}_1 = U_b \cdot A_b \cdot (T_{ind} - T_{outd}) \tag{2.10}$$

Where:

U_b = Overall heating coefficient between the building and the environment ($\frac{W}{m^2 \cdot K}$)

A_b = External area of the building (m^2)

The latter will have to be calculated separately for different parts of the buildings, such as walls, glasses etc. The heat transferred through the radiator can by calculated by the following equation:

$$\dot{Q}_2 = K_{rad} \cdot A_{rad} \cdot \Delta T_{lm} \tag{2.11}$$

In the above equation all the terms are defined as in equations (2.5)-(2.6)-(2.7), though here they refer to the radiator instead of the heat exchanger. ΔT_{lm} (K) is the mean logarithmic temperature difference which is typically calculated as shown in the second and third part of Eq. (2.5), but in this case, it can also be calculated as follows:

$$\Delta T_{lm} = \frac{T_{rad,in}+T_{rad,out}}{2} - T_{rad,in} \quad (2.12)$$

Where:

$T_{rad,in}$, $T_{rad,out}$ = Input and output water temperatures, respectively, of the radiator (K)

Traditionally, heating circuits operated in the range 90 to70^{o}C. The circuits in geothermal district heating systems can operate at temperatures as low as 60 to 45^{o}C or even lower. With the development of building insulation and other technologies, lower temperature systems are becoming more and more popular. Low-temperature systems also improve indoor-air quality (Myhren and Holberg, 2008). A common technique is the use of an air velocity component, which forces the air to move through the radiator with increased velocity, causing that way increased heat transfer. (Myhren and Holberg, 2007). Szita (2010) described a three-pipe geothermal district heating system in a town in Hungary, which utilizes geothermal energy at different levels of temperature according to the end-user technology of each building, e.g. radiator, under floor heating etc. The importance of the end-user system is highlighted in this study.

In this connection, it should be noted that there is no unique configuration or operational strategy for geothermal district heating networks. No general conclusions about the operational strategy and the economic feasibility can be made. Everything depends on the conditions of each case, i.e. the flow rate, temperature and quality of geothermal water, the heat density, the distance of the production well to the buildings etc.

In most cases the re-injection of the geothermal fluid is necessary mainly for the following reasons (Steins and Zarrouk, 2012):

- Prevents reservoir depletion, which would otherwise result in declining reservoir pressures and thus a gradually increasing pumping cost.
- It is more environmentally friendly to dispose the brine in the well.

Indeed in high temperature reservoirs, it is sometimes necessary to add additional water to replace that lost to evaporation in cooling towers, so that the reservoir will not get de-pressurized.

In general, it can be concluded that the design of a geothermal district heating system depends greatly on the conditions of the selected area and that there is no single design and operational strategy. Hence few general conclusions can be reached. The most important influences on the design of a geothermal district heating system are the maximum utilization of the geothermal field, and the security of supply of the consumers.

To the best of the author's knowledge no studies about the optimization and simulation of geothermal district heating systems have been carried out to date. Concerning the optimization and simulation of non-geothermal district heating systems, the interested author can find the description and implementation of many different models in the literature such as:

- MODEST (Henning, 1997, amongst many others): It is an optimisation algorithm of dynamic energy system with time dependent components and boundary conditions. In general, MODEST finds the investment and operation decisions that satisfy the energy demand at minimum overall cost in local, regional and national energy systems.
- DESDOP (Weber and Shah, 2011): This algorithm is a mixed integer linear optimisation tool which provides the optimum mix of technologies in order to minimize the emissions. Mixed integer linear optimization techniques have also been used by other researches, such as Gustafsson and Ronnqvist (2008) etc.
- DEECO (Lindenberger *et al.*, 2000): This model which simplex algorithm optimization techniques, in order to examine the maximum integration of solar energy in a district heating system.
- SAFARI (Dotzauer, 2003): This is a mixed integer program used for the mid-term planning of district heating systems.
- GATE/CYCLE (Krause *et al.*, 1999) and TERMIS (Gabrielaitiene *et al.*, 2007): These are commercially available software for the simulation of thermal systems and district heating networks.
- TRNSYS (Heller, 2002, amongst others): It is a commercially available software for the simulation of transient systems.

2.3.4 Basic thermodynamic evaluation

2.3.4.1 Overview

In this section, a brief review of the literature concerning the energetic and exergetic evaluation of geothermal district heating networks will be presented, emphasizing the advantages of exergy analysis. In general, energy analysis alone is not enough to understand the whole system (Hepbasli, 2010, amongst others). For this reason, exergy analysis is necessary in order to get a more complete view of the system energy flows.

It can be briefly said that exergy is the maximum available energy, or in other words the maximum work that can be produced from the system when it is interacting with its surroundings. Energy is based on the 1st law of thermodynamics, while exergy is based on the 2nd law of thermodynamics. In other words, exergy is the optimal use of energy and takes into account all the energy losses that occur due to irreversibilities of the process, as summarised by Ozgener *et al.* (2005a), amongst many others.

Unlike energy, exergy is not subject to a conservation law; it is either consumed or destroyed. This happens due to irreversibilities that take place in any real process. Entropy is generated due to these irreversibilities, which consequently leads to exergy consumption. By implementing exergy analysis, it is possible to determine if (and by how much) it is possible to design more efficient systems. In general, exergy analysis is accepted as the most appropriate way to evaluate a geothermal district heating system, because it can point out the real magnitude of losses, and the parts of the installation that can be improved and it can show how efficiently the system operates.

Parri (2007) states that the use of fossil fuels for heating purposes, i.e. for a desired temperature smaller than 60^{o}C, is a huge waste from an energetic and exergetic point of view. It is far more efficient to use low enthalpy (and thus low exergy fluids), rather than high enthalpy ones. From that point of view, geothermal energy has much to offer in the sustainable development agenda, and the efficient utilization of energy sources. It is also noteworthy that for space heating at about 20^{o}C, a fluid with slightly higher temperature is theoretically usable. But, in that case the effective surface area of the radiator has to be increased considerably. If new, more efficient, radiators are designed in the future, then a temperature of 35^{o}C will be feasible for space heating, increasing the geothermal fields that

are viable for space heating purposes. At the moment, a minimum temperature of 50°C is still necessary for even the best radiators, with many still requiring temperatures in excess of 70°C. An exception to that is the use of underfloor heating systems in the newly built houses, which can operate with temperatures as low as 35°C. Finally, great attention has to be paid to the domestic hot water load, for which a temperature of 60°C is necessary anyway. So, it should be investigated in detail if the latter should be included in the general thermal load of the dwellings or if it should be provided by other means, e.g. electric heating.

Very little research has been carried out into the energetic and exergetic analysis of geothermal district heating systems. As mentioned also before, Turkey has among the highest potentials for geothermal district heating systems worldwide and is an emerging market since 170 geothermal fields have been discovered in the country as stated by Simsek (2001).

2.3.4.2 Basic equations

Summaries of the main equations used for energetic and exergetic evaluation have been given by many authors (Ozgener *et al.*, 2005a,b; Ozgener *et al.*, 2006a,b; Ozgener *et al.*, 2007a,b; Oktay *et al.*, 2008; Kecebas *et al.*, 2011 etc.) and these form the basis of the following listing. These equations can be used to evaluate any geothermal district heating system. Thermal and hydraulic steady-state conditions were assumed in formulating these equations.

- Mass balance:

$$\sum \dot{m}_{in} = \sum \dot{m}_{out} \rightarrow \sum_{wells} \dot{m}_{well} = \dot{m}_r + \dot{m}_{dis} \tag{2.13}$$

Where:

$\dot{m}_{well}$ = Mass flow rate of one geothermal well ($\frac{kg}{s}$)

$\dot{m}_r$ = Re-injection mass flow rate ($\frac{kg}{s}$)

$\dot{m}_{dis}$ = Discharge mass flow rate which takes into account the amount of water that it is not re-injected ($\frac{kg}{s}$)

The latter takes into account both the mass flow rate of the water that is naturally discharged and any leakage, although it is difficult to quantify the latter. In the majority of the studies, Eq. (2.13) is used to calculate the discharge mass flow rate. It should be noted that, depending on the particular case, one of the values of re-injection or discharge may be equal to zero. For example, in Akranes, Iceland, the entire amount of geothermal water is discharged, so the re-injection mass flow rate is equal to zero.

- Energy balance in a control volume:

$$\dot{Q}_{CV} - \dot{W}_{CV} = \sum \dot{m} \cdot (h + \frac{v^2}{2} g \cdot z)_{net} \quad (2.14)$$

Where:

$\dot{Q}_{CV}, \dot{W}_{CV}$ = Heat and work transfer rate through the control volume, respectively (W)

h = Specific enthalpy ($\frac{J}{kg}$)

v = velocity ($\frac{m}{s}$)

g = gravitational acceleration ($\frac{m}{s^2}$)

z = height (m)

The suffix ‘net’ denotes the difference between the input and output values. If there is no heat transfer and work input/output through the boundaries of the network, the above equation reduces to the following:

$$\sum \dot{m} \cdot (h + \frac{v^2}{2} + g \cdot z)_{net} = 0 \quad (2.15)$$

Usually, kinetic energy is considered negligible in these systems. So, if there is no change in the potential energy of the system, the above equation can be simplified to the following form:

$$\sum \dot{m}_{in} \cdot h_{in} = \sum \dot{m}_{out} \cdot h_{out} \quad (2.16)$$

The above equation is the one most commonly used in analysing geothermal district heating systems.

- Exergy balance into a control volume:

$$\sum_k (1-\frac{T_0}{T_k})\cdot \dot{Q}_k - \dot{W} + \sum \dot{m}_{in}\cdot \psi_{in} - \sum \dot{m}_{out}\cdot \psi_{out} = \dot{E}x_{dest.system} \quad (2.17)$$

Where:

T_0 = Temperature in the dead-state conditions (K)

T_k = Temperature in the k_{th} process (K)

ψ = Specific exergy ($\frac{J}{kg}$)

$\dot{E}x_{dest,system}$ = Rate of the exergy destruction through the system (W)

Similarly to the energy balance, if there is no heat or work transfer through the boundaries of the system, the above equation reduces to the following:

$$\sum \dot{m}_{in}\cdot \psi_{in} - \sum \dot{m}_{out}\cdot \psi_{out} = \dot{E}x_{dest,system} \quad (2.18)$$

In geothermal district heating systems, physical exergy is predominant, so eventually the specific exergy will be given by the following equation:

$$\psi = (h-h_0) - T_0\cdot(s-s_0) \quad (2.19)$$

Where:

s = Specific entropy ($\frac{J}{kg\cdot K}$)

h_0 = Specific enthalpy in the dead-state conditions ($\frac{J}{kg}$)

s_0 = Specific entropy in the dead=state conditions ($\frac{J}{kg\cdot K}$)

In the above equation the suffix ‘0‘denotes the dead-state conditions. At dead-state, the mechanical, thermal and chemical equilibria between the system and the environment are satisfied. No further interaction between them is possible. The exergy is by definition equal to zero at that point.

The exergy destruction of a geothermal district heating system is equal to the sum of the exergy destruction of its parts. For a typical system, this is equal to the sum of the

exergy destruction of the heat exchangers, the pumps and the pipelines. All these are defined by the following equations:

$$\dot{E}x_{dest,system} = \sum \dot{E}x_{dest,HE} + \sum \dot{E}x_{dest,pump} + \sum \dot{E}x_{dest,pipe} \quad (2.20)$$

$$\dot{E}x_{dest,HE} = \dot{E}x_{in} - \dot{E}x_{out} \quad (2.21)$$

$$\dot{E}x_{dest,pump} = \dot{W}_{pump} + \dot{E}x_{in} - \dot{E}x_{out} \quad (2.22)$$

$$\dot{E}x_{dest,pipe} = \dot{E}x_{in} - \dot{E}x_{out} \quad (2.23)$$

Where:

$\dot{E}x_{in}$, $\dot{E}x_{out}$ = Input and output exergy rate on each of the aforementioned equipment (W)

$\dot{E}x_{dest}$ = Exergy destruction rate on each of the above equipment (W)

$\dot{W}_{pump}$ = Electrical power provided by the pumps (W)

In energetic and exergetic analyses it is crucial to define the boundaries of the system. Thus it must be noted that in these studies, the system studied was from the production well to the primary heat exchanger: hence only the performance of the geothermal heat extraction was studied. Of course, the above equations are the same for the equipment of the secondary network and can be used in the same way. If there are any other devices in the equipment that cause exergy destruction, these devices also have to be taken into account.

- <u>Efficiencies of the whole system</u>:

Bearing in mind that the previously-studied systems only analysed the primary heat exchanger, the thermal energy efficiency of the whole system will be provided by the following set of equations:

$$\eta_{th} = \frac{\dot{Q}_{out}}{\dot{Q}_{in}} = \frac{\dot{Q}_{sf}}{\dot{Q}_{brine}} \quad (2.24)$$

$$\dot{Q}_{brine} = \dot{m}_G \cdot (h_{brine} - h_0) \quad (2.25)$$

Where:

η = Energetic efficiency (dimensionless)

$\dot{Q}_{sf}$ = Provided by Eq. (2.4)

$\dot{Q}_{brine}$ = Energy rate of the geothermal brine (W)

h_{brine} = Specific enthalpy of the brine ($\frac{J}{kg}$)

In the denominator of the above equation, the suffix 'brine' is used in order to distinguish this energy rate from the energy rate provided by Eq. (2.3), which denotes the actual energy provided by the geothermal fluid. This energy rate will be used in this thesis, while the energy rate used in Eq. (2.24) is closer to the concept of exergy as it provides roughly the maximum energy that can be provided by the geothermal fluid and not the actual energy provided.

In the same way, the total exergetic efficiency of the system will be given by the following set of equations:

$$\varepsilon = \frac{\dot{E}x_{useful,HE}}{\dot{E}x_G} = 1 - \frac{\dot{E}x_{dest,system} + \dot{E}x_r + \dot{E}x_{dis}}{\dot{E}x_G} \quad (2.26)$$

$$\dot{E}x_{useful,HE} = \dot{m}_{sf} \cdot (\psi_{out} - \psi_{in}) \quad (2.27)$$

$$\dot{E}x_G = \dot{m}_G \cdot [(h_G - h_0) - T_0 \cdot (s_G - s_0)] \quad (2.28)$$

Where:

$\dot{E}x_r, \dot{E}x_d$ = Exergy rates of the re-injected and discharged water, respectively (W)

The exergy rates of the re-injected and discharged water can be calculated by an equation similar to (2.28) if the properties of these flows are known. The rest of the exergy rates have been calculated in previous equations.

Finally, the exergetic efficiency of the heat exchanger can be calculated using the following equation:

$$\varepsilon_{HE} = \frac{\dot{m}_w \cdot (\psi_{w,out} - \psi_{w,in})}{\dot{m}_G \cdot (\psi_{G,in} - \psi_{G,out})} \quad (2.29)$$

Where:

$\psi_{w,in}, \psi_{w,out}$ = Input and output exergy rate of the secondary fluid (pure water), respectively ($\frac{J}{kg}$)

$\psi_{G,in}$, $\psi_{G,out}$ = Input and output exergy rate of the geothermal fluid ($\frac{J}{kg}$)

2.3.4.3 Indicative results and discussion

A short review of the above studies and their results will be provided in the table below. All of these studies were based on actual data. Additionally, the pressure and heat losses in the pipelines were not taken into account, although their indirect effects were observed in the real data. For the calculation of water properties the engineering equation solver tool (EES) was used (Kecebas *et al.*, 2011).

Table 2.1 Indicative results of several studies conducted on energetic and exergetic analyses of geothermal district heating systems

GDHS	Date of data used	Energetic efficiency (%)	Exergetic efficiency (%)	Reference
Gonen	1st February 2004	45.91	64.06	Ozgener *et al.* (2005b)
Balcova	1st December 2003	39.36	42.89	Ozgener *et al.* (2006b, 2007b)
Salihli	1st December 2003	59.31	59.58	Ozgener *et al.* (2006b, 2007b)
Balcova	1st February 2004	41.9	46	Ozgener *et al.* (2005a)
Afyon	8th January 2009	37.59	47.54	Kecebas *et al.* (2011)
Bigadic	November 2006	30	36	Oktay *et al.* (2008)
Bigadic	December 2006	40	49	Oktay *et al.* (2008)
Balcova	2nd January 2004	42.36	46.55	Ozgener *et al.* (2006a)

More indicative results can be found in Table 1 of the study of Hepbasli (2010). As already mentioned, the effects of salts and non-condensable gases in the geothermal fluid are neglected (Kanoglu, 2002).

The main exergy losses take place in the heat exchanger, the re-injection of geothermal water and the natural discharge. It has to be mentioned that the re-injected water is not a real loss, since it returns to the reservoir, but it is considered as a loss with the logic that since it was pumped over-ground it delivered a specific amount of energy that could be utilized. The exergy losses in the pipelines and the pumps of the system are much smaller.

The main energy losses of the system occur due to re-injection and natural discharge. The difference between energy and exergy analysis is highlighted through these studies. Though the losses of re-injection are something that cannot be avoided, the losses of natural discharge can be minimized through good design and maintenance of the pipeline system. In most of these systems, a lot of leakages occur due to bad maintenance. In order to improve efficiency, leakage should be minimised. In many of these installations, carbon steel pipes should be replaced by glass reinforced plastic pipes (GRP) for that very reason, as stated by Ozgener *et al.* (2005a).

As can be seen in Table 2.1, in geothermal systems the exergy efficiency is usually higher than the energy efficiency in comparison with conventional thermal systems. Exergy analysis is known to depend a lot on the surroundings of the system, i.e. the dead-state conditions. In geothermal systems, the operating temperatures are near dead-state conditions, so the magnitude of losses is smaller. For example, in a thermal power plant, the boiler reaches a temperature of about 2000^{o}C, while in a geothermal district heating system the maximum temperature is about 100-120^{o}C. It is obvious that in the first system the exergy losses will be much higher. The higher the temperature difference between two streams, the higher are the exergy losses for this process (Oktay *et al.*, 2008). Of course, the lower the re-injection temperature, the higher are the efficiencies of the installation.

Ozgener *et al.* (2007a) produced correlations of the efficiencies with the ambient temperature. In geothermal district heating systems, both the numerator and the denominator depend a lot on the ambient conditions, in comparison to the conventional thermal systems where the dependency of the denominator on ambient conditions is weak since it is usually a fuel stream. So, in most cases the efficiencies increase with an increase of ambient conditions. But it has to be borne in mind that this is not always the case. For

example, Kecebas and Yabanova (2012) found through their model that the energy efficiency increases with increasing ambient temperature, while exergy efficiency decreases. These correlations refer to a specific day of the year. Yuksel *et al.* (2012) investigated the seasonal performance of a geothermal district heating system. Energetic and exergetic analyses were implemented in winter, summer and transition period, where heat loads differ. Highest efficiencies are found in the transition period.

2.3.5 Additional parameters for the energetic evaluation of geothermal district heating systems

2.3.5.1 Specific exergy index

Geothermal fields can be classified according to their temperature as: high enthalpy fields if the reservoir temperature is higher than 150°C; medium enthalpy fields if the reservoir temperature is between 90°C and 150°C; and low enthalpy fields if the reservoir temperature is lower than 90°C (Di Pippo, 2007). In general, this classification is very generic and is not completely agreed between scientists. Furthermore, no information about the quality of the reservoir is provided by this classification. Lee (2001) classified the geothermal fields according to their exergy content. More specifically, the specific exergy index ($SExI$) parameter was proposed. This parameter, which is dimensionless, can be calculated by the following equation:

$$SExI = \frac{h_G - 273.16 \cdot s_G}{1192} \tag{2.30}$$

Where:

h_G = Specific enthalpy of geothermal fluid ($\frac{J}{kg}$)

s_G = Specific entropy of geothermal fluid ($\frac{J}{kg \cdot K}$)

The constant value of the denominator denotes the maximum value of exergy in the wet-steam region of a Mollier diagram, i.e. for saturated steam at 90 bar absolute pressure with triple-point sink, and actually normalizes all the exergy values within the water-steam region (Lee,2001). These exergy values vary between 0 and 1 within the water-steam region. In this way, the values of SExI are almost independent of the sink conditions. According to Lee (2001), if the specific exergy index of a reservoir is higher than 0.5, then

it is a high quality reservoir. If this value is between 0.05 and 0.5, then it is medium quality reservoir. Finally, if this value is lower than 0.05, then the reservoir is of low quality. Ozgener *et al.* (2005a, b; 2007b) applied this equation to their studies, and in most cases the reservoirs were found to be low quality.

A later study by Younger (2015) attempted the classification of geothermal fields according to their enthalpy, which is a more comprehensive and realistic approach compared to the classification according to the temperature of the field. The results of this study are represented graphically in Fig. 2.3, in which the numbers on the lines dividing the different enthalpy categories are approximate values of enthalpies in $\frac{KJ}{kg}$.

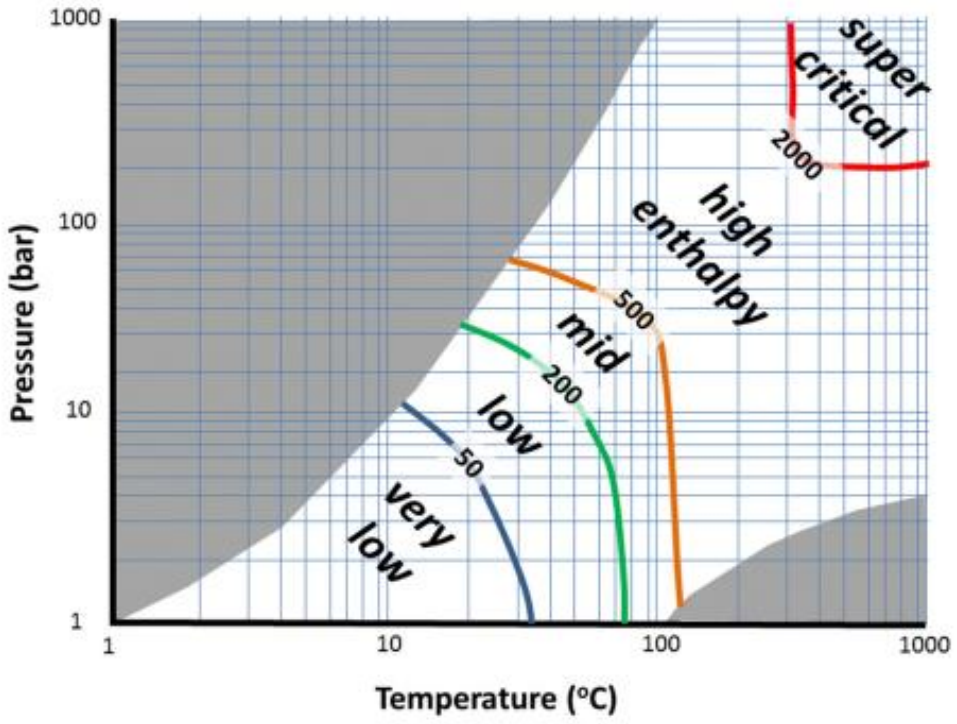

Figure 2.3. *Classification of geothermal fields on the basis of enthalpy (Younger, 2015)*

2.3.5.2 Improvement potential

The following equation can be implemented in order to calculate the maximum exergetic improvement that can be obtained by each process of the network (Hammond and Stapleton, 2001):

$$\dot{IP} = (1 - \varepsilon_{pr}) \cdot (\dot{Ex}_{in} - \dot{Ex}_{out}) \tag{2.31}$$

Where:

$\dot{IP}$ = Improvement potential (W)

ε_{pr} = Exergetic efficiency of the process (Dimensionless)

Ozgener *et al.* (2005a) found that the highest improvement potential exists in the heat exchangers of the system. This highlights the importance of the careful design and selection of the heat exchangers.

2.3.5.3 Other parameters

Very few studies have been carried out concerning other parameters of geothermal district heating systems. Hepbasli (2010), amongst few others, summarizes the concept of energy generation due to friction and heat losses in a system. Ozgener *et al.* (2005b) state the parameters of fuel depletion ratio; relative irreversibility; and productivity lack, which were originally implemented for conventional systems.

Coskun *et al.* (2009) introduced four new parameters which indicate how much the system is renewable and sustainable. These parameters, which were implemented to the Edremit, Turkey, geothermal district heating system are the following: Energetic renewability ratio; exergetic renewability ratio; energetic re-injection ratio; and exergetic re-injection ratio. The first two are defined as the ratio of the renewable energy or exergy, respectively, obtained from the system to the total energy or exergy input (renewable and non-renewable). The latter two are defined as the ratio of renewable energy or exergy, respectively, discharged to environment or re-injected to the well from the system to the total geothermal energy or exergy supplied to the system.

Ozgener and Ozgener (2009) analysed three parameters which describe the total availability of the system. These are the average technical availability; the real availability; and the capacity factor. Technical availability is defined as the ratio of operation hours to total machine hours available in the heating season and takes into account the machine faults of the system. The technical availability of a geothermal system is usually higher than 90%. Real availability is defined as the ratio of generation hours to total machine hours and depends mainly on the non-availability of the system due to possible leakages. If a system is well maintained the real availability can be almost 100%. Finally, the capacity factor is defined as the ratio of the desired actual useful production to the maximum

theoretical production of the system. As shown in this study, the average value of the capacity factor is around 40-42%.

Ozgener (2012) defined the coefficient of performance of a geothermal district heating system as the ratio of the useful energy provided to the summary of all the electrical energy consumed by the pumps of the system.

$$COP = \frac{\dot{E}_{useful}}{\sum_{pumps} \dot{W}_i} = \frac{\dot{E}_G \cdot \eta_{th}}{\sum_{pumps} \dot{W}_i} \tag{2.32}$$

Finally, Hepbasli (2010) introduced four new parameters which take into account the building's circuit. These are: the distribution cycle exergetic ratio; the energy consumption circuit exergetic ratio; the reservoir specific exergy utilization index; and the geothermal brine specific exergy utilization index. Defining further these parameters is out of the scope of this study.

2.3.5.4 Further studies

Sahin and Yazici (2012) and Kecebas *et al.* (2012) studied Afyon, Turkey, geothermal district heating system using artificial neural network (ANN) and adaptive neuro-fuzzy (ANFIS) models. An artificial neural network is a computational tool that mimics the way information is 'learned' by biological neural systems. It consists of an input layer, an output layer and some hidden layers which usually have stored information from some previous data, the so-called 'training'. The use of ANNs has some benefits such as non-linearity, flexibility, speed, simplicity and adaptive learning as noted by Kecebas and Yabanova (2012) amongst others. Artificial neural networks are more appropriate for systems for which no physical model exists, but they can also be used for systems with physical models. An artificial neural network needs some sets of inputs-outputs to determine the connecting weights in the hidden layers. After that, for any given input it is able to provide the output. Aksoy *et al.* (2011) state that 'It has been demonstrated that if there is sufficient number of neurons in the hidden layer of a feedforward ANN, with three layers, then the network can approximate any continuous function at the desired accuracy'. A feedforward ANN is an ANN that the transmission from a layer occurs only to layers following that layer. ANFIS is a hybrid scheme of neural networks and fuzzy logic techniques. It analyses the relation between inputs and outputs and finds the optimal

distribution of membership functions using either a back-propagation gradient descent algorithm or the latter in combination with the least-squares method. Results are compared and it is shown that the ANN models are slightly better in determining energy and exergy rates. Additionally, the correlation factors are very satisfactory. It is shown that ANN and ANFIS can provide a practical and fast solution for the estimation of energy and exergy rates.

Coskun *et al.* (2012) studied a new hybrid system for Edremit, Turkey, geothermal district heating system. The waste heat is re-injected at almost 40ºC, which is a very satisfactory temperature for feeding a heat pump and a biogas power plant, as is proposed. The electricity production of the biogas plant is proposed to be used for the heat pump, the district heating system pumps and all the auxiliary equipment. A biogas power plant needs a constant temperature of about 38ºC to operate. On the other hand, the coefficient of performance of a heat pump rises as the feeding temperature rises. Additionally, heat pumps depend a lot on the price of electricity. In this model, the electricity will be produced effectively for free. Results show that the energetic efficiency increases by 7.5% and the exergetic efficiency by 13%. So, by implementing this hybrid installation several advantages are realised, i.e. increase of efficiencies; increased number of heated residences; reduction of fuel consumption; reduction of emissions; and increase of the system's sustainability. Finally, a basic prerequisite for such a system is that high amounts of agricultural and industrial waste are necessary for the biogas plant to operate.

2.3.6 Economic analysis

2.3.6.1 Conventional economic analysis

After a resource has been found to be viable from an energetic and technical point of view, the last barrier for implementation is the economic feasibility. As already mentioned, a geothermal district heating system is a capital intensive investment (Erdogmus *et al.*, 2006, amongst many others). Additionally, the cost of drilling might render an investment infeasible. In contrast, operational and maintenance costs are quite low.

The total cost can be estimated as the sum of the investment cost, the operational cost and the maintenance cost. Possibly, the salvage cost of the equipment may decrease the total capital cost.

The investment cost consists of the cost of drilling, the cost of electromechanical equipment, i.e. pipeline system; heat exchangers; pumps; end user systems etc., and the cost of infrastructure, i.e. substations; storage tanks; control systems; pipeline burial costs etc. The investment cost can be separated into surface costs, which are easily predicted, and subsurface costs, which contain a lot of risk. The investment cost mainly depends of the following (Erdogmus *et al.*, 2006):

- Depth of resource.
- Distance between resource and consumers.
- Well flow rate and temperature.
- Load factor.
- Composition of geothermal fluid.
- Ease of disposal and re-injection.
- Heat density.

The main operational costs of a geothermal district heating system are the following (Harrison, 1994; Erdogmus *et al.*, 2006):

- Cost of personnel.
- Cost of electricity for the pumps and auxiliary equipment.
- Cost of fuel for peak-up and back-up boilers.
- Cost of tap and make-up water.
- Cost of anti-corrosive and anti-freezing chemicals.
- Cost of marketing.
- Cost of renting facilities.

Vorum and Petterson (1981) indicate that the distribution cost accounts usually more than 25% of the initial investment cost, while the maintenance costs might be even less than 1% of the investment cost. It has to be highlighted at this point that no general conclusions can be made about geothermal district heating systems costs. Depending on each case, allocation of costs might be quite different. In some cases the cost of drilling might be a large portion of the investment cost, e.g. EGS deep systems, while in other cases it might be negligible, e.g. shallow wells. A case study from Dlugosz (2003), for example, shows that the cost of wells is about 8% of the total cost, while transmission and

distribution costs account for more than 66% of the total cost. In other situations the relative costs of these components might be very different.

The main incomes for geothermal district heating systems are usually similar to traditional heating systems and consist of a fixed cost which is used as a minimum guaranteed income and in order to re-pay the initial investment costs and a variable heating cost which is variable and is priced according to the real use of heat. In the latter, the cost is usually calculated by specific meters which count the flow rate through the building, and the temperature of the distribution water before and after the building. These are called Btu-meters or just heat meters and can provide the actual use of heat within each end-user (Bloomquist, 2003). Based on this value, the variable cost of heating is calculated and then is summed with the fixed cost, to form the total income of the investment. Finally, there is the possibility of the extra income due to a financial subsidy that can be provided. This is the case in many countries worldwide which provide subsidies for the promotion and faster commissioning of renewable technologies.

Usually, in the economic analysis of geothermal district heating systems, a comparison with conventional systems is carried out. This comparison is carried out using some economic indicators. Of course, as Hederman and Cohen (1981) state, all the comparisons must be made on a common basis. Consistency must be achieved for taxes, interest rates etc. The main economic indicators are described shortly below and summarised in the works of Erdogmus *et al.* (2006) and Hederman and Cohen (1981).

- Net present value (NPV)

This is the sum of all the future incomes and expenditures at present-day monetary values. The transformation of future values (i-years from now) into present values can be done using the interest rate and the following equation:

$$PV^i = FV \cdot (1 + DR)^{-i} \tag{2.33}$$

Where:

PV = Present value (£)

FV = Future value (£)

DR = Discount rate (Dimensionless)

Therefore, the net present value of an investment with N years investment period can be calculated as:

$$NPV = \sum_{i=0}^{i=N} PV^i \tag{2.34}$$

The higher the net present value, the more economically feasible is a given investment as it denotes a higher net total income throughout the whole investment period.

- Internal rate of return method (IRR)

The IRR is defined as the discount rate which equates the net present value to zero. This can be calculated by solving the following equation for the discount rate:

$$\sum_{i=0}^{i=N} \frac{PV^i}{(1+DR)^i} = 0 \tag{2.35}$$

In general, the present value of the investment in any year can be calculated as the difference between the inflows and the outflows of the investment the specific year, i.e. the net cash flow of the investment. For an investment to be feasible, the IRR has to be higher than the current interest rate. On the other hand, when comparing investments, the one with the higher value of IRR is more feasible as it denotes higher financial security. It should be noted that if the installation is a public investment, the net present value can be very close to zero, since there may be no strong interest in making a profit.

- Unit cost of energy

This is simply the cost of producing one unit of energy. This is the minimum heating fee that the producer could accept in order to have suitable revenues. It is calculated, in general, by the following equations through the annuity method (Krajacic *et al*., 2011):

$$UCE = \frac{CC_{tot} \cdot CRF + C_{O\&M} + C_{misc}}{E_{annual}} \tag{2.36}$$

$$CRF = \frac{IR}{1-(1+IR)^N} \tag{2.37}$$

Where:

UCE = Unit cost of energy ($\frac{£}{kWh}$)

CC_{tot} = Total capital cost (£)

$C_{O\&M}$ = Cost of operation and maintenance of the installation ($\frac{£}{year}$)

C_{misc}= Miscellaneous costs of the installation ($\frac{£}{year}$)

CRF = Cost recovery factor (Dimensionless)

E_{annual} = Annual energy produced (kWh)

IR = Interest rate (Dimensionless)

Other possible costs, such as salvage cost if available, should be also taken into account.

Typical assumed values of interest and discount rate are 6% and 5%, respectively (Sommer *et al.*, 2003), although in many countries, such as UK, the central bank sets in advance the 'base' interest rate to a specific value, which is used as a starting point in any analysis.

Atkinson and Huxtable (1984) highlight the importance of two crucial factors of geothermal district heating systems. These two factors, as mentioned earlier, are the distance between the well and the energy consumption centre and the heat load density. These factors can render an investment infeasible if they are not examined thoroughly.

Erdogmus *et al.* (2006) evaluated the geothermal district heating of Balcova, Turkey, from an economic point of view. The profitability was investigated with the internal rate of return method. Many different scenarios for operating costs and utilized energy price were examined. It was found in that case that the proper monthly utilization price for a 100m^2 building was US$55.5 (equal to £37.95). It is also shown that IRR increases when the heating fee increases and when the operational costs decrease.

Hederman and Cohen (1981) examined the cost of geothermal commercial-scale direct heat applications and compared them with fuel alternatives. Five different projects concerning the well depth and the use of geothermal heat were examined. In general, life-cycle costs of a geothermal installation are much different from those of a conventional unit. A geothermal installation has large initial capital investment costs but low recurrent

operational costs. In contrast, a conventional unit has lower investment costs but quite high operational costs, due to the cost of conventional fuels. For this reason, the life-cycle costs must be taken into account when implementing a comparison between renewable and conventional units. Geothermal energy is found to be cheaper than oil in all circumstances, and cheaper than natural gas in many cases. So, it is shown that geothermal energy can provide a cheap alternative to conventional fuels.

Kanoglu and Cengel (1999) carried out a feasibility study for the combined generation of power and heating or cooling from high enthalpy geothermal resources. They state that in high enthalpy geothermal fields, electricity produced from geothermal energy is about $1/13^{th}$ of the heat power that can be produced from the same source. But, from a thermodynamic point of view, it is not wise to produce heat solely from high enthalpy resources. As previously mentioned, the best solution is the combined generation of heating or cooling and power. Kanoglu and Cengel (1999) also verify the latter from an economic point of view. It is found that heating can provide 3.1 times and cooling 2.9 times the revenue of power alone generation. Additionally, combined heat and power generation can provide 2.1 times the revenue of power alone generation, while combined cooling and power generation can provide 1.2 the revenue of power alone generation. In any case, the integrated use of geothermal energy is more feasible than the use for a single purpose, especially if there is a high enthalpy resource.

Sommer *et al.* (2003) studied the spatial economics of geothermal district heating systems. The commercial software HEATMAP (Bloomquist *et al.*, 2004) was used to examine the feasibility for a low density town in the USA. HEATMAP is a very useful tool which has various inputs, such as: building uses and sizes; a supply source; the source location; the pipeline configuration etc. The outputs that HEATMAP provides are the following: thermal density; sizing of pipelines; total cost estimate; revenues; estimation of viability of the investment; unit cost of energy. In general, costs of geothermal energy vary a lot according to many factors already discussed. Sommer *et al.* (2003) stated the following: ‘An important factor for the economics of geothermal district heating is the trade-off between economies of scale and transportation costs. There is an optimum where the expanding of the network to capture more customers is not worth anymore’. The latter is mainly not worthwhile from the customers’ point of view, because they will have to pay a very high price for heating. Sommer *et al.* (2003), show that the rate of participation, i.e. the proportion of customers in the area that adopts geothermal district heating, is a crucial factor for the viability of the investment. As already discussed, in order to achieve high a

rate of participation, education of the citizens about the benefits of geothermal energy is necessary. A sensitivity analysis on the rate of participation was carried out. It was found that even in the pessimistic case, geothermal energy is competitive at least in the core building district area. But the economies of scale by larger service areas do not necessarily outweigh the higher development costs. The further we get from the core building district, the less feasible is the investment. In general, it is found that no general conclusion can be reached on that aspect. It depends on each case, and careful study is necessary.

Vorum and Petterson (1981) carried out a feasibility analysis of geothermal district heating systems, which indicated that they are competitive with other energy sources, such as fossil fuels, biomass etc. More specifically, two service areas were examined and the unit cost of energy was found to be equal to US$10.3 and US$8.2 per million Btu (roughly equal to £0.024/kWh and £0.019/kWh), respectively. These prices were compared with the prices of electricity, propane and fuel oil, which were respectively US$8.76, US$13.65 and US$11.71 (roughly equal to £0.0204/kWh, £0.0318/kWh and £0.0273/kWh). It was also estimated that an annual saving of about US$480 (c. £330) could be achieved if fuel oil was used before. The competitiveness of geothermal district heating is made clear through this study.

It can be concluded that geothermal district heating is a cheap, or at least competitive, alternative to traditional fossil-fuelled heating systems. The cost of geothermal district heating depends on many factors and can vary widely, but in general geothermal district heating is a cheap solution which together with its low emissions could be a crucial contributor to meeting future energy targets and sustainable development, thus providing many benefits both to the customers and to the society.

2.3.6.2 Exergoeconomic analysis

Exergy analysis is proving to be a powerful tool for finding where improvements can be made. But, only economic analysis can determine the feasibility of such an improvement. For this reason, they are usually implemented together. Exergoeconomic analysis is the combination of exergy and economics for long term operational conditions (Ozgener *et al.*, 2007c, amongst others).

Ozgener *et al.* (2007c) conducted an exergoeconomic study of the Salihli, Turkey, geothermal district heating system implementing mass, energy, exergy and cost analysis.

The relation between thermodynamic losses and capital cost of the whole system and its components is examined with the following equations:

$$\dot{L}_{en} = \dot{E}_{loss} \tag{2.38}$$

$$\dot{L}_{ex} = \dot{E}x_{dest} \tag{2.39}$$

$$R_{en} = \frac{\dot{L}_{en}}{CC_{tot}} \tag{2.40}$$

$$R_{ex} = \frac{\dot{L}_{ex}}{CC_{tot}} \tag{2.41}$$

Where:

$\dot{L}_{en}$ = Energy losses ratio (W)

$\dot{E}_{loss}$ = Energy losses (W)

$\dot{L}_{ex}$ = Exergy losses-destruction ratio (W)

R_{en}, R_{ex} = Ratio of energy and exergy losses to capital cost, respectively ($\frac{W}{£}$)

It is shown that a correlation between capital cost and internal or total exergy losses exists. Internal exergy losses are the losses which occur due to irreversibilities of the process, while external losses are the losses which occur due to interaction of the system with its surroundings. Obviously, the total exergy losses are the sum of internal and external exergy losses. So, usually the total exergy losses are taken into account. No correlation between energy losses and capital cost exists. In general, the prices of the ratio of exergy loss to capital cost of each component tend to be close to each other. So, it seems to be a systematic correlation between exergy losses and capital cost.

It is shown that a successful design must balance the thermodynamic and economic characteristics of the system. As Ozgener *et al.* (2005c) state in their study 'The results suggest that a good design, in terms of balancing efficiency with cost, occurs when the loss-to-capital cost ratios based on exergy for the devices comprising the geothermal district heating system approach the loss-to-capital cost ratio based on exergy for the overall system'. Hence, in a successful design the value of loss to capital cost ratio based on exergy for the components comprising the system must approach an appropriate value, which is usually the loss to capital cost ratio based on exergy for the whole system.

However, the components which need improvement can still be indicated by exergy analysis. Exergoeconomic analysis is very useful to indicate if balance exists between thermodynamic and economic characteristics of the system.

2.4 Thermal energy storage

2.4.1 General

An important parameter for the sustainable development is the maximum utilisation of the available energy sources. Traditionally, if the energy production was higher than the energy consumption, the energy surplus was simply wasted in the environment. On the other hand, in the opposite case expensive equipment and energy sources were used to cover the energy shortages. This mismatch between the production and the demand occurs due to their intermittent nature. For example, in a solar system the energy production is quite changeable throughout the day and it depends on the solar radiation, the cloudiness etc. In contrast, the energy requirements can fluctuate a lot throughout the day depending on the habits of the end-users, amongst many other factors. Lately, the concept of energy storage has been studied extensively as a means of matching the production with the demand. The main idea is to store energy when in excess production and release it when in shortage (Han *et al.*, 2009).

The energy storage systems are, in general, divided in the following categories according to the kind of energy stored: Mechanical, electrical, thermal and chemical energy storage, while less developed are the magnetic and biologic energy storage methods (Dincer and Rosen, 2011). For the sake of simplicity, the thermal energy storage systems will be examined in this section, as well as in the overall thesis, as the studied systems are dealing only with thermal energy both in the production and the demand side. Therefore, the thermal energy storage systems are considered to be the most appropriate for these systems.

The thermal energy storage systems (TES) are further divided in the following categories (Arteconi *et al.*, 2012):

- Sensible TES: In these systems, the energy is stored through the temperature change of the storage medium. The most common storage medium in these

systems is water. A basic advantage of the sensible TES is that the storage medium is safe, cheap, abundant and easy to handle. Furthermore, these are the best established storage systems. In contrast, the basic disadvantage of these systems is that their operation is typically limited by the boiling point of the storage medium, which for water is 100^{o}C. In some cases, solid media, such as concrete, are used for storage, but require generally large storage volumes and are not preferred.

- Latent TES: As its name indicates, in a latent TES the energy is stored through the phase change of the storage medium. The storage media in these systems are called PCMs (Phase Change Materials). Typically, the storage medium is in solid form and when the energy is stored it liquefies. During the discharge phase, the opposite process occurs. A basic advantage is that the system operates in a constant temperature, and the range of the storage temperature is much higher compared to a sensible TES. On the other hand, these systems are more expensive and require better maintenance. The most typical storage media, are water/ice, salt hydrates and polymers.
- Cold TES: This is a special category of the two aforementioned TES and it refers to the thermal energy storage for cold applications. The typical materials that are used are ice, chilled water and some PCMs.
- Thermochemical TES: These systems could also be included in the chemical storage systems and, therefore, will be explained briefly. A reversible chemical reaction is utilised in these systems. Typically, the energy is stored through an endothermic reaction, and the energy is released by performing the reaction in the opposite way. The environmental concerns around these systems have mainly slowed down their development.

Apart from the aforementioned details, when comparing these systems two main parameters are taken into account. These are the energy density of the storage medium and its cost. Concerning the energy density, the thermochemical TES are by far the best option followed by the latent TES and, then, the sensible TES. In contrast, the costs of these systems follow exactly the reverse trend. So, it is a matter of engineering decision which of the previously mentioned TES will be used. Other factors that should be taken into account are the operating temperature, the safety and the available storage volume.

2.4.2 Thermal energy storage in district heating systems

As mentioned earlier, the typical temperatures of the water in a district heating system (including GDHSs) is well below 100^{o}C. Taking this into account together with the fact that water is the working fluid anyway, the use of a sensible TES is an obvious solution. For this purpose, water storage tanks are implemented for the matching between the production and the demand. In a district heating system fed by a CHP unit, the mismatch between the production and the demand can be intensified when the CHP unit is operating in an electrically-driven mode, when the heat production is limited by the electricity production.

Water by its nature displays a natural phenomenon, called stratification, which can influence the operation and effectiveness of the storage. When water is stored in a storage tank, it tends to develop a thermocline and be separated vertically into two different temperature zones. In practice, stratification occurs mainly due to the heat losses to the environment, which creates a zone of colder fluid close to the walls of the tank which tends to move downwards. For the modelling of storage tanks, two main approaches are used: stratified and fully-mixed storage tanks.

In practice, stratification not only occurs naturally but can also be desirable. As mentioned before, the majority of district heating systems are fed by CHP units, in which the temperature of the water provided to the network can be variable (Kostowski and Skorek, 2005; Haeseldonckx *et al.*, 2007). The supply temperature to the end-users should have a specific value according to the end-users' needs. On the other hand, the return temperature to the production unit should be minimised in order to optimise the whole process. So, stratified tanks with a high degree of stratification are used in many cases. Furthermore, the stratification can be enhanced in many different ways on which a lot of research has been carried out (e.g. Verda and Colella, 2011; Garcia-Mari *et al.*, 2013; Kenjo *et al.*, 2007; Jordan and Furbo, 2005)**.** The majority of the studies have shown that stratified storage tanks can provide numerous advantages when coupled with a CHP unit. For example, Verda and Colella (2011) found that the primary energy consumption can be reduced by 12%, while the total costs can be decreased by 5%. Ghaddar (1994) states that a stratified storage tank works more efficiently under a variable temperature, which comes in contrast with the logic of a GDHS. A basic disadvantage of this kind of tank is that the

stratification can be easily destroyed and low flow rates are generally required. This also contrasts with GDHS in which the flow rates are fairly high.

Fully mixed storage tanks have not been studied as extensively as stratified tanks. Pagliarini and Rainieri (2010) studied the effect of a fully mixed storage tank when coupled with a CHP unit for the heating needs of a University campus. The results highlight the energetic and economic benefits of integrating a heat storage in this system. Subsequently, Campos Celador *et al.* (2011) compared the different approaches to modelling of water storage tanks in a CHP plant. More specifically, they used the fully mixed, the actual stratified and the ideal stratified models to simulate the storage tank. It was found that from an energetic point of view, the effectiveness of all the simulations are roughly the same, but from an economic point of view, the stratified approach is more desirable. These results agree partially with the results of Ghaddar (1994) who stated that the stratified approach also substantially improves the results from an energetic point of view.

2.4.3 Thermal energy storage in geothermal district heating systems

As mentioned before, the majority of the studies of hot water storage tanks concerned CHP or solar units, which have a variable feeding temperature which makes the use of stratified tanks unavoidable. To the best of the author's knowledge, there are no published studies which integrate a heat storage into a geothermal district heating system. In contrast with the aforementioned studies, the temperatures across a GDHS and, subsequently, the feeding temperature into the tank, are roughly constant. Furthermore, in these systems the mass flow rates are usually very high (as will also be seen in the following Chapters), which makes the maintenance of stratification quite difficult and costly. Another reason for using a stratified tank is the lack of available area for building a fully mixed tank. In a GDHS, this should not be a problem. Therefore, for all these reasons and in order to increase the knowledge base on fully mixed tanks, in this thesis, a fully mixed storage tank will be used to store hot water and a second fully mixed tank will be used to store cold water. Although it is not very clear, in the studies where fully mixed tanks are used it is assumed that there is only one tank where hot and cold water are stored together. A novelty of this study is that two separate tanks will be used for storing the hot and cold water. As will be seen later, throughout this study the hot water storage tank (HST) will be studied in detail as this will be the main buffer between the heat production and the heat demand. The

cold water storage tank will be used mainly in order to keep the flow rate heading to the geothermal heat exchanger to a constant value. All this will be made clear in the following Chapters.

2.5 Summary

In this Chapter, district heating systems that utilize geothermal energy were reviewed. Heat is extracted from a fluid in the Earth's crust, the so-called geothermal fluid (usually brine), and it is distributed to consumers through a distribution network. The geothermal fluid can be distributed directly to the consumers, or its heat can be provided to a secondary clean water closed system. Usually the latter is the case, because the majority of geothermal fluids have corrosive properties and it is not possible to securely distribute them over large distances. Hence, usually, plate-type counter flow heat exchangers are used for this purpose. Additionally, in most cases, each building has its own secondary heat exchanger, in order to avoid high pressures in the distribution network.

The basic prerequisites for a successful geothermal district heating system are an available resource near to the heat consumption centre and a satisfactory heat density. An adequate temperature of the resource is crucial in order to meet the specific demands of the process in which the geothermal heat will be utilized. As already mentioned, the main processes are space heating and domestic hot water preparation. Developments in the technology of space heating can render many more geothermal wells suitable for space heating. Other uses, either separately or in an integrated way, can be for agricultural purposes, industrial processes, greenhouse heating, balneology, aquaculture, distillation, snow melting etc. Apart from the well temperature, an adequate continuous flow rate is a basic prerequisite. Estimation of these values can be undertaken in many ways, but both of these can only be assured when the drilling takes place, so a high risk is contained in these projects. The risk gets even higher as the cost of drilling increases. As noted in the corresponding section, the drilling is usually a large part of the investment cost. So, a careful estimation of the mass flow rate and the temperature of the well must be done in advance, in order to minimize the drilling risk. Additionally, subsidies are necessary in some cases in order to minimise that risk.

An available geothermal resource, with an adequate temperature and mass flow rate, is not useful if it is far away from the consumers. The transmission and distribution costs are

a large part of the investment cost, sometimes over 50%, so the less distance that the geothermal heat has to be transferred the better. Additionally, a high heat density area is desirable to maximize the income from the investment. The higher the heat density of the area, the higher the amount of heat sold. Additionally, a high rate of participation in the proposed area is also desirable. High participation can be achieved through education, so that people fully appreciate the advantages of geothermal energy. Of course, geothermal expertise is necessary to develop and promote geothermal district heating systems (Lunis, 1985). As already mentioned, initial choices are crucial for these systems. Maximization of heat sold together with maximization of income and maximization of geothermal energy utilized all need to be achieved for a successful geothermal district heating scheme.

Numerous studies have shown the advantages of geothermal energy. It can be concluded that geothermal energy, and therefore geothermal district heating systems, are cleaner than fossil fuels and in most cases cheaper or at least competitive. They result in better indoor air quality, and in countries with high penetration of geothermal energy use, e.g. Iceland, the consumers state that their quality of life has also increased since switching to geothermal energy (Jonasson and Thordarson, 2007). Geothermal energy is also a local energy source, which provides benefits to the local society, and also enhances energy independence.

Finally, with the development and implementation of EGS systems, many new fields are likely to become exploitable, thus substantially increase the geothermal resource base. The refurbishment of old buildings and the construction of new energy-efficient building can go hand in hand with the development of geothermal district heating networks, providing elegant means of achieving targets set to address environmental and energy supply problems.

3 SIZING OF A GEOTHERMAL DISTRICT HEATING SYSTEM

3.1 Introduction

In this Chapter, an integrated model for the sizing of a GDHS is developed. For this purpose, the geothermal data, the heat demand data throughout a whole year and the topology of the studied area are used as the basic inputs. The heat demand data should have a fine time discretization in order to get more accurate results. The output of this model is the complete sizing or dimensioning of the installation, including the number of geothermal wells, the sizing of the storage tank and the sizing of the pipelines amongst others. It should be noted that two components of the installation, i.e. the peak-up boilers and the cold storage tank, will be sized in Chapter 4 as some data from that algorithm are necessary for that purpose. Details on the other data used in this model are given in the next section.

The analysis of the installation is carried out on a daily basis. Therefore, a specific day has to be chosen as the design-day on which the sizing of the installation will be based. The basis of this selection as well as the details of all the mathematical modelling are given in section 3.2. Then, the results of this model are shown in section 3.3. The results are given for real heat demand data, but for arbitrary geothermal data and topology. This is because as the developed model, as well as the others described in this thesis, are generic models and it was not logical to study a geographically specific test-case. The heat demand data are real data however, rather than formulated or arbitrary data, as it was considered that only by using real data could realistic fluctuations be highlighted, and thus the model's advantages and disadvantages made clear. Furthermore, all the results in this thesis are given for three different cases of the design-day. More details on these cases are given in the results section. Finally, in section 3.4 a detailed discussion on the results is provided and in section 3.5 the highlights of this Chapter are summarised.

3.2 Mathematical Modelling

3.2.1 Inputs of the model

As mentioned before, the majority of the inputs of the model will be arbitrary numbers as the developed model is generic. Some of these inputs are initial estimations of some basic values of the installation and will be updated by the algorithm, while the rest are characteristics of the installation and remain constant. The inputs that are updated by the algorithm are the following:

- The ratio of the mass flow rate of working fluid (water) passing through the geothermal heat exchanger to the geothermal flow rate coming from the well (Rm_{init}).
- The thermal efficiency of the hot water storage tank ($\eta_{HST,init}$).
- Temperature drop in the substation ($\Delta T_{sub,init}$).
- Temperature drop per km of the hot transmission pipeline ($\Delta T_{tr.h,init}$).

It should be noted that where the index "*init"* is used, this refers to initial estimations and later in the algorithm the exact values will be calculated. On the other hand, the inputs that remain constant are the following:

- Heat demand data.
- Geothermal, ambient and soil temperatures.
- Mass flow rate of one geothermal well.
- Thicknesses, thermal and physical characteristics of the materials used for the hot water storage tank and the pipelines.
- Length of the transmission and distribution pipelines.
- Burial depth and distance between the pipelines.
- Maximum pressure and tensile strength of the pipelines.
- Absolute roughness of the pipeline.
- Thermal efficiency of the geothermal heat exchanger.
- Thermal efficiency of the substation (η_{sub}). This efficiency takes into account the heat losses of the distribution network as well as the end-user installations.
- Minimum temperature differences on the hot and the cold side of the geothermal heat exchanger.

- Mechanical efficiency of the pumps.
- Air velocity.
- Unit prices of heating and electricity as well as prices of the materials used.
- Interest rate
- Lifespan of the investment.
- Operating hours per year.

Furthermore, the temperature drop in the end of each distribution branch is also used as input. These temperature drops are considered constant throughout the whole study and it is assumed that the heat demand variations will be covered solely by the variation of the mass flow rate. This is one of the basic assumptions of this study. Additionally, for design purposes only, it is considered that the mass flow rate in each branch of the distribution network is equal to a specific proportion of the total mass flow rate on the transmission network. In Chapter 4, where the operation of the installation is studied, the real-time mass flow rates of each branch are taken into account.

Finally, the necessary properties of air and water are written as functions of temperature as the data used are point-data[1]. These data are written in an excel file in order to find the optimum kind of the fitting function. Then, the data are inserted in the algorithm and the best fit function is calculated within the algorithm. The calculated functions have a fitting coefficient of almost 100% and refer to temperatures between 0-120^{o}C, which is the main temperature range in the studied cases. Concerning air, the viscosity is found to be a second order polynomial against the temperature, while the Prandtl number and the thermal conductivity are found to be first order polynomials. Concerning the water, the density and the viscosity are found to be third order polynomials against the temperature, while the specific heat capacity is considered to be constant throughout the studied temperature range and equal to $4190\,\frac{J}{kg \cdot K}$.

It has to be made clear at this point that some variables are point values, while others refer to a whole time interval. In the first category, the temperatures and masses of stored water are included, while in the latter all the other mass exchanges are included. Obviously, the parameters in the first category have one more value than the latter, since the last point of the day is also included. For example, if the time discretization is 1 hour,

[1] http://www.engineeringtoolbox.com

then the first category of variables will have 25 values, while the latter will have just 24 time intervals. In the following, both variables will have the superscript i, but for the first kind of variables it will mean the point-value while for the second kind of variables it will mean the continuous value throughout the time interval i-i+1. The first kind of variables will be called 'points' while the latter are called time-intervals. This distinction will be made clearer in Chapter 4.

3.2.2 First calculation of the basic parameters

In this section, a first calculation of some basic parameters of the network is carried out. Initially, some values of the temperatures of the transmission network have to be calculated. This is done by applying some of the inputs described previously as initial estimations. The points of these temperatures on the transmission network are shown in Fig. 3.1 together with the associated masses. Since the temperature of the geothermal fluid is known, the inlet temperature of the transmission supply pipeline is calculated as:

$$T_{tr,s,i} = T_{G,h} - \Delta T_{h,GHE.,min} \tag{3.1}$$

Where:

$T_{tr,s,i}$ = Temperature in the inlet of the transmission supply pipeline (K)

$T_{G,h}$ = Temperature (hot) of the geothermal fluid (K)

$\Delta T_{h,GHE.,min}$ = Minimum temperature difference in the hot side of the G.H.E. (K)

Then, the temperature in the inlet of the hot water storage tank is calculated by the following equation, which takes into account the heat losses in the supply pipeline:

$$T_{HST,i} = T_{tr,s,i} - L_{tr,s,1} \cdot \Delta T_{tr,s,init} \tag{3.2}$$

Where:

$T_{HST,i}$ = Inlet temperature in the hot water storage tank (K)

$L_{tr,s,1}$ = Length of the transmission supply pipeline between the G.H.E. and the hot water storage tank (km)

$\Delta T_{tr,s,init}$ = Initial estimation of the temperature drop per unit of pipe length in the supply pipeline ($\frac{K}{km}$)

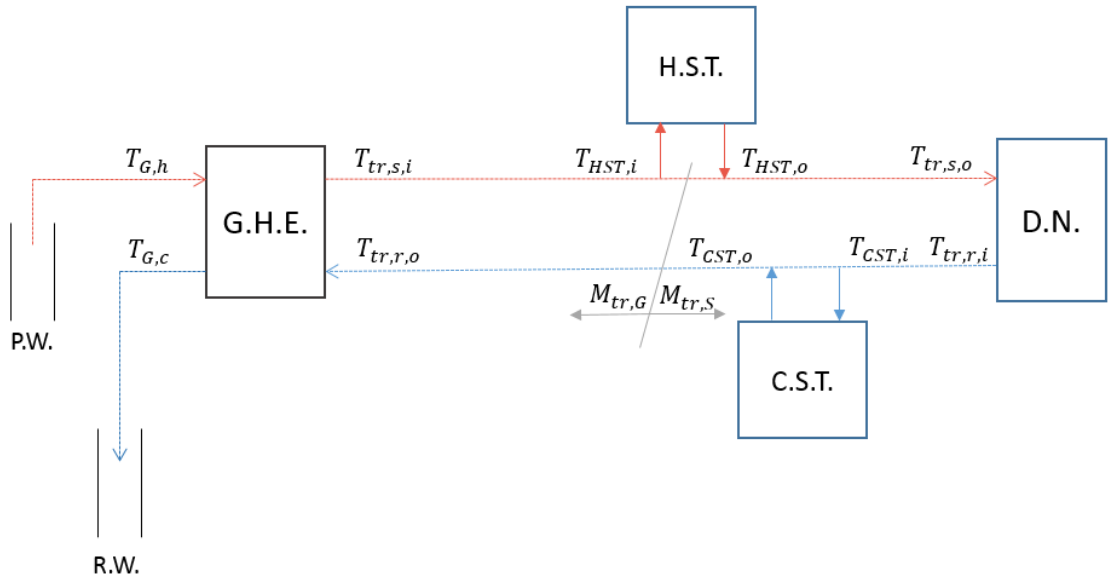

Figure 3.1 *Simplified scheme indicating the temperatures across the transmission pipelines (G.H.E. = Geothermal Heat Exchanger, D.N. = Distribution network, P.W. = Production Well, R.W. = Re-injection Well, H.S.T. = Hot water storage tank, C.S.T. = Cold water storage tank)*

The thermal efficiency of the hot water storage tank is calculated as the proportion of the energy exiting the tank to the energy entering the tank. These energies consist of the thermal energy of the water due to its temperature, and any other forms of energy, such as kinetic energy, are considered negligible. At this stage, the initial estimation of the efficiency will be used, and only the corresponding temperatures will be taken into account since the mass flow rates are not known yet. It should be noted that all these values of the temperatures across the transmission network will be later checked and re-calculated, if necessary, in an iterative loop. So, the temperature at the exit of the hot water storage tank is calculated as:

$$T_{HST,o} = \eta_{HST,init} \cdot \left(T_{HST,i} - T_a\right) + T_a \tag{3.3}$$

Where:

$T_{HST,o}$ = Outlet temperature from the hot water storage tank (K)

$\eta_{HST,init}$ = Initial estimation of the thermal efficiency of the hot water storage tank (Dimensionless)

T_a = Ambient temperature (K)

The outlet temperature of the transmission supply pipeline can be calculated by an equation similar to Eq. (3.2), but, it is proposed the hot water storage tank to be as close as

possible to the substation, so that the response in any change of the demand to be as quick as possible. Therefore, we get:

$$T_{tr,s,o} = T_{HST,o} \tag{3.4}$$

Where:

$T_{tr,s,o}$ = Outlet temperature from the supply transmission pipeline (K)

Afterwards, the inlet temperature of the transmission return pipeline is calculated through the temperature drop in the substation as:

$$T_{tr,r,i} = T_{tr,s,o} - \Delta T_{sub,init} \tag{3.5}$$

Where:

$T_{tr,r,i}$ = Inlet temperature of the return transmission pipeline (K)

$\Delta T_{sub,init}$ = Initial estimation of the temperature drop in the substation (K)

The rest of the temperatures in the transmission return pipeline are calculated with similar equations to those for temperatures in the transmission supply pipeline. More specifically, the following equations are used:

$$T_{CST,i} = T_{tr,r,i} \tag{3.6}$$

$$T_{CST,o} = \eta_{CST,init} \cdot \left(T_{CST,i} - T_a\right) + T_a \tag{3.7}$$

$$T_{tr,r,o} = T_{CST,o} - L_{tr,r,2} \cdot \Delta T_{tr,r,init} \tag{3.8}$$

Where:

$T_{CST,i}$ = Inlet temperature in the cold water storage tank (K)

$T_{CST,o}$ = Outlet temperature from the cold water storage tank (K)

$\eta_{CST,init}$ = Initial estimation of the thermal efficiency of the cold water storage tank (Dimensionless)

$T_{tr,r,o}$ = Outlet temperature from the return transmission pipeline (K)

$L_{tr,r,2}$ = Length of the return transmission pipeline between the cold water storage tank and the G.H.E. (km)

$\Delta T_{tr,r,init}$ = Initial estimation of the temperature drop per unit of pipe length for the return transmission pipeline ($\frac{K}{km}$)

The cold water storage tank is also proposed to be as close as possible to the substation, so that the mass flow rate in both pipelines of the transmission network will be the same. Equation (3.6) arises from this proposition. Furthermore, there are two basic differences in the calculations of the transmission return pipeline compared to the transmission supply pipeline. Firstly, the heat losses of the return pipeline are assumed, at this stage, to be half of the heat losses of the supply pipeline. As will be seen in section 3.2.6, the heat losses of the pipelines are proportional to the temperature difference between the water and the ambient. So, it is quite sensible to assume that the temperature in the return pipeline will be around the middle between the supply and the ambient temperatures and, therefore, the heat losses of the return pipeline to be half of the supply pipeline. Secondly, the heat losses of the cold storage tank are assumed to be half those of the hot storage tank. This is assumed on the same basis as the heat losses of the pipelines. As will also be seen in the results section, both the losses of the pipelines and of the hot water storage tank are quite small, so any wrong estimations in these factors will not cause an important general error. Nevertheless, if these assumptions are not very precise, the only problem that will arise is that the algorithm will need more time to converge (see section 3.2.7 also). So, these two assumptions are definitely acceptable from an engineering point of view.

Concerning the storage tanks, considering that their thermal efficiency can also be defined as $(1 - Losses)$, then the thermal efficiency of the cold storage tank is easily calculated as:

$$\eta_{CST,init} = 1 - \frac{1-\eta_{HST,init}}{2} \tag{3.9}$$

Since all the temperatures of the transmission network are known, the temperature drop of the geothermal water and its temperature at the exit of the geothermal heat exchanger can be, respectively, calculated as:

$$\Delta T_G = R_{m,init} \cdot \frac{T_{tr,s,i} - T_{tr,r,o}}{\eta_{GHE}} \tag{3.10}$$

$$T_{G,c} = T_{G,h} - \Delta T_G \tag{3.11}$$

Where:

ΔT_G = Temperature drop of the geothermal fluid (K)

$R_{m,init}$ = Initial estimation of the ratio of the mass flow rate on the transmission network on the right of the G.H.E. (or left of the hot water storage tank, which will be constant throughout the day as seen on the next) to the geothermal flow rate (Dimensionless)

η_{GHE} = Thermal efficiency of the G.H.E. (Dimensionless)

$T_{G,c}$ = Outlet (cold/ re-injection) temperature of the geothermal fluid (K)

Finally, the total thermal efficiency of the installation is calculated as:

$$\eta_{tot} = \eta_{sub,init} \cdot R_m \cdot \frac{T_{tr,s,o} - T_{tr,r,i}}{\Delta T_G} \tag{3.12}$$

Where:

η_{tot} = Total thermal efficiency of the installation (Dimensionless)

So, through Eqs. (3.1)-(3.12), a first calculation of the basic parameters of the network is carried out. All these values will be checked and updated, if necessary, in later stages of the algorithm. By knowing these initial values, the calculations in the following sections are now possible.

3.2.3 Sizing of the geothermal installation

A basic input of this model is the detailed heat demand over a year. The daily heat demand of each day can be easily calculated as the summary of the separate heat demands over this day.

$$DHD = \sum_{Day} HD^i \tag{3.13}$$

Where:

HD^i = Heat demand per time interval i of the studied day (kWh or J)

DHD = Daily heat demand of the studied day (kWh or J)

So, a list of the daily heat demands over the year of study can be calculated. Then, a specific day is chosen by the user as the design-day. In the design-day, all the heat demand will be covered by geothermal energy only with the assistance of the heat storage and no peak-up boilers will be used. Therefore, the total geothermal energy harvested throughout the day can be calculated by the following equation:

$$E_{G,D,D} = \frac{DHD_D}{\eta_{tot}} \tag{3.14}$$

Where:

$E_{G,D,D}$ = Geothermal energy harvested throughout the design-day (kWh or J)

DHD_D = Daily heat demand of the design-day (kWh or J)

In the above equation, the total efficiency calculated in Eq. (3.12) is used. Then, the above energy term has to be converted in the equivalent power term. This conversion depends on the units of the energy terms which depend on the units of the heat demand data. Commonly, these data are provided in kWh, and therefore the conversion in power terms (in W) is done by dividing the energy term by the hours of the day. For the sake of simplicity, in the rest of this study it is assumed that the heat demand data will be used in kWh.

$$\dot{Q}_{G,D} = \frac{E_{G,D,D} \cdot 1000}{24} \tag{3.15}$$

Where:

$\dot{Q}_{G,D}$ = Geothermal power of the design-day (W)

The term 1000 in the above equation is used to turn the units from kW to W. Since the geothermal power of the design-day is known, the necessary geothermal mass flow rate can be easily calculated as:

$$\dot{m}_{G,D} = \frac{\dot{Q}_{G,D}}{Cp_w \cdot \Delta T_G} \tag{3.16}$$

Where:

$\dot{m}_{G,D}$ = Geothermal mass flow rate on the design-day ($\frac{kg}{s}$)

Cp_w = Specific heat capacity of the geothermal fluid ($\frac{J}{kg \cdot K}$)

The temperature of the geothermal fluid is known from Eq. (3.10) and its specific heat capacity is also a known value. As mentioned in Chapter 2, the properties of the geothermal fluid are the same as those of pure water as the effect of minerals and non-condensable gases is negligible. Then, the necessary number of geothermal wells is calculated by dividing the geothermal mass flow rate by the mass flow rate of one well, which is a known value:

$$N_{wells} = \frac{\dot{m}_{G,D}}{\dot{m}_{well}} \tag{3.17}$$

Where:

N_{wells} = Number of geothermal wells

$\dot{m}_{well}$ = Mass flow rate of each geothermal well ($\frac{kg}{s}$)

Most probably, the above result will be a decimal number which, of course, does not have a physical meaning since it refers to the number of geothermal wells. Therefore, this result has to be rounded. The kind of rounding (floor, bottom or closest integer) depends on the user. In our case, it is selected to round this result to the closest integer, unless for the case where the result is less than 1 where it is rounded to 1. The final number of wells is given by the following equation:

$$\left.\begin{array}{c} If\ N_{wells} < 1: \\ Then:\ N_{wells} = 1 \\ Else:\ N_{wells} = round(N_{wells}) \end{array}\right\} \tag{3.18}$$

So, the final value of the geothermal mass flow rate and the geothermal power are calculated by Eqs. (3.16) and (3.17) properly re-arranged by taking into account the final value of the number of geothermal wells. Therefore, by applying Eqs. (3.13)-(3.18), the geothermal installation is sized and the geothermal power of the design-day are known. The geothermal power of the design-day, is also the maximum geothermal power that can be delivered at any time, since the maximum mass flow rate is used. For that reason, this value is also the geothermal capacity of the installation.

3.2.4 Sizing of the hot water storage tank

The sizing of the hot water storage tank as well as of the rest of the installation will be carried out for the design-day. In our approach, the mass flow rate to the left of the storage tank will be constant throughout the day, while the mass flow rate to the right of the storage tank will be variable according to the heat demand of each time interval (see Fig. 3.1). Since the heat demand is known per time interval, in the following all the calculations will be done for masses per interval (symbolised with M), instead of mass flow rates. So, the masses to the left and the right of the storage tank are calculated, respectively, as:

$$M_{tr,G} = M_{G,D} \cdot R_{m,init} \tag{3.19}$$

$$\left.\begin{array}{l} \boldsymbol{For}\ each\ time\ interval\ i: \\ M_{tr,S}^{i} = \frac{HD^{i}}{Cp_{w} \cdot (T_{tr,s,o} - T_{tr,r,i}) \cdot \eta_{sub}} \end{array}\right\} \tag{3.20}$$

Where:

$M_{tr,G}$ = Mass of water per time interval i in the left of the storage tank (kg)

$M_{tr,S}^{i}$ = Mass of water per time interval i in the right of the storage tank (kg)

Then, by the difference of these values, the masses of charged and discharged water in the storage tank can be calculated, respectively, as:

$$\left.\begin{array}{c} \boldsymbol{For}\ each\ time\ interval\ i: \\ \boldsymbol{If}\ \ M_{tr,G} - M_{tr,S}^{i} \geq 0: \\ \boldsymbol{Then}:\ M_{ch}^{i} = M_{tr,G} - M_{tr,S}^{i} \\ \boldsymbol{Else}:\ M_{ch}^{i} = 0 \end{array}\right\} \tag{3.21}$$

$$\left.\begin{array}{c} \boldsymbol{For}\ each\ time\ interval\ i: \\ \boldsymbol{If}\ \ M_{tr,G} - M_{tr,S}^{i} \geq 0: \\ \boldsymbol{Then}:\ M_{dis}^{i} = 0 \\ \boldsymbol{Else}:\ M_{dis}^{i} = M_{tr,S}^{i} - M_{tr,G} \end{array}\right\} \tag{3.22}$$

Where:

M_{ch}^{i} = Mass of charged water in the storage tank per time interval i (kg)

M_{dis}^{i} = Mass of discharged water from the storage tank per time interval i (kg)

Afterwards, the mass of stored water can be easily calculated by the following equation:

$$\left.\begin{array}{l} \boldsymbol{For}\ i \geq 1: \\ M_{st}^{i} = M_{ch}^{i} - M_{dis}^{i} - M_{st}^{i-1} \end{array}\right\} \quad (3.23)$$

Where:

M_{st}^{i} = Mass of stored water per time interval i (kg)

As a boundary condition in the above equation, it is considered that initially there is no stored water in the hot water storage tank.

$$M_{st}^{0} = 0 \quad (3.24)$$

Finally, the volume of the hot water storage tank will be calculated through the maximum value of stored water during the design-day as:

$$V_{HST} = \frac{\max(M_{st}^{i})}{\rho_{w}(T_{HST.i})} \cdot SF \quad (3.25)$$

Where:

V_{HST} = Volume of the hot water storage tank (m^3)

ρ_w = Density of water ($\frac{kg}{m^3}$)

SF = Security factor (Dimensionless)

In the above equation, the density of water is calculated for the temperature in the inlet of the water tank. This happens because the density of water decreases with increasing temperature. Therefore, the maximum temperature is used, in order to get the minimum density and, subsequently, the maximum storage volume. A security factor SF is also used in the above equation, which in our case is considered to be equal to 1.1. This allows errors of up to 10% during the sizing of the hot water storage tank. Finally, the thickness of the material of the storage tank, which is stainless steel in our case, is calculated through the API Standard 650 (Baker, 2009). This Standard has been originally produced for the sizing of oil storage tanks, but, it is assumed that the same methodology can be applied for water storage tanks without important errors.

In conclusion, by applying Eqs. (3.19)-(3.25), all the mass balances across the transmission network as well as the volume of the hot water storage tank are calculated.

3.2.5 Energy balance in the hot water storage tank

In this section, the methodology for the calculation of the temperature evolution within the hot water storage tank is developed. Furthermore, the calculation of the heat losses from the tank are explained and a definition of the thermal efficiency of the tank is given in order to get a more precise value of it.

For the calculation of the temperature evolution of the stored water, the energy conservation equation in the storage tank is applied within one time interval (similar equation applied by Kostowski and Skorek, 2005):

$$\frac{d(\rho_w \cdot Cp_w \cdot V_{w,st} \cdot T_{st})}{dt} = \dot{Q}_+^i - \dot{Q}_-^i - \dot{Q}_{loss}^i \quad (3.26)$$

Where:

$V_{w,st}$ = Volume of stored water between points i and i+1 (m^3)

T_{st}^i = Temperature of stored water in point i (K)

$\dot{Q}_+^i$, $\dot{Q}_-^i$, $\dot{Q}_{loss}^i$ = Heat surplus due to charging, heat shortage due to discharging and heat losses rate of the storage tank, respectively (W)

In the above equation, the left hand side denotes the accumulation term balanced by the heat surplus due to charging, the heat shortage due to discharging and the heat losses, respectively, in the right hand side. Furthermore, $V_{w,st}$ is the volume of stored water which changes within the time interval. As the specific heat capacity of water has been considered constant, and by replacing the density-times the volume of stored water equal to the mass of stored water, the left hand side of the above equation can be discretised as:

$$\frac{d(\rho_w \cdot Cp_w \cdot V_{w,st} \cdot T_{st})}{dt} = Cp_w \cdot \frac{d(\rho_w \cdot V_{w,st} \cdot T_{st})}{dt} = Cp_w \cdot \frac{d(M_{st} \cdot T_{st})}{dt} = Cp_w \cdot \frac{M_{st}^{i+1} \cdot T_{st}^{i+1} - M_{st}^i \cdot T_{st}^i}{\Delta t} \quad (3.27)$$

Then, both sides of the above equation are multiplied by the time interval (dt) in order to convert the power terms in energy terms which are easier to implement since, as mentioned before, the masses across the network are known and not the mass flow rates.

So, the heat surplus and shortage terms can be calculated by the following equations, respectively:

$$\dot{Q}_{+}^{i} = M_{ch}^{i} \cdot Cp_w \cdot \left(T_{HST,i} - T_a\right) \tag{3.28}$$

$$\dot{Q}_{-}^{i} = M_{dis}^{i} \cdot Cp_w \cdot \left(\frac{T_{st}^{i} + T_{st}^{i+1}}{2} - T_a\right) \tag{3.29}$$

The heat losses of the storage tank include the heat losses from the top, sides and base. Therefore, it is calculated by the following equation:

$$Q_{loss}^{i} = Q_{loss,top}^{i} + Q_{loss,side}^{i} + Q_{loss,base}^{i} \tag{3.30}$$

Where:

$Q_{loss,top}^{i}$, $Q_{loss,side}^{i}$, $Q_{loss,base}^{i}$ = Heat losses rate from the top, sides and base of the storage tank (W)

A basic assumption of this thesis is that the storage tank is considered to be fully mixed. This means that the temperature will be uniform within the tank and equal to the storage temperature (T_{st}). So, the inner surface of the tank will have a temperature equal to the storage temperature at each time-step. The heat losses from the top and sides of the tank occur due to conduction within the different layers of the tank and convection together with radiation to the ambient environment. On the other hand, the heat losses from the base occur due to conduction through the different layers of the tank and the underlying soil. The layers of the storage tank consist of stainless steel, insulation and a cover for the top and sides, and of stainless steel, insulation and a concrete base for the base.

For the calculation of the convective heat transfer coefficient in the top part of the tank, the equations for flow parallel to a horizontal body are used, while for the side part the equations for flow perpendicular to a cylindrical body are used. Therefore, the heat losses in the three parts of the tank can be calculated by the following sets of equations (Kakatsios, 2006), in which all the equations for each part of the tank are referred here as one equation (equation numbering in parentheses below):

- **Top (3.31):**

$$Q^i_{loss,top} = K^i_{top} \cdot A_{top} \cdot (\frac{T^{i+1}_{st}+T^i_{st}}{2} - T_a) \cdot \Delta t$$

$$A_{top} = \frac{\pi \cdot D^2_{st}}{4}$$

$$\frac{1}{K^i_{top}} = \sum_j \frac{t_j}{k_j} + \frac{1}{h^i_{c,top}} + \frac{1}{h^i_{r,\text{top}}}$$

$$h^i_{c,top} = Nu \cdot \frac{k_{air}}{D_{st}}$$

$$Re = \frac{u_{air} \cdot D_{st}}{\nu_{air}}$$

If $Re < 2 \cdot 10^5$:
Then: $Nu = 0.664 \cdot Pr^{1/3} \cdot Re^{1/2}$
Else-if $2 \cdot 10^5 < Re < 5 \cdot 10^5$:
Then: $Nu = 0.029 \cdot Pr^{0.43} \cdot Re^{0.8}$
Else: $Nu = 0.0296 \cdot Pr^{1/3} \cdot Re^{0.8}$

$$h^i_{r,top} = \varepsilon_{cv} \cdot \sigma \cdot ({T^i_{sur}}^2 + T^2_a) \cdot (T^i_{sur} + T_a)$$

- **Sides (3.32):**

$$Q^i_{loss,side} = K^i_{side} \cdot A_{side} \cdot (\frac{T^{i+1}_{st}+T^i_{st}}{2} - T_a) \cdot \Delta t$$

$$A_{side} = \pi \cdot D_{st} \cdot H_{st}$$

$$\frac{1}{K^i_{side}} = \sum_j \frac{t_j}{k_j} + \frac{1}{h^i_{c,\text{side}}} + \frac{1}{h^i_{r,\text{side}}}$$

$$h^i_{c,side} = Nu \cdot \frac{k_{air}}{D_{st}}$$

$$Re = \frac{u_{air} \cdot D_{st}}{\nu_{air}}$$

If $2 \cdot 10^4 < Re < 4 \cdot 10^5$:

Then: $Nu = 0.3 + \frac{0.62 \cdot Re^{1/2} \cdot Pr^{1/3}}{[1+\left(\frac{0.4}{Pr}\right)^{\frac{2}{3}}]^{1/4}} \cdot [1 + \left(\frac{Re}{282000}\right)^{\frac{1}{2}}]$

Else: $Nu = 0.3 + \frac{0.62 \cdot Re^{1/2} \cdot Pr^{1/3}}{[1+\left(\frac{0.4}{Pr}\right)^{\frac{2}{3}}]^{1/4}} \cdot [1 + \left(\frac{Re}{282000}\right)^{\frac{5}{8}}]^{4/5}$

$$h_{r,side}^{i} = \varepsilon_{cv} \cdot \sigma \cdot ({T_{sur}^{i}}^2 + T_a^2) \cdot (T_{sur}^{i} + T_a)$$

- **Base (3.33):**

$$Q_{loss,base}^{i} = K_{base} \cdot A_{base} \cdot (\frac{T_{st}^{i+1} + T_{st}^{i}}{2} - T_{soil}) \cdot \Delta t$$

$$A_{base} = \frac{\pi \cdot D_{st}^2}{4}$$

$$\frac{1}{K_{base}} = \sum_j \frac{t_j}{k_j}$$

Where:

$Q_{loss,top}^{i}$, $Q_{loss,side}^{i}$, $Q_{loss,base}^{i}$ = Heat losses from the top, side and base of the storage tank during time interval i (J)

K_{top}^{i}, K_{side}^{i}, K_{base} = Overall heat transfer coefficient of the top, side and base of the storage tank during time interval i ($\frac{W}{m^2 \cdot K}$)

A_{top}, A_{side}, A_{base} = Top, side and base area of the storage tank (m^2)

D_{st}, H_{st} = Diameter and height of the storage tank (m)

t_j = Thickness of each material j of the storage tank (m)

k_j = Thermal conductivity of each material j of the storage tank ($\frac{W}{m \cdot K}$)

$h_{c,top}^{i}$, $h_{c,side}^{i}$ = Convective heat transfer coefficient of the top and sides of the storage tank for each time interval i ($\frac{W}{m^2 \cdot K}$)

$h_{r,top}^{i}$, $h_{r,side}^{i}$ = Radiative heat transfer coefficient of the top and sides of the storage tank for each time interval I ($\frac{W}{m^2 \cdot K}$)

Nu, Re, Pr = Nusselt, Reynolds and Prandtl numbers, respectively (Dimensionless)

k_{air} = Thermal conductivity of air ($\frac{W}{m \cdot K}$)

u_{air} = Velocity of air ($\frac{m}{s}$)

ν_{air} = Kinematic viscosity of air ($\frac{m^2}{s}$)

ε_{cv} = Emissivity of the cover of the storage tank (Dimensionless)

σ = Stefan-Boltzmann constant for radiative heat transfer which is equal to $5.6703 \cdot 10^{-8} \frac{W}{m^2 \cdot K^4}$

T_{sur}^{i} = Temperature of the surface of the storage tank for each time interval i (K)

It can be seen from the above sets of equations that the average storage temperature between two time intervals is used in each case. In the cases of the top and sides of the tank, the calculations depend on the temperature of the stored water each time and on the outer surface temperature of the tank. Therefore, a temporal superscript is assigned in these calculations. In the case of the base of the tank, the heat transfer coefficient depends only on the materials of the tank and, therefore, it is constant all the time. Furthermore, some of the parameters used in the calculation of the convective heat transfer coefficients are temperature dependent. These parameters, i.e. the Prandtl number and the kinematic viscosity of air, are calculated for the average temperature between the ambient temperature and the outer surface temperature. The latter is also an unknown variable in the problem. For the solution of this problem, it is considered that the heat transfer due to conduction in the different layers of the tank is equal to the heat transfer due to convection and the radiation to the ambient environment. This is schematically illustrated in Figure 3.2, where a cross-sectional area of the side of the tank is shown together with the associated temperatures and heat flows.

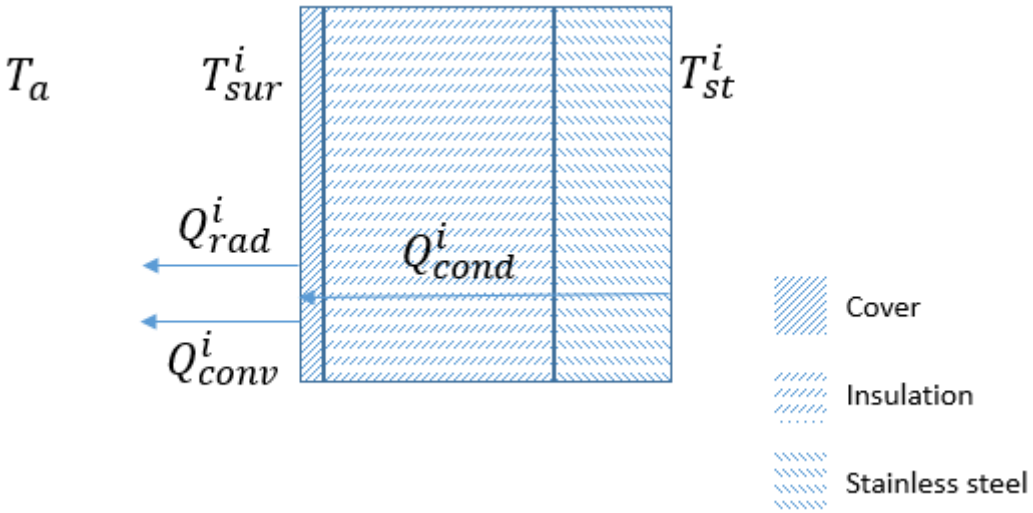

Figure 3.2 *Heat flows and temperatures through the sides of the tank*

By the equality between the heat flows, and by assuming that these are one-dimensional only, we get the following equation:

$$\dot{Q}^i_{cond} = \dot{Q}^i_{conv} + \dot{Q}^i_{rad} \rightarrow$$

$$\sum_j \frac{k_j}{t_j} \cdot (T^i_{st} - T^i_{sur}) = h^i_{conv} \cdot (T^i_{sur} - T_a) + \varepsilon_{cv} \cdot \sigma \cdot ({T^i_{sur}}^4 - T_a^4) \quad (3.34)$$

Where:

$\dot{Q}^i_{cond}$, $\dot{Q}^i_{conv}$, $\dot{Q}^i_{rad}$ = Conductive, convective and radiative heat transfer rates, respectively (W)

As already mentioned, the convective heat transfer coefficient is dependent on the surface temperature, so in order to solve the above equation an iterative method has to be applied. The above equation is valid both for the top and the sides of the tank. For the calculation of the convective heat transfer coefficient, the corresponding equations to (3.31) and (3.33) have to be used. So, for each time interval, the following steps are carried out for the calculation of the storage temperature:

1. An initial estimate for the surface temperature is made.
2. Equation (3.34) is solved iteratively till the real surface temperature is found.
3. The total heat transfer coefficients (K) for each part of the storage tank are calculated through the corresponding equations from the (3.31)-(3.33) sets of equations.

4. Finally, Eqs. (3.26)-(3.30) are applied for the calculation of the heat storage temperature in the next time step.

As a boundary condition for the above process, it is considered that the storage temperature at the beginning of the day is equal to the temperature of the water entering the tank.

$$T_{st}^{0} = T_{HST,i} \tag{3.35}$$

So, the evolution of the stored temperature within the design-day can be calculated. Then, a new value of the thermal efficiency of the storage tank can also be calculated. For that purpose, a new definition which takes into account the mass and temperature variations is defined. The new definition of the thermal efficiency of the storage tank is as follows:

$$\eta_{HST} = \frac{E_{w,out,total}}{E_{w,\text{in,total}}} = \frac{\sum_{i} M_{tr,S}^{i} \cdot Cp_{w} \cdot (T_{HST,o}^{i} - T_{a})}{\sum_{i} M_{tr,G} \cdot Cp_{w} \cdot (T_{HST,i} - T_{a})} \tag{3.36}$$

Where:

$E_{w,in,total}$, $E_{w,out,total}$ = Total energy of water entering and leaving the storage tank, respectively (J)

η_{HST} = Efficiency of the hot water storage tank (Dimensionless)

Figure 3.3 is provided for the better understanding of the above equation and the masses as well as the temperatures that are taken into account in it. As can be seen, the mass and the temperature that are used in the numerator are those after the mixing point with the water coming from the geothermal production, while the mass and the temperature used in the denominator are those before the splitting of the flow to the storage tank. In other words, the energy before the splitting and after the mixing of the flows are taken into account. The temperature of the water after the mixing point has been calculated initially in section 3.2.2, but in this point a more detailed calculation that takes into account the mixing with the water coming from the tank on each time interval can be carried out.

Therefore, by assuming no heat losses at the mixing point, the following energy conservation equation can be applied:

$$\left(M_{tr,G} - \frac{M_{ch}^{i}+M_{ch}^{i-1}}{2}\right)\cdot T_{HST,i} + \frac{M_{dis}^{i}+M_{dis}^{i-1}}{2}\cdot T_{st}^{i} = \left(M_{tr,G} - \frac{M_{ch}^{i}+M_{ch}^{i-1}}{2} + \frac{M_{dis}^{i}+M_{dis}^{i-1}}{2}\right)\cdot T_{HST,o}^{i} \quad (3.37)$$

The above equation was implemented from the middle of each time interval to the middle of the next time interval as the masses are continuous values, while the temperatures are point values as explained earlier. So, for each time interval, all the masses are known by Eqs. (3.19)-(3.22), while the stored temperature is known by the process explained previously. Therefore, by Eq. (3.37) the temperature after the mixing point can be calculated and, finally, by Eq. (3.36) the thermal efficiency of the hot water storage tank can also be calculated.

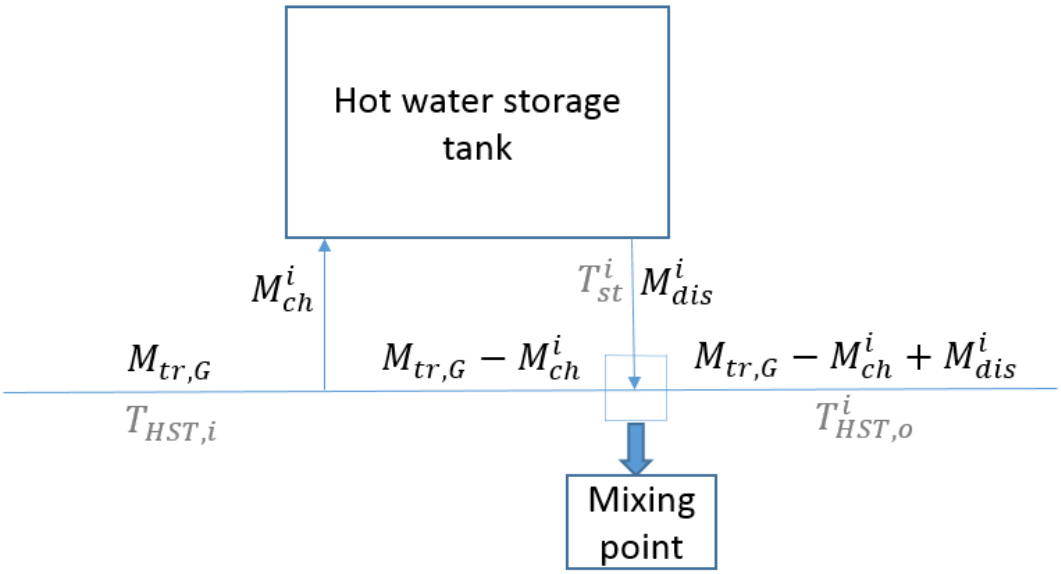

Figure 3.3 *A schematic illustration of the mass balances and temperatures associated with the hot water storage tank*

Concerning the cold water storage tank, it is still assumed that its losses will be still the half of those of the hot water storage tank, and therefore, its value will be calculated through Eq. (3.9), but now taking into account the new value of the thermal efficiency of the hot water storage tank.

3.2.6 Sizing of the pipelines of the network

For the sizing of the pipelines of the network, an optimization algorithm is assembled. The objective function is the total cost of the pipelines which consists of the capital cost, the cost of electricity used by the pumps to overcome the friction losses and the cost of the heat losses. The latter is not a direct cost, but an indirect monetary loss, so it is also taken into account in the total cost. The optimization parameters are the internal diameter of the pipeline and the thickness of the insulation. As a general approach, a system of double pre-insulated underground pipelines will be used. More details on this will be given on the calculation of the heat losses.

$$\mathcal{F}_{min}\left(D_{p,ex}, t_{ins}\right) = CC_p + C_{p.el} + C_{p,hl} \tag{3.38}$$

Where:

CC_p = Capital cost of pipelines (£)

$C_{p.el}$ = Cost of the electricity used by the pumps of the network to overcome the friction losses of the pipelines (£)

$C_{p,hl}$ = Cost of the heat losses of the pipelines (£)

3.2.6.1 Capital cost calculation

The capital cost of the pipelines consists of the cost of the materials, which are selected to be carbon steel and insulation, and the cost of welding. Knowing the dimensions of the pipelines, the total volume of each material can easily be calculated and, then, by multiplying the volume of each material with its unit cost, the cost of each material is calculated. Figure 3.4 shows a cross sectional area of one pipeline for the better understanding of the geometry. The cost of welding is usually a specific cost provided by the manufacturer of the pipelines. In our case, it is considered to have a specific price per weld and meter of diameter. Therefore, the capital cost of the pipelines is calculated by the following equations:

$$V_{c.steel} = \pi \cdot \frac{D_{p,o}^2 - D_{p,i}^2}{4} \cdot L_p \tag{3.39}$$

$$V_{ins} = \pi \cdot \frac{(D_{p.o} + 2 \cdot t_{p,ins})^2 - D_{p.o}^2}{4} \cdot L_p \tag{3.40}$$

$$CC_{mat} = CC_{c,steel} + CC_{ins} = V_{c,steel} \cdot C_{u,c,steel} + V_{ins} \cdot C_{u,ins} \quad (3.41)$$

$$CC_p = 2 \cdot (CC_{mat} + CC_{weld}) \quad (3.42)$$

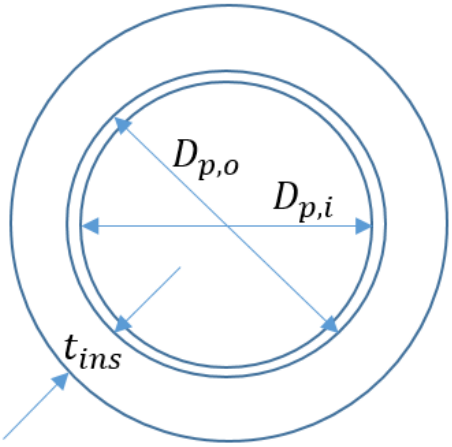

Figure 3.4 *Cross-sectional area of a pipeline with the associated dimensions*

Where:

$V_{c.steel}$, V_{ins} = Volume of carbon steel and insulation used in the pipelines, respectively (m^3)

$D_{p,i}$, $D_{p,o}$ = Inner and outer (not including the insulation) diameter of the pipelines, respectively (m)

L_p = Length of the pipelines (m)

$t_{p,ins}$ = Thickness of the insulation of the pipelines (m)

$C_{u,c,steel}$, $C_{u,ins}$ = Unit cost of carbon steel and insulation, respectively ($\frac{£}{m^3}$)

$CC_{c,steel}$, CC_{ins} = Capital cost of carbon steel and insulation, respectively (£)

CC_{mat}, CC_{weld} = Capital cost of material and welding, respectively (£)

CC_p = Total capital cost of pipelines (£)

In Eq. (3.42), the factor 2 is used in order to take into account both the supply and the return pipelines. In the previous equations, the only parameter that cannot be used in the optimization algorithm is the external diameter of the pipeline. This is calculated through the necessary thickness of the pipeline in order to sustain the internal pressure of the water. For the calculation of the minimum thickness of the pipeline, the following equation is used (Papantonis, 2006):

$$e_{min} = \frac{P_{max} \cdot D_{p,o}}{\sigma \cdot SF} + e_1 \quad (3.43)$$

Where:

P_{max} = Maximum pressure within the pipeline (Bar). Usually, it is equal to $5.5 Bar$.

$D_{p,o} = D_{pi} + 2 \cdot e_{min}$

σ = Tensile strength of the material. For carbon steel it is $1500 \frac{kp}{cm^2}$

SF = Security factor. In this case, it is set equal to 1.7.

e_1 = Corrosion allowance. It is set equal to 1mm.

Furthermore, for the sizing of the pipelines the standardized dimensions are used according to EN10220 (British Standards Institution, 2002). So, after the minimum thickness of the pipeline is calculated by Eq. (3.43), then the result is increased to the next higher value of standardised thickness. It should be noted that only standardised values of external diameters will be used throughout these calculations. Finally, by combining and replacing Eqs. (3.39)-(3.41) and (3.43) into Eq. (3.42), the latter can be written as a function of the internal diameter and the thickness of the insulation, which are the parameters of the initial optimization function.

3.2.6.2 Electrical cost calculation

For the calculation of the electrical cost used by the pumps to overcome the friction losses, it is necessary to calculate the friction losses first. The friction losses are assumed to consist of the linear losses only, which are calculated by the Darcy-Weisbach equation as follows:

$$\delta h_l = \lambda \cdot \frac{L_p}{D_{pi}} \cdot \frac{u_w^2}{2 \cdot g} \quad (3.44)$$

Where:

δh_l = Friction losses (m)

λ = Friction losses coefficient (Dimensionless)

u_w = Velocity of water ($\frac{m}{s}$)

In the above equation, λ is the friction losses coefficient which is calculated through iterations by the Colebrook equation:

$$\frac{1}{\sqrt{\lambda}} = -2 \cdot \log\left(\frac{2.51}{Re \cdot \sqrt{\lambda}} + \frac{\varepsilon_r}{3.71}\right) \quad (3.45)$$

The unknown variables in Eqs. (3.44)- (3.45) can be easily calculated by the following equations:

$$u_w = \frac{4 \cdot \dot{m}}{\rho_w \cdot \pi \cdot D_{p,i}^2} \quad (3.46)$$

$$Re = \frac{u_w \cdot D_{p,i}}{\nu_w} \quad (3.47)$$

$$\varepsilon_r = \frac{\varepsilon_a}{D_{p,i}} \quad (3.48)$$

Where:

ε_r = Relative roughness of the pipeline (Dimensionless)

ε_a = Absolute roughness of the pipeline (m)

In Eq. (3.48), ε_a is the absolute internal roughness of the pipeline, which is assumed to be equal to 0.1mm. The density and the kinematic viscosity of water are calculated for the average temperature of water within the pipeline. These temperatures will be known after the heat losses are calculated. Therefore, this part has to be combined with the next one also. But, since these temperatures are defined, then the friction losses can be written as a function of the internal diameter only through Eqs. (3.45)-(3.48). Afterwards, the electrical power that has to be provided to the pumps is given by the following equation:

$$P_{el} = \frac{\dot{m} \cdot g \cdot \delta h_l}{\eta_{pump}} \quad (3.49)$$

Where:

P_{el} = Electrical power of the pump (W)

η_{pump} = Mechanical efficiency of the pump (Dimensionless)

The mechanical efficiency of the pump (η_{pump}) is assumed to be equal to 70%. So, the cost of the electricity can be easily found by multiplying the electrical power of the pumps by the operating hours per year and by the unit cost of electricity. Additionally, since the capital cost refers to all the years of the investment, then the electrical cost has to be taken

into account for all the years of operation too. Eventually, the electrical cost used in the objective function is calculated as:

$$C_{p,el} = \sum_{i=1}^{i=N} \frac{P_{el} \cdot AOH \cdot C_{u,el}}{(1+\mathrm{IR})^{i}} \tag{3.50}$$

Where:

$C_{p,el}$ = Total cost of electricity used by the pumps (£)

$C_{u,el}$ = Unit cost of electricity ($\frac{£}{kWh}$)

AOH = Annual operating hours of the installation

IR = Interest rate (Dimensionless)

In the above equation, the factor 2 is not used as it is in Eq. (3.42) because the electrical cost is not the same between the two pipelines. This happens because the temperatures within the pipelines are different and, subsequently, the properties of water are different and, finally, the electrical cost is different. So, in the final objective function, the electrical cost of each pipeline has to be taken into account separately.

With the process explained in this section, it was shown that through Eqs. (3.44)-(3.49), the electrical cost of the pumps can be expressed as a function of the internal diameter only. Therefore, this part of the total cost can be replaced in the initial objective function.

3.2.6.3 Cost of heat losses

In order to calculate the cost of the heat losses, first the heat losses have to be calculated. For this purpose, a system of double pre-insulated underground pipelines is considered (see Fig. 3.5). As a beginning, the equations summarised by Bohm (2000) will be used.

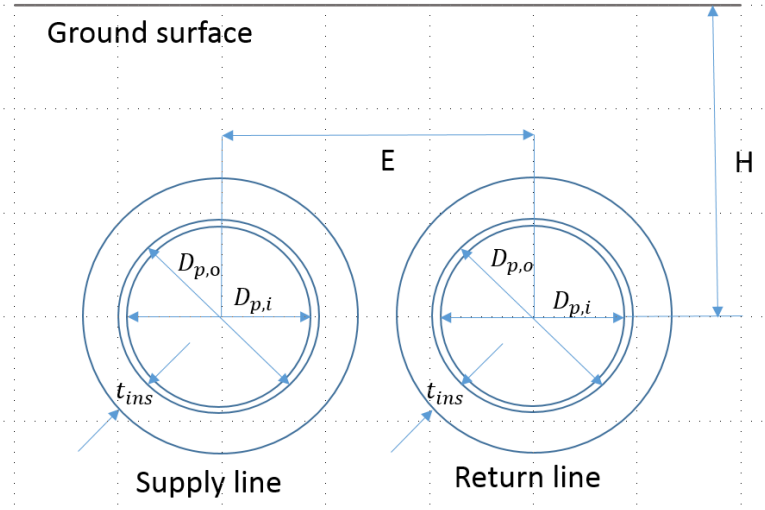

Figure 3.5 *Studied system of double pre-insulated underground pipes*

These equations are the following:

$$\dot{q}_s = (U_1 - U_2) \cdot \left(\frac{T_s+T_r}{2} - T_{soil}\right) + (U_1 + U_2) \cdot \left(\frac{T_s-T_r}{2}\right) \quad (3.51)$$

$$\dot{q}_r = (U_1 - U_2) \cdot \left(\frac{T_s+T_r}{2} - T_{soil}\right) - (U_1 + U_2) \cdot \left(\frac{T_s-T_r}{2}\right) \quad (3.52)$$

$$U_1 = \frac{R_g+R_i}{(R_g+R_i)^2-R_n^2} \quad (3.53)$$

$$U_2 = \frac{R_n}{(R_g+R_i)^2-R_n^2} \quad (3.54)$$

$$R_i = \frac{1}{2\cdot\pi\cdot k_{ins}} \cdot \ln\left(\frac{D_{ins}}{D_{p,o}}\right) + \frac{1}{2\cdot\pi\cdot k_p} \cdot \ln\left(\frac{D_{p,o}}{D_{p.i}}\right) \quad (3.55)$$

$$R_g = \frac{1}{2\cdot\pi\cdot k_{soil}} \cdot \left[\ln\left(\frac{4\cdot\acute{H}}{D_{ins}}\right) - \frac{S_n}{S_d}\right] \quad (3.56)$$

$$R_n = \frac{1}{4\cdot\pi\cdot k_{soil}} \cdot \ln\left[1 + \left(\frac{2\cdot\acute{H}}{E}\right)^2\right] \quad (3.57)$$

$$S_n = \left(\frac{D_{ins}}{2\cdot E}\right)^2 + \left(\frac{D_{ins}}{4\cdot\acute{H}}\right)^2 + \frac{D_{ins}^2}{4\cdot(4\cdot\acute{H}^2+E^2)} \quad (3.58)$$

$$S_d = \frac{1+\beta}{1-\beta} - \left(\frac{D_{ins}}{2\cdot E}\right)^2 \quad (3.59)$$

$$\beta = \frac{k_{soil}}{k_{ins}} \cdot \ln(\frac{D_{ins}}{D_{p,o}}) \quad (3.60)$$

$$D_{ins} = D_{p,o} + 2 \cdot t_{p,ins} \quad (3.61)$$

$$D_{p,o} = D_{p,i} + 2 \cdot e_p \quad (3.62)$$

$$\acute{H} = H + \frac{k_{soil}}{h_{gs}} \quad (3.63)$$

Where:

$\dot{q}_s$, $\dot{q}_r$ = Heat losses rate of the supply and return pipelines, respectively (W)

k_{ins}, k_p, k_{soil} = Thermal conductivities of the insulation, the material of the pipelines and the soil, respectively ($\frac{W}{m \cdot K}$)

T_{soil} = Soil temperature (K)

D_{ins} = Total diameter of the pipelines, including the insulation (m)

e_p = Thickness of the material of the pipeline (m)

E, H = Distance between the pipelines and their burial depth, respectively (m)

Equation (3.63) is used to take into account the convection and radiation occurring due to the ground surface. In this equation, $\acute{H}$ is the equivalent depth and h_{gs} is the convective heat transfer coefficient in the ground surface which also takes into account the radiation. According to Kvisgaard and Hadvig (1980, as cited in Bohm, 2000), the value of h_{gs} can be considered constant and equal to $14.6 \frac{W}{m^2 \cdot K}$.

In general, Eqs. (3.51)-(3.63) are defined for a system of double pre-insulated underground pipelines with a unique temperature across their length (T_s for the supply pipeline and T_r for the return pipeline). But, in our case the temperature drop has to be taken into account. For this purpose, each pipeline will be discretised in space and in each element the temperature will be considered to decrease linearly (see Fig. 3.6). Then, the average temperature in each element of each pipeline will be used in Eqs. (3.51)-(3.63).

For each spatial element:

$$T_s = \frac{T_s^j + T_s^{j+1}}{2} \quad (3.64)$$

$$T_r = \frac{T_r^j + T_r^{j+1}}{2} \quad (3.65)$$

It should be noted that Eqs. (3.55)-(3.57) refer to 1 meter of pipeline, therefore in order to take into account the space discretization each of these variables has to be divided by the value of the space discretization in meters.

Then, the following definition of the heat losses will also be used in each spatial element of the pipelines:

$$\dot{q}_s = \dot{m}_p \cdot Cp_w \cdot (T_s^j - T_s^{j+1}) \quad (3.66)$$

$$\dot{q}_r = \dot{m}_p \cdot Cp_w \cdot (T_r^{j+1} - T_r^j) \quad (3.67)$$

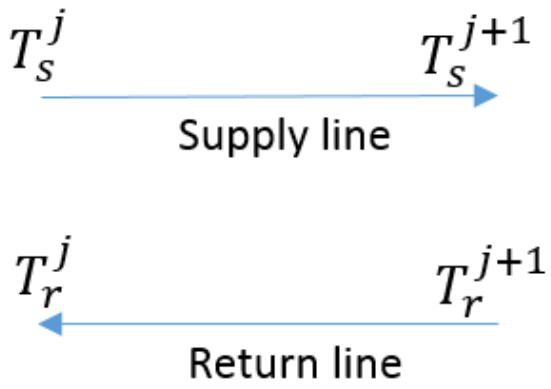

Figure 3.6 *Inlet and outlet temperatures in each spatial element of the pipelines*

Therefore, by combining Eqs. (3.51)-(3.65) with Eqs. (3.66) and (3.67), we end up in the following two equations for each spatial element:

$$A_1 \cdot T_s^j + A_2 \cdot T_s^{j+1} + A_3 \cdot T_r^j + A_3 \cdot T_r^{j+1} = A_4 \quad (3.68)$$

$$A_3 \cdot T_s^j + A_3 \cdot T_s^{j+1} + A_2 \cdot T_r^j + A_1 \cdot T_r^{j+1} = A_4 \quad (3.69)$$

Where:

$A_1 = A_5 - A_6 - A_3$

$A_2 = -A_5 - A_6 - A_3$

$A_3 = \frac{U_2}{2}$

$$A_4 = -A_7 \cdot T_{soil}$$
$$A_5 = \dot{m}_p \cdot Cp_w$$
$$A_6 = \frac{U_1 - U_2}{2}$$
$$A_7 = U_1 - U_2$$

Where all the variables have been defined previously.

If the pipelines are discretised in N spatial elements, then the unknown variables are $2N + 2$ in total. Furthermore, by writing down the Eqs. (3.68) and (3.69) for each element, we get $2N$ equations. In order to solve this problem the following two considerations are made:

- The inlet temperature in the supply line (T_s^0) will be a known value.
- The temperature difference in the boundary of the pipelines ($T_s^N - T_r^N$) will also be a known value.

So, with these considerations the previous system of $2N$ equations with $2N + 2$ variables, is transformed in a system of $2N + 1$ equations with $2N + 1$ variables. Therefore, this system can be solved in order to provide the temperatures along the lengths of both pipelines.

It should be noted that the process developed up to now in this section can provide the temperature distribution over a system of double pre-insulated underground pipelines if the inlet temperature of the supply pipeline and the temperature difference between the ends of the pipelines are known. In the studied system, the temperatures over the transmission network have been estimated up to now, while the temperature drops between the ends of the distribution network are known. In the next section, the method for applying integration of this algorithm to the whole system will be explained.

The heat losses of each pair of pipelines can, then, be easily calculated as the summary of the heat losses of the supply and return pipeline:

$$q_{hl,pp} = \sum_{s,r} q_{hl,p} = \sum_{s,r} \dot{m}_p \cdot Cp_w \cdot (T_{p,in} - T_{p,out}) \tag{3.70}$$

Where:

$q_{hl,pp}$ = Heat losses of a pair of pipelines (J)

$q_{hl,p}$ = Heat losses of one pipeline (J)

$\dot{m}_p$ = Mass flow rate through one pipeline ($\frac{kg}{s}$)

$T_{p,in}$, $T_{p,out}$ = Inlet and outlet temperature in one pipeline, respectively (K)

In the above equation, the indexes s and r denote the supply and return pipelines. Finally, the cost of the heat losses can be easily calculated by multiplying the total heat losses with the unit cost of heating. Similarly, all the years of operation have to be taken into account before the heat losses cost can be used in the objective function. Therefore, the final equation for the heat losses cost is the following:

$$C_{p,hl} = \sum_{i=1}^{i=N} \frac{\sum_{pipes} q_{hl,pp} \cdot C_{h,u}}{(1+IR)^i} \tag{3.71}$$

Where:

$C_{p,hl}$ = Total cost of heat losses (£)

$C_{u.h}$ = Unit cost of heat losses ($\frac{£}{kWh}$)

In conclusion, by applying Eqs. (3.68) and (3.69) together with the boundary conditions and the process explained in this section, the temperatures across a pair of pipelines can be calculated. Then, by applying Eqs. (3.70) and (3.71) the cost of the heat losses of the pipelines are calculated for a given set of dimensions.

3.2.6.4 Integrated algorithm for the sizing of the pipelines

As mentioned earlier, standardised values of internal diameters of the pipeline will be used according to EN10220. Concerning the thickness of the insulation, discrete values of the thickness from 1 to 30cm will be used with a discretization of 1cm. Therefore, both the internal diameter and the thickness of the insulation (which are the optimization parameters) will get only discrete values.

For the optimum sizing of all the pipelines of the network, the following process is followed:

a) For each branch of the distribution network it is considered that the inlet temperature in the supply pipeline is equal to the outlet temperature of the transmission supply pipeline ($T_{d,s,i}^{j} = T_{tr,h,o}$). The latter is calculated in section 3.2.2.

b) **For** each combination of discrete sizes of internal diameter ($D_{p,i}$) and thickness of insulation ($t_{p,ins}$) and **for** each branch of the distribution network:

   1. Equation (3.43) is used to calculate the thickness of the pipelines or their external diameter ($D_{p,o}$).
   2. The process of section 3.2.6.3 is applied for the calculation of the temperatures and the cost of the heat losses of each branch of the distribution network.
   3. Since the temperatures along the pipelines are known, the process explained in section 3.2.6.2 is applied to calculate the electrical cost of each pipeline.
   4. The capital cost is calculated through the process explained in section 3.2.6.1.
   5. These costs are added together.

c) The dimensions for which the total cost is minimized are identified. These are the optimum dimension for each branch of the distribution network. The temperatures across each branch of the distribution network are also known.

d) Since the outlet temperature from each return pipeline of the distribution network is known, an energy conservation equation is applied in the mixing point connecting the end of the cold distribution pipeline with the beginning of the cold transmission pipeline in order to find a new value of the inlet temperature of the return transmission pipeline ($T_{tr,c,i}$).

e) Eqs. (3.3) and (3.4) are applied using the new value of the thermal efficiency of the hot water storage tank (Eq. 3.36), in order to find a new value of the temperature at the inlet of the hot water storage tank ($T_{st,h,i}$). In the same way, a new value of the temperature at the exit of the cold water storage tank ($T_{st,c,o}$) is calculated through Eqs. (3.6)-(3.7) and (3.9).

f) As mentioned in section 3.2.2, both the storage tanks are in the boundary of the transmission network. Therefore, it can be considered that the temperature drop in the boundary of the transmission network is equal to $T_{st,h,i} - T_{st,c,o}$. The inlet temperature of the supply line of the transmission network ($T_{tr,h,i}$) is calculated in section 3.2.2 and will remain constant throughout the calculations as it depends only on the temperature difference in the hot side of the geothermal heat exchanger.

g) The process explained in step b is now applied in the transmission network. Its optimum dimensions as well as new values of $T_{st,h,i}$ and $T_{st,c,o}$ are now known.
h) Equations (3.26)-(3.37) are applied in order to determine a new value of the outlet temperature of the transmission supply pipeline ($T_{tr,h,o}$).
i) **If** this value is different that the value calculated in section 3.2.2, then steps a-h are repeated till convergence is achieved.

Eventually, through this process the optimum dimensions of both the transmission and distribution network will be known. Furthermore, the capital cost of each pair of pipelines will be known as well as new values of the temperatures across the network. So, all the temperatures of the transmission network will have updated values compared to those calculated in section 3.2.2, apart from the inlet temperature in the supply pipeline ($T_{tr,h,i}$), which is constant, as mentioned before.

3.2.7 Integrated model

By applying the methodology explained in sections 3.2.2-3.2.6, the sizing of the installation can be carried out if some initial estimations are done. But, in the end of section 3.2.6, the temperatures across the transmission network have an updated value. On the other hand, these temperatures have been calculated through the initial estimations in section 3.2.2 and based on these values the rest of the calculations, including those on section 3.2.6, were carried out. Therefore, all the calculations have to be done again till convergence achieved. All the values that had the suffix *init* (initial estimations) and a renewed value was calculated, the renewed value will be used in the new calculations.

For better supervision of the process, the parts of the methodology are separated in different functions in which one uses the results from the previous and feeds the next function. The whole programming in Python (Python Software Foundation, 2016) was also carried out in this way. Each function will contain several equations of those shown up to now. In the following, the short name of each function is shown in bold letters, the equations used in the parenthesis and the use of each function in brackets. So, the functions used are the following:

- **TFC** (3.1-3.8) "First calculations of the temperatures of the transmission network"

- **TFF** (3.9-3.12) "Thermal efficiency of the installation"
- **GS** (3.13-3.18) "Sizing of the geothermal installation"
- **HST** (3.19-3.25) "Sizing of the hot water storage tank"
- **THL** (3.26-3.37) "Hot storage tank heat losses"
- **PS** (3.38-3.71) "Sizing of the pipelines"

So, the steps that are followed in the integrated model for the sizing of the installation are the following:

1. **TFC** function is used for the first calculation of the temperatures of the transmission network.
2. Since the temperatures of the network are known, T**FF** function is used for the calculation of the thermal efficiency of the installation as well as of the thermal efficiency of the hot water storage tank.
3. By having calculated a first value of the thermal efficiency of the installation, then **GS** function is applied for the sizing of the geothermal installation.
4. The mass flow rates across the network are known through step 3, therefore **HST** function is implemented for the sizing of the hot water storage tank.
5. **THL** function is applied for the calculation of the heat losses of the storage tank. A new thermal efficiency of the hot water storage tank is found.
6. **PS** function is used for the optimum sizing of all the pipelines of the network. New values of the temperatures across the whole network are found.
7. If the thermal efficiency of the hot water storage tank found in step 5 and the temperatures of the transmission network found in step 6 are different from those in steps 2 and 1, respectively, then the new values are implemented and steps 2-6 are repeated till convergence of the problem. The convergence limits used are 10^{-12} for the thermal efficiency and 10^{-6} for the temperatures.

Eventually, when the problem converges, the whole sizing of the installation will be known. More details on the outputs of the algorithm will be given in section 3.2.9.

3.2.8 Possible sources of error

Three main sources of error can arise from the results of the above explained algorithm. Firstly, the mass of stored water in the hot water storage tank can get negative values. This is unphysical, and it basically means that more hot water is needed in the network, which subsequently leads to the use of the peak-up boilers. This also comes in contrast with the initial concept of the design-day for which it was stated that all the heat demand will be covered by geothermal energy only. Secondly, the outlet temperature of the return transmission pipeline ($T_{tr,r,o}$) can get higher values than the re-injection temperature of the geothermal water ($T_{G,c}$). In other words, the temperature difference on the cold side of the geothermal heat exchanger ($\Delta T_{c,GHE}$) can get negative values. This is of course something unacceptable as in a heat exchanger the temperatures of the heating fluid in the inlet and the outlet have to be higher than the corresponding temperatures of the heated fluid. Thirdly, the temperature that arrives in the end-users might have a temperature lower than the needs of the end-users. For the sake of simplicity, a minimum value of the outlet temperature of the supply transmission pipeline ($T_{tr,s,o,min}$) is defined, which is estimated through the minimum end-users requirements and the estimated heat losses. So, the third source of error is defined as the case in which the value of the outlet temperature of the return transmission pipeline is found to be lower than the minimum acceptable value.

The first source of error cannot be solved automatically in the developed code as this error is due to the fluctuation of the heat demand within the specific day. For example, two days can have the same daily heat demand, yet differ greatly in the degree of variation of the heat demand within the day. So, in one case the mass of stored water can be always positive or zero while in the other case negative values can occur. If this problem arises, the only solution is to select the day with the closest daily heat demand to that of the initially selected design-day as the new design-day. If this does not work, then this process has to be repeated. It was shown that, in the worst case, three selections of the design-day are enough. Therefore, this source of error can be relatively easily solved. The only disadvantage is the higher computational time needed, but this is negligible for the timescale of the planning or research for this type of installation.

The second and the third sources of error occur due to the physics of the problem. Two variables of the problem that are initially estimated and kept constant throughout the whole algorithm can have a big effect on its physics. These variables are the temperature

difference on the hot side of the geothermal heat exchanger ($\Delta T_{h,GHE}$) and the ratio of the mass flow rate on the left of the storage tank to the geothermal mass flow rate (R_m). For the first variable, its minimum value which is provided by the manufacturer, while for the second variable an estimation of the user are used in the developed algorithm. The temperature difference can increase above this minimum value and the ratio of the mass flow rates can either increase or decrease compared to the initial estimation. In general, it is desired to keep the ratio of the mass flow rates in the maximum possible value as, in this way, more geothermal energy is harvested (see Eq. 3.10).

A loop that checks if any of these two sources of error arise in the end of the algorithm was built. The main scope of this loop was to fix the values of the variables that might present an error by adjusting the aforementioned variables that affect them. Furthermore, the cost of the pipelines and the number of wells should be kept in the minimum possible value. A preliminary analysis (Appendix A) has shown the following:

- As the temperature difference in the hot side of the geothermal heat exchanger ($\Delta T_{h,GHE}$) increases, the temperature difference in the cold side of the geothermal heat exchanged ($\Delta T_{c,GHE}$) increases, the outlet temperature of the supply transmission pipeline ($T_{tr,s,o}$) decreases, the capital cost of the pipeline is variable and mainly decreases after a steep initial increase, and finally, the number of wells is not affected significantly.
- As the ratio of the mass flow rates (R_m) increases, the temperature difference on the cold side of the geothermal heat exchanger ($\Delta T_{c,GHE}$) decreases, the outlet temperature of the supply transmission pipeline ($T_{tr,s,o}$) is almost constant, the capital cost of the pipelines presents small and stochastic variations and the number of wells decreases.

Initially, the algorithm is run with the initial estimations of the temperature difference and the ratio of the mass flow rates. If any of the errors arise, then by taking into account the above observations, the following if-loop of four different cases is used for the solution of the errors running the algorithm as many times as required by the following conditions:

- **If** $\Delta T_{c,GHE} < \Delta T_{c,GHE,min}$ **and** $T_{tr,s,o} > T_{tr,s,o,min}$:

  Then:

  While $T_{tr,s,o} > T_{tr,s,o,min}$: $\Delta T_{h,GHE} \uparrow$

  If (still) $\Delta T_{c,GHE} < \Delta T_{c,GHE,min}$:

  Then:

  While $\Delta T_{c,GHE} < \Delta T_{c,GHE,min}$: $R_m \downarrow$
- **If** $\Delta T_{c,GHE} < \Delta T_{c,GHE,min}$ **and** $T_{tr,s,o} < T_{tr,s,o,min}$:

  Then: Assistance by a heat pump is needed
- **If** $\Delta T_{c,GHE} > \Delta T_{c,GHE,min}$ **and** $T_{tr,s,o} < T_{tr,s,o,min}$:

  Then:

  While $\Delta T_{c,GHE} > \Delta T_{c,GHE,min}$: $\Delta T_{h,GHE} \downarrow$

  If (still) $T_{tr,s,o} < T_{tr,s,o,min}$:

  Then: Assistance by a heat pump is needed
- **If** $\Delta T_{c,GHE} > \Delta T_{c,GHE,min}$ **and** $T_{tr,s,o} > T_{tr,s,o,min}$:

  Then:

  While $\Delta T_{c,GHE} > \Delta T_{c,GHE,min}$ **and** $T_{tr,s,o} > T_{tr,s,o,min}$: $R_m \uparrow$

It should be mentioned that the fourth case of the above if-loop is not an error of the algorithm, but by increasing the ratio of the mass flow rates, then the economically optimum solution is found. This happens because by increasing the ratio of the mass flow rates the number of wells, on the one hand, decreases with a subsequent big decrease of the total cost, and the cost of the pipelines changes stochastically. But, it can be definitely said that the reduction in the cost due to less wells being needed is much greater than any change caused by the cost of the pipelines. It is assumed that the other costs of the installation are not affected importantly by this change. Therefore, the last case represents a kind of economical optimization when there are no errors caused by the initial estimations.

By observing the above four-case if-loop, it can be observed that in some cases the use of a heat pump is needed. This denotes mainly that the specific geothermal potential is unavailable to provide with heat the specific end-users. Consequently, the use of a heat pump to lift of the temperature to the desired level is needed. This case is out of the scope of this thesis and will not be studied further.

In general, it can be intuitively stated that if the temperature of the geothermal fluid is some degrees higher than the needs of the end-users, then by the proper adjustment of the two variables shown above, the algorithm can work and the installation can be properly sized. This was also shown in the studied case. More details on this will be given in the results section. An aspect that requires careful consideration is the case where some end-users require a much higher temperature than the others. In a case like that, then these users either cannot be provided with heat or a heat pump should be implemented only for them. So, the above if-loop could be applied with the condition of the temperature for the average users and, then, a heat pump could be applied to those users which require a higher temperature. Finally, another solution would be the rejection of a part of the load as an error would also indicate that the whole load cannot be covered in this way. The latter is a rare case as, normally, this would have been identified in the very early stages of the design of the installation.

To summarise, in this section some possible sources of errors that can arise during the application of the developed algorithm have been identified. Then, a solution for each of these errors was presented and it was shown that, in most of the cases, either with the selection of a day with a very similar heat demand as the design-day or with the proper adjustment of some input variables the problem can be solved. Usually, the problem will not be solved when the temperature of the geothermal fluid is lower or just a bit higher than the needs of the end-users or when some end-users have much higher temperature needs. In these cases, the use of a heat pump is required either for a part or for all the users, but normally, this problem will have been identified in the very first design stages, so the developed algorithm would provide a solution in the vast majority of the cases.

3.2.9 Outputs of the model

In this section, a collective mapping of the outputs of this model will be given. In section 3.2.1, the inputs of the model were explained and in sections 3.2.2-3.2.8, the developed algorithm was explained in detail. For better understanding, the outputs divided in the following groups:

- **Main results:** Necessary number of geothermal wells; Volume and dimensions of the hot water storage tank; Temperature drop of the geothermal fluid; Total thermal efficiency of the installation; Geothermal capacity; Mass flow rate on

the left of the storage tanks; and Ratio of the mass flow rate on the left of the storage tank to the geothermal mass flow rate.

- **Transmission network data:** Design temperatures (Inlet/outlet of supply and return pipelines); Inner diameter; Outer diameter; Thickness of insulation; Capital Cost.
- **Distribution network data:** For each branch of the distribution network, the same data as for the transmission network are provided.
- Plots of the evolution of the mass and temperature of the stored water.
- Design-day heat demand.

3.3 Results

In this section, the results of the above explained algorithm are presented. As mentioned earlier, the heat demand data used are real data, while the rest of the inputs are arbitrary data. The heat demand data were provided by the Estates and Buildings office of the University of Glasgow and refer to some buildings managed by the University. The annual heat demand is around 38500MWh with an average and a peak demand of around 4.4 and 14MW, respectively. The time discretization of the data is 30 minutes. A plot of the data for the year of study can be seen in Fig. 3.7. Some other basic input data are shown in Table 3.1.

As already mentioned, throughout the developed model a specific day is chosen as the design-day and based on this day, the sizing of the whole installation will be carried out. In our case, three different and very discrete days have been chosen as the design-day. More specifically, the chosen days are those that their daily heat demand corresponds to the 25^{th}-, 50^{th}- and 75^{th}- centile of the daily heat demands of the whole year. For the sake of simplicity, these cases will be called 25%ile, 50%ile and 75%ile in the rest of this study, respectively. In Fig. 3.8, the curve that sorts the daily heat demands from the lower to the higher in a percentage base is shown. The chosen days are those which their daily heat demand corresponds to the 25, 50 and 75% of this figure. So, three very different cases of sizing have been selected and will be studied.

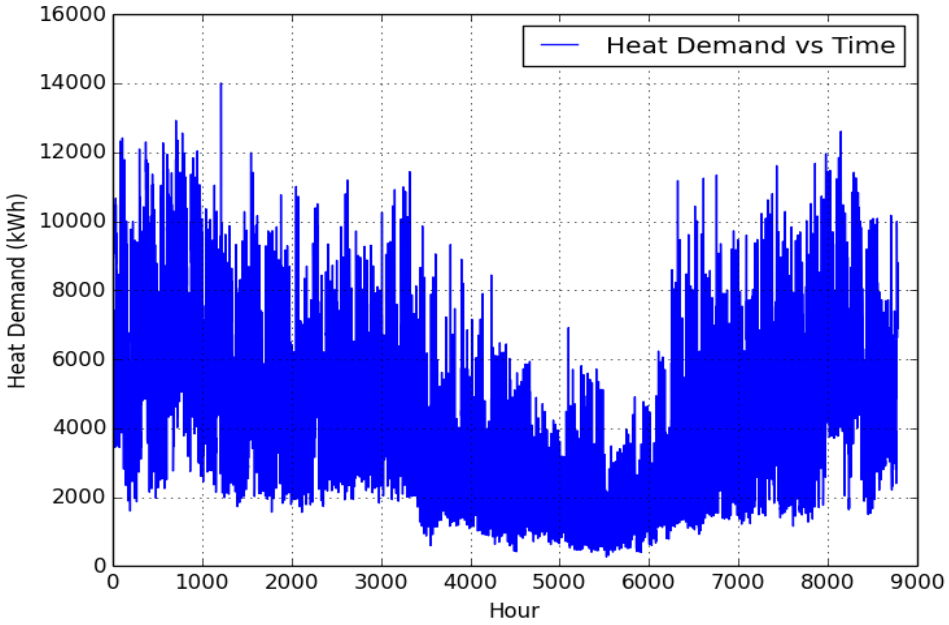

Figure 3.7 *Heat demand data for the year of study*

Table 3.1 *Main input data*

Data	**Value**
Mass flow rate of each geothermal well ($^{kg}/_{s}$)	20
Temperature of the geothermal fluid (K)	353.15
Minimum temperature difference on the hot side of the G.H.E. (K)	5
Ambient design temperature (K)	280.15
Soil temperature (K)	280.15
Minimum temperature at the outlet of the supply transmission pipeline (K)	334.65
Lifespan of the investment (Years)	30

As the daily heat demand for the day based on which the sizing is done increases, the total fraction of heat demand that is covered by geothermal energy increases with the size of the geothermal installation. Therefore, by applying the model in three different cases, the effect of sizing the geothermal installation will be made clear both from an energetic, economic and environmental point of view. Additionally, the algorithm is not applied for a higher sizing of the geothermal installation as, in this case, the installation will work at partial load the majority of time and this will likely make the investment unfeasible.

The main results of the model are shown in Table 3.2 and refer to the design-day for each case. It should be noted that the height-to-diameter ratio of the hot water storage tank was selected to be equal to 1. Therefore, since its volume is known for each case, then, its height and diameter can also be easily calculated. The volume of stored water in the hot water storage tank throughout the design day can be seen for each case in Figs. 3.9-3.11, while its temperature evolution can be seen in Figs. 3.12-3.14. Concerning the pipelines of the transmission network, the design temperatures can be seen in Table 3.3, while the dimensions can be seen in Table 3.4. Similarly, the design temperatures and the dimensions for each branch of the distribution network are shown in Tables 3.5 and 3.6, respectively. In our case, it was assumed that the distribution network consists of 5 branches. Furthermore, the temperature drop per length for each pipeline of the network is shown on Table 3.7 and the capital cost of each pair of pipelines, together with their lengths, are shown on Table 3.8.

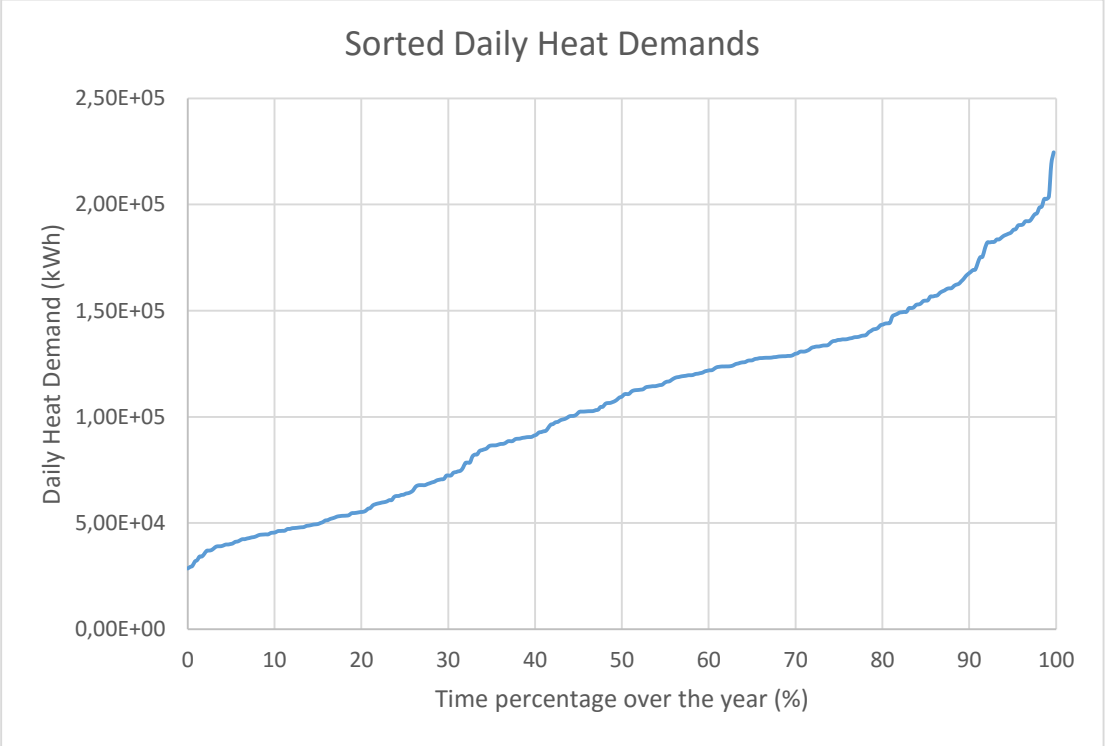

Figure 3.8 *Sorted daily heat demands on a percentage basis*

Table 3.2 Main results of the sizing of the installation

Case	25%ile	50%ile	75%ile
No of wells	1	2	3
Geothermal mass flow rate, $\dot{m}_G$ (kg/s)	20	40	60
Mass flow rate on the left of the storage tank, $\dot{m}_{tr,S}$ (kg/s)	29.87	60.10	92.26
Geothermal capacity, $\dot{Q}_{G,D}$ (kW)	2520.6	5006.5	7502.4
Temperature drop of the geothermal fluid, dT_G (K)	30.079	29.872	29.843
Total thermal efficiency, η_{tot} (%)	86.886	87.431	87.610
Volume of the hot water storage tank, V_{HST} (m^3)	341.93	592.34	1132.30
Diameter and height of the hot water storage tank, D_{HST}, H_{HST} (m)	7.579	9.102	11.297

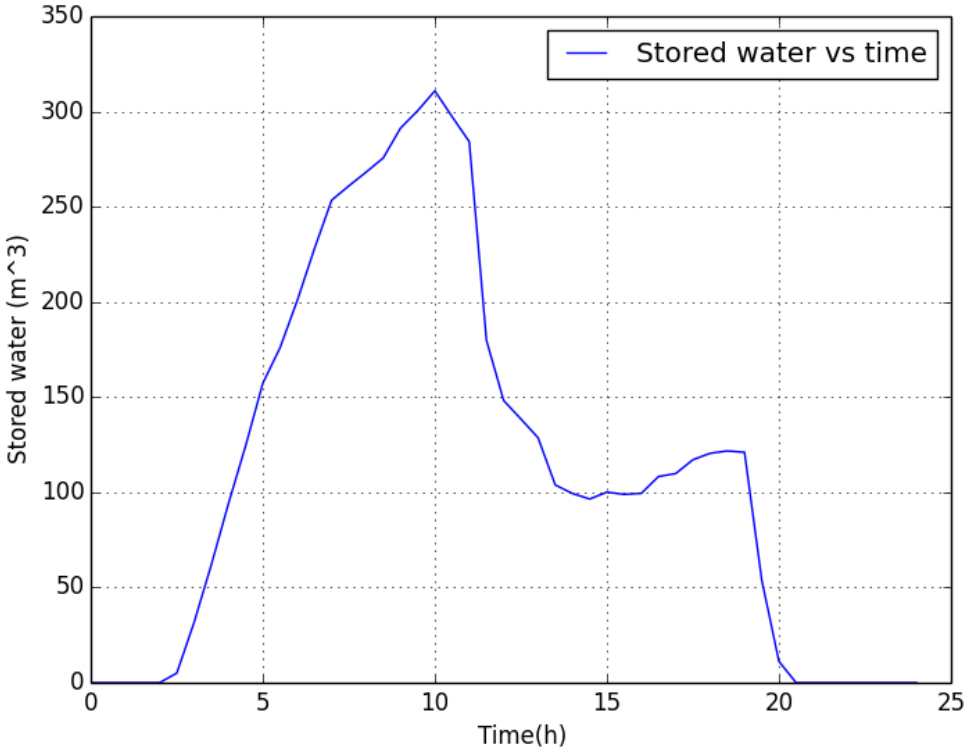

Figure 3.9 Volume of stored water over time (25%ile sizing)

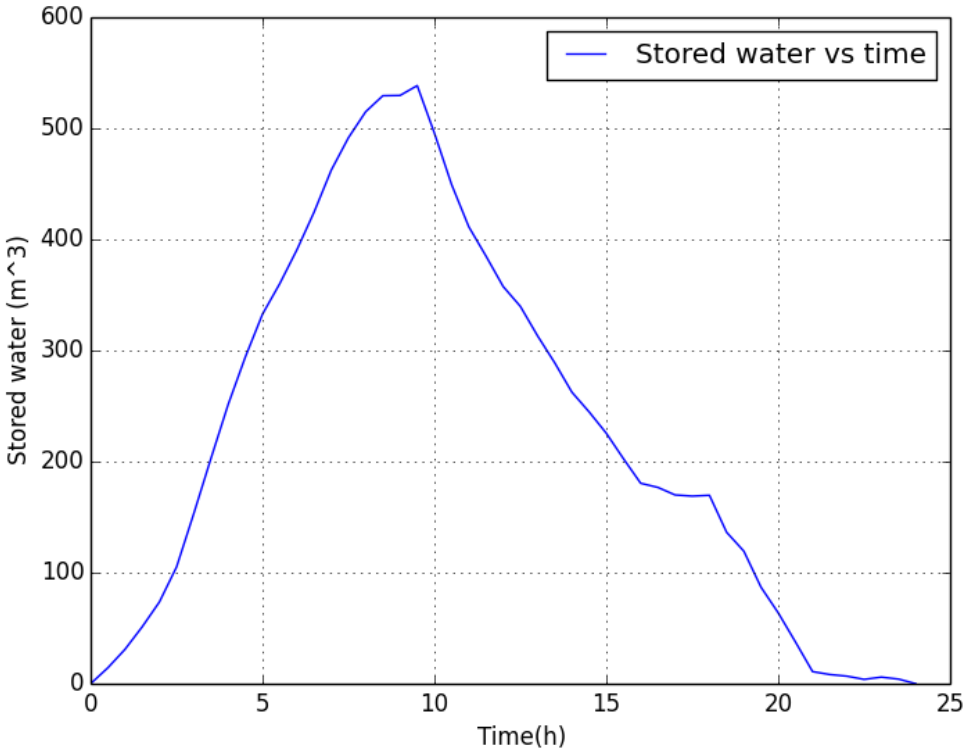

Figure 3.10 *Volume of stored water over time (50%ile sizing)*

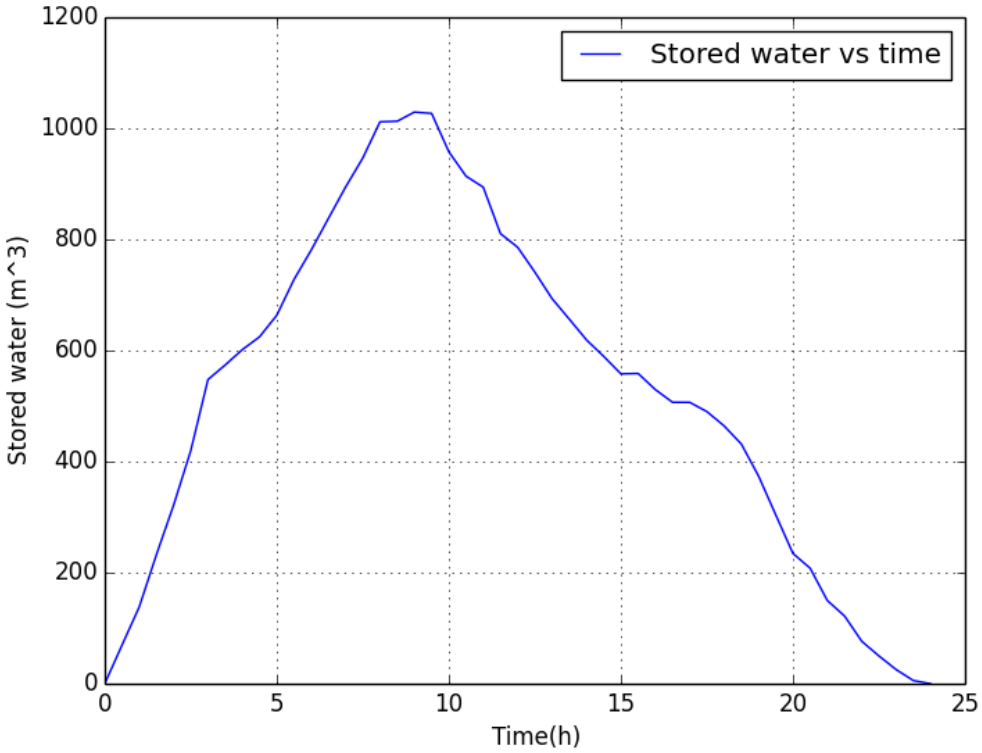

Figure 3.11 *Volume of stored water over time (75%ile sizing)*

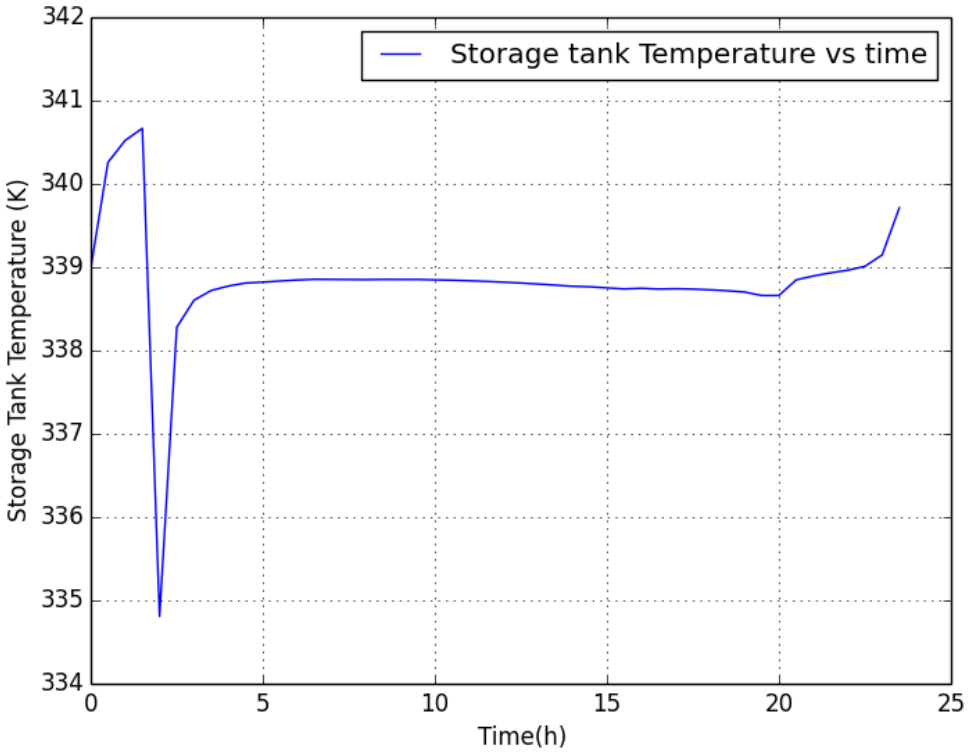

Figure 3.12 *Temperature evolution of stored water over time (25%ile sizing)*

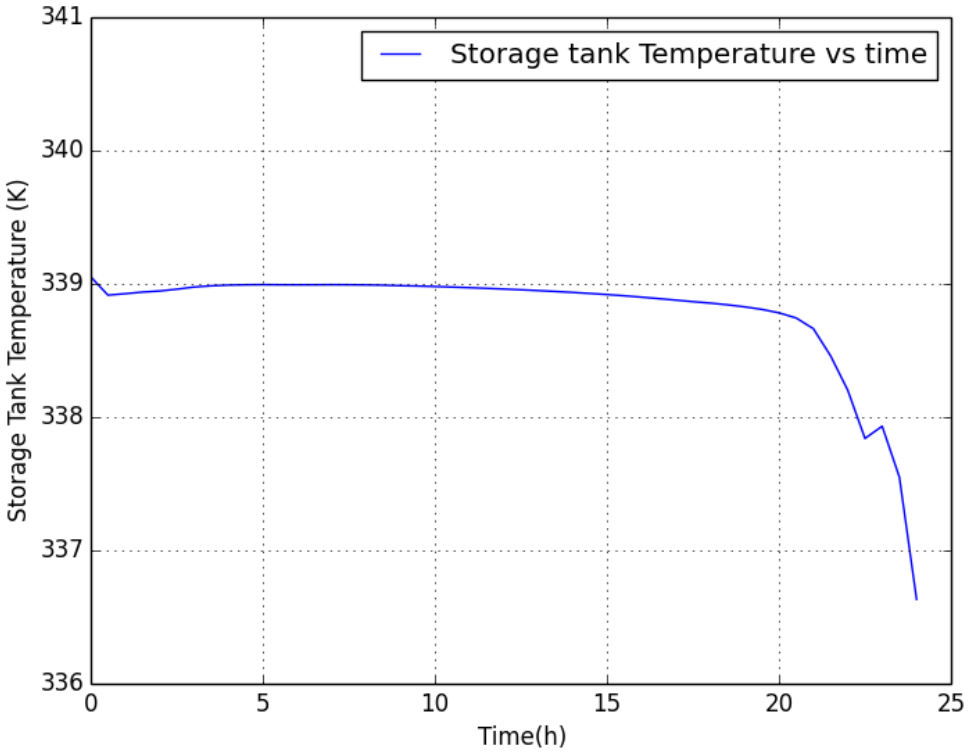

Figure 3.13 *Temperature evolution of stored water over time (50%ile sizing)*

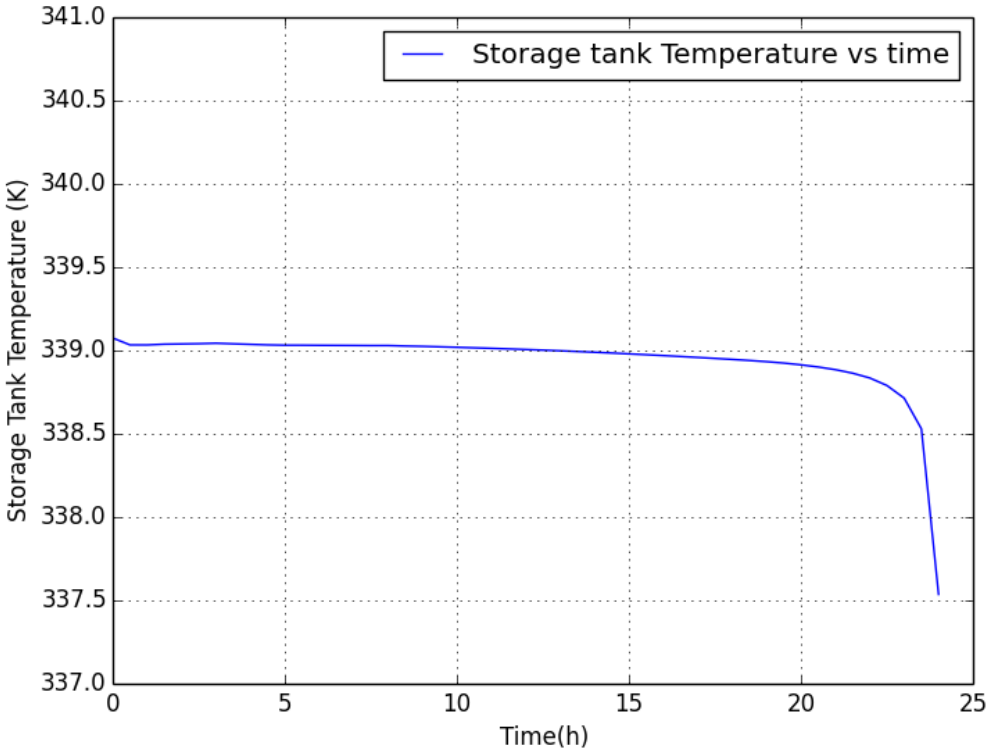

Figure 3.14 *Temperature evolution of stored water over time (75%ile sizing)*

Table 3.3 *Design temperatures of the transmission network (K)*

Case	25%ile	50%ile	75%ile
Supply-Inlet	339.150	339.150	339.150
Supply-Outlet	338.968	339.043	339.066
Return-Inlet	320.013	320.199	320.263
Return-Outlet	319.909	320.141	320.221

Table 3.4 *Optimum dimensions of the transmission network's pipelines (cm)*

Case	25%ile	50%ile	75%ile
Inner diameter	21.45	26.78	34.92
Outer diameter	21.91	27.3	35.56
Thickness of insulation	20	20	21

Table 3.5 Design temperatures of the distribution network (K)

Case	25%ile	50%ile	75%ile
Branch 1			
Supply-Inlet	338.968	339.043	339.066
Supply-Outlet	338.914	339.011	339.045
Return-Inlet	321.914	322.011	322.045
Return-Outlet	321.878	321.990	322.030
Branch 2			
Supply-Inlet	338.968	339.043	339.066
Supply-Outlet	338.766	338.935	338.992
Return-Inlet	320.766	320.935	320.992
Return-Outlet	320.629	320.862	320.941
Branch 3			
Supply-Inlet	338.968	339.043	339.066
Supply-Outlet	338.851	338.976	339.017
Return-Inlet	318.851	318.976	319.017
Return-Outlet	318.777	318.933	318.985
Branch 4			
Supply-Inlet	338.968	339.043	339.066
Supply-Outlet	338.897	339.005	339.041
Return-Inlet	323.897	324.005	324.041
Return-Outlet	323.845	323.977	324.023
Branch 5			
Supply-Inlet	338.968	339.043	339.066
Supply-Outlet	338.703	338.887	338.956
Return-Inlet	318.703	318.887	318.956
Return-Outlet	318.533	318.788	318.885

Table 3.6 Optimum dimensions of the distribution network (cm)

Case	25%ile	50%ile	75%ile
Branch 1			
Inner diameter	7.33	11.11	13.61
Outer diameter	7.61	11.43	13.97
Thickness of insulation	16	17	18
Branch 2			
Inner diameter	11.11	13.61	16.43
Outer diameter	11.43	13.97	16.83
Thickness of insulation	17	18	19
Branch 3			
Inner diameter	11.11	16.43	21.45
Outer diameter	11.43	16.83	21.91
Thickness of insulation	17	19	19
Branch 4			
Inner diameter	5.75	7.33	8.57
Outer diameter	6.03	7.61	8.89
Thickness of insulation	15	16	17
Branch 5			
Inner diameter	8.57	13.61	16.43
Outer diameter	8.89	13.97	16.83
Thickness of insulation	16	18	18

Table 3.7 Temperature drop per length for the pipelines of the network (K/km)

Case	25%ile	50%ile	75%ile
Transmission Network			
Supply pipeline	0.121	0.071	0.056
Return Pipeline	0.069	0.039	0.028
Distribution Network			
Branch 1			
Supply pipeline	0.450	0.267	0.175
Return Pipeline	0.300	0.175	0.125
Branch 2			
Supply pipeline	0.316	0.169	0.116
Return Pipeline	0.214	0.114	0.080
Branch 3			
Supply pipeline	0.234	0.134	0.098
Return Pipeline	0.148	0.086	0.064
Branch 4			
Supply pipeline	0.888	0.475	0.316
Return Pipeline	0.650	0.350	0.225
Branch 5			
Supply pipeline	0.379	0.223	0.157
Return Pipeline	0.243	0.141	0.101

Table 3.8 Capital Cost and length of each pair of pipelines (Costs in £, lengths in m)

Case	CC (25%ile)	CC (50%ile)	CC (75%ile)	Length
Transmission Network	177429	217827	287616	1500
Distribution Network				
Branch 1	5001	7185.4	8779	120
Branch 2	38322	46821	56529	640
Branch 3	29939	44163	56087	500
Branch 4	2690	3334	3918	80
Branch 5	33182	51211	60407	700

Finally, a sensitivity analysis was carried out for the heat losses of the pipelines against some basic parameters of this process. The analysis was carried out for the transmission pipeline of the 75-C case. The results are shown in Figs. 3.15-3.19, where the heat losses of the pipelines are presented against their burial depth, the distance between them, the inlet water temperature, their internal diameter and the mass flow rate through them, respectively.

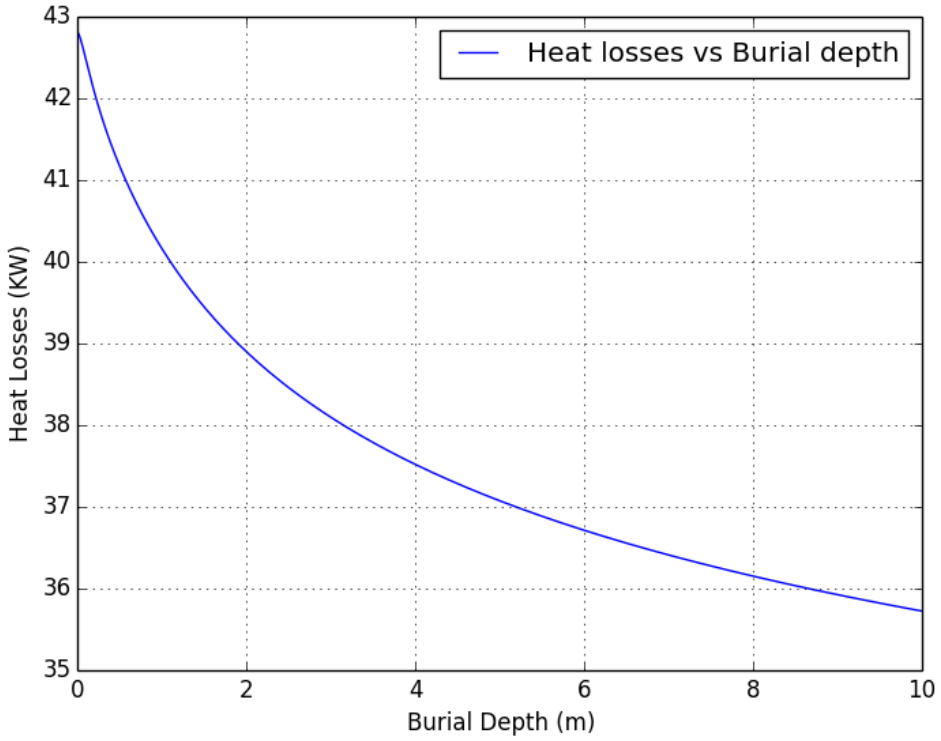

Figure 3.15 Heat losses of the pipelines against their burial depth (75-C case)

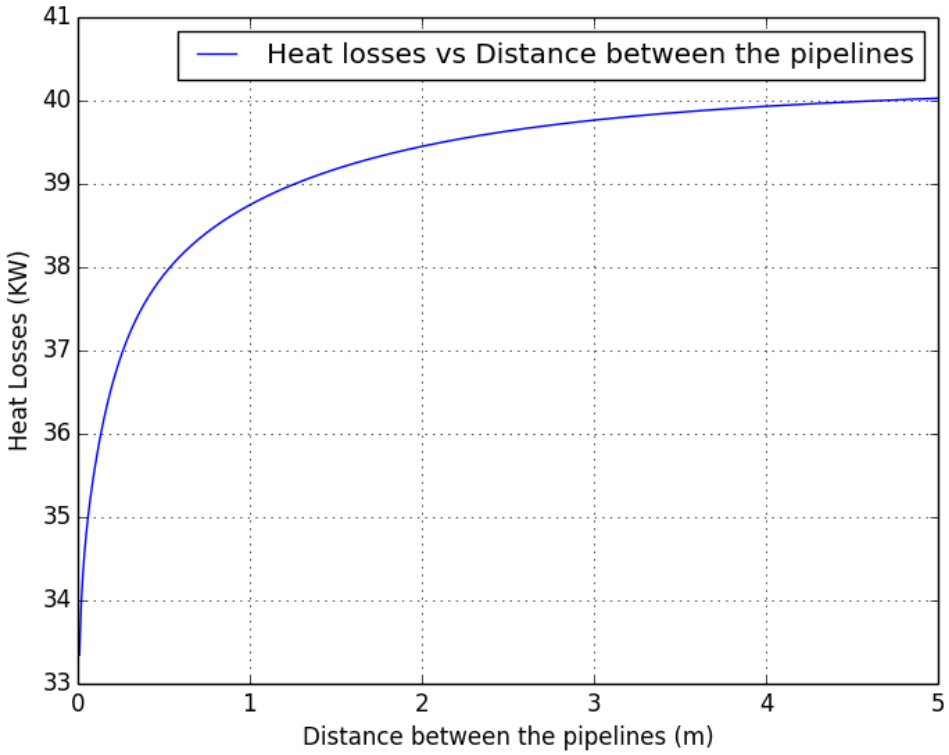

Figure 3.16 *Heat losses of the pipelines against their between distance (75-C case)*

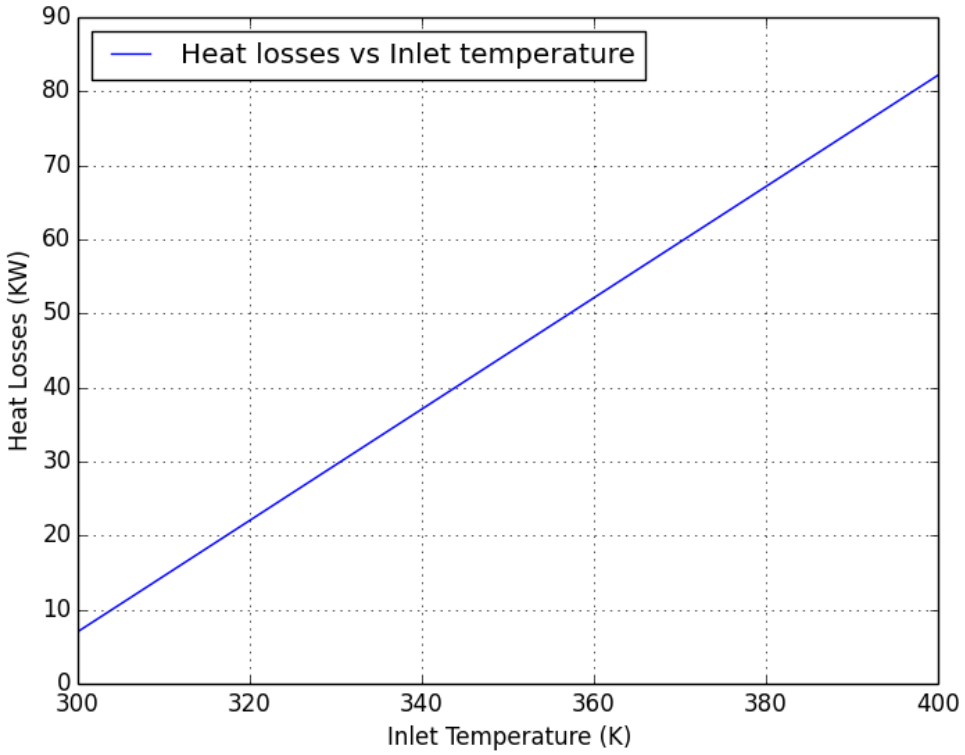

Figure 3.17 *Heat losses of the pipelines against the inlet temperature (75-C case)*

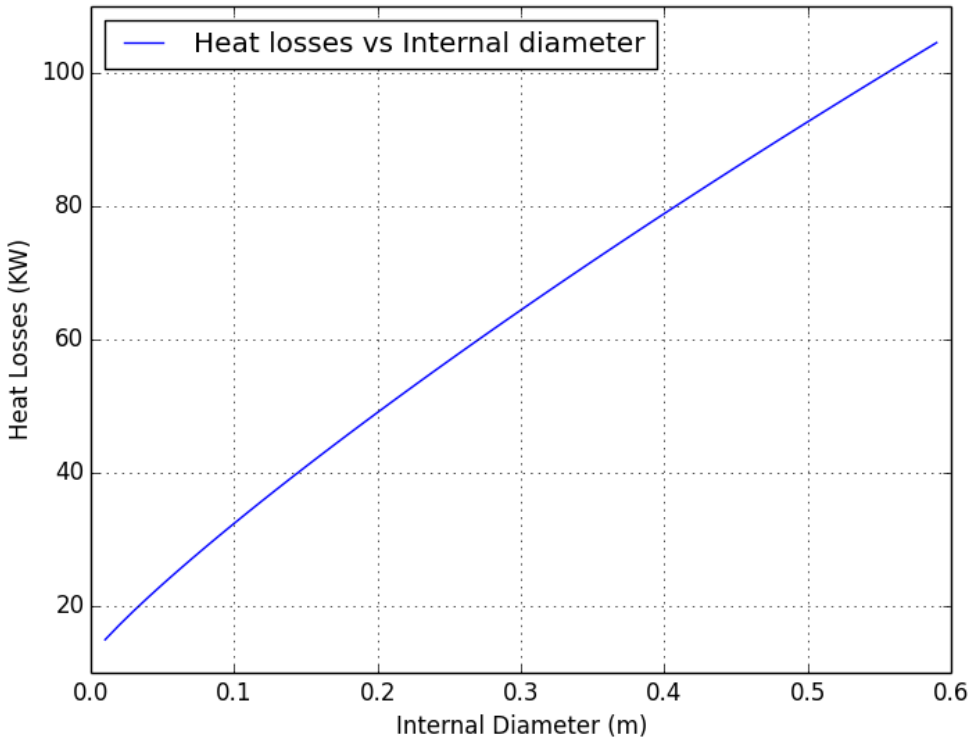

Figure 3.18 *Heat losses of the pipelines against their internal diameter (75-C case)*

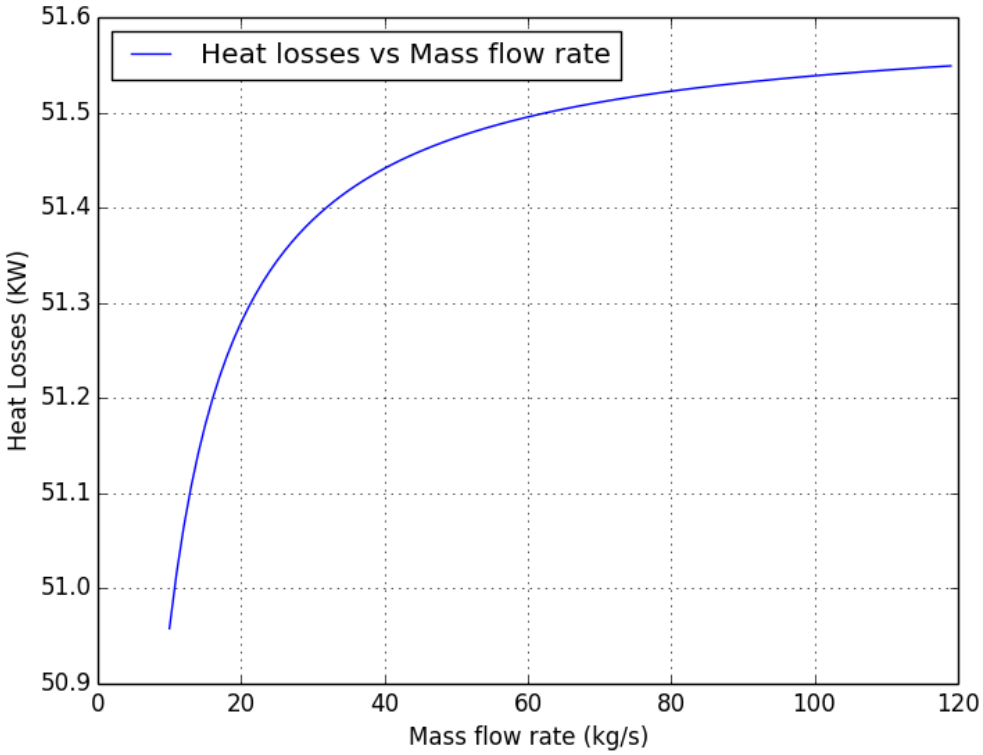

Figure 3.19 *Heat losses of the pipelines against the mass flow rate (75-C case)*

3.4 Discussion

A first important observation which is not visible directly is that the algorithm was able to produce results and there was no need to use a heat pump. As can be seen in Table 3.1, the temperature of the geothermal fluid is roughly 19K higher than the needs of the end-users. Although this temperature difference is not that big, it is believed that even if it was smaller, then the algorithm would also be able to provide results. Therefore, the earlier intuitive clam that a temperature somehow higher than the needs of the end-users can be functional is, at least, partially verified.

The main results of the developed model were shown on Table 3.2 and refer to the design-day for each case of sizing. As can be seen in this table, the number of wells and, subsequently, the geothermal flow rate increase as the sizing of the installation (i.e. the heat demand coverage by geothermal energy) increases. This is totally expected, as in order to cover a higher fraction of the heat demand by geothermal energy, higher geothermal flow rate is necessary. Subsequently, this is also depicted in the number of the necessary geothermal wells. Additionally, it is observed that the temperature drop of the geothermal fluid is almost the same in each case and is roughly equal to 30K degrees. Therefore, and by taking into account Eq. (3.16) properly re-arranged, the geothermal capacity increases almost proportionally with the number of wells. This is normal, as the geothermal capacity depends on the geothermal flow rate and the temperature drop of the geothermal fluid. Since, the latter is almost constant, then, it can be said that the geothermal capacity is roughly proportional to the geothermal flow rate or to the number of wells. Another important finding is that the total thermal efficiency of the installation increases as the sizing also increases. So, it can be said that as more geothermal energy is harvested the whole process becomes more efficient.

The volume of the hot water storage tank, on the other hand, increases with the increase of the coverage by geothermal energy as expected, but not proportionally. This happens because the mass or volume of stored water, and the volume of storage tank subsequently, depend strongly on the fluctuation of the heat demand within the specific design-day. Two days might have the same daily heat demand, but the fluctuation within the day can be very different. For example, one day can have a very peaky heat demand while the other day can have a rather constant heat demand. Intuitively, it is understood that in the first case the volume of the storage tank will be bigger as higher storage capacity will be needed in order

to accommodate the sharp changes of the heat demand within the day. But, in general, it can be definitely stated that the volume of the storage tank will increase with the size of the installation.

Furthermore, it can be seen that the ratio of the mass flow rate on the left of the storage tank to the geothermal flow rate ($\dot{m}_{tr,S}/\dot{m}_G$) is almost the same in all three cases and is equal to around 1.5, but these not exactly equal as this value, which is symbolised as R_m in the model, is a value provided as output of the model. An initial estimation of this value is given as input, but as mentioned in section 3.2.9, this value might be changed if the physics of the problem require this. Since these values are slightly different, it means that the algorithm has changed the initially provided value in some or all the cases. This result is in accordance with the literature: Harrison (1987) states that this value has to be higher than 1. It can also be observed that the mass flow rate is quite large as will be the mass exchanges between the network and the storage tank. This would make the conservation of the stratification of the tank quite difficult. This fact justifies the choice of a fully mixed storage tank as a logical selection for this kind of process.

In Figs. 3.9-3.11, the volume of stored water in the hot water storage tank throughout the design-day was presented for each case. It is observed that all the graphs represent a similar trend, in which the maximum amount of stored water is achieved in almost the same, early morning, hours. This is something expected as the heat demand is generally low over the night, so in this period of time the majority of produced water would be stored for later use. Then, a relatively sharp decrease occurs between 10.00-15.00 hours, and subsequently the decrease of the amount of stored water is smoother. Of course, this variation depends a lot on the end-users. In our case, the end-users are buildings managed by the University, so the heat demand is expected to be high in the aforementioned hours. If the heat demand referred to typical dwellings, then an even sharper decrease of the amount of stored water would be expected during the early morning hours (typically 06:00-08:00), in which there is usually the peak demand, then the stored water would increase till the evening hours (typically 19:00-22:00), where there is a second peak demand which is typically lower than the morning peak demand. This statement makes clear why the case of geothermal district heating is very case-specific by its own nature and, therefore, it is quite difficult to extract completely generalised conclusions in many aspects.

The temperature evolution of the stored water is shown in Figs. 3.12-3.14. It can be seen that the higher temperature decreases occur during the first and, mainly, the last hours of the day in which the storage tank is almost empty. During the rest of the day the temperature is almost constant, indicating negligible heat losses. The only exception is the graph that depicts the temperature evolution for the lower sizing (Fig. 3.12), where especially in the early hours there is a much steeper decrease in the temperature of stored water. This happens because, as can be seen in Fig. 3.9, there is no stored water for many hours and the mathematical model shows some instability. These figures highlight the effect of the insulation thickness, which is equal to 20cm in our case, showing that the heat losses in a well-insulated tank can be minimised. The thickness of the insulation is also in agreement with published values (Chan *et al.*, 2013).

In order to further quantify the effect of the insulation, a sensitivity analysis was carried out for the simple cooling of the storage tank. More specifically, the storage tank of the 75%ile case was considered to be full of water at 350K degrees and the time needed to cool down the water by 10K degrees was calculated for different insulation thicknesses. The results of this sensitivity analysis are shown on Table 3.9. It can be seen that when insulation is used a very long period of time is required to cool down the water, indicating that the heat losses are quite small. In this case, the storage tank is considered to be always full, so stratification phenomena will occur which are not taken into account in this sensitivity analysis. These phenomena might affect the final results, but the general trend and scale of the results will be the same. It is also seen that the cooling time increases almost linearly with the thickness of the insulation. So, both from Table 3.9 and from Figs. 3.12-3.14, the effect of the insulation on the minimization of the heat losses is highlighted and it is considered that the process followed is appropriate.

Table 3.9 *Sensitivity analysis of the storage tank heat losses*

Thickness of the insulation (cm)	**Time (h) needed to cool the water by $\Delta T = 10K$**
20	2022
15	1523
10	1023
5	523
0	12

Concerning the sizing of the pipelines, the design temperatures of the transmission and distribution network are shown on Tables 3.3 and 3.5, respectively. The corresponding temperature drop per km of pipeline, which depicts the heat losses of the pipeline, is shown on Table 3.7. A first important observation is that the calculated values of the heat losses are rather lower than published values (see Kanoglu and Cengel, 1999, for example). In many cases, the heat losses are even a scale of magnitude lower than similar published values. This is because in the developed algorithm, the heat losses of the pipelines are taken into account in the objective function and quite thick insulation is used. This can also be verified by Tables 3.4 and 3.6, where the dimensions of the pipelines of the transmission and distribution network are presented, respectively. In order to further verify this argument, the proportion of each cost for the transmission pipeline of the 75%ile case of sizing is shown in Table 3.10. It can be seen that, indeed, the heat losses cost account for a big fraction of the total cost and this justifies the thick insulation used. Probably in practice, the heat losses would not be taken into account as much as they should be and a thinner insulation would be used. Additionally, the fact that these are simulation results and not real data might be partially a reason for this discrepancy.

Table 3.10 *Proportion of each part of the cost during the sizing of the transmission pipelines (75%ile case)*

Part of the total Cost	**Proportion (%)**
Capital cost	52.76
Electrical cost	17.04
Heat losses cost	30.2

On the other hand, although the heat losses are lower than the published values, it can be observed that there are some important differences between them. This happens because the optimization algorithm does not take into account only the heat losses, but also the capital and electrical costs. For example, by combining the results of Tables 3.4, 3.6 and 3.7, it can be observed that the smaller pipelines have increased heat losses compared to the bigger ones. This happens because as the diameter of the pipeline decreases, the friction losses increase (see Eq. 3.44) and, therefore, the electrical cost increases. So, for smaller pipelines, the heat losses are a smaller fraction of the total cost, as the electrical cost becomes much more important. Therefore, the heat losses will be higher in this case.

Another important finding from the results is that the size of the pipelines increases as the overall size of the installation increases. This is to be expected, as larger sizing entails higher flow rates and, therefore, larger pipelines will be needed to deal with these higher flow rates.

In Table 3.8, the capital cost for each pair of pipelines is shown. Two important observations can be drawn from this table. Firstly, the capital cost of the pipelines increases as the sizing increases. This is also to be expected because, as mentioned above, larger sizing means higher flow rates and, subsequently, larger pipelines. Secondly, it can be observed that the capital cost increases with the length of the pipeline, but not proportionally. This happens because each component of the total cost is affected differently with the change in the length and this is taken into account explicitly in the objective function. So, it can be stated that all the above observations indicate the power and usefulness of the developed algorithm for the optimum sizing of the pipelines of the network.

Finally, in Figs. 3.15-3.19, the heat losses of the pipelines are shown against some basic parameters that influence the phenomenon of heat loss. Some important observations can be made on these figures which can be useful for the initial design stages of the pipeline system. These observations can also be generalised for any system of pipelines which transfer a hot fluid, as the governing equations will be the same. Firstly, it is observed from Fig. 3.15 that the heat losses of the pipelines decrease as the burial depth increases. This means that the pipelines should be buried as deeply as possible. This, on the other hand, can significantly increase the cost, so an optimum solution should be found taking this into account. Secondly, in Fig. 3.16 it is seen that the heat losses decrease as the pipelines are laid closer to each other. This indicates that the pipelines should be laid as close to each other as possible. Then, in Fig. 3.17 is it shown that the heat losses increase proportionally with the inlet temperature. This is something expected as with the increase of the inlet temperature, the temperature gradient between the pipelines and the surrounding soil increases and, therefore, the heat losses will increase. Almost the same trend is presented in Fig. 3.18, in which it is shown that the heat losses increase almost proportionally with the increase of the internal diameter of the pipelines. The latter is also expected as an increase in the diameter of the pipeline indicates an increase in the heat transfer area which, subsequently leads to higher heat losses. Eventually, Fig. 3.19 shows an increase of the heat losses with the increase of the mass flow rate through the pipelines. This is expected intuitively, but also through Eqs. (3.66)-(3.67). An interesting observation is that

the heat losses increase more rapidly at lower flow rates, but after a point the rate of the increase levels off.

3.5 Summary

This Chapter presented the first developed model of this thesis, which concerns to the sizing of a geothermal district heating system. First, the mathematical modelling was presented in detail together with a synoptic review of the inputs and outputs. Subsequently, the results for three different cases of sizing were provided, followed by an extended discussion on these which highlight some important observations that can be quite useful in the design of such systems.

The developed model mainly uses as inputs the geothermal data, the heat demand data throughout at least one year, and the topology of the installation. Other case-specific data, such as the ambient design and soil temperatures or the physical properties of water, are used as inputs also. The model was designed to be as generic as possible and, therefore, the majority of the data are user-defined inputs. In our case, only the heat demand data were real data while the rest of the data were arbitrary inputs by the author. By applying the mathematical model developed in section 3.2, the sizing of the installation will be achieved. More specifically, the main outputs of the model will be the necessary number of wells, the sizing of the hot water storage tank and the sizing of the pipelines. A simplistic illustration of the process is presented in Fig. 3.20.

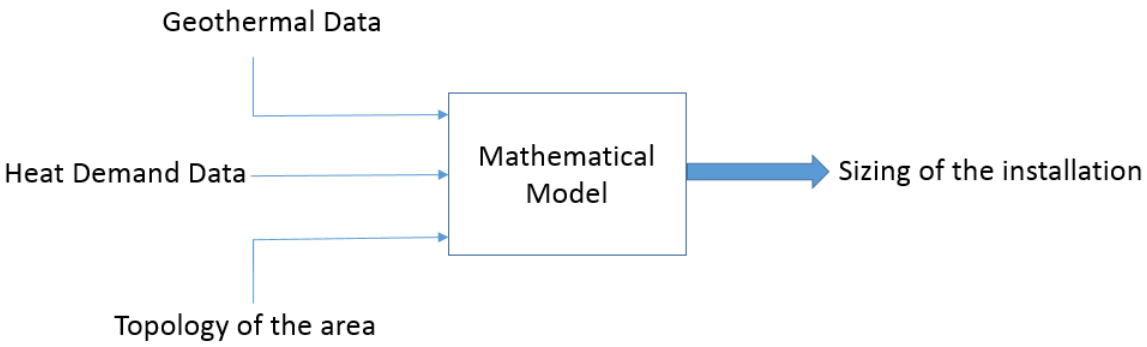

Figure 3.20 *Schematic illustration of the process*

The developed model was then applied for three different cases of design-day, which affects the sizing of the whole installation. More specifically, the sizing was carried out for those days that their daily heat demand is equal to the 25^{th}-, 50^{th}- and 75^{th} centile of the daily heat demands of the whole year. The most important conclusions that were drawn by the results and discussion sections were the following:

- The total thermal efficiency is quite high for any case of sizing and is about 86.8-87.6%, and it also increases with the overall sizing.
- The temperature drop of the geothermal fluid is around 30K degrees for any case.
- The mass flow rates across the network are quite high, justifying the selection of a fully mixed storage tank instead of a stratified tank.
- The heat losses of the storage tank are negligible when a thick insulation is used. Only in the times when the storage tank is almost empty is the temperature drop noticeable, but again the heat losses, in total, are quite small.
- The importance of the heat losses of the pipelines at the initial design stage was highlighted. It was shown that by using the developed optimization algorithm for the sizing of the pipelines, the heat losses are much smaller than previously published values. This indicates that the heat losses were probably underestimated in the past, but this is inadvisable as it was shown that these are a big fraction of the total cost. Therefore, the power of this algorithm was highlighted.
- The heat losses of the pipelines increase as the sizing gets smaller because there is a trade-off between the heat losses and the electrical cost, which are both taken into account in the sizing of the pipelines.
- The capital cost of the pipelines increases with the increase in the sizing, as bigger pipelines are needed to deal with the higher flow rates of the bigger sizing.

In conclusion, it can be said that there seem to be two controversial trends concerning the sizing of the installation. On the one hand, as the sizing of the installation increases the cost of the installation will increase as bigger pipelines, bigger storage tanks, and more geothermal wells (amongst other things) will be needed, which of course, will increase the initial capital cost. On the other hand, the total thermal efficiency increases (however slightly) as the sizing increases and together with the decrease of the heat losses, this is an

indicator that the whole process improves with the increase in size. This can potentially lead to lower operational costs which might level-off the difference in the capital cost. All these will be studied in detail on Chapter 5, where a detailed economic, energetic and environmental comparison between the proposed and the traditional case of operation as well as between the different cases of sizing, will be carried out.

4 OPERATION OF A GEOTHERMAL DISTRICT HEATING SYSTEM

4.1 Introduction

In this Chapter, the operation of a geothermal district heating system will be studied in detail. More specifically, two different models have been developed for this purpose that their main input is the output of the model of Chapter 3, i.e. the sizing of the installation. In other words, the operation of the installation that can theoretically be built based on the outcome of Chapter 3 is now studied.

Firstly, a model that provides the operational strategy of the installation over a random day has been built. By operational strategy is defined the complete knowledge of the operation of the installation within one day, since the installation is scheduled on a daily basis. The inputs of this model are the sizing of the installation and the heat demand over a random day. The first set of inputs will be the same for every day, while the heat demand will obviously be changeable from day to day. So, with this model the operational strategy of the sized installation will be known for a given heat demand. In general, the main outputs of this model will be the necessary geothermal mass flow rate; when and by how much should the storage tank be charged or discharged; when and by how much should the peak-up boilers used; all the mass flow rates across the installation; the cost of electricity for the pumps; the cost of the fuel needed for the peak-up boilers; and the temperature in the critical points of the installation. The concept of critical points in a district heating system was first introduced by Pinson *et al.* (2009). It is stated that in a district heating system, it is usually not important to know what happens at every single point of the network, but only at some specific points, which are called the critical points of the network. In this work, the critical points of the network are the inlet and the outlet of each pipeline of each branch of the distribution network, the inlet and the outlet of each pipeline of the transmission network, the points before and after the storage tank as well as the point after the peak-up boilers. This algorithm would be quite useful for the operators of the installation as they would know in advance how they should operate the installation the next day or days if the heat demand of this day is known or can be predicted.

Secondly, a model that studies the operation of the installation over a whole year has been built. For this purpose, the model of a random day has been extended over a whole

year. In the model of the random day, some inputs from the previous day are necessary to run the algorithm and some of the outputs are data for the next day. More details on this will be given below. So, in this case the model of the random day will be run serially for all the days of the year and each day will provide the necessary data for the next day and will be fed with the necessary data from the previous day. The outputs of this model are the same as of those of the random day, but some of them are those of interest for further study. More specifically, those are the total cost of electricity to run the pumps and the total fuel used over the year. These two comprise the main operational costs of the installation and will be used in the economic analysis in Chapter 5. Furthermore, through this model, the cold water storage tank and the peak-up boilers will be sized as shown on the corresponding section.

In this section, a brief introduction on the developed models was provided. In section 4.2, the mathematical modelling for both models will be presented in detail, while in section 4.3 indicative results will be given for random days together with the results of the annual operation of the installation. Afterwards, these results will be discussed in section 4.4 and a brief conclusion of this Chapter will be provided in section 4.5.

4.2 Operation over a randomly-selected day

4.2.1 Input data

In this section, all the input data used in the developed algorithm will be presented. As mentioned before, there will be some data that are independent of the day of study, and thus constant (such as the size of the system), and some other data that change day-by-day, such as the heat demand data. These two kinds of data will be clearly separated below.

All the input, as well as the output data of all the models are in txt files, which is the simplest way to store data, but at the same time it is quite easy to handle them for post-processing, such as importing into an Excel file. The only matter that the user of the model will have to be careful of is to write the variables in each txt file in the correct order, because within the Python code each line of the txt file refers to a different and specific variable. So, the code “knows” that a specific line of a specific txt file will be a specific variable and never anything else. So, the user will have to be very careful on writing the variables in the correct order otherwise the model will provide completely wrong results.

In order to be better understandable, the input data will be separated in different groups according to their origin or purpose. The input data that are independent of the day of study are the following:

- Installation data: Temperature of the geothermal fluid ($T_{G,h}$); temperature in the inlet of the supply transmission pipeline ($T_{tr,s,i}$); ratio of the mass flow rate on the left of the storage tank to the geothermal mass flow rate (R_m); thermal efficiency of the geothermal heat exchanger (η_{GHE}); thermal efficiency of the in-house installations (η_{dw}); time discretization of heat demand data.
- Sizing data: Number of wells (N_{wells}); mass flow rate of each well ($\dot{m}_{well}$); minimum mass flow rate of each well ($\dot{m}_{well,min}$); volume and height to diameter ratio of the hot water storage tank.
- Design day approximations: Outlet temperature of the supply transmission pipeline ($T_{tr,s,o,init}$); inlet temperature of the return transmission pipeline ($T_{tr,r,i,init}$); outlet temperature of the return transmission pipeline ($T_{tr,r,o,init}$); total thermal efficiency of the installation ($\eta_{tot,init}$); temperature drop of the geothermal fluid ($\Delta T_{G,init}$).
- Transmission network data: Length of the transmission pipeline (L_{tr}); dimensions of the pipelines as calculated in Chapter 3.
- Distribution network data: Length of each branch of the distribution pipelines; dimensions of the pipelines (as calculated in Chapter 3) and temperature drop on their boundaries.
- Pipeline data: Data referring to the heat transfer phenomenon of the pipelines of the system as presented in section 3.2.6.3.
- Hot storage tank data: Data referring to the calculation of the heat losses of the hot water storage tank as presented in section 3.2.5.
- Boiler data: Thermal efficiency of the peak-up boilers (η_b), lower heating value of the fuel used (LHV_f) and temperature of the water provided by the boiler ($T_{b,out}$).
- Ambient data: Air temperature (T_a); Soil temperature (T_{soil}); air velocity (u_{air}).

It should be noted that the temperature in the inlet of the supply transmission pipeline will be the same every day and equal to the value calculated for the design day. This value will also remain constant throughout the algorithm. On the other hand, the values included

in the design-day approximations are those calculated in the design-day, but are used only as initial approximations and their values will change through the calculations.

Additionally, the inputs of the algorithm that change for each day are the following:

- Total heat demand: Heat demand for each time interval (HD^i)
- Discretised heat demand: Heat demand for each branch of the network and for each time interval (HD_j^i)
- Previous day storage data: Mass and temperature of the stored water in the last point of the previous day (M_{st}^0,T_{st}^0 respectively). These are used as the values of the first point of the studied day. As mentioned before, the mass and temperature of stored water are point data, in contrast with the next variables which are continuous values.
- Previous day masses: Masses in the left and right of the storage tank, masses of charged and discharged water and mass of water provided by the boiler during the last time interval of the previous day ($M_{tr,G}^P$,$M_{tr,S}^P$,M_{ch}^P, M_{dis}^P and M_b^P, respectively).
- Previous day distribution mass flow rates: Mass flow rates of each branch of the distribution network over the last time interval of the previous day ($\dot{m}_{d,j}^P$).

As in the model explained in Chapter 3, the Python language has been used to develop this model too. This model is based on a functional logic of code developing. This means that the code is broken into some functions, which work like the subroutines of classical programming, and each function may call other functions. Using this logic, the code is more readable and understandable, and so is the logic of the calculations. Each function has some inputs and outputs and within the function there are all the necessary calculations. So, in the next section each function will be explained separately and in the end the general logic and hierarchy between the functions will be explained. The model of Chapter 3 was also developed using the functional logic, but it was not explained in that Chapter because the calculations were more straightforward. In this case, the calculations and the logic are more complex, so it is considered that in this way the whole logic will be better understood.

4.2.2 Functions used in the model

In this section, the functions used in this model will be described. In the case where functions from the model of Chapter 3 are used, these will be briefly presented. In each case, the input values, the main equations used as well as the output values will be specified. It should be noted that the functions will be presented in the same order as they are written in the code. Some functions which are written later on the code will call earlier functions which will often provide as input a value which is first calculated by them. So, some inputs on the early functions will not be fully understandable initially, since some of their inputs will be calculated by later functions which are then calling them. This will be totally clear in the next session, where the hierarchy of the functions will be presented.

4.2.2.1 Water mass balances function

The inputs used in this function are the following:

- M_{st}^{0}: Mass of stored water in the first point.
- $M_{tr,S}^{i}$: Mass on the transmission network on the right of the storage tank in each time interval. This will be calculated within a following function.
- $\dot{m}_{G,1}$: First estimation of the geothermal mass flow rate. This will also be calculated within a following function.

First, a more accurate value of the geothermal mass flow rate has to be calculated. The exact value will be calculated in a following function. At the moment, it has to be checked if the value of the first estimation lies within the limits of available geothermal mass flow rate. So, the following loop is used for this purpose and additionally in order to calculate the number of wells which should operate at this day:

$$\left.\begin{array}{c} \boldsymbol{If}\ \dot{m}_{G,1} \geq \dot{m}_{G,max} = \dot{m}_{well} \cdot N_{wells}: \\ \boldsymbol{Then}:\ \dot{m}_G = \dot{m}_{well} \cdot N_{wells} \\ N_{wells,oper} = N_{wells} \\ \boldsymbol{Else-if}\ \dot{m}_{G,1} < \dot{m}_{min,well}: \\ \boldsymbol{Then}:\ \dot{m}_G = \dot{m}_{min,well} \\ N_{wells.oper} = 1 \\ \boldsymbol{Else}:\ \dot{m}_G = \dot{m}_{G,1} \\ N_{wells,oper} = a + 1 \end{array}\right\} \quad (4.1)$$

Where:

$N_{wells,oper}$ = Operating wells at the specific day of study

In the above loop, a is the division remainder of the division of $\dot{m}_{G,1}$ with $\dot{m}_{well}$. The first and the second cases of the loop refer to the initial estimation of the geothermal flow rate being higher than the maximum or lower than the minimum available flow rate, respectively. In these cases, the geothermal flow rate will be set to be equal to the maximum or minimum available value, respectively. The third case refers to the initial estimation being between the maximum and minimum available flow rates and, therefore, remains the same. Therefore, a more accurate geothermal mass flow rate as well as the number of operating wells have been calculated. Then, the mass flow rate on the transmission network in the left of the storage tank as well as the correspondent mass during a time interval can be calculated, respectively, as:

$$\dot{m}_{tr,G} = R_m \cdot \dot{m}_G \tag{4.2}$$

$$M_{tr,G} = \dot{m}_{tr,G} \cdot 60 \cdot TimeMesh \tag{4.3}$$

It is reiterated that the above values are constant throughout the whole day. Since the mass of water on the transmission network in the right of the storage tank is known as an input, then the masses of charged and discharged water can be calculated as:

$$\left.\begin{array}{c} \boldsymbol{For}\ each\ time\ interval\ i: \\ \boldsymbol{If}\ \ M_{tr,G} \geq M_{tr,S}^{i}: \\ \boldsymbol{Then}:\ M_{ch}^{i} = M_{tr,G} - M_{tr,S}^{i} \\ M_{dis,1}^{i} = 0 \\ \boldsymbol{Else}:\ M_{ch}^{i} = 0 \\ M_{dis,1}^{i} = M_{tr,S}^{i} - M_{tr,G} \end{array}\right\} \tag{4.4}$$

The terms in Eqs. (4.2)-(4.4) have been explained in Chapter 3. The above loop is similar to Eqs. (3.21)-(3.22) with the difference being in the mass of discharged water. The above calculated value is not the final one as it does not take into account the case that the storage tank is empty. Therefore, the number '1' is in its suffix. In this case, it is impossible to discharge water from the tank. The exact mass of discharged water will be calculated in the end of this function.

Afterwards, the mass of stored water as well as the mass provided by the boiler will be calculated. It is assumed that the time interval are quiet small, so that within one time interval it won't be needed to discharge both the storage tank and put the boiler in operation. The mass of stored water in the beginning of the day is an input to the function and in order to proceed to the next time intervals, a simple mass conservation law, similar to Eq. (3.23) has to be applied as follows:

$$\left.\begin{array}{c} \boldsymbol{For}\ each\ time\ interval\ i\text{:} \\ A = M_{st}^{i} + M_{ch}^{i} - M_{dis}^{i} \\ \boldsymbol{If}\ \ A < 0\text{:} \\ \boldsymbol{Then}\text{:}\ M_{st}^{i+1} = 0 \\ M_{b}^{i} = abs(A) \\ \boldsymbol{Else}\text{:}\ M_{st}^{i+1} = A \\ M_{b}^{i} = 0 \end{array}\right\} \tag{4.5}$$

Where:

M_b^i = Mass of water provided by the boiler to the network in each time interval i (kg)

In the above loop, the first case refers to when the boiler has to be used to cover a part of the demand, while the second case refers to when the boiler does not have to be used. Finally, since the mass of stored water is known, the accurate value of discharged water can be calculated with the following loop:

$$\left.\begin{array}{c} \boldsymbol{For}\ each\ time\ interval\ i\text{:} \\ \boldsymbol{If}\ \ M_{st}^{i} = 0\text{:} \\ \boldsymbol{Then}\text{:}\ M_{dis}^{i} = 0 \\ \boldsymbol{Else-if}\ \ M_{st}^{i} > 0\ \ \boldsymbol{and}\ \ M_{st}^{i+1} = 0\text{:} \\ \boldsymbol{Then}\text{:}\ M_{dis}^{i} = M_{st}^{i} \\ \boldsymbol{Else}\text{:}\ M_{dis}^{i} = M_{dis,1}^{i} \end{array}\right\} \tag{4.6}$$

The second case of the above loop refers to the case when the storage tank gets discharged within the specific time interval, and therefore only the mass of the previously stored water can be discharged from the storage tank.

So, by applying expressions (4.1)-(4.6), all the masses across the transmission network will be known. More specifically, the outputs of this function are the following:

- Geothermal flow rate ($\dot{m}_G$).
- Mass flow rate on the left of the storage tank ($\dot{m}_{tr,G}$)
- Masses of charged and discharged water for each time interval (M_{ch}^i and M_{dis}^i, respectively.
- Mass of stored water throughout the day (M_{st}^i).
- Mass provided by the boiler in each time interval (M_b^i).
- Necessary operating wells (N_{wells}).

4.2.2.2 Dimensioning of the hot water storage tank function

In this function the basic dimensions of the hot water storage tanks are calculated. The calculations included in this function were also used and explained in Chapter 3. So, a simple reference will be made here. The inputs of this function are the volume of the hot water storage tank (V) and its height-to-diameter ratio (hdr), while the outputs will be the following:

- Height of the storage tank (H_{HST}).
- Diameter of the storage tank (D_{HST}).
- Thickness of the material of the storage tank (t_{st}).
- The area of the side, base and top surface, respectively, of the hot water storage tank (A_{side}, A_{base} and A_{top}).

It should be noted that the above values could be calculated separately and used as inputs in this model, but it was decided to have them calculated within this function in order to minimize the input values of the code.

4.2.2.3 Hot water storage tank heat balance function

This case is not actually one function but a number of smaller functions feeding a bigger one which calculates the heat losses of the storage tank. The majority of these functions has also been explained in Chapter 3 and more specifically in section 3.2.5. So, in this section the main differences from the function of the previous model will be explained.

The main idea behind this function is to apply the energy conservation equation to the storage tank for each time interval and through this equation to find the evolution of the temperature within the storage tank, as well as the temperature at the exit of the storage tank. The smaller functions are used to calculate the heat losses coefficients of the base, top and side parts of the storage tank (see Eqs. (3.31-3.33)). The main inputs of this function are the following:

- Temperature in the inlet of the storage tank ($T^i_{HST,i}$). The basic difference with the previous model is that this temperature is not constant throughout the day, but it is variable at each point. This temperature will be calculated within a later function in order to be used as input in this function.
- Temperature of stored water at the first point (T^0_{st}).
- Mass of stored water at each point (M^i_{st}).
- Mass of water on the transmission network on the left of the storage tank during one time interval ($M_{tr,G}$). This value is constant throughout the day.
- Mass of water on the right of the storage tank throughout the day ($M^i_{tr,S}$).
- Masses of charged and discharged water from the storage tank throughout the day (M^i_{ch} and M^i_{dis}, respectively).
- Mass of water provided by the peak-up boilers throughout the day (M^i_b). All these masses are calculated and provided as an input by the function explained in section 4.2.2.1.
- The basic dimensions of the storage tank as calculated in section 4.2.2.2.

Initially, the temperature evolution of the water stored in the hot water storage tank will be calculated. For this purpose, the methodology explained in section 3.2.5 will be applied. The only difference compared to this section is that the temperature of the water at the inlet of the storage tank will be variable, and not constant as in Chapter 3, and this has to be taken into account. Therefore, instead of calculating the heat surplus to the tank due to charging by Eq. (3.28), it is calculated by the following equation:

$$\dot{Q}^i_+ = M^i_{ch} \cdot Cp_w \cdot \left(T^i_{HST,i} - T_a\right) \tag{4.7}$$

So, the temperature evolution of the stored water can be easily calculated and, afterwards, the temperature evolution at the exit of the storage tank and after the mixing point (see Fig. 3.3) can be calculated. In order to do this calculation an equation similar to

(3.37) is used, but in this case the variation of the temperature at the inlet of the storage tank has to be taken into account again. So, the corresponding equation as follows:

$$\left(M_{tr,G} - \frac{M_{ch}^{i} + M_{ch}^{i-1}}{2}\right) \cdot T_{HST,i}^{i} + \frac{M_{dis}^{i} + M_{dis}^{i-1}}{2} \cdot T_{st}^{i} =$$
$$(M_{tr,G} - \frac{M_{ch}^{i} + M_{ch}^{i-1}}{2} + \frac{M_{dis}^{i} + M_{dis}^{i-1}}{2}) \cdot T_{HST,o}^{i} \quad (4.8)$$

By applying the above equation the temperature after the mixing point of the storage tank is calculated. Several notes that differentiate further the calculations in this case compared to those of Chapter 3 have to be made:

- At the first time interval, the term of the mass on the transmission network on G.H.E.'s side ($M_{tr,G}$) should be replaced by $\frac{M_{tr,G}^{P} + M_{tr,G}}{2}$, since the energy equation takes into account the second half of the last period of the previous day. This is the first time that the data of the previous day are needed.
- At the last time interval, under the same logic the mass data of the first interval of the next day are needed. Since these are unknown, it is assumed that they are equal to the data of the last period of the studied day. So, in this case, the temperature at the last point of the studied day may not be totally accurate. But, this point will be the first point of the next day, and it will be calculated very accurately. So, from an engineering point of view this assumption and the possible subsequent error is not important.
- For each time interval, if the water provided by the boiler is positive, which means that there is no water discharge, then the temperature after the mixing point is set directly equal to the temperature of the water before the mixing point ($T_{HST,i}^{i}$), since the above equation can cause some instabilities and the results are not accurate.

The outputs of this function will be the following:

- Temperature evolution of the stored water throughout the day (T_{st}^{i}).
- Temperature of the water after the mixing point throughout the day ($T_{HST,o}^{i}$).

4.2.2.4 Pipeline temperatures function

In this function, the temperature distribution across the pipelines is calculated. As mentioned earlier, the calculation of the temperature in the critical points of the network is adequate. This function is the basis of the next two functions and uses the method explained in section 3.2.6.3 and, more specifically, Eqs. (3.51)-(3.69). As explained in the aforementioned section, in order to calculate the temperature distribution across a set of double pre-insulated underground pipes, the temperature in the inlet of the supply pipeline as well as the temperature drop in the boundary of the pipeline has to be known. These two values have to be provided as an input to this function together with the geometrical characteristics (Dimensions, burial depth and distance between the pipelines) of the pipelines. The outputs of this function are the temperatures in the critical points of the pair of pipelines, i.e. the temperatures at the inlet and outlet of each pipeline.

4.2.2.5 Single iteration temperatures function

The function of this section together with the next one are the basic functions of this model. In this function the first calculation of the temperatures of the network for each point throughout the day will be carried out, while with the next function, as will be explained later, the complete calculation of all the variables of the network will be done. This function will be called by the next one, and will get some inputs that will be calculated at the beginning of the next function. The calculations are quite similar to those of section 3.2.6.4, but are limited only in the calculation of the heat losses or temperatures of the pipelines. These will be explained briefly here. The inputs of this function are as follows:

- Temperature at the inlet of the storage tank for each point ($T^{i}_{HST,i}$).
- Initial temperature of the stored water (T^{0}_{st}).
- The temperature of the water provided by the boiler ($T_{b,out}$).
- The mass provided by the boiler in each time interval (M^{i}_{b}).
- The mass of charged and discharged water of the storage tank in each time interval (M^{i}_{ch} and M^{i}_{dis}, respectively).
- The mass of stored water in each point (M^{i}_{st}).

- The mass of water in the transmission network in the left and the right of the storage tank, as well as the correspondent mass flow rates ($M_{tr,G}$, $\dot{m}_{tr,G}$, $M^i_{tr,S}$ and $\dot{m}^i_{tr,S}$, respectively).
- The mass flow rate on each branch of the distribution network for each time interval ($\dot{m}^i_{d.j}$).
- The temperature drop in the boundaries of each branch of the distribution network ($\Delta T_{d,j}$).
- The dimensions of the transmission network.
- The dimensions of all the branches of the distribution network.
- The dimensions of the storage tank.

It should be noted that most of the inputs of this function are calculated in the next function. Actually, this function operates as an intermediate step for the complete calculation of the variables of the network.

Some important assumptions made in Chapter 3 are recalled in this point. More specifically, it was assumed that the peak-up boiler is right after the storage tank and that both of these devices are very close to the substation. This is quite realistic, since with this approach a quicker response to the peak demands can be achieved. So, the heat losses between the storage tank and the peak-up boiler as well as the substation will be neglected. Additionally, it can be assumed that the hot transmission pipeline is up to the inlet of the storage tank. The cold storage tank will be at the beginning of the cold transmission pipeline. So, it can be said that both the pipelines of the transmission network have the same mass flow rate ($M_{tr,G}$). Finally, the total length of the transmission network will be used for the calculation of the heat losses, without causing an important error to the calculations.

The general method for the calculation of the temperatures of the whole network is as follows:

- Given the temperature at the inlet of the storage tank, by calling the function of hot storage tank heat balance, the temperature evolution at the outlet of the storage tank ($T^i_{HST,o}$) will be known.

- In order to calculate the temperature at the exit of the hot transmission pipeline, i.e. taking into account the possible influence of the incoming water by the boiler, the following energy conservation equation will be used:
$\left(M_{tr,G} - M_{ch}^{i} + M_{dis}^{i}\right) \cdot Cp_w \cdot \left(T_{HST,o}^{i} - T_a\right) + M_b^i \cdot Cp_w \cdot \left(T_{b,out} - T_a\right) = M_{tr,S}^{i} \cdot Cp_w \cdot (T_{tr,s,o}^{i} - T_a)$
- By applying the same discretization method as in section 3.2.2.4 for the calculation of the temperature after the mixing point of the storage tank, the temperature at the exit of the hot transmission pipeline will be known for each point ($T_{tr,s,o}^{i}$).
- Then, it is assumed that the outlet temperature of the hot transmission pipeline, calculated above, will be equal to the inlet temperature of all the hot pipelines of the transmission branches: $T_{trho}^{i} = T_{dho,j}^{i}$.
- For each branch of the distribution network, the inlet temperature of the hot pipeline is known as well as the temperature drop on its boundaries. So, for each branch and for each time-point, the function of the pipeline temperatures can be applied in order to find the temperatures in the critical points of the branches of the distribution network. These are $T_{d,s,o,j}^{i}$, $T_{d,r,i,j}^{i}$ and $T_{d,r,o,j}^{i}$, respectively.
- The mass flow rates of the return pipelines of the branches of the distribution network are mixed before they pass to the return pipeline of the transmission network. The heat losses in the mixing point are neglected and by applying the energy conservation equation in the mixing point, the inlet temperature in the cold transmission pipeline is calculated for each point ($T_{tr,s,i}^{i}$). The energy equation that is applied is the following: $\sum_j \dot{m}_{d,j}^{i} \cdot T_{d,r,o,j}^{i} = \dot{m}_{tr,S}^{i} \cdot T_{tr,r,i}^{i}$
- Then, for each point the temperature at the inlet of the storage tank (T_{sthi}^{i}) and the inlet of the cold transmission pipeline (T_{trci}^{i}) are known. So, taking into account the assumption made previously about what is considered as the transmission pipeline and by neglecting the thermal interference of the cold water storage tank, the temperature drop at the boundary of the transmission network can be calculated for each point as $\Delta T_{tr}^{i} = T_{HST,i}^{i} - T_{tr,s,i}^{i}$.
- The inlet temperature of the hot transmission pipeline is also known, as it is a basic input of the model. So, for each point the pipeline temperature function can be applied for the transmission network in order to find the temperatures at

the critical points of the transmission network. These are $T^i_{HST,}$, $T^i_{tr,s,i}$ and $T^i_{tr,s,o}$. It should be noted that the first of the above calculated temperatures is used as an input also.

The outputs of this function, as mentioned earlier, are the temperatures in the critical points of the whole network throughout the day. It should be noted that within this function only one calculation or one iteration of the temperatures is carried out. The name of this function comes from this fact. In the next function, a big loop for the accurate calculation of the temperatures of the network will be created and this function will be used within the loop.

4.2.2.6 Network calculation function

As mentioned before, the complete calculation of the variables of the network will be carried out within this function. The function described in section 4.2.2.5 will be used as a basis for that purpose. The inputs of this function are the following:

- Total heat demand data throughout the day (HD^i).
- Discretized heat demand data throughout the day (HD^i_j).
- The temperature at the inlet of the hot transmission pipeline, which is known and constant throughout the day ($T_{tr,s,i}$).
- The first approximation for the temperatures at the outlet of the supply transmission pipeline as well as the inlet and the outlet of the return transmission pipeline ($T_{tr,s,o,init}$, $T_{tr,r,i,init}$ and $T_{tr,r,o,init}$, respectively).
- The first approximation of the temperature drop of the geothermal fluid ($\Delta T_{G,init}$).
- The first approximation of the thermal efficiency of the installation ($\eta_{tot,init}$).
- The temperature of the water provided by the peak-up boiler ($T_{b,out}$).
- The previous day storage data, i.e. the mass and temperature of the stored water at the beginning of the day (M^0_{st} and T^0_{st}, respectively).
- Dimensions of both the transmission and distribution network.
- The temperature drop along the boundaries of each branch of the distribution network ($\Delta T_{d,j}$).
- The thermal efficiency of the in-house installation (η_{dw}).

It should be noted that the last two inputs will be calculated accurately in subsequent functions, and iterative processes will be used in order to find their precise values. So, actually, this function has as input a temperature drop and an efficiency and it does not matter if it is a precise or an estimated value. But, within this function all the other variables will be calculated precisely. For the sake of simplicity, in this section the symbol of initial estimation will be neglected for all the variables. It should also be noted, that it cannot be known in advance if the peak-up boilers will be used or not during the day, so it is assumed that the input of the efficiency equals to the total thermal efficiency of the installation. If the peak-up boilers are used, then this efficiency should be equal to the thermal efficiency of the geothermal part of the installation. This distinction will be made clear in the following functions.

A few equations used in Chapter 3 will also be used here in a very similar way. These equations will be written in full for reasons of completeness. Firstly, the daily heat demand of the studied day is calculated as:

$$DHD = \sum_{Day} HD^{i} \tag{4.9}$$

Subsequently, the geothermal energy and the corresponding geothermal power needed to cover the above demand can be calculated by:

$$E_{G,D} = \frac{DHD}{\eta_{tot}} \tag{4.10}$$

$$\dot{Q}_G = \frac{E_{G,D}}{24 \cdot 1000} \tag{4.11}$$

Where:

$E_{G,D}$ = Daily energy provided by geothermal energy in the studied day (kWh)

$\dot{Q}_G$ = Geothermal power provided in the studied day (W)

In this case, there is some stored water at the beginning of the day. The thermal power of this stored water has to be taken into account and is provided by the following equation:

$$\dot{Q}_{st}^{0} = \frac{M_{st}^{0} \cdot Cp_w \cdot (T_{st}^{0} - \min(T_{tr,r,o}^{i}))}{24 \cdot 3600} \tag{4.12}$$

Where:

$\dot{Q}_{st}^{0}$ = Thermal power of initially stored water in the hot water storage tank (W)

It should be mentioned that the minimum outlet temperature of the return transmission pipeline is used as the reference temperature, since this is the lowest temperature in the network. The above value is necessary for the calculation of the mass flow rate of geothermal water since it is an amount of energy/power that can also cover a part of the daily heat demand. So, the above value should be reduced from the necessary geothermal power for the cover of the heat demand. This mass flow rate will be the first estimation that is used as an input in the Water mass balances function (1.3.1). The mass flow rate of geothermal water will then be equal to:

$$\dot{Q}_G - \dot{Q}_{st}^{0} = \dot{m}_{G,1} \cdot Cp_w \cdot \Delta T_G \rightarrow \dot{m}_{G,1} = \frac{\dot{Q}_G - \dot{Q}_{st}^{0}}{Cp_w \cdot \Delta T_G} \quad (4.13)$$

This mass flow rate will be the first estimation that is used as an input in the Water mass balances function (4.2.2.1).

Since the characteristics of the distribution network together with the discretised heat demand are inputs of this function, the mass flow rate in each branch of the network is calculated with the following loop:

$$\left.\begin{array}{l} \textbf{\textit{For}}\ \textit{each branch } j\ \textit{of the network}\ \textbf{\textit{and for}}\ \textit{each time interval } i: \\ \dot{m}_{d,j}^{i} = \frac{HD_j^i}{Cp_w \cdot \eta_{dw} \cdot \Delta T_{d,j}} \end{array}\right\} \quad (4.14)$$

In the above expression, probably some transformations should be made in the numerator or the denominator in order to obtain the same units in both cases. Subsequently, the mass flow rate on the transmission network on the right of the storage tank can be easily calculated as the summation of the mass flow rates of the branches of the distribution network.

$$\dot{m}_{tr,S}^{i} = \sum_{j} \dot{m}_{d,j}^{i} \quad (4.15)$$

The correspondent value for the whole time interval is then calculated as:

$$M_{tr,S}^{i} = \dot{m}_{tr,S}^{i} \cdot TimeMesh \cdot 60 \tag{4.16}$$

In the above equation, $TimeMesh$ denotes the time discretization of the heat demand data in minutes. As a next step, the water mass balances function is called. Some inputs of that function have already been calculated within the studied function. By calling the water mass balances function, and using the above calculations, all the mass flow rates and mass exchanges of the network will be determined. Then, depending on the fluctuation of the heat demand throughout the day, it can be possible to use the peak-up boiler when it is not necessary, i.e. when there is more geothermal energy that can be provided. So, in order to minimize the use of the peak-up boiler and maximize the utilization of geothermal energy, the following loop is used:

$$\left.\begin{array}{c} \textbf{\textit{For}}\ each\ time\ interval\ i: \\ \textbf{\textit{While}}\ M_b^i > 0\ \textbf{\textit{and}}\ \dot{m}_{G,1} < \dot{m}_{well} \cdot N_{wells}: \\ \textbf{\textit{Then}}:\ \dot{m}_{G,1} = \dot{m}_{G,1} + 0.01 \\ \textbf{\textit{Call}}\ Water\ Masses\ Function \rightarrow \\ New\ values\ of\ M_b^i\ and\ of\ all\ the\ other\ outputs \end{array}\right\} \tag{4.17}$$

The second criterion in the above loop was set so that the geothermal flow rate will not become higher than the maximum available one. So, with the above calculations, the minimization of peak-up boiler use is achieved. Of course, the peak-up boilers are not necessarily phased out as the maximum geothermal flow rate might not be enough to cover the load. Then, another condition that should be satisfied is that the stored water volume must not exceed the capacity of the storage tank. For that purpose, the following loop is used:

$$\left.\begin{array}{c} \textbf{\textit{For}}\ each\ time\ interval\ i: \\ \textbf{\textit{While}}\ \frac{M_{st}^i}{\rho_w} > V_{HST}: \\ \textbf{\textit{Then}}:\ \dot{m}_{G,1} = \dot{m}_{G,1} - 0.01 \\ \textbf{Call}\ \text{Water Masses Function} \rightarrow \\ New\ values\ of\ M_{st}^i\ and\ of\ all\ the\ other\ outputs \end{array}\right\} \tag{4.18}$$

Where:

V_{HST} = Volume of the hot water storage tank, which is a general input in the algorithm (m^3)

In the above loop, the criterion for the maximum geothermal flow rate is not used, since the geothermal flow rate is decreased only, so it cannot be higher than the maximum available flow rate. Therefore, now, all the final mass flow rates and mass exchanges of the network are known for each time interval.

The dimensioning of the hot storage tank function will then be called, so that the dimensions of the storage tank will be known. All the necessary inputs for the function explained in section 4.2.2.5 are now available, so, in order to calculate the temperatures of the whole network the following steps are carried out:

- First, the following initial estimations are made: $T^i_{HST,i}$=$T_{tr,s,o,init}$, $T^i_{tr,r,i} = T_{tr,r,i,init}$ and $T^i_{tr,r,o} = T_{tr,r,o,init}$.
- **Call** One Iteration Temperatures function→ New values of $T^i_{HST,i}$, $T^i_{tr,r,i}$ and $T^i_{tr,r,o}$ are now known together with the other results of this function.
- For the final calculation of all the temperatures of the network a correction of the estimated temperatures should be made. This is done by the following iterative loop:

  For each point:
  While $abs\left(T^i_{HST,i,new} - T^i_{HST,i}\right) > 10^{-6}$ **or** $abs\left(T^i_{tr,r,i,new} - T^i_{tr,r,i}\right) > 10^{-6}$ **or** $abs\left(T^i_{tr.r.o.new} - T^i_{tr,r,o}\right) > 10^{-6}$:
  Then: $T^i_{HST,i} = T^i_{HST,i,new}$, $T^i_{tr,r,i} = T^i_{tr,r,i,new}$ and $T^i_{tr,r,o} = T^i_{tr,r,o,new}$
  Call One Iteration Temperatures Function→ $T^i_{sthi,new}$,$T^i_{trci,new}$ and $T^i_{trco,new}$

It should be noted that the above iteration concerns the temperatures of the network, so the object of the iteration concerns the points rather than the time intervals. When the above multiple iteration converges, all the temperatures of the network will be calculated for each point, apart from the temperatures between the hot storage tank and the substation ($T^i_{HST,o}$ and $T^i_{tr,s,o}$). The hot storage tank losses function is called in order to calculate these values. So, finally, all the temperatures across the network have been calculated.

The outputs of this function, which are the main outputs of the whole model, are the temperatures of the critical points of the whole network throughout the whole day, all the

mass exchanges of the network and the corresponding mass flow rates; the geothermal mass flow rate; as well as the number of wells that should be operated during that day.

4.2.2.7 Optimum ΔT_G function

As already referred, the function described in section 4.2.2.6 calculates all the variables of the network having as input a temperature drop of the geothermal fluid as well as an efficiency of the installation. As a first step, these are the initial estimates used as inputs in the whole model. But, then, these values have to be renewed in order to find them precisely for the studied day, because these values will not be the same every day. Furthermore, as will be seen in Eq. (4.19), the temperature drop of the geothermal fluid is different at each point during the day, while these results depend on the initial value used in section 4.2.2.6. In order to overcome the dependency of the results on the initial estimation of the temperature drop, an optimum value of the temperature drop that minimizes this difference has to be found. In practice, this will be the final average temperature drop throughout the day. The function described in this section will be the objective function that will be called in a later function and will find the optimum value of the temperature drop of the geothermal fluid. In this function, the only input is a temperature drop of geothermal fluid.

Firstly, the network calculation function is called for the calculation of the variables of the network. The rest of the inputs of this function will be provided by the later function that is calling the objective function described here. Then, the temperature drop of the geothermal fluid is calculated as follows:

$$\left.\begin{array}{l} \boldsymbol{For}\ each\ point: \\ \Delta T_G^i = R_m \cdot \frac{T_{tr,s,i} - T_{tr,r,o}^i}{\eta_{GHE}} \end{array}\right\} \tag{4.19}$$

Where all the terms have been explained in previous sections

The difference of the above calculated values compared to the input value of temperature drop can be easily calculated as:

$$\left.\begin{array}{l} \boldsymbol{For}\ each\ point: \\ \Delta T^i = abs(\Delta T_G - \Delta T_G^i) \end{array}\right\} \tag{4.20}$$

Finally, the objective function, i.e. the output of this function, will be the summary of the above residuals:

$$\Delta T_{tot} = \sum_{i} \Delta T^{i} \tag{4.21}$$

Later on, in the function that will call this objective function, the minimization of ΔT_{tot} will be the objective. Finding the value of the geothermal temperature drop that provides the minimum value of ΔT_{tot} means that this is the optimum estimate, which is the target of this section.

4.2.2.8 Efficiencies function

In this function, the thermal efficiency of the geothermal part of the installation as well as the total thermal efficiency of the installation will be calculated. In the beginning of the model, an efficiency is used as an input. This efficiency is initially considered equal to both of the previously referred efficiencies. If the peak-up boilers are used within the day, these efficiencies will be different and will be calculated in this function, otherwise a more precise value of the unique thermal efficiency will be calculated. The inputs of this function are a temperature drop of the geothermal fluid (ΔT_G), a value of total thermal efficiency (η_{tot}) and the thermal efficiency of the peak-up boilers (η_b).

Initially, the network calculation function is called for the calculation of all the variables of the network. As happens in the function described in section 4.2.2.7, the rest of the inputs will be calculated in the next, and final function, that will call the function described here.

The heat energy of the stored water at the first point (Q_{st}^{0}) can be calculated by Eq. (4.12) without dividing by the time frame ($24 \cdot 3600$), while for the last point can be calculated in a similar way as:

$$Q_{st}^{N} = M_{st}^{N} \cdot Cp_{w} \cdot (T_{st}^{N} - \min(T_{tr,r,o}^{i})) \tag{4.22}$$

Then, it is assumed, that the feeding water of the peak-up boiler is pumped from the cold storage tank, whose temperature is assumed to be 1 degree lower than the average temperature of the inlet of the return transmission pipeline. The cold storage tank will be

very close to the substation, so the temperature of the water pumped in the tank will be equal to that of the inlet of the return transmission pipeline. On the other hand, the 1 degree is assumed to be the heat losses of the tank, taking into account the heat losses of the hot storage tank as found in Chapter 3; it is likely an overestimation of its real value. Of course, from an engineering point of view, this is acceptable as the error will not be that big and a possible overestimation will lead (as will be seen below) to values of fuel used being higher than the real ones.

$$T_{b,in} = average\left(T_{tr,r,i}^{i}\right) - 1 \tag{4.23}$$

Where:

$T_{b,in}$ = Input water temperature in the peak-up boilers (K)

The total mass of water provided to the network by the boiler can be easily calculated as:

$$M_{b,tot} = \sum_{i} M_{b}^{i} \tag{4.24}$$

So, the heat provided by the boiler to the network and the heat input of the fuel to the boiler are calculated as:

$$Q_{b,tot} = M_{b,tot} \cdot Cp_{w} \cdot (T_{b,out} - T_{b,in}) \tag{4.25}$$

$$Q_{f,tot} = \frac{Q_{b,tot}}{\eta_{b}} \tag{4.26}$$

The heat provided by geothermal energy throughout the day will be calculated using the new value of geothermal flow rate, which is provided by the network calculation function which is called in the beginning of this function, and the temperature drop of the geothermal fluid which is used as input in this function.

$$Q_{G} = \dot{m}_{G} \cdot Cp_{w} \cdot \Delta T_{G} \cdot 24 \cdot 3600 \tag{4.27}$$

Afterwards, the total thermal efficiency of the installation can be calculated with the following equation:

$$\eta_{tot} = \frac{DHD + Q_{st}^{N}}{Q_{st}^{0} + Q_G + Q_{f,tot}} \quad (4.28)$$

In order to define the thermal efficiency of the geothermal part of the installation, the part of the daily heat demand that is covered by geothermal energy has to be calculated. For this purpose, the following equations are used:

$$M_{tr,S,tot} = \sum_{i} M_{tr,S}^{i} \quad (4.29)$$

$$DHD_G = DHD \cdot (1 - \frac{M_{b,tot}}{M_{tr,S,tot}}) \quad (4.30)$$

Where:

$M_{tr,S,tot}$ = Total amount of water during the studied day in the right of the storage tank (kg)

DHD_G = Part of the daily heat demand covered by geothermal energy (kWh)

So, the thermal efficiency of the geothermal part of the installation can be easily calculated in a similar way as for the total thermal efficiency as:

$$\eta_G = \frac{DHD_G + Q_{st}^{N}}{Q_{st}^{0} + Q_G} \quad (4.31)$$

Obviously, if the peak-up boiler is not used, all the heat demand will be covered by geothermal energy and the two efficiencies will be identical. Finally, in order to calculate the necessary amount of fuel for each time interval, the following set of equations is used:

$$\left.\begin{array}{c} \textbf{\textit{For}}\ each\ time\ interval\ i\text{:} \\ Q_b^i = M_b^i \cdot Cp_w \cdot (T_{b,out} - T_{b,in}) \\ Q_f^i = \frac{Q_b^i}{\eta_b} \\ M_f^i = \frac{Q_f^i}{LHV_f} \end{array}\right\} \quad (4.32)$$

Where:

Q_b^i = Heat provided by the peak-up boilers to the water in each time interval (J)

Q_f^i = Heat provided by the fuel in the peak-up boilers in each time interval (J)

M_f^i = Amount of fuel used by the peak-up boilers in each time interval (kg)

LHV_f = Lower heating value of the fuel used in the peak-up boilers ($\frac{J}{kg}$)

The final outputs of this function will be a renewed value of the total thermal efficiency of the installation and of the geothermal part of the installation (η_{tot} and η_G, respectively) as well as the quantity of fuel used in the boiler at each time interval (M_f^i).

4.2.2.9 Final results function

This is the final function of the model, which provides the final results for the studied day. Actually, in this function there are very few calculations carried out and mainly the previous functions are called for that purpose. It should be noted that this is the only function which is called in the main body of the code. All the other functions are called either within this function or within other functions. The inputs of this function are the following:

- Total heat demand data (HD^i).
- Mass and temperature of stored water at the last point of the previous day (M_{st}^0 and T_{st}^0).
- Initial estimations of the temperatures of the transmission network ($T_{trho,init}$, $T_{trci,init}$ and $T_{trco,init}$).
- Initial estimation of the temperature drop of the geothermal fluid ($\Delta T_{G,init}$).
- Initial estimation of the total thermal efficiency of the installation ($\eta_{Tot,init}$).

In order to minimize the inputs in this function, it is noted that it is necessary to use as inputs in any function in Python, those variables that can change during the calculations. Although in previous functions, some constant variables have been used as inputs, this does not happen in this case as the number of inputs in this case would be very big.

Firstly, the optimum temperature drop of the geothermal fluid has to be found. For that purpose, the objective function described in section 4.2.2.7 will be used. Python programming language has a lot of built-in optimization algorithms. The optimization method that is used in this case is the bounded Brent's method (see, for example, Gonnet,

2002). The bounds of the optimization will be $\pm 5K$ around the initial estimation. It was shown in practice that this range of boundaries includes the optimum solution in most of the cases and provides a very acceptable computational time.

So, by applying this optimization method, the optimum value of the temperature drop of the geothermal fluid is calculated. Then, the function described in section 4.2.2.8 is called in order to find the values of the total thermal efficiency of the installation as well as of the geothermal part of the installation. It is recalled that that the optimum value of the temperature drop of the geothermal fluid will be used as an input in this function. Then, the following loop is used in order to find the final values of efficiencies:

$$\left.\begin{array}{c} \textbf{While } abs\left(\eta_G - \eta_{tot,init}\right) > 10^{-6}: \\ \textbf{Then: } \eta_{tot,init} = \eta_G \\ \textbf{Call } \text{Efficiencies Function} \rightarrow \text{ New values of the efficiencies} \end{array}\right\} \quad (4.33)$$

It should be noted that in the above loop, the thermal efficiency of the geothermal part of the installation is compared with the initial estimation of the total thermal efficiency. As already mentioned, in the initial estimation it is assumed that the peak-up boilers are not used. So, when the above loop converges, the final efficiencies of the installation will be known as well as the mass of fuel used per time interval.

Then, in order to calculate the final results, the network calculation function (see section 4.2.2.6) is called. The optimum value for the temperature drop of the geothermal fluid is used as well as the final thermal efficiency of the geothermal part of the installation, which have been both calculated before. Finally, since all the mass flow rates across the network are known, Eqs. (3.44)-(3.49) are applied to each time interval for the calculation of the electrical power provided by the pumps. The final outputs of this function, which are the final outputs of the whole model, will be summarised in section 4.2.3.

4.2.2.10 Hierarchy of functions

In the following figure, the hierarchy of the functions used in this model is shown in order to make the whole process more comprehensible. For the sake of simplicity, the functions described in sections 4.2.2.1-4.2.2.9 will be assigned with the following abbreviations:

- **WMB** (section 4.2.2.1) "Water mass balances "
- **DHST** (section 4.2.2.2) "Dimensioning of the hot water storage tank"
- **HSTHB** (section 4.2.2.3) "Hot water storage tank heat balance"
- **PT** (section 4.2.2.4) "Pipeline temperatures"
- **SIT** (section 4.2.5) "Single iteration temperatures"
- **NC** (section 4.2.6) "Network calculation"
- **ODT** (section 4.2.7) "Optimum ΔT_G"
- **EFF** (section 4.2.8) "Efficiencies"
- **FR** (section 4.2.9) "Final results"

The beginning of each arrow shows the callable function and the correspondent end shows the function within which is called. For example, function 5 calls functions 3 and 4, while functions 5 is called by function 6.

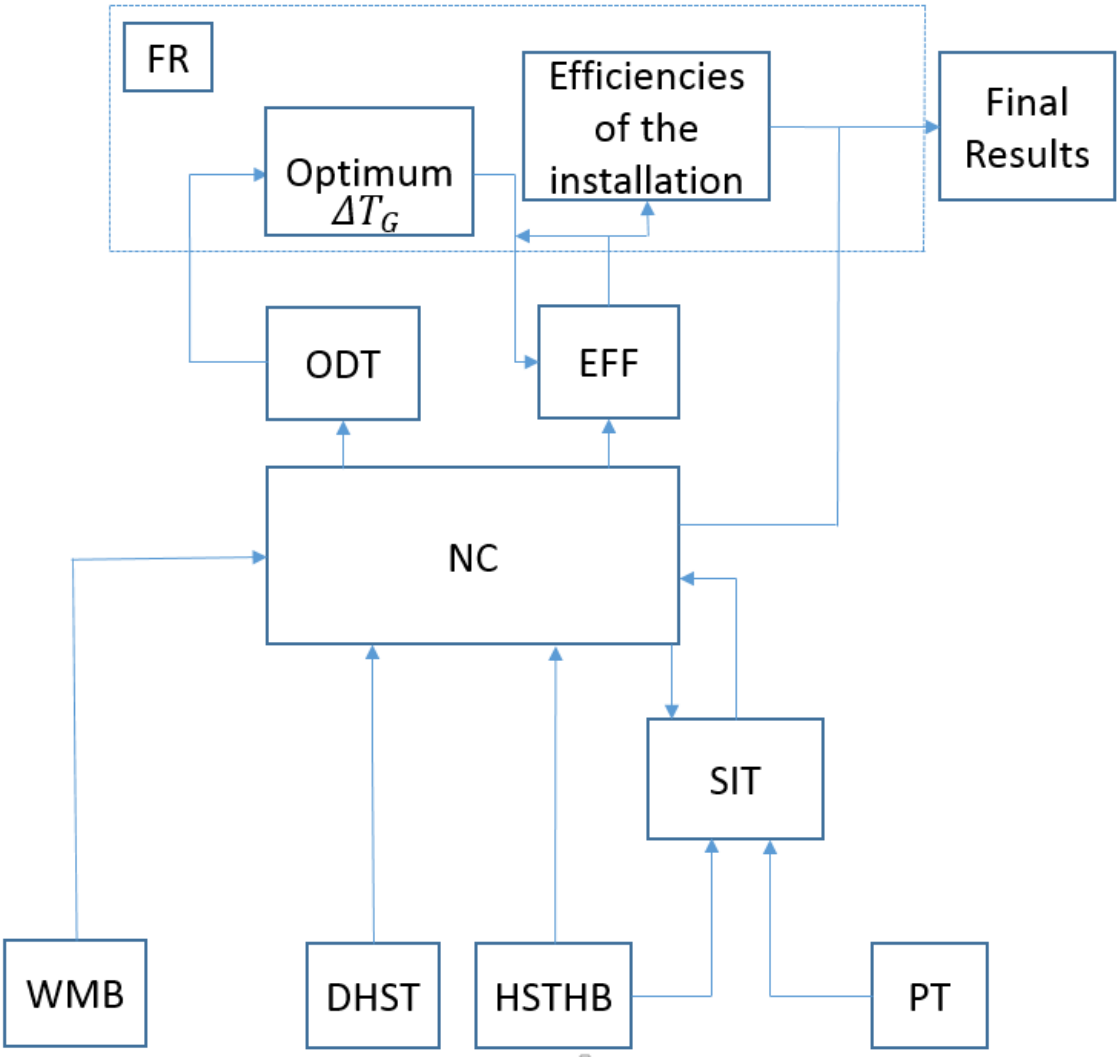

Figure 4.1 *Hierarchy of functions used in the developed model*

4.2.3 Output data

As mentioned before, the outputs of the model will be the outputs of the final results function described in sections 4.2.2.9. The outputs of this model are a number of different txt files, since most of the variables have a number of different values throughout the day. Those variables are recognised below by the superscript “i” and their result is an array or a matrix of values. So, storing the results in different files makes the distinction of the variables of different category much easier. A txt file is the simplest way of storing data, but, at the same time, is the easier way to handle them and pass them in any other kind of post-processing that the user might want. The results are divided to four main categories which are the general results, the results of the mass balances across the network, the results of the temperatures of the network and the data of the last point or time interval of the day that are necessary to run the algorithm the next day. Of course, each category can contain numerous txt files according to the nature of the variable stored. Furthermore, the exact way of storing the data depends also on the user. In our case, the way that the outputs will be written below do not necessarily represent the exact way they are stored, but they are written in the most understandable way.

The general results of this model are the following:

- The necessary geothermal flow rate ($\dot{m}_G$).
- The mass flow rate on the transmission network on the left of the storage tank ($\dot{m}_{tr,G}$).
- The number of wells in operation (N_{wells}).
- The average temperature drop of the geothermal fluid, which is the optimum value found by the function described in section 4.2.2.7 ($\Delta T_{G,opt}$).
- The thermal efficiency of the geothermal part of the installation (η_G).
- The total thermal efficiency of the installation (η_{tot}).
- The total electrical energy used by the pumps over the day ($C_{el,day}$).

The results of the mass balances across the network that are provided by this model are as follows:

- Main results: mass flow rate and the corresponding mass over a time interval of charged water in the storage tank ($\dot{m}_{ch}^{i}$ and M_{ch}^{i}, respectively); mass flow rate

and the corresponding mass over a time interval of discharged water from the storage tank ($\dot{m}_{dis}^{i}$ and M_{dis}^{i}, respectively); mass flow rate and the corresponding mass over a time interval of the water provided to the network by the peak-up boilers ($\dot{m}_{b}^{i}$ and M_{b}^{i}, respectively); mass flow rate and the corresponding mass over a time interval of fuel used in the peak-up boilers ($\dot{m}_{f}^{i}$ and M_{f}^{i}, respectively); mass flow rate and the corresponding mass over a time interval of the water on the transmission network in the right of the storage tank ($\dot{m}_{tr,S}^{i}$ and $M_{tr,S}^{i}$, respectively).

- Mass of stored water throughout the day (M_{st}^{i}). This variable is not written on the main results as it contains one value more.
- Mass flow rates on each branch of the distribution network throughout the day ($\dot{m}_{d,j}^{i}$).

Then, the results of the temperatures of the network are divided into the following two groups:

- Transmission network: temperature at the inlet of the hot water storage tank ($T_{HST,i}^{i}$); temperature of the stored water (T_{st}^{i}); temperature at the outlet of the hot water storage tank ($T_{HST,o}^{i}$); temperature at the outlet of the supply transmission pipeline ($T_{tr,s,o}^{i}$); temperature at the inlet of the return transmission pipeline ($T_{tr,r,i}^{i}$); temperature at the outlet of the return transmission pipeline ($T_{tr,r,o}^{i}$).
- Distribution network: temperature at the inlet of the supply distribution branches ($T_{d,s,i}^{i}$); temperature at the outlet of the supply distribution branches ($T_{d,s,o}^{i}$); temperature at the inlet of the return distribution branches ($T_{d,r,i}^{i}$); temperature at the outlet of the return distribution branches ($T_{d,r,o}^{i}$).

Finally, the results of the last point or time interval of the studied day that are necessary for the calculations of the subsequent day are the following (see also section 4.2.1):

- Masses per time interval: mass on the transmission network on the left of the storage tank ($M_{tr,G}$); mass on the transmission network on the right of the storage tank ($M_{tr,S}^{N}$); mass of charged water in the storage tank (M_{ch}^{N}); mass of

water discharged from the storage tank (M_{dis}^{N}); mass of water provided by the boiler (M_{b}^{N}).

- Storage data: temperature of stored water (T_{st}^{N}); mass of stored water (M_{st}^{N}).
- Mass flow rates on each branch of the distribution network ($\dot{m}_{d,j}^{N}$).

As the last category of output refers to the last point or time interval of the studied day, they are assigned the temporal superscript N. The only exception is the mass on the transmission network on the left of the storage tank which is constant throughout the day.

4.3 Operation over a year

The second model of this Chapter studies the operation of the installation over a whole year. The model of section 4.2 that studies the operation over a random day is used as a basis for that purpose. More specifically, this model is applied in series for each day across the year and the data of the last time interval or point of one day are used on the following day as the data of their first time interval or point and then a few more calculations are carried out. Although the model of this section uses many times the previous model, their natures are quite different. The model of a random day will actually be used as a tool by the technicians of the installation in order to know in advance how they should operate the installation a random day given the heat demand. On the other hand, the model developed here will theoretically be used before the construction of the installation in order to calculate several energetic, economic and environmental indices of the installation and compare these with the corresponding indices of a traditional geothermal district heating system that does not use a heat storage. This will indicate if eventually the inclusion of a heat storage is worthwhile or not and will be done with the methodology explained in Chapter 5. In other words, this model provides mainly the necessary inputs for Chapter 5. Furthermore, in this section the cold water storage tank and the peak-up boilers will be sized, since this requires installation data over the whole year rather than for a specific day, as occurred in the main sizing of the installation in Chapter 3.

The inputs of this model are the same as of those of the previous model apart from the heat demand data (total and discretized), where obviously the data of the whole year are used. Then, within the model these data are separated on the corresponding data for each different day and a counter is assigned on each day so that the proper heat demand data are used each time. Additionally, the model developed in section 4.2 requires some data from

the previous day in order to carry out the calculations. In this case, the same data are also required for the first day of the whole year, but cannot be known since theoretically the installation has not been built yet. Additionally, these data will have a small impact on the final results as the model will run for a whole year and, therefore, any error will diminish over time. So, an initial estimation of these values has to be made in the beginning of the algorithm. A logical initial estimation can be based on the results from the design-day.

Afterwards, the algorithm of section 4.2 is applied for every day of the year and the outputs explained in section 4.2.3 are available for each day of the year. As the nature of this algorithm is different, only some of these data are of interest for this model. Those data are either the necessary data for the rest of the calculations of this model or are the necessary input data for Chapter 5 and are direct outputs. Since these data are available for each day, they can be easily stored together in bigger arrays, so that the results of the whole year, and not of each day separately, are available for post-processing. In the rest of this section, the variables over the whole year will be indexed with the subscript *an* (annual). For example, if M_{st}^{i} is the mass of stored water for each point over a day, $M_{st,an}^{i}$ will be the mass of stored water for each point over the whole year. The only difference is that, in this case, the counter i will refer to the time interval over the whole year. The data of interest in this case are the following:

- The electrical power used by the pumps to overcome friction losses ($P_{el,an}^{i}$)
- The geothermal mass flow rate ($\dot{m}_{G,an}^{i}$).
- The mass on the transmission network in the right of the storage tank ($M_{tr,S,an}^{i}$).
- The mass of water provided by the boiler ($M_{b,an}^{i}$).
- The mass of fuel provided to the boiler ($M_{f,an}^{i}$).
- The temperature at the inlet of the return transmission pipeline ($T_{tr,r,i,an}^{i}$).
- The temperature at the outlet of the supply transmission pipeline ($T_{tr,s,o,an}^{i}$).

The last variable is used only in order to have an overview if at any time of the year the temperature at the outlet of the supply transmission pipeline falls below the minimum value set by the requirements of the end-users (see section 3.2.8).

The total electrical energy used by the pumps throughout the year is calculated as:

$$E_{el,tot} = \sum(P_{el,an}^{i} \cdot TimeMesh/60) \tag{4.34}$$

In the above equation, the final result will be in Wh or kWh depending on whether the power used is expressed in W or kW, respectively. It is a user choice to get the results in these units as it is more helpful for their post-processing.

In a similar way, the total mass of fuel provided to the boilers throughout the year can be easily calculated by summing all their individual values.

$$M_{f,tot} = \sum_{i} M_{f,an}^{i} \tag{4.35}$$

Then, the heat input to the boiler for each time interval can be calculated by Eqs. (4.25) and (4.25). The maximum of these values equals the capacity of the peak-up boilers as this value represents the maximum heat that has to be provided by the boilers. Therefore, theoretically no more heating power more than this will have to be provided. Of course, in reality, the boilers will probably be bigger in case of a geothermal system breakdown. So, the size of the peak-up boilers will be calculated by the following equation:

$$\dot{Q}_{pb} = \max\left(\frac{M_{b,tot} \cdot Cp_w \cdot (T_{b,out} - T_{b,in})}{\eta_b \cdot TimeMesh \cdot 60}\right) \tag{4.36}$$

In the above equation, the terms $TimeMesh$ and 60 in the denominator are used in order to get the result directly in units of power (Watts).

The sizing of the cold water storage tank will be done on the hypothesis that this storage tank will operate as a more general storage device compared to the hot water storage tank which will operate based on the fluctuation of the heat demand. In other words, it should be taken into account that the cold water storage tank should be able to store a bigger amount of water than the hot water storage tank in times of low load where the flow rates around the network will be quite small. At these times, there will be an increased need for storing a large amount of water that would otherwise circulate around the installation. On the other hand, in a case of very big fluctuations of the heat demand within a day there is the case that the hot water storage tank will be completely discharged

to cover the heat demand and right after that for the heat demand to be quite small, so that all this amount of water will need to be stored in the cold water storage tank. A logical intuitive assumption is that the volume of the storage tank will be equal to the volume of the hot water storage tank increased by the equivalent volume which is necessary to store the maximum amount of water in the left of the storage tank over three consecutive time intervals. Taking into account the maximum amount of water on the left of the storage tank over three consecutive time intervals seems to be an acceptable and adequate solution from an engineering point of view. So, the volume of the storage tank is calculated by the following equations:

$$\left.\begin{aligned} V_{CST} &= V_{HST} + \frac{\max(M_{+}^{i})}{\rho_w(\overline{T})} \\ M_{+}^{i} &= M_{tr,S}^{i-1} + M_{tr,S}^{i} + M_{tr,S}^{i+1} \\ \overline{T} &= average(T_{tr,r,o,an}^{i}) \end{aligned}\right\} \quad (4.37)$$

Where:

V_{CST} = Volume of the cold water storage tank (m^3)

The second part of the above expression is applied for every time interval apart from the first and the last one, as the calculations cannot be carried out in these cases. Furthermore, the reference density of water is calculated for the average temperature around the year of the inlet supply transmission pipeline, as this is the inlet temperature on the cold storage tank also. A more precise solution would be to take into account the density based on the temperature at each different time interval on which the mass surplus is calculated. But, in general, the fluctuation of the temperature at the inlet of the supply transmission pipeline is very small, so the fluctuation of the density is even smaller as the influence of the temperature on the density of water is quite small. Therefore, this selection is definitely acceptable for the studied case. So, by using expression (4.36) the volume of the cold water storage tank is found. Then, by applying the dimensioning of the hot water storage tank function, the dimensions of the tank are also calculated. It is recalled that this function can be used for any storage tank as it includes calculation on the geometry of the tank and calculations based on the internal pressure of the tank which are both independent of the temperature within the tank. So, with this process the cold storage tank is sized and with Eq. (4.36) the peak-up boilers are also sized. These were the two parts of the installation which were not sized with the methodology of Chapter 3 as data of the whole year were necessary for that purpose. So, the sizing of the installation is also

complete now. Finally, the average geothermal flow rate around the year is calculated by the following equation:

$$\overline{\dot{m}_G} = average(\dot{m}^i_{G,an}) \tag{4.38}$$

So, the final outputs of the whole model are the following:

- Total electrical energy used by the pumps ($E_{el,tot}$).
- Total mass of fuel used by the boilers ($M_{f,tot}$).
- Size of the peak-up boilers ($\dot{Q}_{pb}$).
- Volume of the cold water storage tank (V_{CST}).
- The average geothermal mass flow rate ($\overline{\dot{m}_G}$).

4.4 Results

4.4.1 Operation over random days

As mentioned before, the model that studies the operation of the installation over a random day will be mainly used as a tool by the technicians of the installation in order to know in advance how to operate the installation over any day with a known heat demand. So, only indicative results of random days can be shown here. Therefore, several indicative days have been chosen to show the effect of the sizing of the installation over its operation. The daily heat demands of the three days that were chosen as design-days in Chapter 3 are shown on Table 4.1. The days chosen in this section have daily heat demands that lie between the heat demands of the design-days for each case of sizing. For the case of simplicity, these days are named Day 1, Day 2, Day 3 and Day 4, respectively, and their daily heat demands are shown on Table 4.2. As can be seen on this table, the four selected days cover a big range of daily heat demands, from very low to very high heat demands. The mass of stored water for the four selected days for each case of sizing are shown in Figs. 4.2-4.13, respectively.

Table 4.1 *Daily heat demands of the design-day for each case of sizing as calculated in Chapter 3*

Case	Daily heat demand (kWh)
25%ile	51242
50%ile	102497
75%ile	157000

Table 4.2 *Daily heat demands of the random days chosen for study in this section*

Case	Daily heat demand (kWh)
Day 1	44696
Day 2	96340
Day 3	112459
Day 4	195378

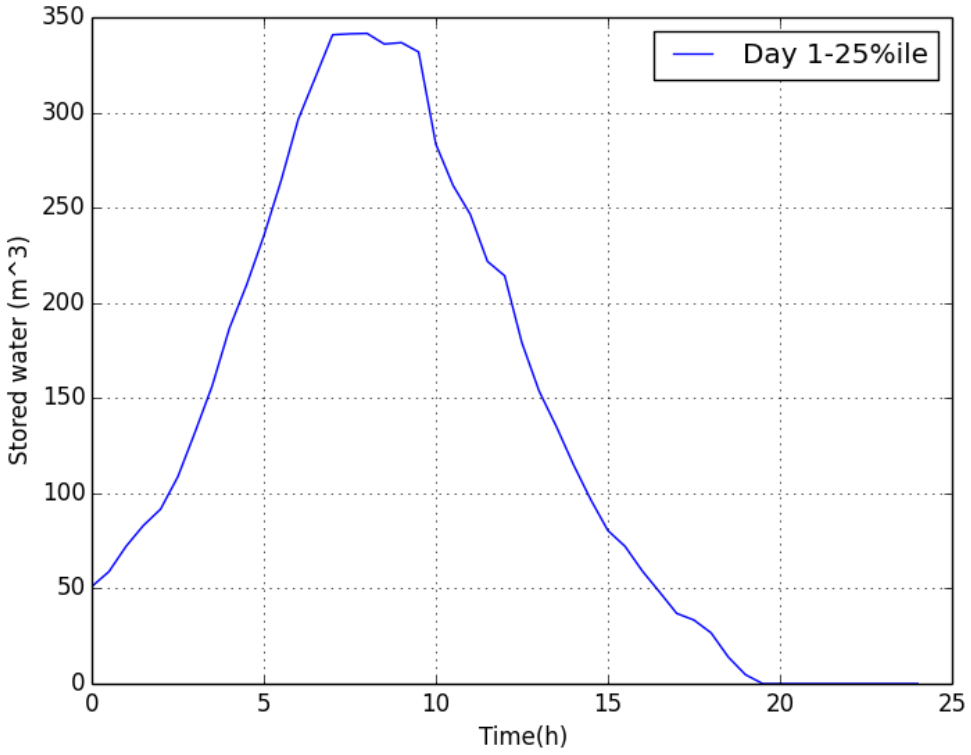

Figure 4.2 *Mass of stored water for Day 1 (25%ile sizing)*

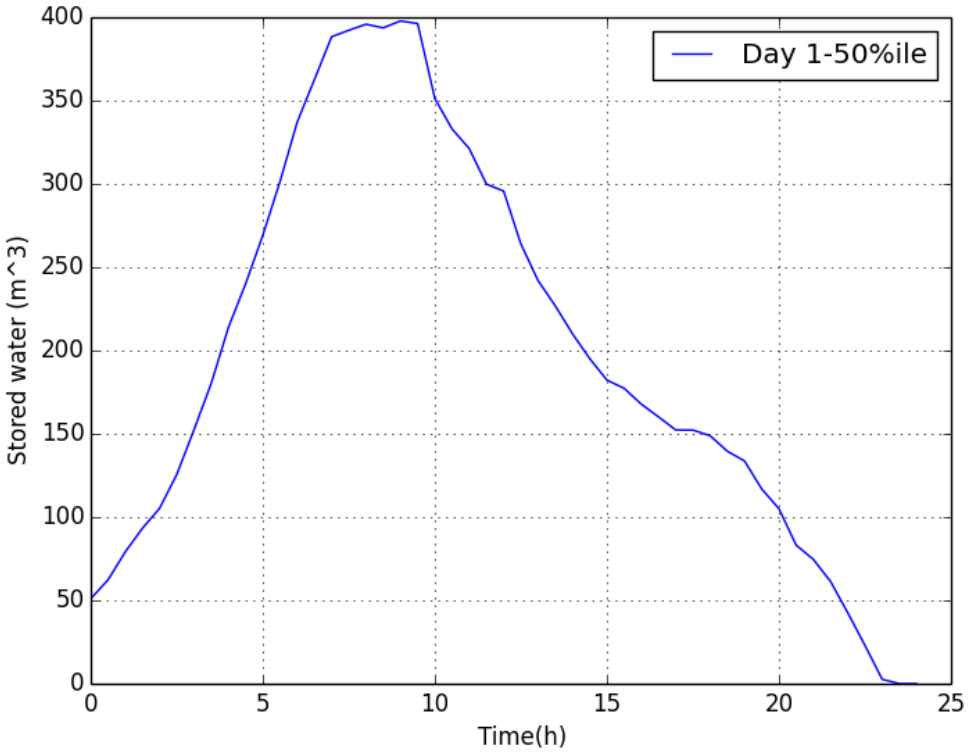

Figure 4.3 *Mass of stored water for Day 1 (50%ile sizing)*

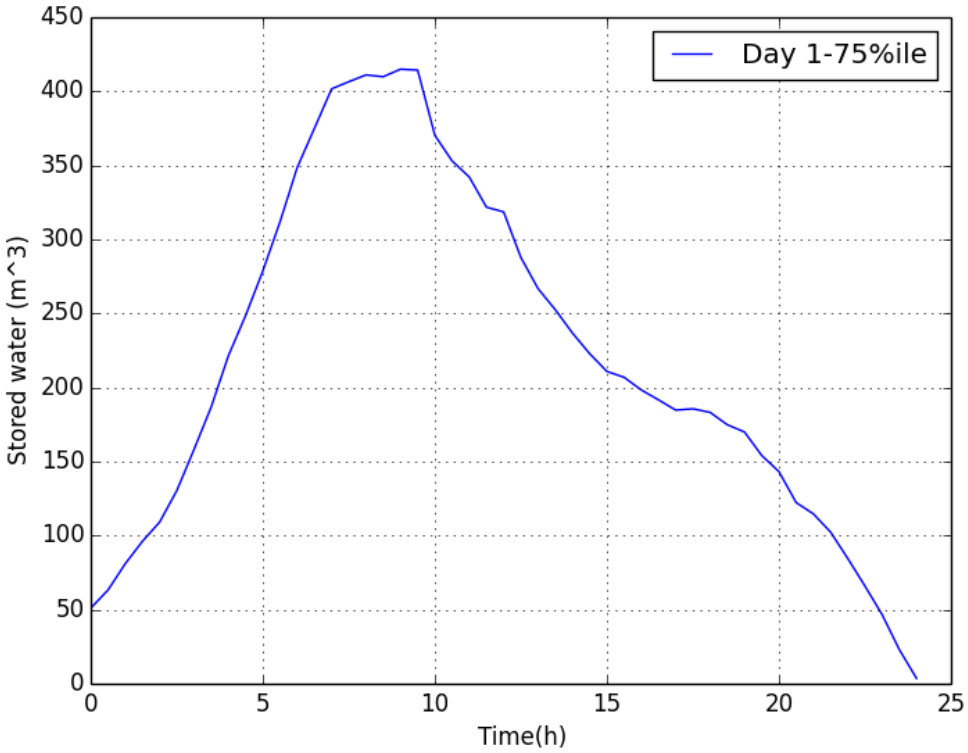

Figure 4.4 *Mass of stored water for Day 1 (75%ile sizing)*

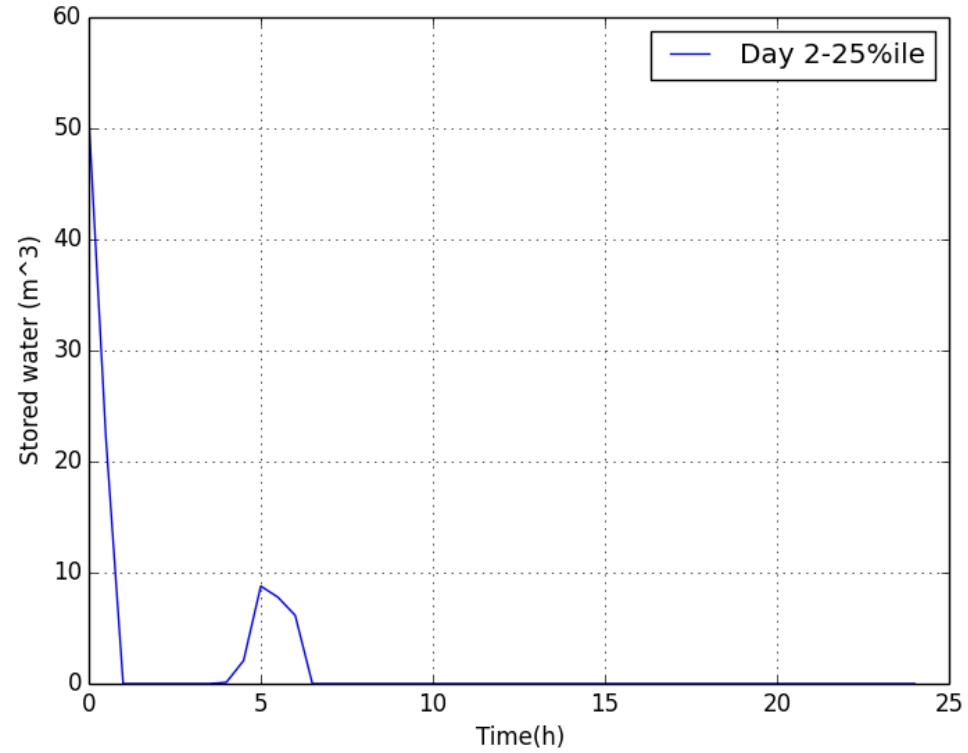

Figure 4.5 *Mass of stored water for Day 2 (25%ile sizing)*

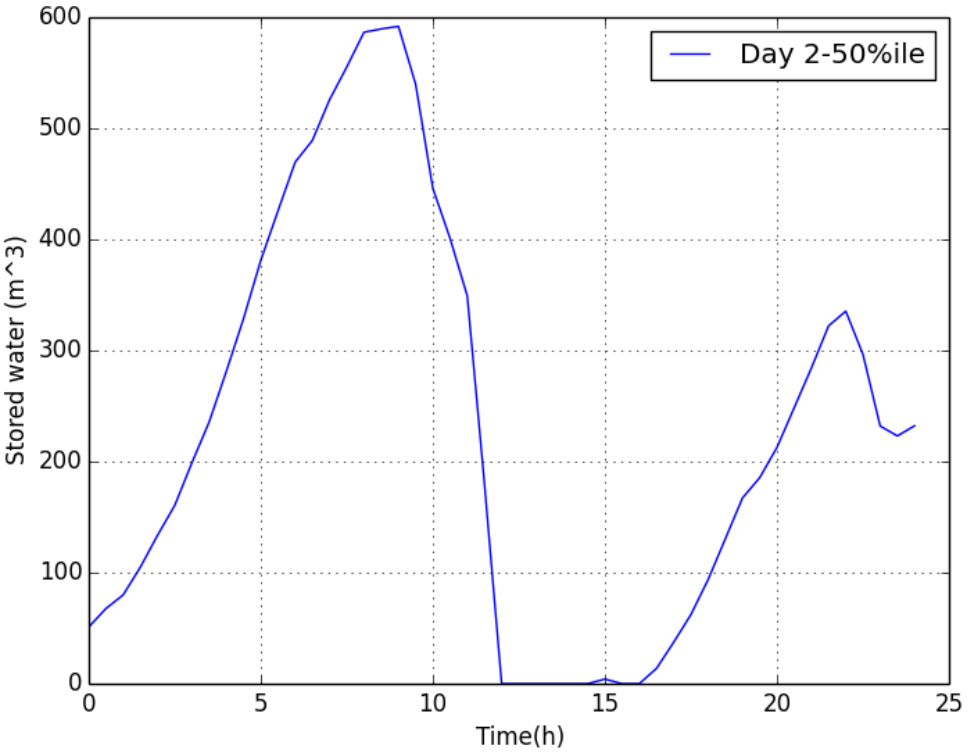

Figure 4.6 *Mass of stored water for Day 2 (50%ile sizing)*

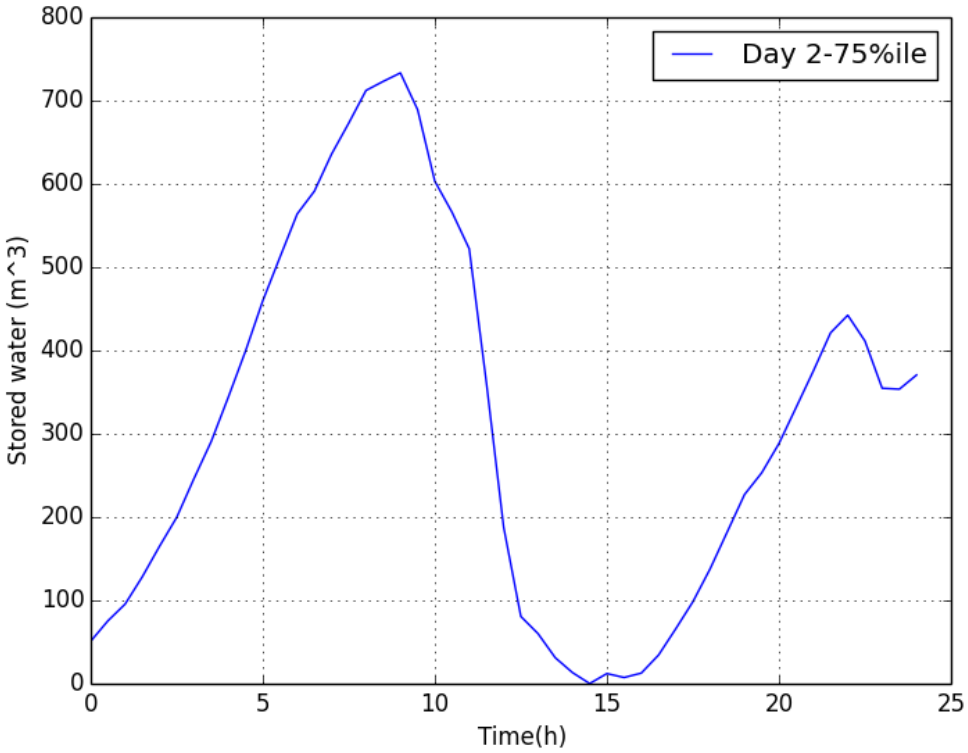

Figure 4.7 *Mass of stored water for Day 2 (75%ile sizing)*

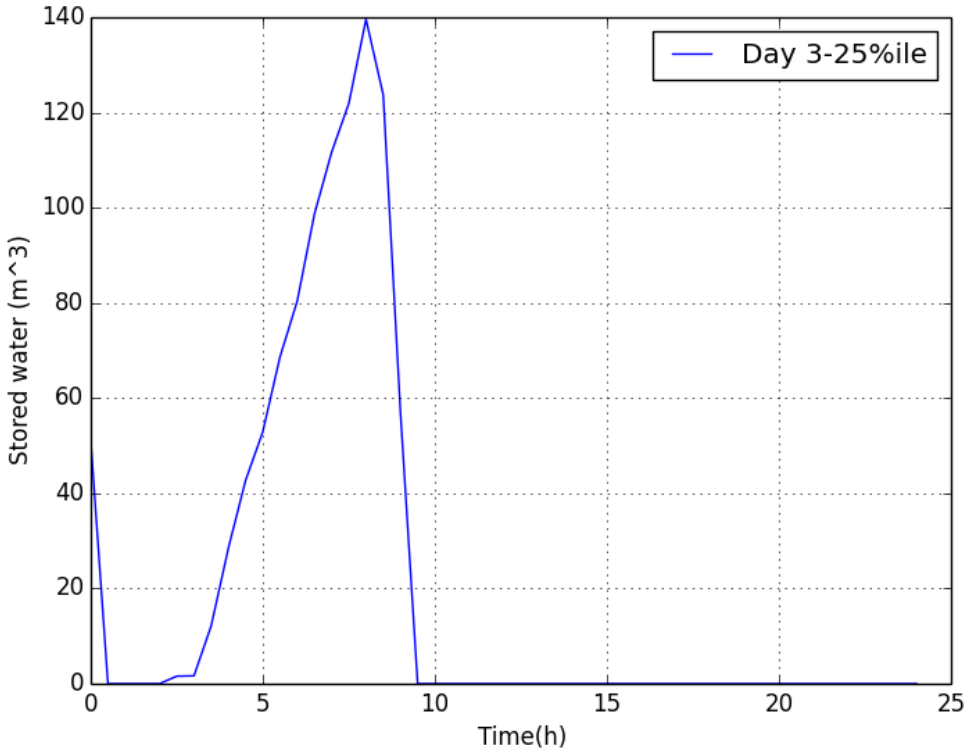

Figure 4.8 *Mass of stored water for Day 3 (25%ile sizing)*

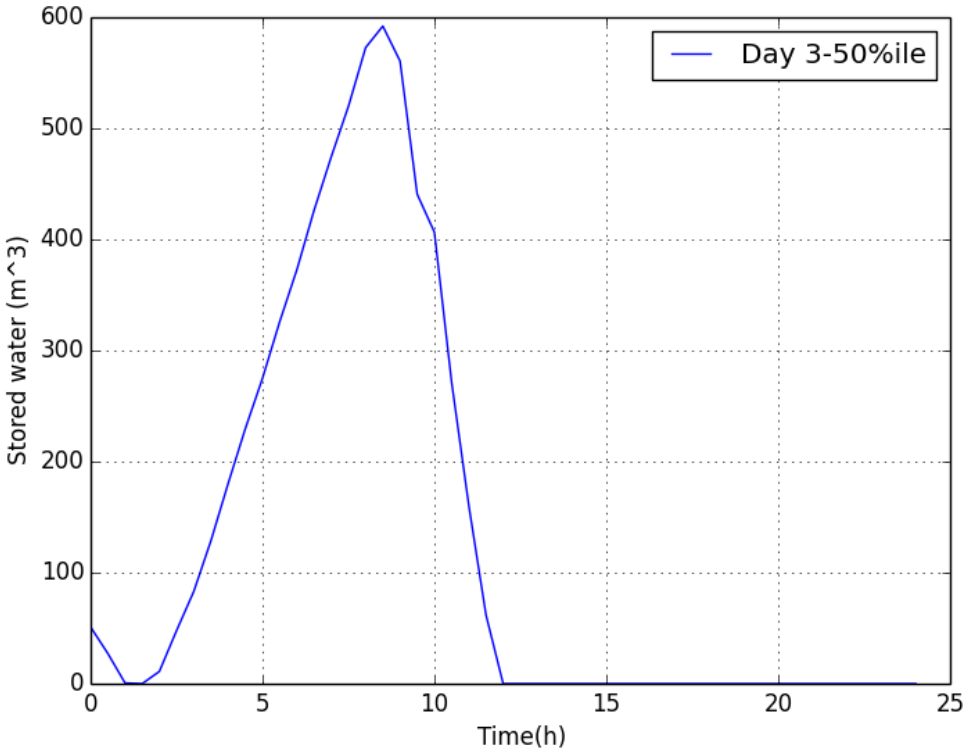

Figure 4.9 *Mass of stored water for Day 3 (50%ile sizing)*

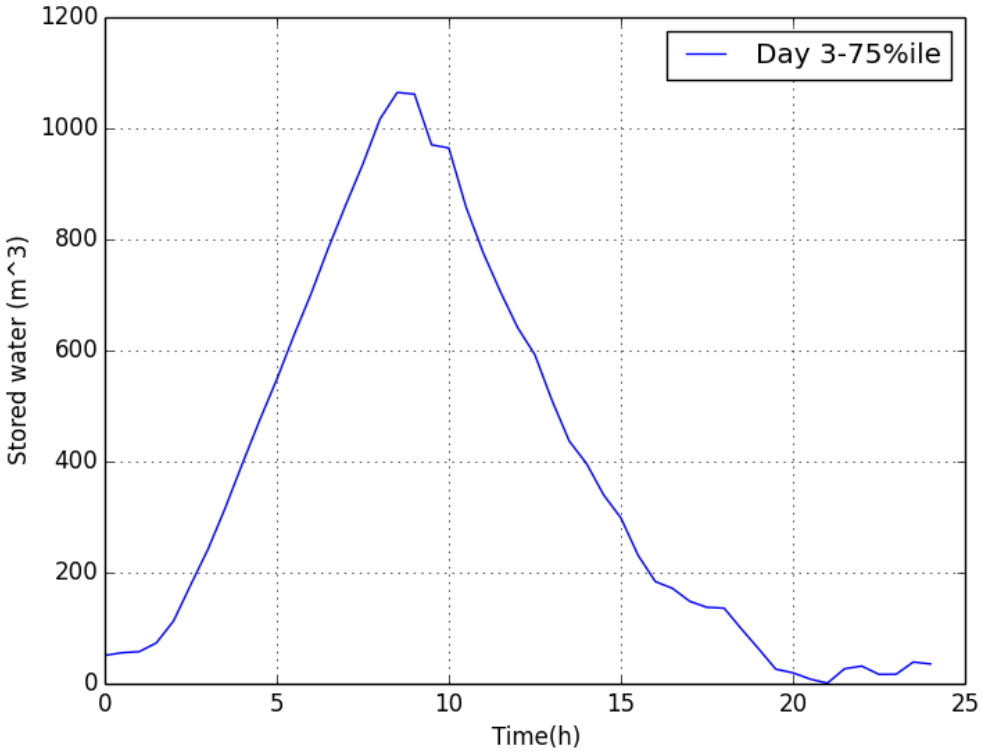

Figure 4.10 *Mass of stored water for Day 3 (75%ile sizing)*

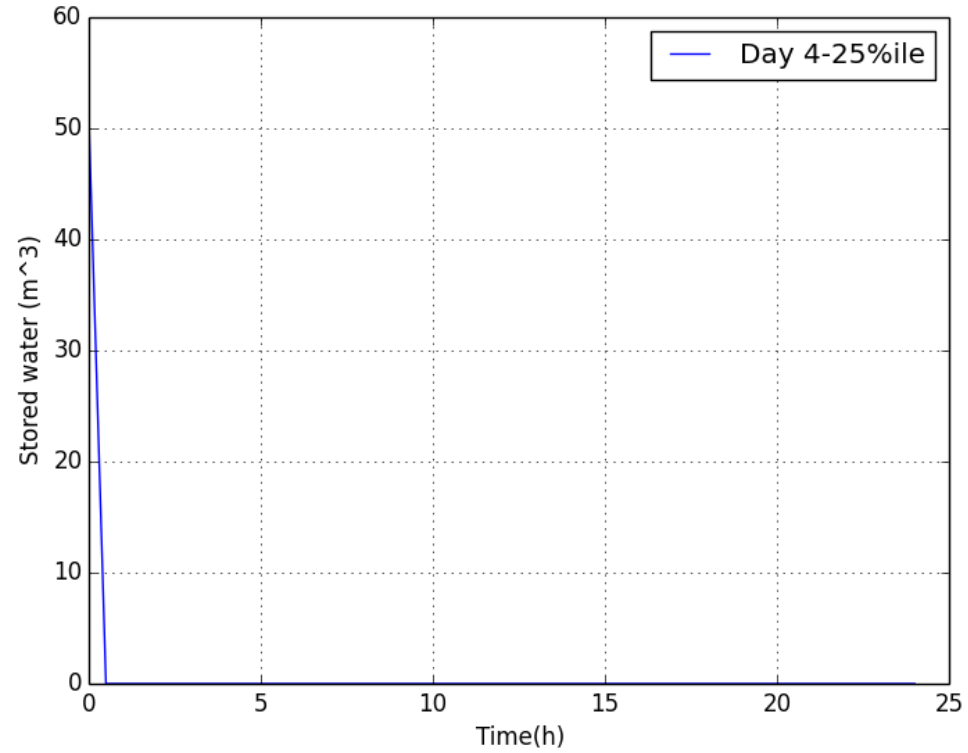

Figure 4.11 *Mass of stored water for Day 4 (25%ile sizing)*

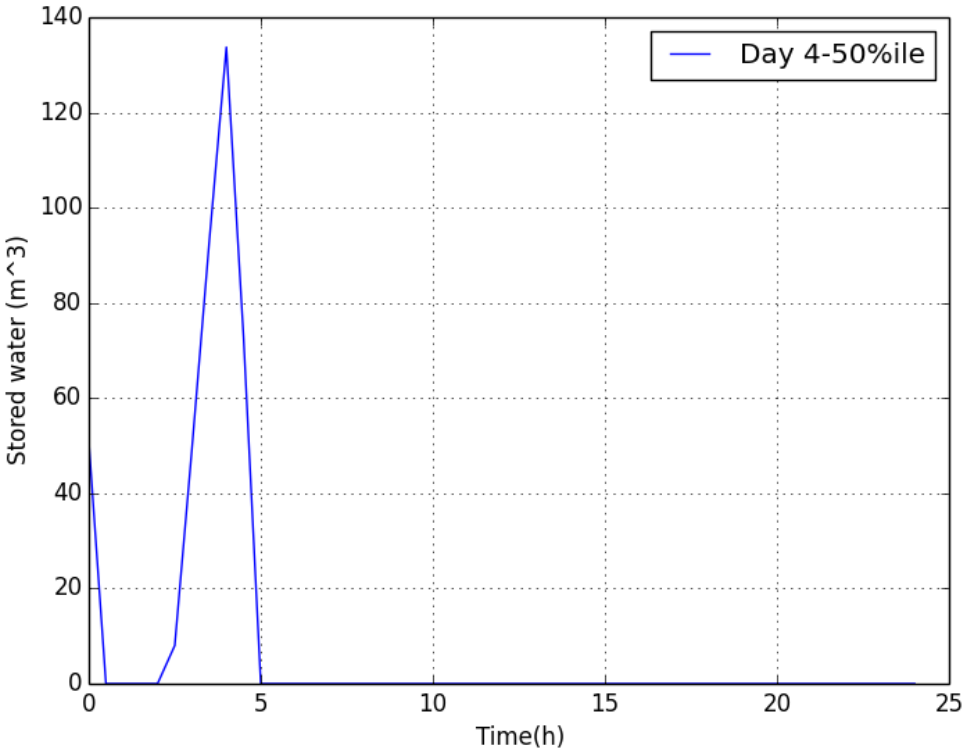

Figure 4.12 *Mass of stored water for Day 4 (50%ile sizing)*

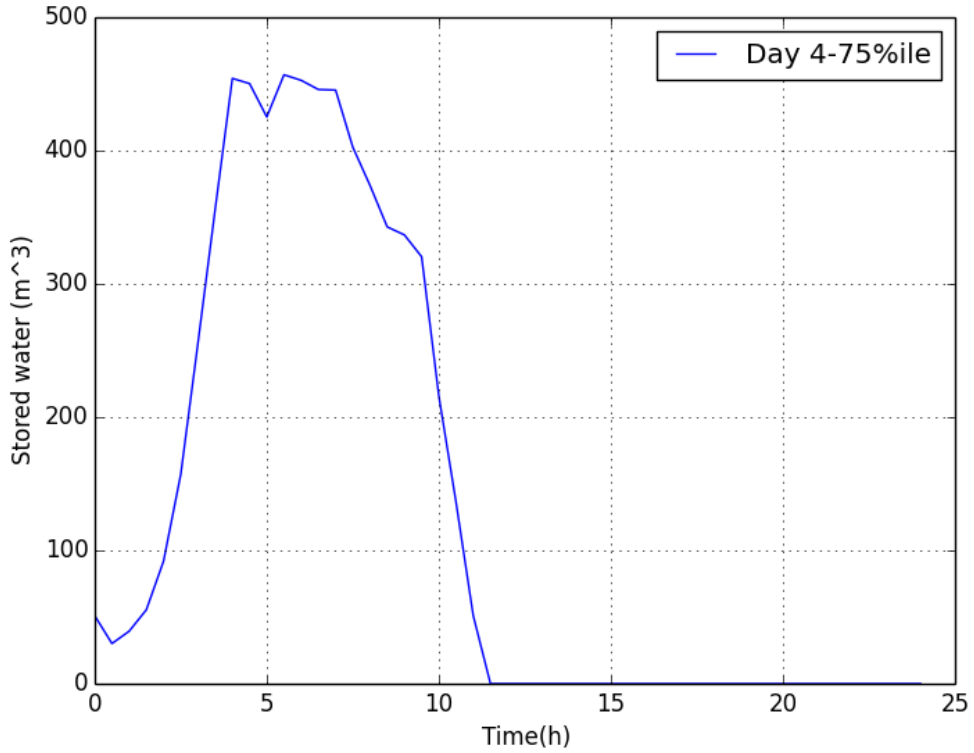

Figure 4.13 *Mass of stored water for Day 4 (75%ile sizing)*

Furthermore, in Table 4.3 the total mass of fuel used during the day for each case is shown, while in Table 4.4 the necessary geothermal flow rate for each case is shown.

Table 4.3 *Total mass of fuel (kg) used over the day for each case*

Case	**25%ile**	**50%ile**	**75%ile**
Day 1	440.08	43.75	0
Day 2	4471.05	486.71	0
Day 3	6069.25	2680.60	0
Day 4	14214.80	8891.59	3324.07

Table 4.4 Necessary geothermal flow rate (kg/s) for each case

Case	25%ile	50%ile	75%ile
Day 1	15.09	12.61	16.50
Day 2	20	36.01	38.66
Day 3	20	32.33	42.28
Day 4	20	40	60

4.4.2 Annual operation

In this section, the main results of the model of the annual operation of the installation will be presented, while the main results will also be presented for the traditional case of operation of a geothermal district heating system, i.e. without a heat storage. The traditional case is defined as the following case:

- No heat storage is used.
- The mass flow rate is not constant throughout the day, but follows the heat demand all the time.
- When the geothermal energy cannot cover all the heat demand, peak-up boilers are used.
- Apart from the heat storage, the rest of the installation has exactly the same dimensions as found in Chapter 3.

In other words, in the traditional case, the operation of an identical installation without the heat storage which is operated in the traditional way is studied. The main results of the studied case are shown on Table 4.5 for each case of sizing, while the results of the traditional operation are shown on Table 4.6. By comparing these two tables, the advantages of the proposed case will be identified. Finally, in Figs. 4.14-4.16 the volume of water stored in the hot water storage tank throughout the whole year is shown for each case of sizing, respectively.

Table 4.5 Main results of the studied case

Case	25%ile	50%ile	75%ile
Total energy used by the pumps (kWh)	1118013	297220	107323
Total fuel used by the boilers (kg)	1904221	712402	112402
Average geothermal flow rate (kg/s)	19.34	32.25	38.69
Size of peak-up boilers (kW)	15507	12607	8251
Size of cold storage tank (m^3)	1365.22	1606.04	2155.57

Table 4.6 Main results of the traditional operation of the installation

Case	25%ile	50%ile	75%ile
Total energy used by the pumps (kWh)	1116824	297141	107296
Total fuel used by the boilers (kg)	1992312	1002647	245580
Average geothermal flow rate (kg/s)	18.78	32.11	37.25
Size of peak-up boilers (kW)	15828	13272	9755

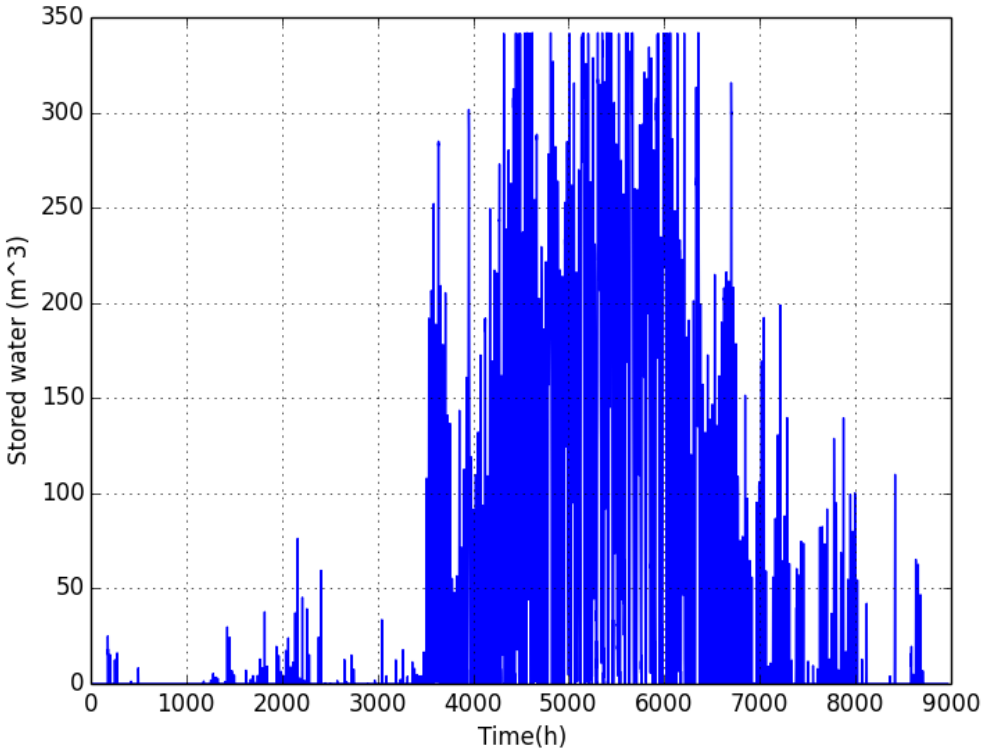

Figure 4.14 Volume of stored water over the year (25%ile sizing)

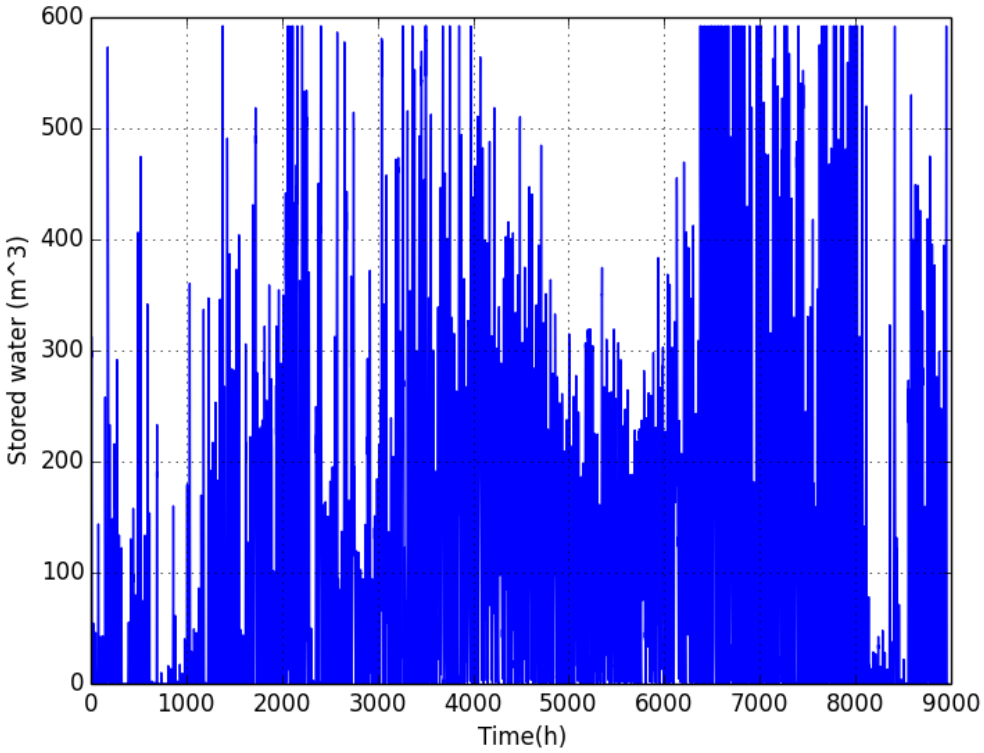

Figure 4.15 *Volume of stored water over the year (50%ile sizing)*

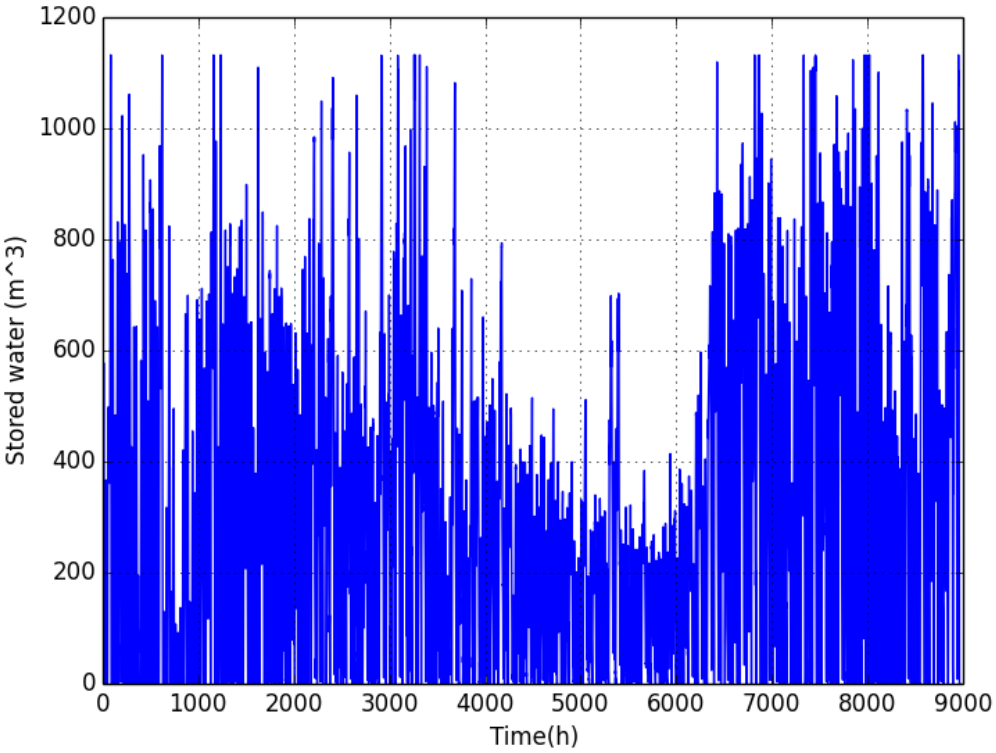

Figure 4.16 *Volume of stored water over the year (75%ile sizing)*

4.5 Discussion

Concerning the model of the operation over a random day, several interesting observations can be made through the corresponding results. Firstly, it is shown that for the same day of study as the sizing of the installation increases less fuel is used. This is totally expected because as the sizing increases, more geothermal energy is available to cover the heat demand. So, in the majority of the cases more geothermal energy is used for that purpose. An interesting exception in the observation of the higher geothermal flow rate is in Day 1, in the medium sizing of the installation, where the geothermal flow rate is lower than that of the low sizing of the installation. This occurs either because of the limitations of the geothermal flow rate (see Eq. (4.1)) or because the geothermal energy is much better harvested in this case due to the higher storage capacity. Furthermore, the heat storage also increases, which means that more geothermal energy can be stored in times of low load. So, all these lead to the conclusion that a larger sizing of the geothermal installation leads to a higher fraction of the load being covered by geothermal energy with subsequent decrease of the use of fuel.

The second observation concerns the influence of the increase of the daily heat demand for the same sizing of the installation. It can be seen that as the heat demand increases more fuel is used to cover the heat demand which is expected as the geothermal installation has a specific capacity and can never produce more heat than this capacity. This happens although the geothermal flow rate also increases as the heat demand increases (see Table 4.4). The only exception is the case of the medium sizing of the installation between Days 2 and 3 where the geothermal flow rate is lower in the second case, which is not expected as the heat demand is higher. This might occur for the same reasons as in the previous paragraph. So, in general, it can be said that, for a specific installation, as the heat demand increases both the geothermal flow rate and the fuel used will increase. If the heat demand is relatively low compared to the capacity of the installation (see 75%ile case in Table 4.3), the mass of fuel used will be zero and all the heat demand will be covered by geothermal energy.

A third observation that arises from Table 4.3 in conjunction with Tables 4.1 and 4.2 is that when the heat demand of a specific day is lower than the heat demand of the design-day of the specific installation, then all the heat demand will not be necessarily covered by geothermal energy. This is made clear on the case of Day 1: both in the low and the

medium sizing there is some fuel used to cover the heat demand, although the heat demand of the design day of both cases is higher than for Day 1. This happens because, as mentioned many times before, not only the total heat demand is important but also its fluctuation within the day. So, a specific day can have such a fluctuation of its heat demand from one time interval to the other that the heat demand at a specific time cannot be covered without the help of the peak-up boilers. This observation makes clear the importance of the fluctuation of the heat demand within the day.

Concerning the results of the annual operation of the installation, some very interesting points can be made both for the different sizing of the installation when the heat storage is used as well as between the cases where the heat storage is used and not. Firstly, when the heat storage is used, it is seen by Table 4.5 that the energy used by the pumps decreases when the sizing of the installation increases. This is justified by the fact that bigger pipelines are used when the sizing increases, so the friction losses, and subsequently the power required by the pumps, will decrease (see also section 3.2.6.2). Therefore, the total energy used by the pumps throughout the year will decrease. Then, it is observed that as the sizing of the installation increases the average geothermal flow rate throughout the year will increase. This is totally expectable as the annual heat demand is obviously the same in each case and since more geothermal energy is available as the sizing increases, more geothermal energy will be harvested. Another interesting observation on the geothermal flow rate is that the increase between the large and medium sizing is not so big as between the medium and the low sizing. Intuitively, the medium sizing is expected to be closer to the average demand throughout the year. So, in the case of the larger sizing, the geothermal installation will be under-utilized leading to an average geothermal flow rate which is higher than that of the medium sizing, but much smaller than its maximum flow rate (see Table 3.2).

On the other hand, more geothermal energy harvested means that a higher fraction of the annual heat demand is covered by geothermal energy, which in turn means that a smaller fraction of this demand has to be covered by the peak-up boilers. So, the fact that the fuel used throughout the year decreases as the sizing of the installation increases is totally justified. For the same reason, the size of the peak-up boilers also decreases as the sizing increases, since the peak demands that will have to be covered by the boilers will be lower. Finally, as the system sizing increases the size of the cold storage tank increases. This is expected as the size of the hot storage tank also increases as the system size increases, as seen in Chapter 3, while the second component which defines the size of the

cold storage tank will be almost the same for each case. This happens because its numerator will be exactly the same for each case and its denominator, which is the density of water, will be roughly the same as the density of water is almost constant for the range of the temperature used. In other words, the size of the cold storage tank will be almost directly proportional to the size of the hot storage tank for a specific heat demand throughout the year. So, as the sizing increases, the size of the hot storage tank increases and, subsequently, the size of the cold storage tank will increase.

By comparing Tables 4.5 and 4.6, an initial comparison between the studied case and the traditional operation of a geothermal district heating system can be made. First, it can be seen that the energy used by the pumps throughout the year is almost the same whatever the heat storage is used or not, for each case of sizing. This indicates that the total flow rate throughout the installation over a whole year will be almost the same without being affected by the presence of the heat storage. Then, it is observed that when the heat storage is used, the amount of fuel used throughout the year decreases. This indicates that with the inclusion of the heat storage, geothermal energy is utilised in a more optimal way decreasing the reliance on the peak-up boilers. This observation is among the most important of this thesis. It can also be observed that the average geothermal flow rate increases when the heat storage is used, but only slightly. This increase of the geothermal flow rate does not justify the decrease of the fossil fuel consumption, enhancing in this way the role of the heat storage in better matching demand and supply of heat.

Another interesting observation concerning the mass of fuel used, is that the absolute decrease when the heat storage is used in the low and large sizing cases is smaller than in the medium sizing. This happen because in the low sizing, the geothermal capacity is low compared to the heat demand on the majority of the times around the year, so all the geothermal energy will be sent time directly to the heat demand most of the time during the year. This can also be observed by Fig. 4.14 where it is seen that for a large amount of time around the year the amount of stored water is relatively low for the low sizing of the installation. So, the heat storage will not have a big impact in this case and the amount of fuel used will be roughly the same either whether the storage is used or not. On the other hand, in the large sizing of the installation the geothermal capacity is big enough to cover alone the heat demand the majority of time. So, the amount of fuel used will be small anyway and the decrease in the fuel consumption will be relatively small. All these indicate that the heat storage is better utilised in the case of the medium sizing of the installation, although a decrease in fuel consumption is observed in any case. This comes

in agreement with Figs. 4.14-4.16 where it is observed that in the medium sizing of the installation, more water is stored compared to the maximum capacity of the storage in each case. In the low sizing of the installation, as mentioned before, a large amount of time the storage is not used as all the geothermal production is sent directly to the load, while in the large sizing of the installation, the storage is not used that much mainly in periods of low load (summer months) as the heat demand can be covered solely by the adjustment of the geothermal flow rate in the appropriate value.

Finally, the size of the boilers increases when the heat storage is not used, which is expected as more and probably higher peak demands will occur in this case. But, the increase in the size of the peak-up boilers when the heat storage is not used is small compared to the increase in the mass of fuel used. This denotes that the peak demands throughout the year will be roughly the same numerically no matter whether the heat storage is used or not, but these will be much more frequent when the heat storage is not used. This reconciles the apparent disagreement between the increase of the size of the peak-up boilers and the increase in fuel consumption. A more detailed comparison between the studied and the traditional case will be carried out in Chapter 5, where economic, environmental and further energetic details will be calculated.

4.6 Summary

This Chapter studies in detail the operation of the installation sized in Chapter 3 either for a random day or for a whole year. So, two models were developed for the study of these two cases. The model that studies the operation of the installation over a random day was explained in section 4.2, while the model that studies the annual operation was explained in section 4.3. Then, the results for both models were shown in section 4.4 followed by an extensive discussion in section 4.5.

In the first model, the inputs are the sizing of the installation from Chapter 3. The topology of the installation that was also used as an input in Chapter 3 together with the heat demand of the random studied day are the other inputs of this model. Furthermore, some initial estimations which are derived from the design-day of the specific case are also used as inputs. By applying the model described in section 4.2, the operational strategy of the installation for the studied day will be known. It is recalled that the operational strategy is defined as the complete knowledge of the operation of the installation during the studied

day, i.e. the necessary geothermal flow rate, when and by how much should the storage tank be charged or discharged, when and by how much should the peak-up boilers be used etc. Furthermore, an analytical mapping of the temperatures in the critical points of the installation will also be known over the day. Finally, the electricity used by the pumps as well as the fuel used by the peak-up boilers throughout the day will also be known with the application of this model.

In other words, this model shows how the installation that is already built should be operated in a day with a known or predicted heat demand. Practically, it is much easier to predict the weather conditions rather than the heat demand of a specific (usually the next) day. For that purpose, an attempt to connect the given heat demand with the weather conditions of the area was attempted in Appendix B. The results of this Appendix are discouraging as it is shown that the correlation between the heat demand and the weather conditions is not always straightforward as other factors, such social factors or the heat capacity of the building, greatly influence the heat demand. These factors are, in general, difficult to predict, so this correlation is difficult to be produced. Of course, general conclusions cannot be made as this correlation and its influencing factors are very case-specific and in our case are not known. Theoretically, if this correlation is achieved, then by integrating this correlation with the model developed in section 4.2, the operation of the installation can be known the next day given the weather conditions. Intuitively, this is more useful than predicting the heat demand for any day as the weather forecasts are typically provided by professionals on the field and the accuracy is much higher than predicting the heat demand. So, if a robust correlation is built between the heat demand and the weather conditions, then one of the basic inputs of the model will be much more accurate and, subsequently, the operational strategy provided will be more precise and close to the reality. The other two main inputs of the model, i.e. the sizing and the topology of the installation, are constant and cannot cause any errors to the results. So, if the third input is more accurate, then, the accuracy of the results will increase a lot.

In the second model, the first model is used as a basis and is applied serially for each day of the year. In the first model, some variables from the previous day of study are needed as inputs, while some of the results from the last time interval will be used as inputs in the next day. In this case, the outputs of the previous day are used automatically as inputs of the next day. In general, the inputs of this model are the same as in the previous model apart from the heat demand, where the heat demand of the whole year is used. The outputs of this model are the same as for the previous one, but they concern the whole year

obviously. The outputs of interest in this case are mainly the total electricity used by the pumps and the mass of fuel used by the peak-up boilers throughout the year and the average geothermal flow rate. The first two comprise the main operational costs of the installation and will be among the main inputs in the economic analysis of the installation that will be presented in the next Chapter, while the average geothermal flow rate will be used for the calculation of the main energetic indices of the installation. Finally, this model provides also the size of the cold water storage tank as well as of the peak-up boilers, filling the gap in the model of Chapter 3.

As the first model studies the operation of the installation over a random day, it was applied to four random days around the year with daily heat demands between the limits set by the three design-days for each case of sizing. The main findings of this model are the following:

- For the same day of study, as the sizing of the installation increases, more geothermal energy is used leading to the reduction of the fuel used. So, a bigger fraction of the daily heat demand is covered by geothermal energy.
- For the same sizing of the installation, as the daily heat demand of the studied day increases, then both the geothermal flow rate and the mass of fuel increase.
- If the daily heat demand is lower than the daily heat demand of the design-day of the specific installation, then it is not necessary for all the heat demand to be covered by geothermal energy only. The fluctuation of the heat demand across the day is equally important for the operation of the installation with the daily heat demand.

The second model is then applied for the three cases of sizing using the heat demand around the year and an initial comparison is carried out with the traditional operation of these systems where no heat storage is used. The main findings in this case are as follows:

- In the case of using the heat storage, as the sizing of the installation increases, then the electricity used by the pumps decreases, the mass of fuel used by the peak-up boilers decreases, and the size of the peak-up boilers decreases, while on the other hand, the average geothermal flow rate and the volume of the cold water storage tank increase.

- For the same sizing of the installation, when comparing the case of using the heat storage and the traditional case, it is observed that the electricity used by the pumps is roughly the same, the mass of fuel used by the boilers decreases when the heat storage is used with a subsequent decrease in the size of the boilers, while on the other hand the average geothermal flow rate increases.
- The heat storage seems to be better utilised in the medium sizing of the installation (50%ile).

A more comprehensive and detailed comparison between the studied case of including a heat storage in the system and the traditional case will be carried out in the next Chapter, where the main findings of the second model of this Chapter will be used as input. So, concluding, the first model in this Chapter is a very useful tool for the technicians of the installation that can know in advance how to operate the installation over a day with a given (or predicted) heat demand, while the second model sizes the rest of the installation that could not be sized in Chapter 3, and provides the main running costs of the installation together with the average geothermal flow rate. All these will be among the main inputs in the next Chapter.

5 ECONOMIC, ENVIRONMENTAL AND ENERGETIC ANALYSIS OF A GEOTHERMAL DISTRICT HEATING SYSTEM

5.1 Introduction

In this Chapter, the economic, environmental and energetic feasibility of the proposed operation of a geothermal district heating system (GDHS) with a storage tank will be studied and a comparison with the traditional case will be carried out. The main goal of this Chapter is to compare the studied case of this thesis with the traditional operation of these systems in order to conclude eventually if it is worthwhile integrating a storage tank or not. In other words, this Chapter does not compare the studied case with alternative technologies, but only with the traditional case (i.e. with no storage). For that purpose, as will be made clear later on this Chapter, some parameters that will be considered common between the two cases will be neglected. So, some of the results might not depict their actual values in terms of real installations and, therefore, a straight comparison with typical values of other technologies should not be made. But, these values are considered adequate to make a comparison between the studied and the traditional case. This comparison will be made for each case of sizing of the installation in order to identify the influence of the sizing on the economics of the installation.

The main inputs of this Chapter are the outputs of the model of the annual operation of the installation that was studied in section 4.3, and the capital costs of several parts of the unit. In this Chapter, the inputs are much less than in the previous two Chapters, so these will not be explained in a separate section. Then, through the methodology presented the basic economic, environmental and energetic indices of the studied case will be calculated and a comparison with the traditional case (for which the same indices will also be calculated), will be made. The final answer that will be attempted to be provided in this Chapter is the following: “Is it worthwhile including a heat store within the proposed operation of a geothermal district heating system or not?”

In this section, a brief introduction in this Chapter was given. In section 5.2, the methodology for all the necessary calculations will be explained in detail, while in section 5.3 the results of the studied and the traditional case will be shown. Finally, a discussion on

the results will be provided in section 5.4, followed by some concluding remarks in section 5.5.

5.2 Methodology

5.2.1 Economic analysis

In this section, the calculation of the basic economic indices both of the studied installation as well as of the traditional case will be explained. The calculations are the same for both cases (apart from the capital cost of the storage tanks that will be zero in the traditional case as there is no storage in this case). The cash flows for these two cases will be also explained for that purpose. Initially, the financial outflows and incomes of the investment have to be calculated. These will be explained in detail in the following two sections.

5.2.1.1 Calculation of the investment expenditure

The investment expenditure consists of the following parts:

- Initial capital cost.
- Capital cost of some units that will be replaced after some years of operation.
- Running costs in the first year of operation.
- Running costs in subsequent years.

The calculation of these parts, which are necessary for all the subsequent calculation will be explained in this section. First, it is assumed that the installation is built in year n=0 and it starts operating in year n=1. Both the initial capital and running costs will be calculated for the year n=0, but for the cash flows, the running costs from year n=1 and onwards will be taken into account, as the installation will operate in these years. The initial capital cost of the installation is calculated by the following equation:

$$CC_{tot}^{0} = CC_{dr}^{0} + CC_{HST}^{0} + CC_{CST}^{0} + CC_{pb}^{0} + CC_{np}^{0} + CC_{ot}^{0} \quad (5.1)$$

Where:

CC_{tot}^{0} = Total initial (year n=0) capital cost (£)

CC_{dr}^{0}, CC_{HST}^{0}, CC_{CST}^{0}, CC_{pb}^{0}, CC_{np}^{0}, CC_{ot}^{0} = Initial capital cost of several equipment used during the construction of the installation (Drilling, hot and cold water storage tanks, peak-up boilers, network pipelines and other costs, respectively) (£)

In applying the above equation, typical costs for specific components of the capital expenditure were assembled on the basis of discussion with UK practitioners in the geothermal direct use sector. For the drilling costs, it was assumed that the first deep borehole would cost £1.5M, decreasing to £1M for later boreholes. The latter are cheaper as ground conditions would be better known in advance and the risk of drilling would decrease. Furthermore, it is assumed that one re-injection well will also be drilled in each case of study in order to maintain the flow of geothermal fluid in the underground and avoid the degradation of the geothermal resource. It should be pointed out that the number of wells calculated in Chapter 3 are the production wells, as based on these the available geothermal flow rate was calculated. So, if the number of production wells calculated in Chapter 3 are N_{wells}, then the total number of wells will be $N_{wells} + 1$ and the cost of drilling will be given in million £ as follows:

$$CC_{dr}^{0} = 1.5 + N_{wells} \cdot 1 \tag{5.2}$$

The capital cost of the network pipelines includes the cost of materials, which are carbon steel and mineral wool (insulation), the cost of welding and the civils costs for burying the pipes underground. The cost of the material is calculated by Eqs. (3.41)-(3.42) since the dimensions of the pipelines are known. The unit cost of carbon steel is estimated at £400/tonne and the cost of mineral wool at £60/m^3. The cost of welding is assumed to be £1000 per weld and meter of diameter and there will be one welding every 6 meters of pipeline. Finally, the civils costs are assumed to be £300 per meter of pipeline. So, for each pair of pipelines, their capital cost will be calculated by the following equations:

$$CC_{np}^{0} = 2 \cdot (CC_{mat}^{0} + CC_{weld}^{0}) + CC_{civil}^{0} \tag{5.3}$$

$$CC_{weld}^{0} = 1000 \cdot D_{p,o} \cdot \frac{L_p}{6} \tag{5.4}$$

$$CC_{civil}^{0} = 300 \cdot L_p \tag{5.5}$$

Where:

CC_{mat}^{0} = Capital cost of the materials of the pipelines in year n=0 (£)

CC_{weld}^{0} = Capital cost of the welding of the pipelines in year n=0 (£)

CC_{civil}^{0} = Civils costs for the burying of the pipelines in year n=0 (£)

$D_{p,o}$ = External diameter of the pipelines (not including the insulation) (m)

L_p = Length of each pipeline (m)

In Eq. (5.3), the factor 2 is used in the first two terms in order to account for both the supply and the return pipeline. On the other hand, it is not used in the calculation of the civil costs as one excavation will be done for each pair of pipelines. The costs in Eqs. (5.3)-(5.5) are all given in £.

Concerning the costs of the tanks, these include the materials, civils costs, the erection on slab and other minor costs. The materials of the storage tanks include carbon steel as the main material of the tank, mineral wool for insulation, mild steel as the material of the cover of the tank and concrete which is used as the base of the tank. The thickness of carbon steel has been calculated in Chapter 3, while the thickness of the mineral wool is assumed to be 20cm, the thickness of the cover is assumed to be 3mm and the thickness of the concrete base to be 50cm. So, since the diameter of each storage tank is known from Chapters 3 and 4, respectively, the volume of each material can be easily calculated. Then, the volume of each material is calculated by the unit costs in order to identify the cost of each material. Finally, all the costs are summed together for the calculation of the cost of each tank. So, indicatively, the cost of materials of the hot water storage tank will be given as:

$$CC_{mat,HST}^{0} = V_{c,steel} \cdot C_{u,c,steel} + V_{ins} \cdot C_{u,ins} + V_{cov} \cdot C_{u,cov} + V_{con} \cdot C_{u,con} \quad (5.6)$$

Where:

$CC_{mat,HST}^{0}$ = Initial capital cost of the materials of the hot water storage tank (£)

$V_{c,steel}$, V_{ins}, V_{cov}, V_{con} = Volumes of the carbon steel, insulation, cover and concrete used in the hot water storage tank, respectively (m^3)

$C_{u,c,steel}$, $C_{u,ins}$, $C_{u,cov}$, $C_{u,con}$ = Unit cost of carbon steel, insulation, cover and concrete, respectively ($\frac{£}{m^3}$)

In the above equation, the unit costs of carbon steel and of the insulation are the same as those for the pipelines, while the unit cost for the cover is assumed to be the same as that of carbon steel. Furthermore, the unit cost of concrete is assumed to be equal to £50/m^3. The other costs of the tank are assumed on the basis of recent projects in the UK. More details on these assumptions can be found in Appendix C. Eventually, the capital cost of the hot water storage tank, for example, will be calculated as:

$$CC^0_{HST} = CC^0_{mat,HST} + \sum CC_i \tag{5.7}$$

In the above equation, the second part refers to the other costs included in the calculation of the capital cost of the tanks.

Moreover, for the cost of the peak-up boilers, an average capital cost of £200/kW[2] is assumed for industrial gas boilers. So, the capital cost of the peak-up boilers is calculated as:

$$CC^0_{pb} = 200 \cdot Q_{pb} \tag{5.8}$$

In the above equation, the thermal power of the peak-up boilers (Q_{pb}) has been calculated in Chapter 4, and has to be used in units of kW. Finally, other minor costs include pumps, heat exchangers, in-house installations, salaries of workers etc., all of which have been estimated from recent analogous projects in the UK. So, by applying Eqs. (5.1)-(5.8) the calculation of the initial or up-front capital cost of the installation is possible. As mentioned before, in the traditional case of operation, the costs of the hot and cold storage tank will not be calculated by Eq. (5.7), but will be equal to zero as no storage tank is built in this case.

As mentioned before, several parts of the installation will need to be replaced after several years of operation, since they have a limited lifetime. More specifically, it is assumed that the peak-up boilers will be replaced after 20 years of operation, while the heat exchangers and the pumps will be replaced after 15 years of operation. Their cost at the time of the replacement will be calculated based on their initial capital cost and an average annual increase of the equipment which can be either set equal to the discount rate

[2] http://2050-calculator-tool-wiki.decc.gov.uk/cost_categories/82

or another value depending on the specific market and its trends. So, these costs are calculated by an equation like the following:

$$CC_x^n = CC_x^0 \cdot (1 + AAI_{CC,x})^n \quad (5.9)$$

Where:

CC_x^n = Capital cost of x equipment of the installation in year n (£)

CC_x^0 = Capital cost of x equipment of the installation in year n=0 (£)

$AAI_{CC,x}$ = Average annual increase of the capital cost of x equipment (%)

The above equation refers to any of the aforementioned equipment. In our case, the average annual increase of any part of the capital cost is assumed to be 3%. These costs of replacement will have to be taken into account in the calculation of the cash flows of the installation.

The running costs of the installation include the cost of fuel used by the boilers, the cost of electricity used by the pumps, the salaries of workers, the carbon taxes and other minor costs. The calculation of these costs for the first year of operation will be shown, and then the calculation of their values in the next years which are necessary for the cash flows will be explained.

The total fuel used over the year as well as the total electricity used by the pumps has been calculated in Chapter 4. Then, for the calculation of the unit cost for gas, which is the fuel used and electricity, their historic prices for non-domestic users are used. These historic prices were found on the website of the Department of Energy and Climate Change of the UK[3]. A chart of these prices is included in Appendix D. Then, the values for 2013 have been used as unit costs for gas and electricity. So, the initial running costs of the fuel and electricity are calculated, respectively, as:

$$RC_f^0 = M_{f,tot} \cdot C_{u,f} \quad (5.10)$$

$$RC_{el}^0 = E_{el,tot} \cdot C_{u,el} \quad (5.11)$$

[3] https://www.gov.uk/government/statistical-data-sets/gas-and-electricity-prices-in-the-non-domestic-sector

Where:

RC_f^0, RC_{el}^0 = Annual running cost of fuel and electricity in year n=0 (£)

$M_{f,tot}$ = Total mass of fuel used by the peak-up boilers per year (kg)

$E_{el,tot}$ = Total electricity used by the pumps per year (kWh)

$C_{u,f}$ = Unit cost of fuel ($\frac{£}{kg}$)

$C_{u,el}$ = Unit cost of electricity ($\frac{£}{kWh}$)

The salaries of workers are quite case-specific, so in our case these are assumed based on an average salary of £2500 per month. Then, the cost of carbon taxes is assumed to be £15 per tonne of CO_2 emitted in the environment. The latter will be calculated in a following section. So, the initial running cost of carbon taxes is calculated as:

$$RC_{ct}^0 = 15 \cdot M_{CO_2,tot} \tag{5.12}$$

Where:

RC_{ct}^0 = Annual running cost for carbon taxes in year n=0 (£)

$M_{CO_2,tot}$ = Annual CO_2 emissions of the installation (tn)

In the above equation, the total mass of CO_2 emitted has to be used (in tonnes). This value will be calculated in section 5.2.2. Finally, the other running costs include any other costs that might occur during the operation of the installation and are assumed to be equal to £30000 for every case. Therefore, the total initial running cost of the installation is calculated by the following equation:

$$RC_{tot}^0 = RC_f^0 + RC_{el}^0 + RC_w^0 + RC_{ct}^0 + RC_{ot}^0 \tag{5.13}$$

Where:

RC_{tot}^0 = Total annual running cost of the installation in year n=0 (£)

RC_w^0, RC_{ot}^0 = Annual running costs of workers and others in year n=0 (£)

As mentioned earlier, the installation is assumed to be operating from year n=1 onwards. So, the running costs used in the calculation of the cash flows will be calculated from that year and after, although the initial running costs will be used in the calculation of some economic indices as will be seen later. Therefore, an average annual increase for

each part of the running cost will be considered and its value after n years will be calculated by an equation similar to Eq. (5.9).

$$RC_x^n = RC_x^0 \cdot (1 + AAI_{RC,x})^n \quad (5.14)$$

Where:

RC_x^n = Annual running cost of x kind in year n (£)

RC_x^0 = Annual running cost of x kind in year n=0 (£)

$AAI_{RC,x}$ = Average annual increase of the running cost of x kind (%)

So, an average annual increase for each part of the running cost has to be considered. For the case of the fuel, the charts of its historic prices is used as happened for the calculation of its unit prices that was used in Eq. (5.10). In this case, the unit price of fuel over the last ten years is considered and its annual increase from year to year is calculated. Then, the average of these annual increases is calculated and is assumed that the annual increase from now onwards will be equal to this average annual increase of the previous ten years. Exactly the same process is followed for the calculation of the average annual increase of the electricity cost.

The average annual increase of the salaries of workers is assumed to be 2.5%, while the average annual increase of other running costs is assumed to be equal to the discount rate, which in our case is assumed to be 5%. Finally, the cost of the carbon taxes is assumed to be constant over the years, as there is no certainty over its evolution in the future. So, its average annual increase will be 0%.

5.2.1.2 Calculation of income

The income in this study consists of the following three parts:

- A fixed cost per day which guarantees a certain income and is used for the repayment of the initial capital cost. For each case, it is fixed in such a value so that the initial capital cost is repaid within 10 years.
- A variable cost which depicts the real consumption of energy. As a base case for this research, the variable cost is fixed at £0.02/kWh of heating provided.

- A financial incentive recently established in the UK, the so-called RHI (Renewable Heat Incentive), which provides £0.05/kWh of renewable heat provided. This value increases by 2.5% each year and the incentive is provided for the first 20 years of operation of the installation.

So, the incomes of the investment in year n=0 are calculated by the following equations:

$$IC_{tot}^{0} = IC_{fix}^{0} + IC_{var}^{0} + IC_{RHI}^{0} \tag{5.15}$$

$$IC_{fix}^{0} = \frac{CC_{tot}^{0}}{\sum_{i=1}^{i=10}(1+AAI_{hp})^{i}} \tag{5.16}$$

$$IC_{var}^{0} = AHD \cdot C_{hp,u}^{0} \tag{5.17}$$

$$IC_{RHI}^{0} = AHD_{G} \cdot 0.05 \tag{5.18}$$

Where:

IC_{tot}^{0} = Total income of the investment in year n=0 (£)

IC_{fix}^{0}, IC_{var}^{0}, IC_{RHI}^{0} = Fixed, variable and income from the RHI in year n=0 (£)

AAI_{hp} = Average annual increase of the price of heating (%)

$C_{hp,u}^{0}$ = Unit price of heating in year n=0 ($\frac{£}{kWh}$)

AHD = Annual heat demand (kWh)

AHD_{G} = Annual heat demand covered by geothermal energy, which is calculated in section 5.2.4 (kWh)

It is recalled that the installation will start operating at year n=1, so the incomes will also start from this year onwards. The calculation of the above values is taking place only for computational purposes and in order to make the following calculations easier.

As mentioned before, the fixed cost is calculated on the basis of repaying the initial capital cost in 10 years. By observing Eq. (5.16), it is seen that the counter in the denominator starts from i=1. This happens because the installation starts operating in year n=1, so the revenue will start from that year, as stated previously. Furthermore, it is seen

that in order to get the value of the fixed cost, a simple division by the number of years is not made, but an average annual increase in the heating price is taken into account. This happens, because the price of heating should increase every year in order to compensate for the increase in the expenditure and general year-on-year inflation.

So, the fixed cost will increase over the following years with an average annual increase of the heating price which, in our case, is assumed to be 3% lower than the average annual increase of the fuel. The same average annual increase will also apply to the variable cost of heating. Finally, as mentioned before, the income from the RHI subsidy will increase by 2.5% each year. So, the income of the investment the following years will be given by the following equations:

$$IC_{tot}^{n} = IC_{fix}^{n} + IC_{var}^{n} + IC_{RHI}^{n} \tag{5.19}$$

$$IC_{fix}^{n} = IC_{fix}^{0} \cdot (1 + AAI_{hp})^{n} \tag{5.20}$$

$$IC_{var}^{n} = IC_{var}^{0} \cdot (1 + AAI_{hp})^{n} \tag{5.21}$$

$$\left.\begin{array}{c} \boldsymbol{If}\ n \leq 20: \\ \boldsymbol{Then}:\ IC_{RHI}^{n} = IC_{RHI}^{0} \cdot (1 + 0.025)^{n} \\ \boldsymbol{Else}:\ IC_{RHI}^{n} = 0 \end{array}\right\} \tag{5.22}$$

$$AAI_{hp} = AAI_{RC,f} - 0.03 \tag{5.23}$$

Where:

IC_{tot}^{n} = Total income of the investment in year n (£)

IC_{fix}^{0}, IC_{var}^{0}, IC_{RHI}^{0} = Fixed, variable and income from the RHI in year n (£)

$AAI_{RC,f}$ = Average annual increase of the running cost of fuel (%)

5.2.1.3 Calculation of the financial indices

Initially, the comparison between the studied and the traditional case of a geothermal district heating system will be based on the comparison of several financial indices of each case. The calculation of the necessary capital and running costs has been done in the

previous section. The definitions and explanations of the following economic indices were well summarised in Chapter 2.

The first financial index used is the levelised cost of heating (LCH), i.e. the minimum price that heat should be sold to the consumers in order to have a feasible investment and is equivalent to the unit cost of energy (UCE) described in Chapter 2. This is calculated by Eqs. (2.35) and (2.36) properly formulated for our problem as follows:

$$LCH = \frac{CC_{tot} \cdot CRF + RC_{tot}^{0}}{AHD} \tag{5.24}$$

$$CRF = \frac{IR}{1-(1+IR)^{N}} \tag{5.25}$$

Where:

LCH = Levelised cost of heating ($\frac{£}{kWh}$)

CRF = Cost recovery factor (Dimensionless)

In Eq. (5.24), the whole capital cost should be included, taking into account both the initial capital cost as well as the cost of replacement of any units in the future, as explained earlier. For that purpose, no temporal superscript has been assigned to this variable. The capital cost of the next years should be reduced in current values through the discount rate. So, the total capital cost that will be used in Eq. (5.24) is calculated through the following equation:

$$CC_{tot} = \sum_{n=0}^{n=N} \frac{CC_{tot}^{n}}{(1+DR)^{n}} \tag{5.26}$$

Where:

DR = Discount rate (Dimensionless)

Then, the running cost of year n=0 is also used in the numerator of Eq. (5.24). So, it is seen that the values of the total capital cost and of the running cost both in year n=0 are used for the calculation of the levelised cost of heating. Furthermore, the cost recovery factor is used in Eq. (5.24) in order to break down the capital cost over the whole investment period. As can be observed in this equation, the running cost of one year, and

more specifically of year n=0, is used. This is the only case where the running cost of year n=0, which does not exist in reality, will be used. Furthermore, the capital cost that refers to one year has to be used also. Although the total capital cost is all spent in specific years of the investment, and mainly in year n=0, it actually refers to all the years of operation and, theoretically, has to be re-paid in these years. Therefore, the cost recovery factor is implemented so that both the capital and the running costs refer to one year of operation of the installation. The levelised cost of heating cannot provide useful information for one investment, but for the comparison between two or more investments. When comparing two or more investments, the investment with the lower levelised cost is the more feasible one, as a lower levelised cost indicates that this investment can be equally feasible with the other one even if the heat is sold cheaper. In other words, for the same selling price of heat, the income and the benefits of the installation with lower levelised cost will be higher.

The second financial index that is used is the net present value (NPV) of the investment, which is defined as the summary of the discounted cash flows over the whole investment period. In other words, the net cash flow is calculated for each year of operation and the discount rate is used in order to transform this in today's value. Then, all these discounted values are summed together and provide the net present value of the investment. So, the net present value is calculated by the following equations:

$$\left.\begin{array}{c} \boldsymbol{For}\ each\ year\ of\ operation\ n: \\ NCF^n = IC^n_{tot} - CC^n_{tot} - RC^n_{tot} \\ DNCF^n = \frac{NCF^n}{(1+DR)^n} \end{array}\right\} \quad (5.27)$$

$$NPV = \sum_{n=0}^{n=N} DNCF^n \quad (5.28)$$

Where:

NCF^n = Net cash flow in year n (£)

$DNCF^n$ = Discounted net cash flow of year n (£)

In Eq. (5.27) the net cash flow in year n=0 has to be taken into account also. Theoretically, if the net present value is positive, this indicates that the investment is feasible. From another point of view, when comparing two investments the investment

with the higher net present value is the more feasible one. The discount rate that is used in this study is assumed to be constant and equal to 5%.

The third financial index that is used is the internal rate of return of the investment (IRR). This is defined as the discount rate that nullifies the net present value. So, in this case, the net present value is set equal to zero in Eq. (5.28) and then this equation together with expression (5.27) are solved for the discount rate. So, the internal rate of return is calculated by the following expression.

$$IRR = DR\ (for\ NPV = 0) \tag{5.29}$$

In theory, the value of the internal rate of return when compared with the current interest rate can indicate how feasible an investment is. If the IRR is higher than the interest rate, then the investment is feasible, while if it is lower the investment is unfeasible. When comparing two or more investments, the one with the higher IRR is the more feasible and financially "safe" investment as it is further from the current interest rate.

The fourth, and final, financial index is the benefits-to-costs ratio of the investment (BCR). This index is defined as the sum of the discounted benefits of each year divided by the sum of the discounted capital costs of each year. In the numerator, the benefits are defined as the difference of the income minus the running costs, so the capital costs are not taken into account there, but only in the denominator. In other words, the benefits-to-costs ratio is the ratio of the earnings to the capital expenditures. Therefore, the BCR is calculated by the following expressions:

$$\left.\begin{array}{c} \boldsymbol{For}\ each\ year\ of\ operation\ n: \\ ABF^n = IC_{tot}^n - RC_{tot}^n \\ DABF^n = \frac{ABF^n}{(1+DR)^n} \end{array}\right\} \tag{5.30}$$

$$\left.\begin{array}{c} \boldsymbol{For}\ each\ year\ of\ operation\ n: \\ DCC^n = \frac{CC_{tot}^n}{(1+DR)^n} \end{array}\right\} \tag{5.31}$$

$$BCR = \frac{\sum_{n=0}^{n=N} DABF^n}{\sum_{n=0}^{n=N} DCC^n} \quad (5.32)$$

Where:

ABF^n = Annual benefits in year n (£)

$DABF^n$ = Discounted annual benefits in year n (£)

DCC^n = Discounted capital cost in year n (£)

The benefits-to-costs ratio can indicate either if one investment is feasible or not, but it can also indicate which investment if more feasible among two or more investments. For an investment to be feasible, the benefits-to-cost ratios has to be higher than 1, i.e. the net benefits to be higher than the capital expenditures. When comparing two or more investments, the investment with the higher value of the benefits-to-costs ratio is more feasible as it indicates higher values of benefits.

In this section, the calculation of four different financial indices that can indicate if the proposed solution is more feasible than the traditional case from an economic point of view was explained. As mentioned before, all the indices have the capability to show which of the two cases is more feasible, while the NPV, the IRR and the BCR can also show if an investment is feasible, in general, or not without comparing both of them. For example, if the values of the IRR for the two cases are 1% and 2%, respectively, this indicates that the second case is more feasible than the first one, but in reality, both these values are lower than the current interest rates (around 6% or more). So, none of these investments are feasible. Therefore, not only a comparison between the two cases should be made, but the values of these indices should also indicate that the investments are feasible. Furthermore, it should be mentioned that the IRR, the BCR and, partially, the LCH provide qualitative information about the investment, and not quantitative. In other words, their values are independent of the size of the investment. Two investments with completely different capital costs and incomes can have the same values of the above indices. Only, the NPV provides quantitative information about the investment and is a very good indicator of the economic size of the investment. Finally, these indices are used since they can indicate the more feasible of two possible investments; however, if the results are close one another, then one of the indices might not depict the truth. So, all of them are used together in order to obtain more robust results.

5.2.1.4 Cash flows of the investment

The cash flow of an investment is a graph which depicts the monetary value of the investment at each specific period over time. It includes all the expenditure that occurs from the construction and during the operation of the installation, i.e. all the capital and running costs, as well as the income. In order to calculate the cash flow of an investment the following steps have to be implemented:

- The capital and the running costs of the installation are calculated for each year of operation. In our case, this has been carried out with Eqs. (5.1)-(5.9) and (5.10)-(5.14), respectively.
- The total income is calculated for each year of operation through Eqs. (5.15)-(5.23). Both the income and the aforementioned costs are calculated on their real value at the specific year and are not discounted.
- The net cash flow for each year of operation is calculated by reducing the capital and running costs of each year from the total income.
- Finally, the cumulative net cash flow is calculated for each year and this result is plotted against time.

So, since the capital and running costs as well as the total income are calculated for each year, the following equations are applied for the calculation of the cash flow of the investment:

$$NCF^n = IC_{tot}^n - CC_{tot}^n - RC_{tot}^n \tag{5.33}$$

$$\left.\begin{array}{l}\boldsymbol{For}\ each\ year\ of\ operation\ from\ 1\ to\ n: \\ \qquad CNCF^n = CNCF^{n-1} + NCF^n\end{array}\right\} \tag{5.34}$$

Where:

$CNCF^n$ = Cumulative net cash flow in year n (£)

As seen above, Eq. (5.34) is valid from year n=1. This happens because, obviously, if it was applied in year n=0, the calculation of the cumulative net cash flow in year n=-1 would be necessary. This value does not exist, so the cumulative net cash flow in year n=0 is calculated as:

$$CNCF^0 = NCF^0 = -CC_{tot}^0 \quad (5.35)$$

So, by applying Eqs. (5.33)-(5.35), the cumulative net cash flow has been calculated and the cash flow graph can be drawn. At this point, it is very important to note, that in year n=0 that the installation is theoretically constructed, there are neither running costs nor any income. Therefore, the net cash flow in year zero is calculated by the proper form of Eq. (5.33) as shown in the second part of Eq. (5.35), where only the initial capital cost is taken into account.

5.2.2 Environmental analysis

In this section, the methodology that has to be carried out for the environmental analysis of the installation will be shown. Because the main scope of this Chapter is to compare the proposed solution with the traditional case only, the local environmental impact, i.e. the local emissions, will be taken into account. It is assumed that the emissions during the construction of the installation as well as of its spare parts will be roughly the same between the two cases. So, only the emissions during the operation of the installation will be taken into account. These emission are assumed to arise from the following three sources:

- Combustion of fossil-fuel in the peak-up boilers.
- Electricity used by the pumps.
- Emissions by the geothermal production itself.

The emissions by the geothermal production are assumed to be negligible (Rybach, 2003, amongst others), while the emissions from the electricity used by the pumps are not taken into account. The latter is because, as shown in Chapter 4, the amount of electricity used both in the proposed and in the traditional case is almost the same. So, the emissions that will arise by the use of electricity will be roughly the same between the two cases. Since the scope of this Chapter is to do, mainly, a comparison between the two cases and not with other technologies, these emissions will not be taken into account. Therefore, the emissions of the installation will include only the emissions from the combustion of the fuel in the peak-up boilers.

In general, the emissions that arise from the combustion of a fuel (fossil or not) depend mainly on the composition of the fuel and, secondly, on the excess air and the conditions of the combustion. In our case, the following assumptions are made:

- The fuel used is natural gas, which consists 100% from methane.
- The air-to-fuel ratio is above the stoichiometric value required for this combustion. Therefore, all the methane is combusted and there is no methane in the exhaust gases.
- The combustion is perfect and since the fuel is methane, the only direct emission is carbon dioxide (CO_2), while there are no other carbon or sulphur oxides in the exhaust gases. The other substances contained in the exhaust gases will be water, nitrogen and possibly some oxygen which are not pollutants.
- The peak-up boilers operate with NO_x elimination technologies and, therefore, the NO_x will be neglected.

So, the only emissions of the installation that will be taken into account are the carbon dioxide emissions that occur during the combustion of methane. The combustion of methane in excess air obeys the following simplified formula:

$$CH_4 + 2 \cdot O_2 \rightarrow CO_2 + 2 \cdot H_20 \quad (5.36)$$

By applying, the analogy of moles between the methane combusted and the produced carbon dioxide in the above formula, then for 1 mole of methane combusted there is 1 mole of produced carbon dioxide. Then, in order to convert this analogy into analogy of masses, the molecular weight for methane and carbon dioxide have to be used. The molecular weights of these two substances have the following values[4]:

$$M_{r,CH_4} = 16.044 \quad (5.37)$$

$$M_{r,CO_2} = 44.01 \quad (5.38)$$

The units in the molecular masses are grammars per mole of the substance. In other words, 1 mole of methane is equal to 16.044 grammars. Therefore, by applying the

[4] http://www.engineeringtoolbox.com/molecular-weight-gas-vapor-d_1156.html

molecular masses shown above to the mole analogy, we can get the mass analogy through the following reasoning path:

$$\left.\begin{array}{c} 1\ mol\ of\ CH_4 = 1\ mol\ of\ CO_2 \\ 16.044\ gr\ of\ CH_4 = 44.01\ gr\ \ of\ CO_2 \\ 1\ gr\ of\ CH_4 = \frac{44.01}{16.044} = 2.743\ gr\ of\ CO_2 \\ 1\ kg\ of\ CH_4 = 2.743\ kg\ of\ CO_2 \end{array}\right\} \quad (5.39)$$

So, with the above expression it is shown that for each kilogram of methane combusted, there will be 2.743 kilograms of carbon dioxide emitted in the atmosphere. The total amount of fuel used in each case has been calculated in Chapter 4. So, the total annual emissions of carbon dioxide can be easily calculated by the following equation:

$$M_{CO_2,tot} = 2.743 \cdot M_{f,tot} \quad (5.40)$$

This will be the only pollutant from the whole process that will be taken into account for the comparison of the two cases.

5.2.3 Energetic indices of the installation

In this section, the way of calculating two energetic indices of the installation will be explained. These two indices are the load factor (LF) of the installation and the fraction of the annual heat demand that is covered by geothermal energy (ε_G). The load factor is defined as the proportion of the average geothermal mass flow rate throughout the year to the maximum available geothermal flow rate. So, this index is calculated by the following equation:

$$LF = \frac{\overline{\dot{m}_G}}{\dot{m}_{G,max}} \quad (5.41)$$

Where:

$\overline{\dot{m}_G}$ = Average geothermal flow rate ($\frac{kg}{s}$)

$\dot{m}_{G,max}$ = Maximum available geothermal flow rate ($\frac{kg}{s}$)

The numerator of the above equation has been calculated in Chapter 4, through the application of the algorithm of the annual operation. The denominator is calculated in

Chapter 3, Table 3.2, and is the geothermal flow rate of the design-day for each case of sizing of the installation. The maximum available geothermal flow rate can also be calculated as the product of the number of production wells by the mass flow rate of one well.

$$\dot{m}_{G,max} = N_{wells} \cdot \dot{m}_{well} \tag{5.42}$$

So, with these equations the load factor of the installation can be easily calculated. As observed by Eq. (5.41), the load factor indicates how close the operation of the installation is to the full load operation. A high value of load factor shows that the installation is working on average close to the full load. In geothermal energy, as well as in the other renewables, it is desirable for the operation to be as close as possible to the full load, as in this way the maximum utilisation of the source is achieved. For renewable energies, which in general have a very low running cost, it is of the utmost importance to obtain the maximum potential of the source, since it is usually rather expensive to build the installation. So, since the expensive installation is built, the maximum use of the source is desired.

The second energetic index of the installation is the fraction of the annual heat demand that is covered by geothermal energy to the total annual heat demand.

$$\mathcal{E}_G = \frac{AHD_G}{AHD} \tag{5.43}$$

It should be noted that in the above equation, the values of the heat demand over the whole year are used, in contrast to Eq. (4.29) where the equivalent values for the studied day are used. The denominator of the above equation can be easily calculated as the summary of the heat demand over the whole year which is a basic input of the whole study. This value is independent of the case of sizing, as it obviously depends on the heat users only, and is always constant. In our case, the total annual heat demand is equal to:

$$AHD = 37486216\ kWh \tag{5.44}$$

For the calculation of the annual heat demand that is covered by geothermal energy, the calculation of the annual heat demand that is covered by the peak-up boilers is necessary. The total amount of fuel that is used in the peak-up boilers throughout the year has been

calculated for each case in Chapter 4. Then, the heat provided by the combustion of the fuel to the network is calculated by the following equation:

$$Q_{f,tot} = M_{f,tot} \cdot LHV_f \cdot \eta_b \quad (5.45)$$

Where all the variables have been explained in Chapter 4.

The thermal efficiency of the boiler is assumed to be constant and equal to 88%, while the lower heating value of the fuel will always be known by the composition of the fuel. A part of this heat will reach the end users and will be the part of the annual heat demand that is covered by the peak-up boilers. This is defined by taking into account all the possible heat losses from the boilers to the end users. As mentioned earlier in this thesis, it is assumed that the peak-up boilers are very close to the substation. So, any possible heat losses in the transmission network are neglected. Furthermore, it is assumed that the heat losses in the substation are also negligible. So, the only heat losses that have to be taken into account are those in the distribution network. For that purpose, the following efficiencies for each branch of the supply and return distribution pipelines, respectively, are defined:

$$\eta_{d,s,j} = \frac{T_{d,s,o,j} - T_a}{T_{d,s,i,j} - T_a} \quad (5.46)$$

$$\eta_{d,r,j} = \frac{T_{d,r,o,j} - T_a}{T_{d,r,i,j} - T_a} \quad (5.47)$$

Where:

$T_{d,s,o,j}$, $T_{d,s,i,j}$, $T_{d,r,o,j}$, $T_{d,r,i,j}$ = Supply/return outlet and inlet temperatures of pipeline j, respectively (K)

By the two above equations, the efficiencies of the supply and return pipelines of each branch of the distribution network are calculated. In our case, for the sake of simplicity an average thermal efficiency of the supply and return pipelines will be used. These are calculated as follows:

$$\overline{\eta_{d,s}} = average(\eta_{d,s,j}) \quad (5.48)$$

$$\overline{\eta_{d,r}} = average(\eta_{d,r,j}) \quad (5.49)$$

The above two average efficiencies account for all the heat losses that occur from the boilers to the end-users. The thermal efficiency of the boilers has already been taken into account in Eq. (5.45). A final factor that has to be taken into account for the calculation of the heat demand that is provided by the peak-up boilers is the thermal efficiency of the in-house installation. This thermal efficiency is considered to be constant for each case and equal to 92%. Eventually, the annual heat demand that is covered by the peak-up boilers will be calculated as:

$$AHD_{pb} = Q_{f,tot} \cdot \overline{\eta_{d,s}} \cdot \overline{\eta_{d,r}} \cdot \eta_{dw} \quad (5.50)$$

Finally, the annual heat demand that is covered by geothermal energy can be easily calculated by reducing the annual heat demand that is covered by the peak-up boilers from the total annual heat demand.

$$AHD_G = AHD - AHD_{pb} \quad (5.51)$$

So, by applying Eqs. (5.43)-(5.51) the fraction of the total heat demand that is covered by geothermal energy can be calculated. It is easily understood that the higher possible value of this fraction is desired, because this would mean the maximum contribution of geothermal energy to the heat demand coverage and the minimum contribution (or usage) of the peak-up boilers.

In this section, the calculations for two basic indices that will be used for the energetic evaluation of the installation have been shown. These indices are the load factor and the fraction of the heat demand that is covered by geothermal energy. It is desirable for both of these factors to attain the maximum possible value. For the load factor, this would indicate that the installation is operating as close as possible to its full load, which is always something desirable for renewable energy sources, while for the fraction this would indicate that the contribution of geothermal energy to the heat demand coverage would be maximised, with subsequent minimisation of the use of peak-up boilers.

5.3 Results

In this section, the results of the economic, environmental and energetic analysis of the studied case as well as of the traditional operation of the installation will be shown for each case of sizing. The economic results will be shown both for the case that the RHI (Renewable Heat Incentive), which is a financial subsidy as explained before, is included and not. In this way, it is attempted to highlight any potential advantages that a financial subsidy can have in a renewable project.

Initially, in Table 5.1 the unit prices of fuel and electricity are shown for each case. As mentioned in section 5.2.1, these prices depend on the amount of fuel and electricity use, respectively, so for different cases of sizing these can be different. Then, in Table 5.2 the equivalent average annual increase of the prices of fuel and electricity are also shown. All these values are necessary for the next results and are shown here in order to have a complete overview of the results. In both tables, the results are shown both for the studied and the traditional case.

Table 5.1 *Unit prices of fuel and electricity for each case of sizing*

Case	**25%ile**	**50%ile**	**75%ile**
Operation with the storage tank			
Unit price of fuel (£./kWh)	0.028882	0.028882	0.031206
Unit price of electricity (£/kWh)	0.088820	0.108690	0.108690
Operation without the storage tank			
Unit price of fuel (£/kWh)	0.028882	0.028882	0.028882
Unit price of electricity (£/kWh)	0.088820	0.108690	0.108690

Table 5.2 Average annual increase of the price of fuel and electricity for each case of sizing

Case	25%ile	50%ile	75%ile
Operation with the storage tank			
Average annual increase of fuel price (%)	12.0118	12.0118	10.9747
Average annual increase of electricity price (%)	11.7732	9.3553	9.3553
Operation without the storage tank			
Average annual increase of fuel price (%)	12.0118	12.0118	12.0118
Average annual increase of electricity price (%)	11.7732	9.3553	9.3553

The main initial capital costs for each case of sizing are shown in Table 5.3 both for the studied and the traditional case. The corresponding running costs in year n=0 for the same cases are shown in Table 5.4. In these and the rest of this section, the studied case of using the heat storage will be assigned with the abbreviation Wi, while the traditional case without the heat storage will be assigned with the abbreviation Wo.

Table 5.3 Main initial capital costs of the studied and the traditional case for each case of sizing

	CC_{dr}^{0}	CC_{HST}^{0}	CC_{pb}^{0}	CC_{np}^{0}	CC_{tot}^{0}
25%ile Wi	3500000	35478	3101400	1636274	10012558
25%ile Wo	3500000	0	3165600	1636274	10018887
50%ile Wi	5000000	53644	2521400	1737049	11069181
50%ile Wo	5000000	0	2654400	1737049	11108465
75%ile Wi	6500000	90221	1650200	1860405	11896085
75%ile Wo	6500000	0	1951000	1860405	12028422

Table 5.4 Main initial running costs of the studied and the traditional case for each case of sizing

	RC_f^0	RC_{el}^0	RC_{tot}^0
25%ile Wi	763682	106407	1043876
25%ile Wo	799011	106302	1082975
50%ile Wi	285707	41000	448052
50%ile Wo	402109	40991	577217
75%ile Wi	48771	20360	164076
75%ile Wo	98489	20357	219652

Then, the results of the financial indices of the investment are shown in Tables 5.5 and 5.6 for the cases that the RHI is taken into account and not. In both tables, the results are shown for each case of sizing and both for the studied and the traditional case. It should be noted that the levelised cost of heating does not depend on the RHI, since the income of the investment is not taken into account for its calculation, so it has the same value either if the RHI is taken into account or not. As can be seen in these tables and will be explained further in the next section, the NPV, the IRR and the BCR are negative for the low sizing of the installation which means that the investment is not feasible. For that purpose, the cash flows will be shown for this case, but only for the other two cases of sizing. These cash flows are shown on Figs. (5.1)-(5.4).

Table 5.5 Financial indices of the studied and the traditional case (RHI included)

	LCH (£/kWh)	NPV (£· 10^6)	IRR (%)	BCR (-)
25%ile Wi	0.04988	<0	<0	<0
25%ile Wo	0.05098	<0	<0	<0
50%ile Wi	0.03574	60.478	29.10	5.689
50%ile Wo	0.03932	46.661	25.83	4.581
75%ile Wi	0.02885	92.521	34.00	8.045
75%ile Wo	0.03092	86.647	32.55	7.433

Table 5.6 Financial indices of the studied and the traditional case (RHI not included)

	***LCH* (£/kWh)**	***NPV* (£· 10^6)**	***IRR* (%)**	***BCR* (-)**
25%ile Wi	0.04988	<0	<0	<0
25%ile Wo	0.05098	<0	<0	<0
50%ile Wi	0.03574	36.371	16.90	3.819
50%ile Wo	0.03932	25.108	13.78	2.927
75%ile Wi	0.02885	63.135	20.58	5.808
75%ile Wo	0.03092	58.431	18.88	5.338

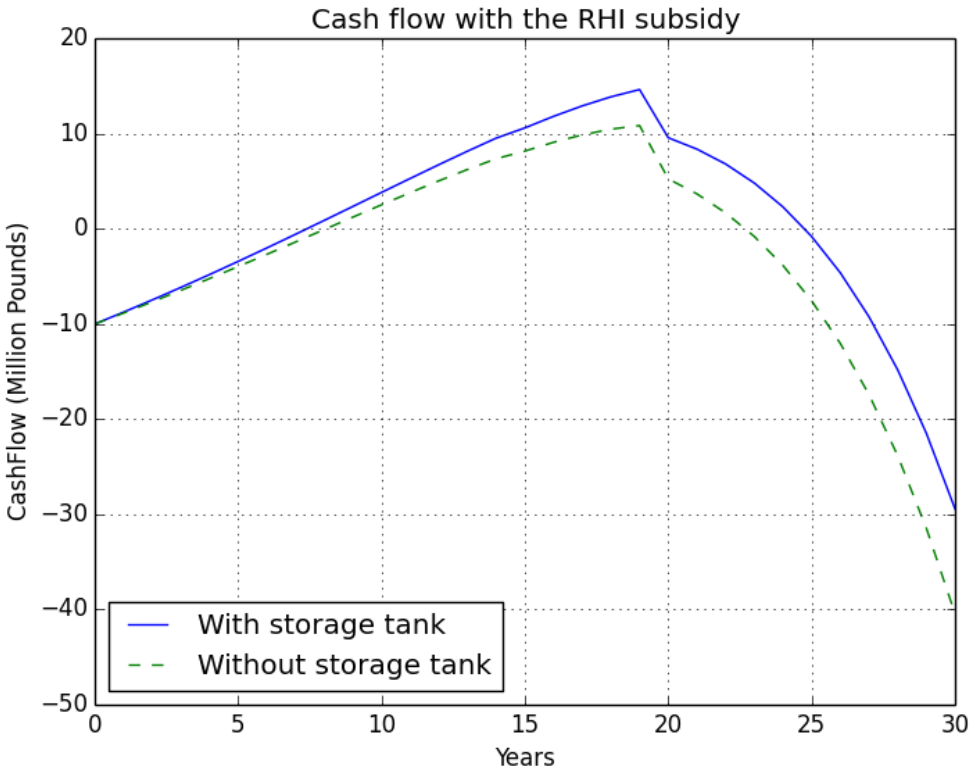

Figure 5.1 Cash flow of the investment with the RHI subsidy (25%ile sizing)

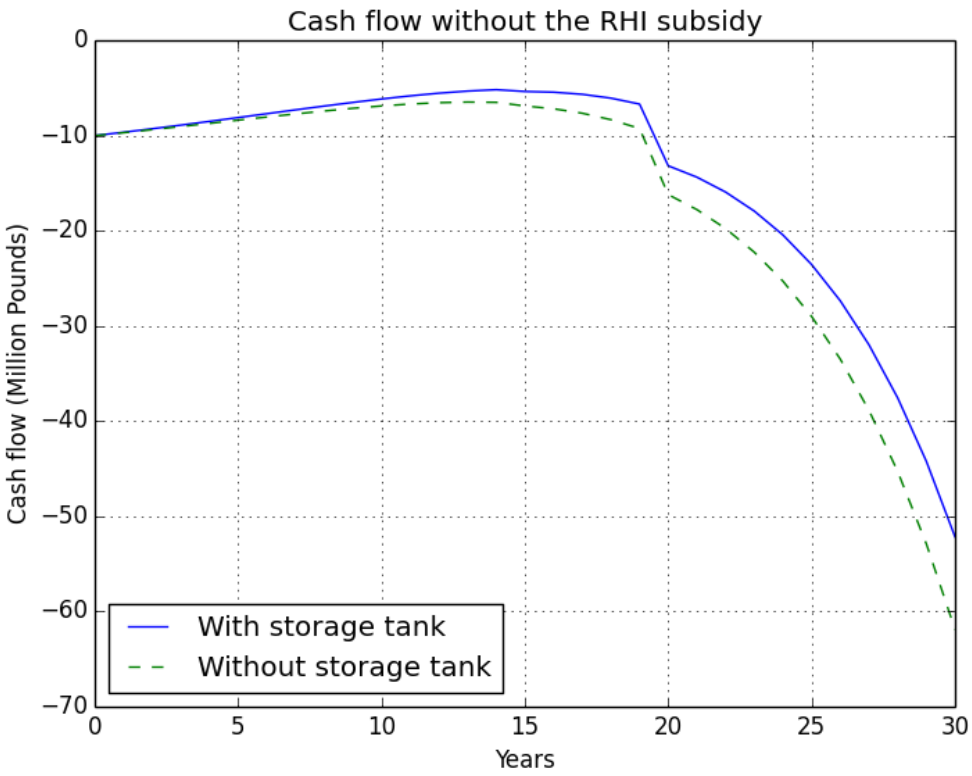

Figure 5.2 *Cash flow of the investment without the RHI subsidy (25%ile sizing)*

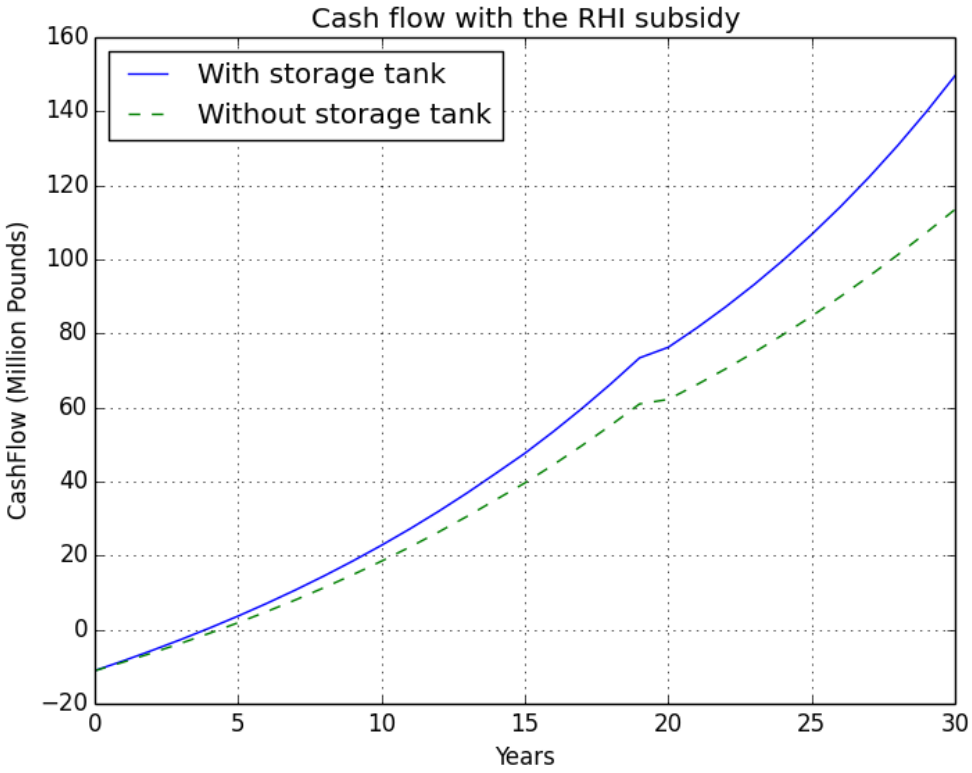

Figure 5.3 *Cash flow of the investment with the RHI subsidy (50%ile sizing)*

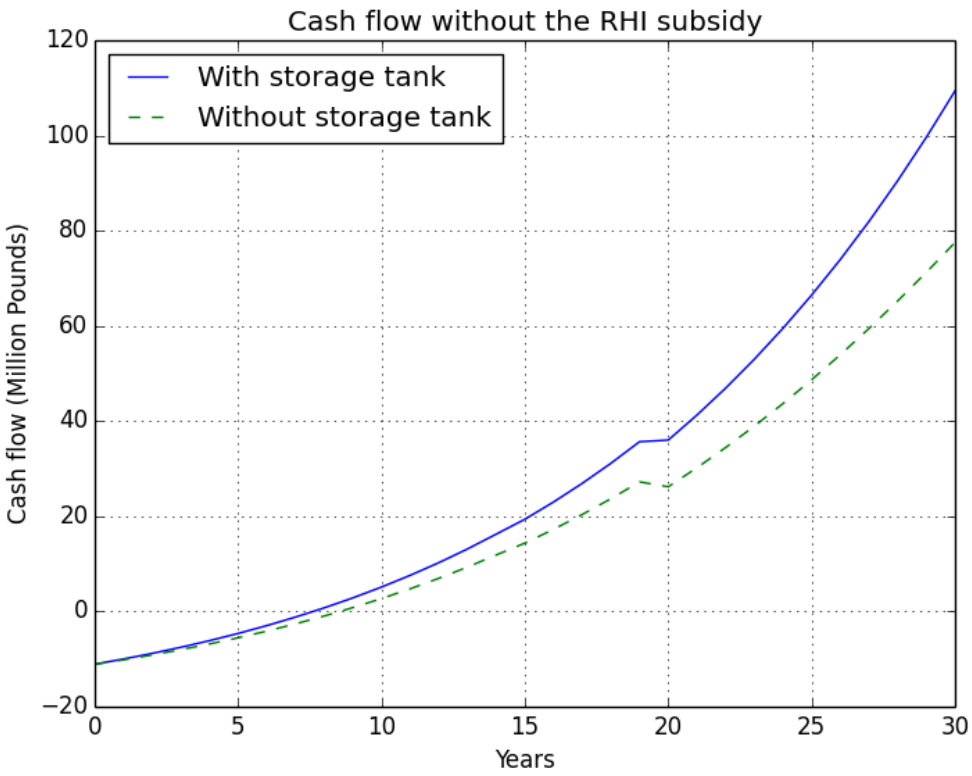

Figure 5.4 *Cash flow of the investment without the RHI subsidy (50%ile sizing)*

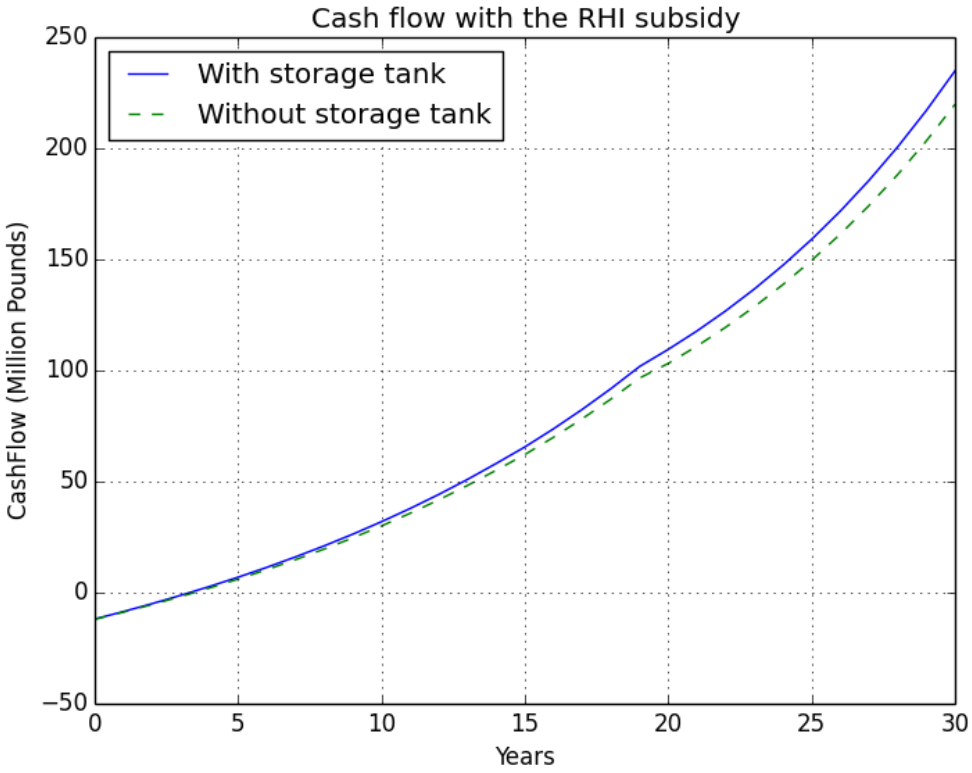

Figure 5.5 *Cash flow of the investment with the RHI subsidy (75%ile sizing)*

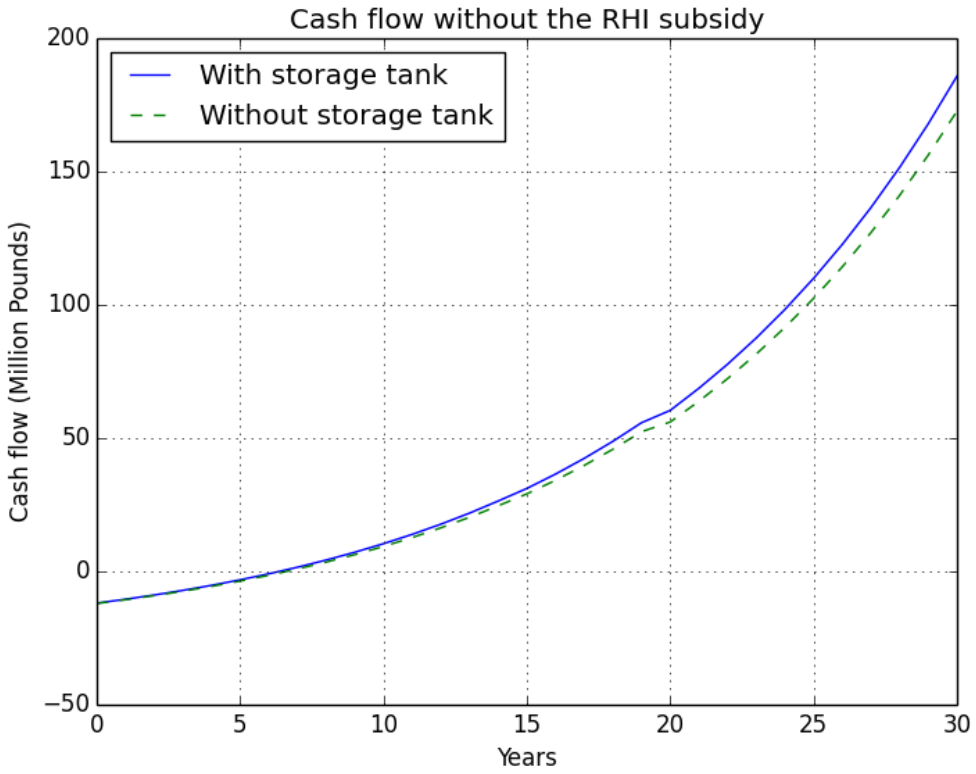

Figure 5.6 *Cash flow of the investment without the RHI subsidy (75%ile sizing)*

Finally, the results of the environmental and energetic analysis both for the studied and the traditional case and for each case of sizing are shown in Table 5.7.

Table 5.7 *Results of the environmental and energetic analysis of the installation*

	Annual CO_2 emissions (kg)	**Load factor (%)**	**Proportion of heat demand covered by geothermal energy (%)**
25%ile Wi	5223278	96.695	44.967
25%ile Wo	5478858	93.882	42.421
50%ile Wi	1954119	80.631	79.364
50%ile Wo	2750260	80.267	70.957
75%ile Wi	308319	64.647	96.742
75%ile Wo	673626	62.084	92.883

5.4 Discussion

The first important observations of this Chapter arise from Tables 5.1 and 5.2 in which the unit price of fuel and electricity as well as their average annual increases are shown for each case of sizing both for the studied and the traditional case. Firstly, it is observed that these values can be different between some cases because, as mentioned before these values depend on the annual use of fuel and electricity, respectively. Furthermore, it is seen that discrete values are obtained only and do not lie in a continuous range of values. If the annual use of either fuel or electricity lies within a specific range, then its unit price and its average annual increase will get a specific value defined by the historical data. Secondly, it is observed that as the sizing of the installation increases both the unit price of fuel and electricity increase too. As it was shown in Chapter 4, both the use of fuel and electricity decrease as the sizing of the installation increases. These denote, in simple words, that when more fuel or electricity is used, then its price decreases, which is intuitively sensible from a market point of view. Thirdly, it is observed that as the sizing of the installation increases, the average annual increase of fuel and electricity prices both have a decreasing trend. So, under the same reasoning as previously, this shows that when more fuel or electricity is used, its average annual increase rises, which has an opposing trend to its unit price. In other words, when more fuel or electricity is bought, its price is lower but its average annual increase will be higher. Obviously, these observations apply both for the studied and the traditional case.

The main capital costs of the installation can be seen in Table 5.3 from which important conclusions can be drawn both for cases of different sizing as well as between the studied and the traditional case for the same sizing of the installation. Firstly, it can be observed that both the capital cost of drilling and the capital cost of the pipelines is exactly the same between the studied and the traditional case for the same case of sizing. This is totally expected, as between the studied and the traditional case the only differences are the use of the heat storage under a different operational strategy, while the rest of the installation is the same. So, the number of wells and the pipelines, and subsequently their capital cost, will be exactly the same between these cases. Secondly, it is seen that as the sizing of the installation increases, both the capital cost of drilling and the capital cost of the pipelines increase. These are also expected because, as seen in Chapter 3, a larger sizing of the installation requires more wells to be drilled, which of course increases the total cost of drilling, while on the other hand, a larger sizing of the installation denotes higher mass

flow rates and, subsequently, bigger pipelines which are required to compensate with these higher flow rates. The latter obviously leads to an increased capital cost for the pipelines and is in agreement with the results of Chapter 3 concerning the size of the pipelines.

Thirdly, it is noted that for the same case of sizing, the cost of the heat storage tank is obviously higher in the studied case, since in the traditional case there is no heat storage and its cost is zero. Furthermore, it can be seen that as the sizing of the installation increases, the cost of the heat storage tank increases. The latter is also expected because the larger sizing of the installation requires bigger heat storage, as can be identified from Chapter 3, which increases its capital cost. Fourthly, the cost of the peak-up boilers has a decreasing trend as the sizing of the installation increases and is also smaller for the studied case. Both of these results are in agreement with the results of the size of the peak-up boilers shown in Chapter 4. Taking into account these results and the fact that the cost of the boilers is assumed to be directly proportional to their size, then the impacts on their cost shown in Table 5.3 are justified. Furthermore, it can be observed that as the sizing of the installation increases, the total capital cost increases which is sensible taking into account the previous observations and the fact that larger sizing denotes bigger installation and, subsequently, higher capital cost. Finally, the most important observation of Table 5.3 is the fact that for the same case of sizing, the total capital cost will be higher in the traditional case than in the studied case. So, the studied case has a lower capital cost compared to the traditional case, although the extra cost of the heat storage tank is taken into account. This happens, mainly, because of the higher capital cost of the peak-up boilers in the traditional case, which offsets the difference due to the heat storage.

Then, in Table 5.4 the annual running costs of the installation for each case are shown. It is observed that the cost of fuel for the same case of sizing is higher for the traditional case in which the heat storage is not used, while this cost decreases as the sizing of the installation increases. Both these observations are expected taking into account the mass of fuel used for each case as shown in Tables 4.5 and 4.6, respectively, and the fact that the cost of fuel is proportional to its total amount used. Furthermore, it is shown that for the same case of sizing the cost of electricity is almost the same between the studied and the traditional case, while the cost of electricity decreases as the sizing of the installation increases. This is also expected for the same reasons as for the cost of fuel. Taking this into account, the fact that the total running cost decreases as the sizing of the installation increases is totally sensible. Finally, it is shown that for the same case of sizing the total running cost will be lower in the studied case. So, a first major conclusion of this Chapter

is that both the capital and the running costs will be lower for the studied case than for the traditional case of operation of a geothermal district heating system.

The main financial indices of the investment for each case of sizing are shown in Tables 5.5 and 5.6 for the cases that the RHI subsidy in taken into account and not, respectively. These two tables highlight some very important drawbacks. Firstly, it is shown that for the same case of sizing all the financial indices improve when the heat storage is used. More specifically, the levelised cost of heating decreases, while the NPV, the IRR and the BCR all increase. For example, the difference in the RHI denotes an increased potential annual income of £42350-137830 depending on the case of sizing. The maximum increase in annual income is for the medium case of sizing, which denotes that the best improvement in the financial performance occurs in this case. The second interesting drawback highlighted by these tables is the influence of the sizing of the installation on the financial viability of the investment. It can be seen, that all the financial factors improve when the sizing of the installation increases. This happens mainly because, as will also be seen later, a larger sizing of the installation indicates that more geothermal energy is used to cover the heat demand, which subsequently leads to increased income from the RHI incentive. Another factor that causes the higher viability of the larger sizing are the lower running costs in this case, which increase the net annual income of the investment. So, it can be said that if there is no restricting factor such as non-favourable geological conditions, the geothermal installation should be sized on the maximum possible sizing, even if the heat storage impacts most affect the medium sizing, as shown previously.

A third really important observation which arises from the comparison of Tables 5.5 and 5.6 is the influence of the RHI subsidy in the viability of the investment. As it can be clearly seen, all the financial indices improve a lot when the RHI is taken into account. For example, the NPV can increase up to 84%, the IRR can increase up to 87%, while the BCR can increase up to 56% when the RHI is taken into account. The only financial index which remains the same is the levelised cost of heating which does not depend on the RHI. Therefore, these results definitely prove the tremendous impact of a financial subsidy in a renewable project.

Up to this point, the discussion was focused on whether the studied case is more viable than the traditional case. By observing these two tables, it can also be seen if each investment alone is feasible or not. It can be seen that the investment is not viable for the

lower sizing of the installation either if the RHI is taken into account or not, because the NPV, the IRR and the BCR are all negative. This definitely indicates that this investment is not viable. A further investigation on the viability of this investment will be carried out on the next section in which two solutions which can improve its viability will be examined. For the cases of larger sizing, it can be seen that the investments are definitely viable for the case that the RHI is taken into account, while for the case that the RHI is not taken into account the viability or, more properly said, the economic attractiveness of the medium sizing is somehow questionable. This happens because of the values of the IRR shown. As mentioned before, the value of the IRR has to be higher than the current interest rate of the market. In our case, this is definitely the case. But in practice, the values of the IRR have to be typically higher than 15% in order to have greater security and in order to take into account any non-predicted factors that can influence the investment. So, although this case is definitely viable as the results show, it might not be very attractive for investors. For the case of the larger sizing of the installation, the investment is viable and very attractive even when the RHI is not included. In general, it can be stated that the investment is feasible for the medium and the large sizing of the installation and the feasibility is greatly enhanced with the inclusion of the RHI subsidy.

All these observations concerning the financial feasibility of the investments, are also depicted in Figs. 5.1-5.6 in which the cash flows of each investment are shown. As expected, the cash flow for the lower sizing of the installation will have negative values as shown in Figs. 5.1 and 5.2 since the investment is not viable. Then, it is observed that for each case of sizing, the studied case is more viable as the monetary flow is higher at each time. The fact that the storage impacts most the medium sizing is also observed as the difference between the two lines is bigger in this case compared to the larger sizing case. The change in the inclination in the 20^{th} year of the investment occurs, firstly because the RHI stops being provided after that year, as explained in the methodology section, and secondly in this year the peak-up boilers are replaced. The latter are a relatively expensive item as seen in Table 5.3, so this change in inclination is justified even in the cash flows where the RHI is not taken into account. Furthermore, the influence of the RHI is also made clear through these cash flows as it can be seen that the monetary values are much higher when the RHI is taken into account. Finally, it can be seen that the pay-back period of the investment is quite low when the RHI is taken into account, while it increases a lot when it is not taken into account, although these pay-back periods can still be regarded as very acceptable. More specifically, the pay-back period is around 4 and 3 years for the medium and larger sizing of the installation, respectively, when the RHI is taken into

account, while the same values are around 7-8 and 6 years, respectively, when the RHI is not taken into account. The latter shows again the influence of the RHI and the fact that the investment with the larger sizing has the higher viability as mentioned before also.

Concerning the annual CO_2 emissions of the installation, it can be seen in Table 5.7 that these decrease when the heat storage is used for every case of sizing. This is totally expected, since the emissions are directly proportional to the mass of fuel used and, as it was shown in Chapter 4, this decreases when the heat storage is used. The relative decrease of the emissions in the lower case of sizing is small since, as mentioned before, almost all the geothermal production is sent directly to the heat load and, therefore, the change in the operation of the peak-up boilers, and subsequently their emissions, will not be very high. On the other hand, the highest absolute decrease of the emissions is for the medium case of sizing, which indicates again that the storage impacts are greatest in this case. An interesting observation is also that the highest relative decrease of the emissions is for the larger case of sizing, where the absolute decrease is around 50%. But, in this case, the emissions are relatively low anyway, so it can be indeed stated that the medium case of sizing is impacted more. It can also be observed that as the sizing of the installation increases, the emissions will decrease as the amount of fuel used will also decrease. Since the sizing of the installation increases, more geothermal energy and less fuel are used, so the emissions will decrease.

As for the load factor of the geothermal part of the installation, it can be seen in Table 5.7 that it increases when the heat storage is used. This indicates that when the heat storage is used, the geothermal part of the installation operates at a higher average flow rate, thus increasing the utilization of geothermal energy compared to the traditional case of operation. On the other hand, it is also shown that the load factor decreases as the sizing of the installation increases. This happens because, as the sizing of the installation increases, the potential geothermal production also increases, so there can be many times over the year that the heat demand can be covered just by a part of the geothermal production. In other words, more geothermal energy that is available for the same overall heat demand as the sizing increases, so the smaller the fraction of it that will be used to cover the same heat demand. In the lower case of sizing, the potential geothermal production is low, so almost all the geothermal production is sent directly to the heat demand. For example, in our case, the load factor is 96.695% when the heat storage is used, which means that the geothermal installation is working very close to its full capacity all over the year.

Finally, in Table 5.7 the proportion of the total heat demand that can be covered by geothermal energy is shown. It is observed that when the heat storage is used, a higher proportion of the heat demand is covered by geothermal energy. This is expected from the previous results, where it was shown that when the heat storage is applied, more geothermal energy is utilised and less fuel is used. This indicates that a higher proportion of the heat demand will be covered by geothermal energy. Furthermore, as the sizing of the installation increases, more geothermal energy is available, so obviously, a higher proportion of the heat demand will be covered by geothermal energy.

5.5 Further investigation on the financial viability of the investment

As shown in the previous section, the case of the lower sizing of the installation (25%ile case) is not financially viable. In this section, two potential solutions in order to overcome this problem will be examined. The first of the following potential solutions and, under certain circumstances that will be explained later in this section, the second too, can also be applied in the other cases of sizing either in order to increase their viability or if these are not viable too.

The first possible solution that could increase the viability of the investment is to increase the income of the investment. The most obvious way to do this is by increasing the variable cost of heating, which up to now was priced at £0.02/kWh of heat delivered to the end-users. Practically, this value was quite low as in reality the variable cost of heating is £0.05/kWh or higher. So, the same analysis which was explained in section 5.2.1 will be applied for higher values of the variable cost of heating. In this case, only the curves for the studied case with the use of the heat storage will be shown as it is not attempted to check if it is worthwhile including a heat storage or not, but to check the general viability of the investment. Nevertheless, it was clearly shown in the previous two sections that it is financially worthwhile including a heat storage in a geothermal district heating system. The results of this analysis for the 25%ile sizing case and for the cases that the RHI is taken and not taken into account are shown in Figs. 5.7 and 5.8, respectively.

As expected, the increase of the variable cost of heating can definitely increase the viability of the investment. As shown on Figs. 5.7 and 5.8, the increase of the variable cost of heating increases the monetary value of the investment in any period of time. Furthermore, by comparing these two figures with Figs. 5.3-5.6, it is observed that for the

lower case of sizing a similar cash flow is achieved at a variable cost of £0.05/kWh when compared to the medium sizing and at a variable cost of £0.06-0.07/kWh when compared to the larger sizing of the installation. This shows that more than a two-fold increase is required in the lower case of sizing to achieve the same cash flow as with the other cases. Even if not the same cash flow is desirable, it is shown in the two above figures that the case with a variable cost of £0.03/kWh is barely viable and not so attractive.

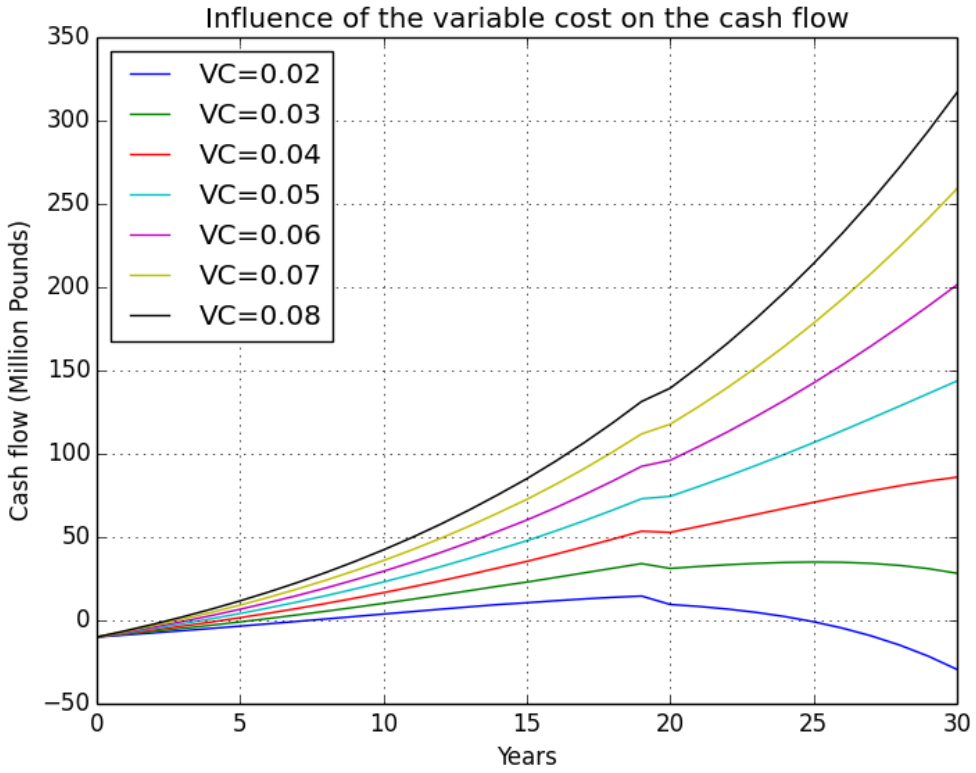

Figure 5.7 *Influence of the variable cost of heating on the cash flow of the investment (RHI included-25%ile sizing)*

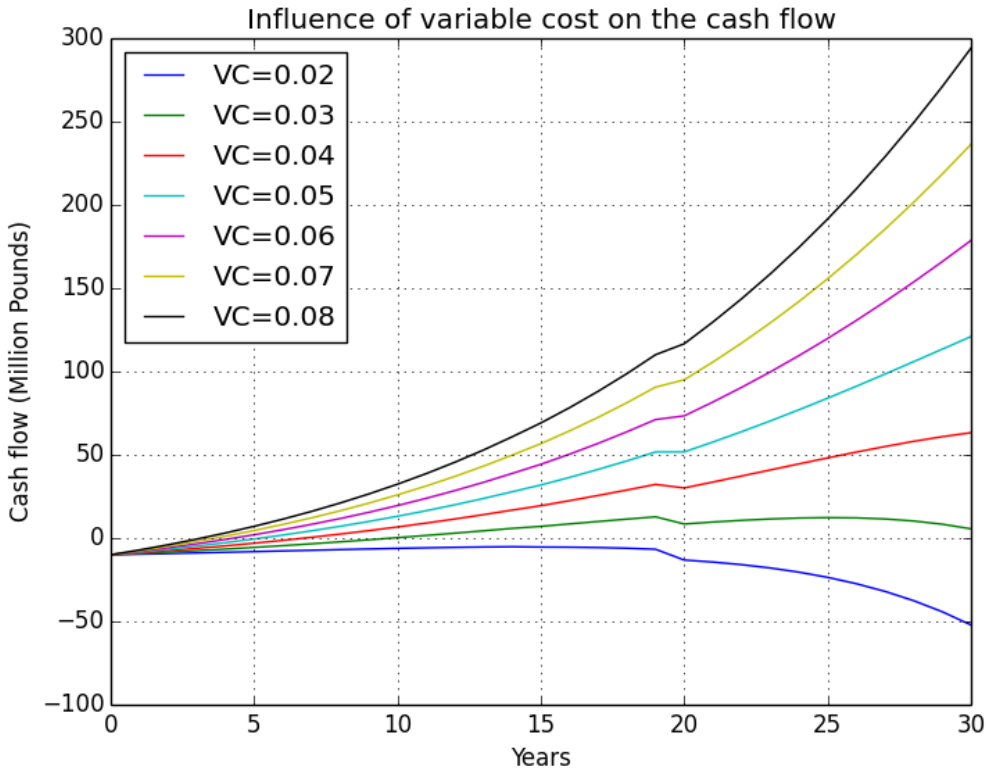

Figure 5.8 *Influence of the variable cost of heating on the cash flow of the investment (RHI not included- 25%ile sizing)*

So, the first viable case is for the variable cost of heating to be £0.04/kWh which is double the initially used value. Although this value is double compared to the other cases of sizing, it remains relatively low when compared to variable costs that are applied in the traditional heating systems. So, with this analysis it was shown that by increasing the variable cost of heating within logical limits, and usually below the values of traditional heating systems, it can make investment feasible.

The second solution that could increase the viability of the investment is the decrease of the investment expenditure. By observing in detail Table 5.3, it can be seen that the total capital cost between the three cases of sizing is not very different, especially when taking into account that this refers to the whole period of the investment. On the other hand, it is observed in Table 5.4 that the running cost is considerably more different between the three cases compared to the capital cost and it is maximum for the lower case of sizing. The running cost consists mainly of the cost of fuel and the cost of electricity used by the pumps, as mentioned before. The cost of fuel cannot be controlled easily as it depends on the heat demand. On the other hand, the cost of electricity depends mainly on the mass flow rate and the dimensions of the pipelines. With the approach followed throughout this thesis, the mass flow rates over the transmission network depend roughly on the sizing of

the installation, while those over the distribution network depend on the heat demand. The heat demand is constant for each case of sizing, so the mass flow rates on the distribution network will be roughly the same over the year for each case of sizing. It should be noted that this statement refers to the whole year and not the design-day, where (as shown in Chapter 3) the mass flow rates on the distribution network will obviously be different. So, since the mass flow rates will be the same, it seems a sensible choice to increase the size of the pipelines of the distribution network in order to decrease the friction losses, and subsequently the cost. This change will increase the capital cost of these pipelines which is contradictory to the decrease of the running cost. Whether this change improves the viability of the investment will be examined below.

So, the same analysis will be carried out for two different cases for the sizing of the distribution network. For the sake of simplicity, these two cases will refer to the sizing of the distribution network for the medium and large cases of sizing. In other words, the only difference in the next two studied cases will only be the size of the distribution network, while everything else (including the number of wells, the size of the storage tank and the size of the peak-up boilers) will be the same as in the lower case of sizing. These two cases will be symbolised as 25T-50D and 25T-75D, respectively, in the following. The graphs of the cash flows for these two cases are shown in Figs. 5.9-5.12 both for the cases that the RHI is included and not included. By comparing these cash flows with the ones showed in Figs. 5.1 and 5.2 which refer to the 25%ile sizing, both for the transmission and distribution network, it can be clearly seen that the feasibility of the investment increases very slightly in the two new cases. Sizing the distribution network for a larger case of sizing seems to improve the feasibility of the investment. But this improvement is so slight as to be barely visible in the graphs, and it definitely does not make the investment feasible. So, it can be concluded that this solution does not improve the feasibility of the investment importantly and it is thus not recommended.

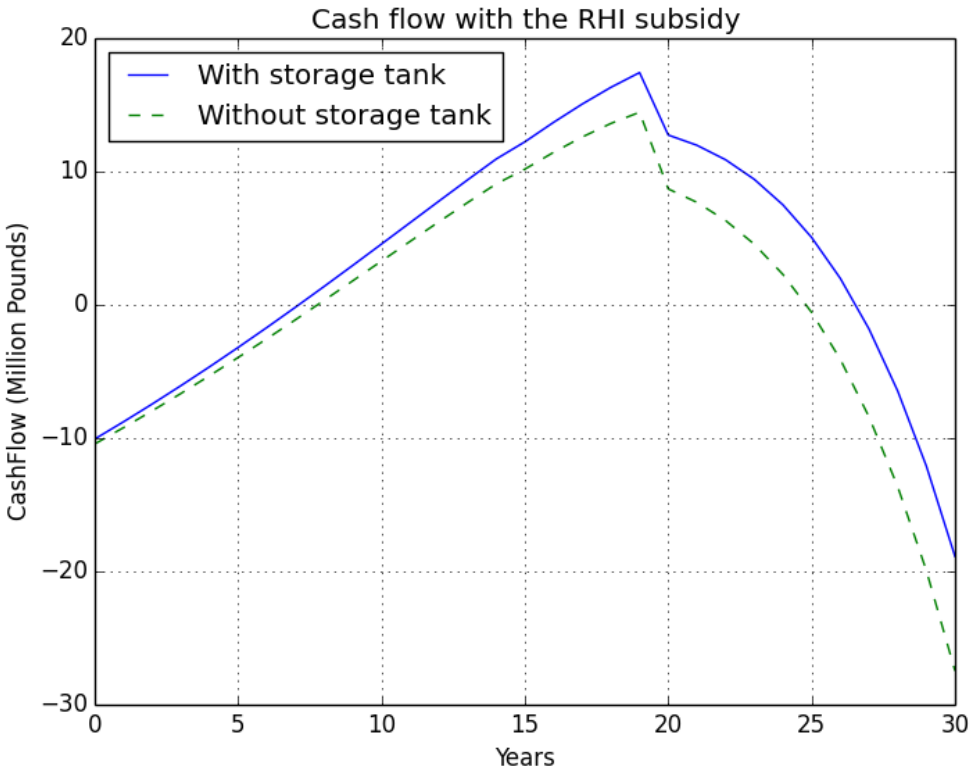

Figure 5.9 *Cash flow of the investment with the RHI subsidy (25T-50D sizing)*

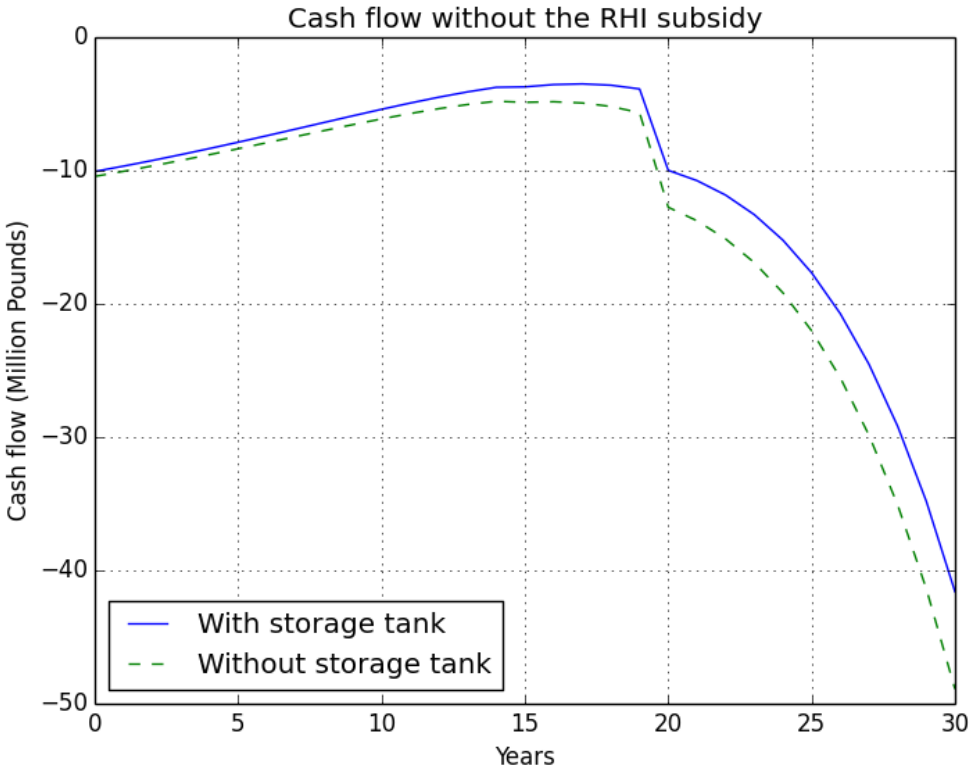

Figure 5.10 *Cash flow of the investment without the RHI subsidy (25T-50D sizing)*

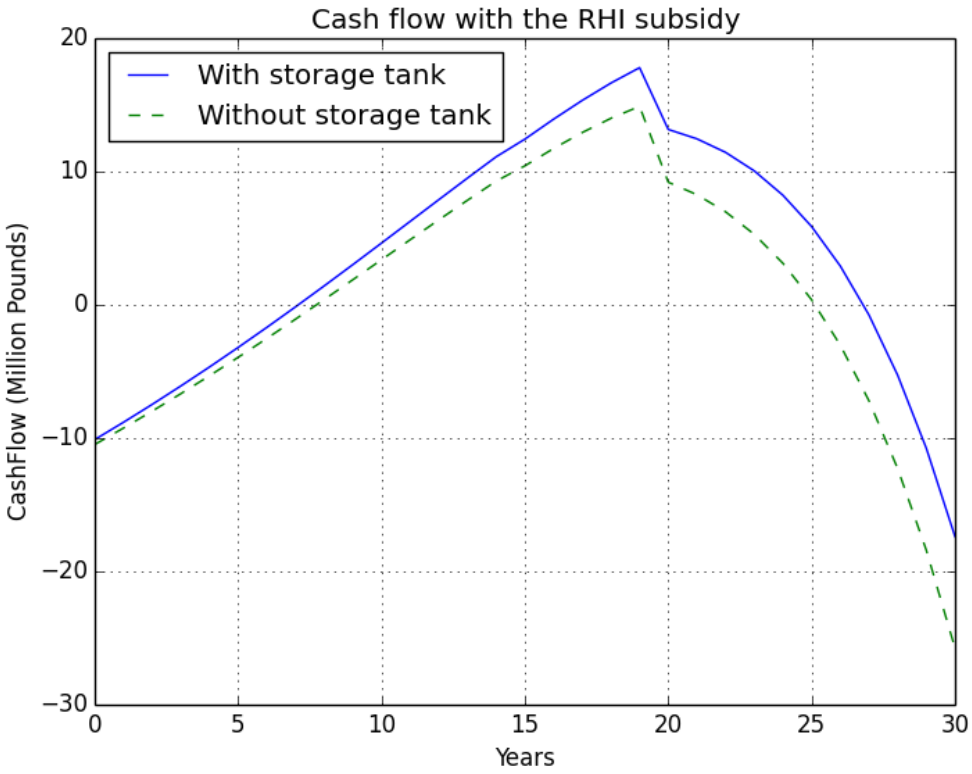

Figure 5.11 *Cash flow of the investment with the RHI subsidy (25T-75D sizing)*

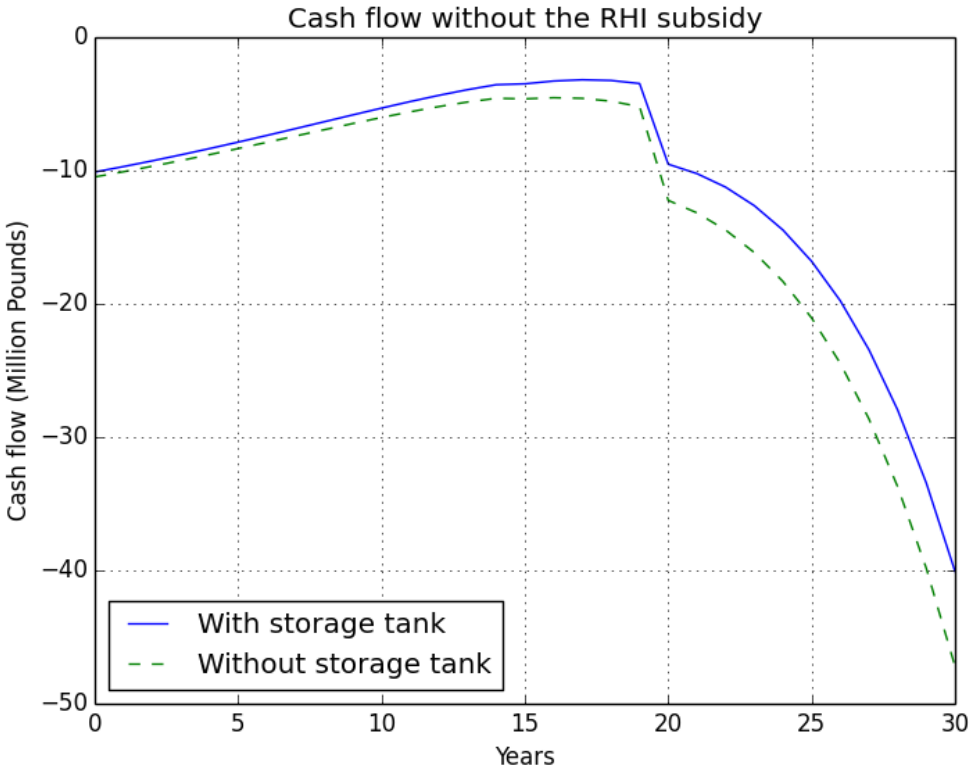

Figure 5.12 *Cash flow of the investment without the RHI subsidy (25T-75D sizing)*

By the analysis shown in this section, it can be concluded that if a geothermal district heating system with or without the heat storage is not financially viable, the only effective solution to that problem is to increase the income of the investment by increasing the variable cost of heating. It was further proved that this increase of the variable cost usually lies within the margins of the variable cost of alternative heating technologies. So, it can be stated that, even if the initially selected variable cost has to be increased, this technology will remain competitive to other heating technologies. Finally, the effect of a financial subsidy in a renewable heat project was once again highlighted as it was shown that the investment reaches the financial attractiveness of the cases of larger sizing with a lower variable cost of £0.01-0.02kWh in the case that the RHI is taken into account. In other words, if a financial subsidy is provided, then the necessary increase of the variable cost of heating that will turn the investment to viable will be lower compared to the case that a subsidy is not provided.

5.6 Summary

In this Chapter, an economic, environmental and energetic analysis of a geothermal district heating with a heat storage, which is the studied case in this thesis, was carried out and a comparison with the traditional case of not using a heat storage was done. Concerning the economic analysis of the investment, the main capital and running costs were initially calculated for both cases as well as the capital costs of replacement of some parts of the installation and the evolution of the running costs over the investment period. Afterwards, using these capital and running costs, several financial indices of the investments were calculated in order to make the comparison between the two cases. Then, the annual emissions of carbon dioxide were calculated for the environmental analysis of the installation, while for the energetic analysis two separate energetic indices were used. The first energetic index that was used was the load factor of the installation which depicts how close to the nominal load the installation is operating over the year, while the second energetic index was the proportion of the annual heat demand that is covered by geothermal energy.

The results have highlighted some very important insights on the economic, environmental and energetic aspects either when the studied case is compared with the traditional case, which is the main point of interest of this Chapter, as well as when cases

of different sizing of the geothermal part of the installation are compared with each other. The main concluding remarks of this Chapter are the following:

- Both the capital and running costs of the installation are lower in the studied case compared to the traditional case for any case of sizing.
- The capital cost of the installation increases as the sizing of the installation increases, while on the other hand, the running costs of the installation is decreased as less fuel and electricity are used when the sizing increases.
- All the financial indices show that the studied case of using a heat storage in a geothermal district heating system is more attractive than the traditional case of not using a heat storage. More specifically, the levelised cost of heating decreases, while the NPV, the IRR and the BCR all increase. This is the case for any case of sizing of the installation.
- The effect of a financial subsidy, such as the Renewable Heat Incentive (RHI) in our case, was highlighted. All the financial indices of the installation increase a lot when the RHI is taken into account.
- The most attractive case of sizing from an economic point of view is the larger case of sizing. This happens mainly because more geothermal energy is used to cover the heat demand and, therefore, the income from the RHI increases. Furthermore, the running costs will be lower in the cases of larger sizing. Therefore, it can be said that, as long as other circumstances allow this, the sizing of the geothermal component of the installation should be as large as possible.
- On the other hand, the heat storage seems to impact more the medium case of sizing as in this case, the higher relative increases of the financial indices occur.
- The emissions of the installation decrease when the heat storage is used for each case of sizing as less fuel is used to cover the peak demands.
- The emissions decrease as the sizing of the installation increases as less fuel is used as well.
- As happens with the economic analysis, the medium sizing of the installation is impacted most from an environmental point of view when the heat storage is used.
- The load factor of the installation increases when the heat storage is used, also for each case of sizing. This means that for the studied case more geothermal

energy is utilised from the same geothermal installation, which is something desirable as for any renewable energy source.

- Furthermore, the load factor of the installation decreases as the sizing of the installation increases, which means that the installation is working further from its full or nominal capacity. This is expected as the maximum available geothermal energy is increased, so for the same annual heat demand the load factor will decrease.
- Finally, the proportion of the heat demand that is covered by geothermal energy increases when the heat storage is used. This proportion also increases as the sizing of the installation increases, which is something expected as more geothermal energy is available to cover the same heat demand.

In general, it can be concluded that by applying a heat storage under the proposed operational strategy in a geothermal district heating system, both the capital and the running costs decrease, while the overall production of heat is cheaper. The latter is probably the most important conclusion of this thesis. Furthermore, the peak-up boilers are used less and more geothermal energy is utilised compared to the traditional case. This leads to less emissions to the environment and a higher fraction of the heat demand to be covered by geothermal energy. So, all these results support a definite answer to the question given in the beginning of this Chapter, which defined the scope of it. It can be definitely said that the proposed case is better than the traditional case, from the economic, environmental and energetic points of view.

6 CONCLUSION

6.1 Achievement of aim and objectives

A comprehensive study of geothermal district heating systems (GDHSs) was carried out in this thesis. Initially, a detailed literature review was presented, in which it was identified that there was a gap in the way of operation of these systems. More specifically, there was no published research which examined the operation of a GDHS, but only practical experience is known about that. For that purpose, the study of the operation of a GDHS was a major part of this thesis. Furthermore, as for any renewable system it is desirable to maximise the utilisation of the lowest-carbon source, which in our case is geothermal energy. This is particularly important for renewable systems as these are capital intensive investments and it is of the utmost importance to maximise their utilisation in order to increase the cost-effectiveness of the investment. These two factors are the main drivers for the focus of this study.

Traditionally, a GDHS varies its heat output according to the heat demand up to its maximum capacity and in the cases that geothermal energy cannot cover all the heat demand, fossil-fuel peak-up boilers are implemented. In this study, it is proposed to keep the geothermal production constant throughout the day and integrate a fully-mixed hot water storage tank where hot water can be stored in times of low load, which can subsequently be released into the network to relieve peak demands. The operation of the installation will be scheduled on a daily basis, while it is re-iterated that the studied units are assumed to be heat production only units (which is common for geothermal energy) and offer higher flexibility compared to CHP units. It is also recalled that through this approach it is not intended to totally phase out the peak-up boilers (as this would probably render the investment unfeasible), but to reduce their use.

The **aim** of this thesis was to study the energetic, economic and environmental effect of including a heat storage in a geothermal district heating system under the proposed novel operational strategy. The aim of the thesis was achieved by fulfilling the three objectives defined in section 1.1.

The **first objective** was to develop a model for the sizing of a GDHS which would operate under this mode of operation. Through the developed algorithm, a specific

representative day is chosen as the design-day and the whole sizing is based on this day. In our case, three very different and discrete days were chosen as the design-days in order to show the influence of the sizing of the installation on the results. More specifically, those days where the days that their daily heat demand is equal to the 25^{th}-, 50^{th}- and 75^{th} centile of the daily heat demands of the whole year. The results show that the efficiency of the installation is very high and approximately 86.8-87.6% depending on the case of sizing. It was also shown that the mass flow rates throughout the network were quite high which makes the use of a fully-mixed tank (instead of a stratified tank) a sensible and logical choice. Probably the most important conclusion drawn from this part of the study was the importance of the insulation on the heat losses of the storage tank and the pipelines. More specifically, it was shown that the heat losses of the storage tank will be negligible if a thick insulation (in our case the thickness selected was 20cm) is used. For the pipelines of the network, an optimization algorithm was built which took into account their capital cost, the cost of electricity used to overcome the friction losses and the cost of the heat losses. By applying this algorithm, the obtained values of the heat losses were much smaller than other published values, which indicates that the heat losses were probably underestimated previously and have to be taken into account during the initial design of the pipeline system. This highlights the power of this optimisation algorithm

The **second objective** is the development of a model for the detailed study of the operation of the installation. In this model, the outcomes of the first model were used as inputs. Firstly, an algorithm that provides the operational strategy of the installation over a random day with a given heat demand was built. By operational strategy is defined the complete knowledge of the operation of the installation this day, such as the knowledge of the temperatures and the mass flow rates throughout the installation and for each time interval. This algorithm can be potentially a powerful tool for the operators of the installation who will know in advance how to operate the installation on any day if they know (or can predict) its heat demand. Then, this model was extended in order to build an extended model for the study the operation of the installation over a whole year. The main outputs of this model are the amount of electricity used by the pumps of the installation as well as the amount of fuel used by the peak-up boilers, both for the whole year, and comprise the main running costs of the installation. A comparison of these values for the studied and the traditional case of operation of GDHS was carried out and it was found that when the heat storage is implemented less fuel is used and more geothermal energy is utilised, while the amount of electricity used is roughly the same. Furthermore, the results indicate that the heat storage impacts most the medium sized installation. On the other

hand, it was shown that as sizing increases proportionately less fuel is used and more geothermal energy is utilised. So, it can be concluded that although the impact of the storage is higher in a modest sizing of the installation, the installation should be sized as big as possible in order to maximise the use of geothermal energy.

The **third** and last **objective** of this study was the development of an integrated model for the calculation of the economic, energetic and environmental indices of the installation together with a comparison with the traditional case. It was shown that when heat storage is used, both the capital and running costs of the installation are lower when compared to the traditional case. Therefore, all the financial indices obtained more favourable values for the studied case compared to the traditional operation. More specifically, the levelised cost of heating decreases, while the NPV, the IRR and the BCR all increase. Additionally, the effect of a financial subsidy, such as the Renewable Heat Incentive (R.H.I.) in our case, in a renewable heating project was highlighted, as all the financial indices increased importantly when the R.H.I. was taken into account. Yet again, a conflicting point arose, as on the one hand the storage impacts more the medium case of sizing from an economic point of view, but on the other hand, the most financially attractive case is the larger case of sizing. Of course, the second case is usually preferred and as proposed before, the geothermal part of the installation should be sized as large as possible. Furthermore, it was shown that when the heat storage is used the load factor of the installation increases, which means that the installation is working for more hours in its full load and more geothermal energy is used. Subsequently, a larger part of the total heat demand will be covered by geothermal energy. Finally, by implementing the heat storage, the annual emissions of the installation will decrease.

By the conclusions drawn from the last part of the study, a definite answer can be given to the main question of this thesis, which was whether it is worthwhile including a heat storage under the proposed operational strategy in a GDHS or not. It was clearly shown that for any case of sizing of the installation, by applying the heat storage the overall production of heat is cheaper and the peak-up boilers are used less. The utilisation of geothermal energy, which has numerous advantages as explained earlier, is increasing with subsequent reduction in the emissions of the installation. So, it can be definitely stated that the integration of a heat storage under the proposed mode of operation is beneficial for a GDHS from economic, energetic and environmental points of view. Therefore, the **aim** of this thesis has been fully achieved.

6.2 Summary of contributions of the thesis

The aim of this thesis was fully achieved together with its main objectives. The main contributions of this thesis in the field can be summarised as:

- The proposition of the integration of a heat storage in a geothermal district heating system under a novel operational strategy. It was shown that this proposition is beneficial for the system under an economic, energetic and environmental point of view.
- The provision of a robust algorithm for the sizing of the installation which would operate under the new operational strategy.
- Useful insights were obtained for the sizing and operation of several parts of the installation. The most important insight was the importance of the heat losses of the pipeline which was revealed by the optimisation algorithm that was developed for their sizing. This algorithm can also be used for the sizing of any pair of underground pre-insulated pipelines, if the boundary conditions are known. This is a contribution out of the main line of the thesis.
- The provision of a model that can provide the operational strategy of the installation in any day with a known heat demand. This model can theoretically be used by the operators of the installation if they can calculate or predict the heat demand of the studied day one day in advance which is reasonably achievable using weather forecasts. If the heat demand is known, this model will provide them with all the necessary information about how they should operate the installation throughout the day.
- The provision of a model that can provide useful information about the operation of the installation over a whole year.
- The provision of a model that can calculate the economic and energetic indices of the installation as well as its annual emissions. A second model was also built that can provide the same values of a traditional GDHS.
- The provision of a model that is coupled with the latter model and can make a robust comparison of the aforementioned indices which can show if the proposed solution is beneficial against the traditional case or not. In our case, the results of this model showed the first mentioned, and most important, contribution of this thesis, i.e. the economic, energetic and environmental effectiveness of this proposition.

6.3 Recommendations for future work

In this final section of the thesis, some recommendations for future work will be given. These include recommendations on the improvement and enrichment of the algorithms and proposal of further steps that should be taken using these algorithms. Finally, a similar approach for the modelling of a future energy system based on geothermal district heating will be proposed.

The first part of this study presented a robust algorithm for the sizing of a GDHS under the proposed operational strategy. A first improvement on the model would be to add the sub-models of other parts of the installation, mainly of the geothermal heat exchanger and of the substation, which in this study were considered as black-boxes. The geothermal heat exchanger was not further studied in this thesis as it is considered that it is a standardised equipment and that it was not worthwhile studying it further, while a possible study for its optimisation would be quite long and beyond the scope of this thesis. On the other hand, the substation of the installation was not also studied further, as no details could be found in the literature about these and it is envisaged that their configuration will be very case-specific and, therefore, difficult to model generically. Furthermore, depending on the case a substation might not even exist in an installation.

Moreover, the models for the sizing and the operation of the installation did not take into account the behaviour of the end-users, but took into account only the temperature drop in the boundaries of the branches of the distribution network. In other words, the boundary of the study were the boundaries of the "main" branches of the distribution network. The models could be further extended in order to take into account more details of the distribution network as well as the characteristics and the interface of each end-user (or at least of each different kind of end-user). Obviously, these additions would also affect the economic, energetic and environmental analysis which should be properly modified.

A basic disadvantage of all the models, and especially of the sizing model, is that they have not been validated against real data. This happened partially due to the lack of real data as some parts of the installation are not (or not known to be) deployed yet in reality, such as the proposed fully mixed tank, while for other parts, such as the pipelines, it was really hard to get real data from third parties. So, the validation of the developed models against real data is crucial for their possible practical and real-life application. If the

validation takes place, it is strongly believed that these models can be directly (or with few modifications) applied in real projects.

The whole analysis in this thesis was applied for three different discrete cases of sizing of the installation which were explained in detail in Chapter 3. These cases were the days whose daily heat demands correspond to the 25^{th}-, 50^{th}- and 75^{th}-centile of the daily heat demands of the whole year. These three cases were chosen as logical choices that could depict small, medium and large cases of sizing. A next step could study cases of smaller or larger sizing of the geothermal installation. Concerning the smaller sizing, it is intuitively understood that very small sizing of the geothermal installation is not possible as this would require a very low geothermal flow rate, which would definitely make the investment unfeasible. In other words, when borehole drilling is done for a geothermal well, a minimum flow rate is required otherwise the drilling is not successful or operational. This minimum flow rate excludes the cases of very small sizing of the installation, let's say of less than the 5^{th}- or 10^{th}- centile of the daily heat demands of the year. On the other hand for the case of very large sizing of the installation, in this thesis it was chosen in advance not to study such a case as this would lead to under-utilisation of the geothermal field and would possibly render the investment unfeasible. Whether this case is true depends on how "peaky" are the extreme peak demands. If these are very peaky, this would mean that a part of the geothermal installation would work for only a few hours per year, which is definitely unfeasible. If these peak demands were more frequent and not very peaky, then it might be possible to size the installation for a higher coverage by geothermal energy, albeit it is fairly certain that 100% coverage by geothermal energy would be very costly. After all, as was already mentioned, there will be some boilers in the installation anyway for back-up purposes. For that reason, it is never attempted to achieve 100% coverage by geothermal energy. But, the upper feasible limit of the sizing of the geothermal installation would be a very interesting point. Therefore, a study that would address these issues in detail would be quite useful.

Another issue that could be researched further, which was also explained in Chapter 4, is the development of a tool relating the heat demand data to weather conditions. This relationship can be extremely useful because it can be integrated with the model of the daily operational strategy of the installation developed in Chapter 4, and this model will be able to provide the operational strategy of the installation if the weather data are known (or predicted) instead of the heat demand. This is desirable as it is much easier and more effective to predict the weather conditions of the next day compared to its heat demand. A

first attempt at developing this relationship was made in Appendix B, in which the results were not so encouraging either because the approach was too simplistic or because the data in the studied case are very stochastic. Furthermore, this was not studied further in this thesis as it was out of its scope. So, an obvious further work arising from this thesis would be the development of a robust model that connects the heat demand with the weather conditions.

Finally, a similar study that could be based in the logic of this thesis concerning the management of the geothermal installation would be the integration with a heat pump for the further harvesting of geothermal energy. More specifically, an installation like this can be seen in Fig. 6.1. In such an installation, the cooled water that exits the geothermal heat exchanger instead of being re-injected in the underground (or sent to others uses) will be fed into heat pumps which can upgrade the temperature of fresh water to the desired level. The heated fresh water can either be stored in the hot storage tank or be fed directly in the network. But, the existence of the storage tank is again necessary. The main advantage of this system is that for the same geothermal potential more heat will be harvested through the use of the heat pump. Therefore, for the coverage of the same heat demand the geothermal installation can be smaller.

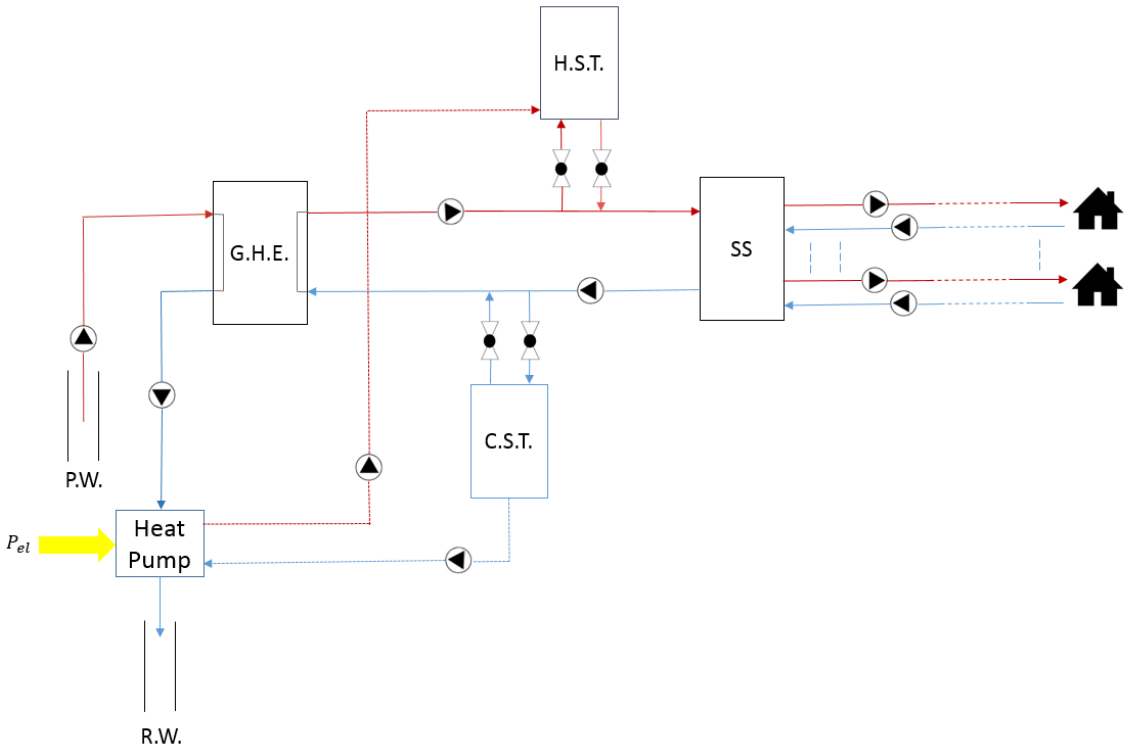

Figure 6.1 *Layout of the proposed system (G.H.E. = Geothermal Heat Exchanger, SS = Substation, P.W. = Production Well, R.W. = Re-injection Well, H.S.T. = Hot Water Storage Tank, C.S.T. = Cold Water Storage Tank, P_{el} = Electrical Power)*

On the other hand, the extra capital cost of the heat pump and of the pipelines connecting it to the network and the storage tanks as well as the extra operational cost of the electrical power used by the heat pump will be the main disadvantages of this proposal. The proposed installation can be operated under three alternative modes. The first alternative is the heat pump to operate in a 24/7 mode. The second alternative is the heat pump to operate only during the night hours in which the price of electricity is usually lower, thus decreasing this additional operational cost. A third alternative which can be applicable in a future energy system is that the heat pump can operate only when there is an excess of electricity in the electrical network, which can be the case in a future electrical system with a high penetration of intermittent renewable energy sources. This proposition on the one hand will make the operation of this system more complex, but on the other hand, will offer very cheap (or even free) electricity to the heat pump as this would be an amount of electricity that would be rejected. The latter would also be an advantage for the renewable electrical producers as this can be a potential additional income for them (as this electricity would be rejected as mentioned before) and this could also increase the stability of the electrical network. Of course, all these alternatives would require a detailed analysis in order to conclude if they are viable or not, but it is strongly believed that under the operation of the system presented in this thesis, these systems would be quite promising.

APPENDICES

Appendix A

Sensitivity analysis of two basic parameters of the system

In this Appendix, a sensitivity analysis of two basic parameters of a geothermal district heating system is carried out in order to examine their effect on the whole system. These parameters are the temperature difference on the hot side of the geothermal heat exchanger ($\Delta T_{h,GHE}$) and the ratio of the mass flow rates of the transmission network (R_m) and they have a crucial effect on the operation of the system. In the beginning of the algorithm explained in Chapter 3, initial values are assigned to these parameters and these are kept constant throughout the whole process. If the final results are physically acceptable, then the algorithm is considered converged, while if this is not the case, then the proper adjustment of these parameters has to be done.

In order to adjust these parameters their effects on several variables of the system have to be evaluated. These effects are studied in this Appendix. More specifically, the influence of the two aforementioned parameters on the temperature difference on the cold side of the geothermal heat exchanger ($\Delta T_{c,GHE}$), the outlet temperature of the supply transmission pipeline ($T_{tr,s,o}$), the capital cost of the pipelines (CC_{pipes}) and the number of wells is analysed. The results of this analysis are shown in the following graphs, and based on these results an iterative loop was added to the basic code for the adjustment of the parameters. More details on this possible source of error, the final loop that is added in the main code and a short discussion on these results are provided in section 3.2.8.

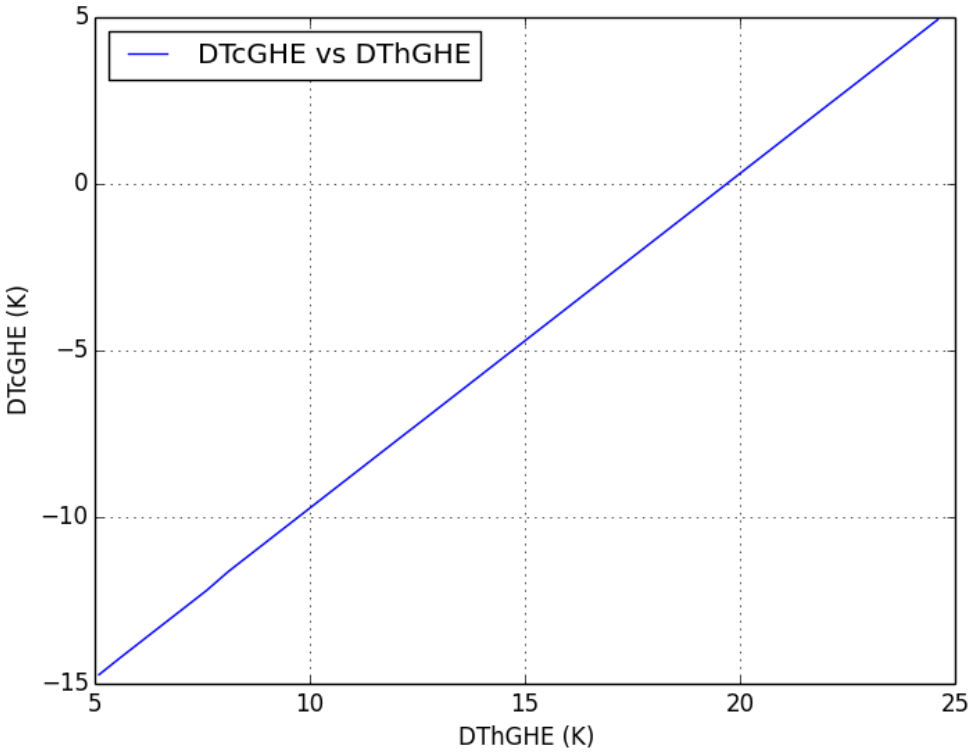

Figure A-A1 *Temperature difference on the cold side of the geothermal heat exchanger vs the temperature difference on the hot side of the geothermal heat exchanger*

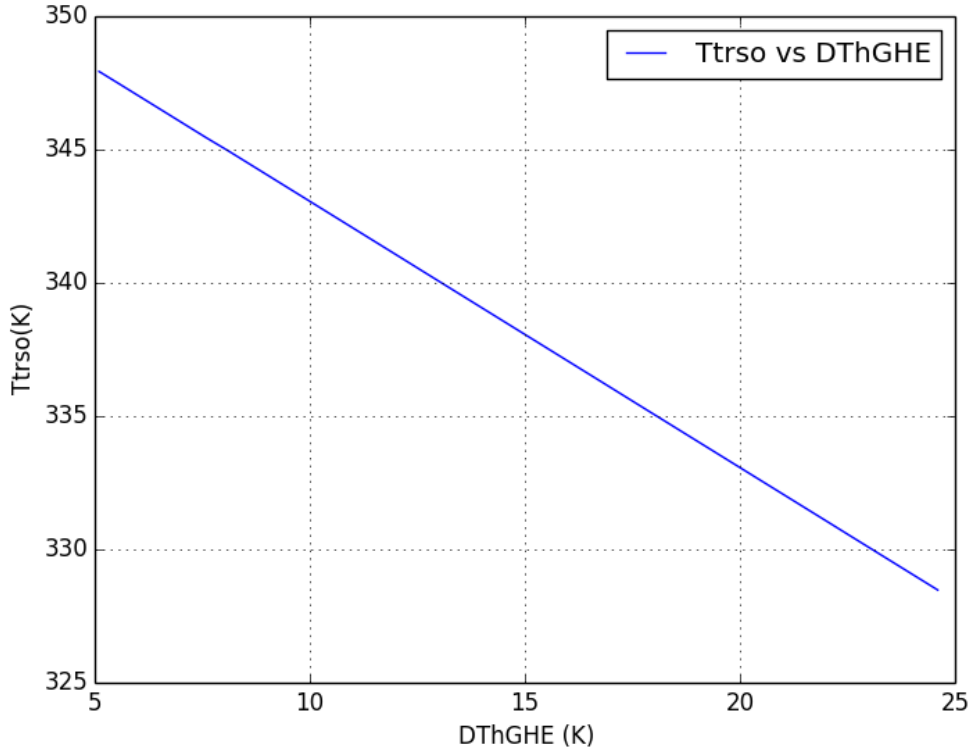

Figure A-A2 *Outlet temperature of the supply transmission pipeline vs the temperature difference on the hot side of the geothermal heat exchanger*

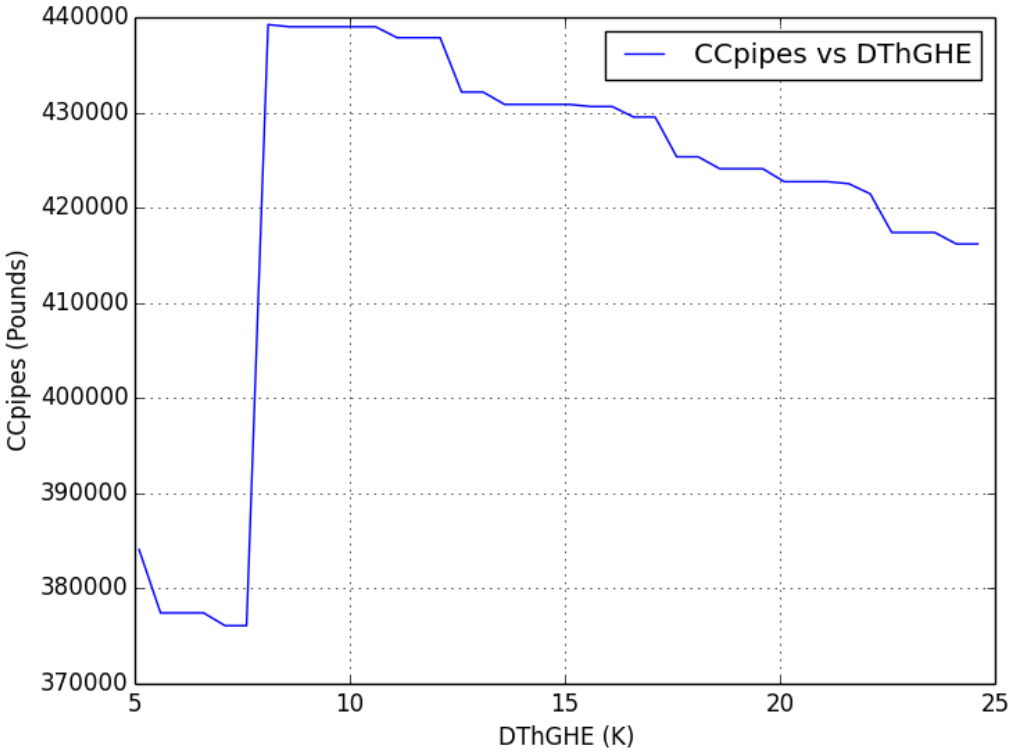

Figure A-A3 *Capital cost of the pipelines vs the temperature difference on the hot side of the geothermal heat exchanger*

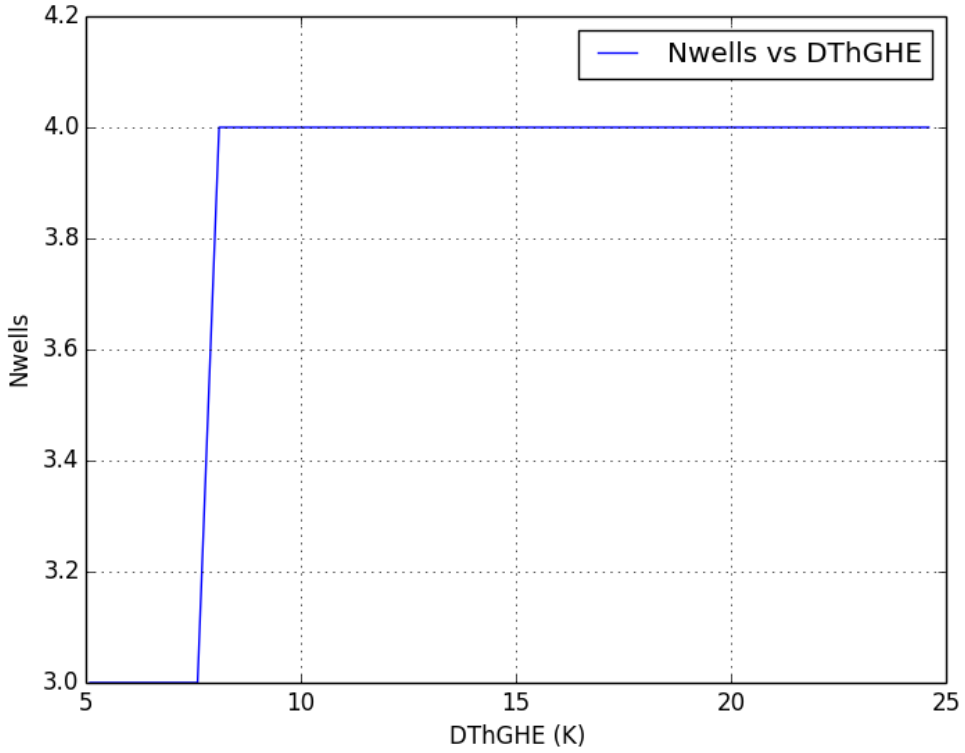

Figure A-A4 *Number of production wells vs the temperature difference on the hot side of the geothermal heat exchanger*

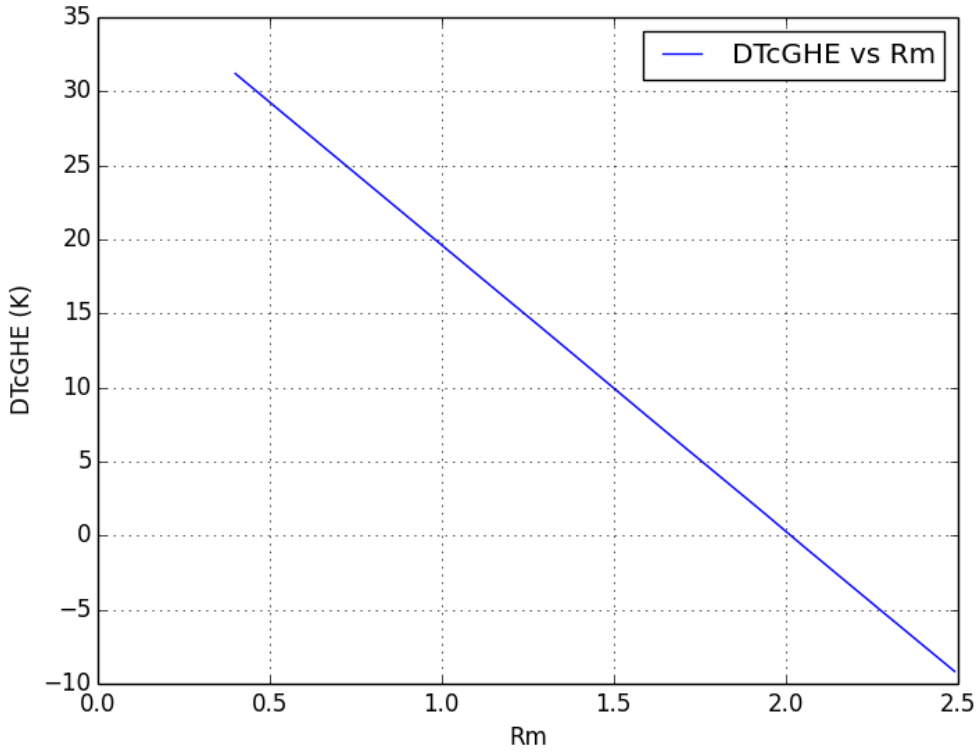

Figure A-A5 *Temperature difference on the cold side of the geothermal heat exchanger vs the ratio of the mass flow rates of the transmission network*

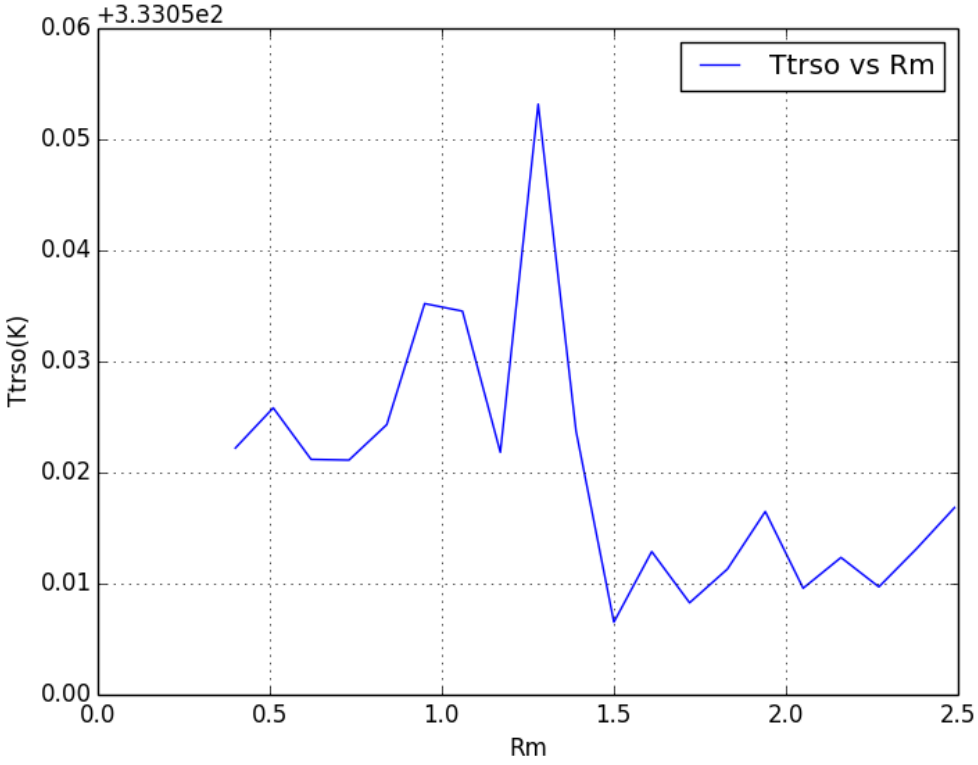

Figure A-A6 *Outlet temperature of the supply transmission pipeline vs the ratio of the mass flow rates of the transmission network*

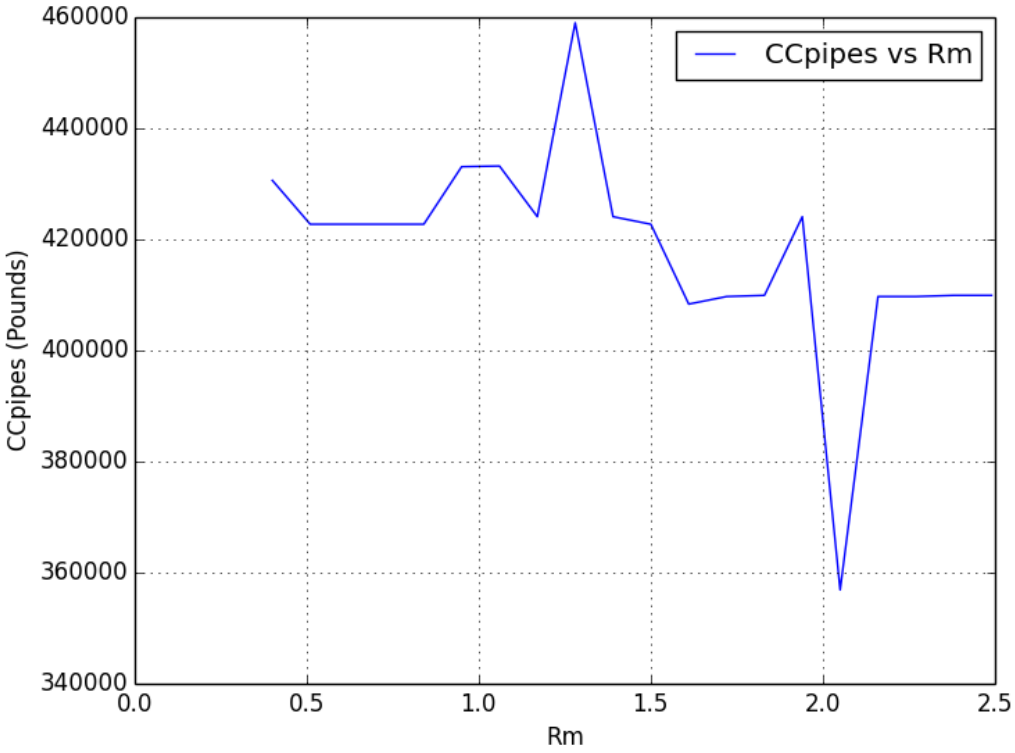

Figure A-A7 *Capital cost of the pipelines vs the ratio of the mass flow rates of the transmission network*

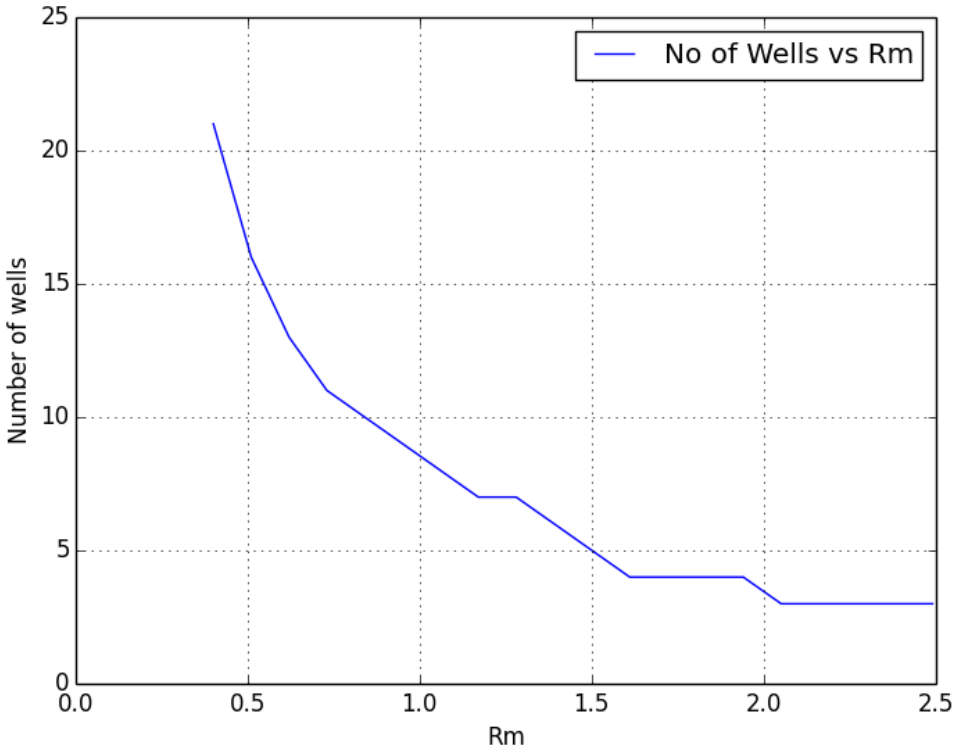

Figure A-A8 *Number of production wells vs the ratio of the mass flow rates of the transmission network*

Appendix B

Relationship between the heat demand and the weather conditions

B1) Introduction

The energy consumption in buildings accounts for a large fraction of the total energy use worldwide. More specifically, in Europe, the energy use in buildings accounts for 40% of the total energy use and 36% of total CO_2 emissions (European Parliament and Council, 2010). Therefore, it is easily understood that in order to fulfil the energy goals set worldwide the building sector should be taken very seriously into account. This can happen by optimising the whole process of energy production, distribution and consumption within the buildings. A crucial factor of the above process is an accurate *a priori* prediction of the energy consumption. An accurate prediction improves the efficiency and performance of the energy production, reducing the environmental impact.

The main energy forms within a building are heating/cooling, hot sanitary water and electricity consumption. In this study, the focus will be on the prediction of the heat demand of the building. A general review of the prediction methods of the energy consumption has been provided by Zhao and Magoules (2012). In general, this problem is quite complex as many factors should be taken into account, such as the weather conditions, the structure of the building, the habits of its occupants (the so-called social factor) and many others. Therefore, many different prediction methods or models have been developed. These can be categorised in the physical or engineering models, the black-box models and the statistical models.

The physical or engineering models are based on the physical principles which govern the heat losses of the building and take into account the different layers throughout its wall, the difference between the ambient and the indoor temperature, the heat gains within the building etc. Many commercial tools have been developed for that purpose, such as TRNSYS and EnergyPlus[5]. Usually, the physical models are quite complex and are not so easy to apply in reality as it is quite difficult to obtain all the characteristics of the building. Therefore, some more simplified methods have been developed. The most well-known method is the degree-day method, which is a very simple method for the calculation of the heat demand knowing only the ambient temperature (Gelegenis, 2009; Schoenau and Kehrig, 1990; Coskun, 2010). This method is very simple and therefore not so accurate. Catalina *et al.* (2013) developed a multiple regression model between the heat demand and the difference between the indoor and the outdoor temperature, the total heat transfer coefficient

[5] http://www.buildingenergysoftwaretools.com/

and the south equivalent surface. The results of this approach were quite satisfactory. Another simplified model was also applied by Afram and Janabi-Sharifi (2015) that predicted the daily energy consumption profile for residential buildings. The interested reader can find more details on the aforementioned methods in the work of Zhao and Magoules (2012).

A black-box model is used when the physical model is not completely known or is very complex to implement practically. In these cases, the inputs and the outputs of the model are known and the black-box approach is used to build the inter-connecting function. The most common types of black-box models are the artificial intelligence methods and these are further divided in the Artificial Neural Networks (ANNs) and the Support Vector Machines (SVMs). A review of these methods in the building energy systems can be found in the works of Krarti (2003) and Dounis (2010). These systems have been used widely the last years for the heat demand forecasting in buildings (Kalogirou, 2006; Kreider *et al.*, 1995; Shamshirband *et al.*, 2015) and the accuracy of the results is usually the best among the methods used. On the other hand, these models need a lot of historical data which are not always available and it is very difficult to point out the optimum parameters of the problem. Finally, the fact that the physics of the problem are not identified through these methods makes a lot of academics, mainly, to avoid these methods.

Another method which is not so common and combines the physical and the black-box models is the grey-box approach, in which there is a theoretical knowledge of the system which is combined with measurements in order to produce its mathematical description. For example, Zhou *et al.* (2008) developed an integrated model for the prediction of the heat demand which uses as inputs the temperature and the relative humidity, that are calculated through a modified grey model, as well as the solar radiation which is calculated through a regressive model. The interested reader can find other applications of the grey-box approach in the work of Guo *et al.* (2011).

The statistical models are producing single or multiple correlations between the heat demand data and, usually, the weather conditions. In general, the statistical methods are divided in the autoregressive models, the integrated models and the moving average models (Popescu *et al.* 2008). Historical data are used for the production of the correlation and, then, this correlation is used to predict the future heat demand. The basic advantage of these models is that they are quite fast and simple to use, but their accuracy is not that good as it is not easy to capture the social factor and the building envelope. An attempt to take into

account the social factor was done by Dotzauer (2002) where it is stated that the social factor is of utmost importance and should be definitely taken into account. So, Dotzauer (2002) separated the heat demand function into two parts, the temperature dependent part and the part that depicts the social behaviour. Popescu *et al.* (2008) are producing multiple correlations between the current weather conditions and data of previous time intervals trying to capture the social factor. The correlation factors are quite satisfying, but when these correlations are tested against new data then the results are quite variable.

In this part of the thesis, simple correlations will be produced between the heat demand data and the weather conditions, in which the social factor and the building envelope will be taken into account. The correlations will be quite simple because, as stated by Dotzauer (2002), there will always be failures in the prediction of the weather which is used for the prediction of the heat demand. Therefore, complex models can provide errors and more simple models can provide the same satisfactory results. In order to take into account the social factor, different correlations will be produced for each season/day/hour. For example, it is expected that for the same temperature the heat demand will be different between summer and winter, or between a working and a non-working day. The optimum splitting of the data will also be researched. Few research has been carried out on the basis of thinning the data. Ma *et al.* (2014) categorised the buildings according to their function and found different correlations for each building, while Yao and Steemers (2005) did a break-down analysis of the load starting from the appliances and building-up the total load. Concerning the building envelope, data of the previous time steps will be used in the correlations. Apart from the work of Popescu *et al.* (2008), there has been no other published work, up to the authors' knowledge, using data of the previous time steps.

The structure of this study is as follows: In this section, a brief introduction in the problem of the heat demand prediction was given. In section B2, the methodology will be explained focusing on the different kinds of data-splitting that will be tested. In section B3, the results will be shown and discussed, while section B4 will conclude this study.

B2) Methodology

In this section, a brief description of the methodology followed will be given. The heat demand data used in the modelling were provided by the Estates and Building Office of the University of Glasgow and refer to a cluster of buildings managed by the University. On the

other hand, the weather data used were obtained by the British Atmospheric Data Centre (BADC)[6] and refer to the Kilpatrick area of Glasgow, which is a village in the west of Glasgow on a straight line distance of almost 14km. The data from the meteorological station of this area were chosen as these were the most precise data, the other operating stations were almost in the same distance and, most importantly, there were very few missing data. There were available data for the whole 2012 and for the first five months of 2013. Therefore, the correlations were done for the 2012 data and, then, these correlations were tested for the 2013 data. As mentioned previously, there were very few missing data from the specific station. More specifically, there were missing data in two days of 2012 and in one day of 2013. These three, in total, days were not taken into account in the calculations.

In order to determine all the correlations, the MATLAB curve fitting tool was used. A novelty of this study, is that for the calculation of the fitting lines/curves the method used was not the typical "least-squares method" in which the sum of the squares of the residuals is minimised, but a special feature of the MATLAB curve fitting tool called "Robust=LAR", in which the sum of the absolute values of the residuals is minimised. The advantage of this method is that it weakens the effects of possible outliers in the data which would lead to not so realistic fittings using the typical method.

For the evaluation of the goodness of the fitting the value of R^2 (Co-efficient of determination) was calculated for each case by the following sets of equations:

$$R^2 = 1 - \frac{SSE}{SST} \quad \text{(A-B1)}$$

$$SSE = \sum(HD_i - \widetilde{HD}_i)^2 \quad \text{(A-B2)}$$

$$SST = \sum(HD_i - \overline{HD})^2 \quad \text{(A-B3)}$$

Where:

R^2 = Coefficient of determination (Dimensionless)

SSE = Sum of squared errors (kWh)

SST = Total sum of squares (kWh)

[6] http://badc.nerc.ac.uk/home/

HD_i, $\widetilde{HD}_i$= Predicted and observed heat demand for each time interval, respectively (kWh)

$\overline{HD}$ = Average predicted heat demand (kWh)

The first part of the modelling is the identification of the optimum set of the dependent variables. In other words, the correlation between the heat demand and different dependent variables will be tested in order to check which one produces the best fitting. The dependent variables will always be two and one of them will always be the temperature at the current time-step as it is assumed to be the main driving force of the heat demand. The other variables that will be checked are the temperature and the heat demand in several previous time-steps in order to capture the effect of the building envelope. At the same time the optimum kind of correlation will be identified.

After the above issues are identified, then the possible correlations will be calculated and tested. In Fig.A-B1, the 2012 data are shown where it is made clear that it is impossible to obtain a single correlation that can fit satisfactorily these very sparse data. Therefore, it is necessary to split the data into different time periods in order to capture possible social variances.

The different temporal data-splitting will be the following:

- Different seasons. The data will be splitted in four different seasons within the year, i.e. January-March, April-June, July-September and October-December.
- Splitting in working and non-working days.
- Different hours. Different correlations will be carried out for each hour of the day. Therefore, there will be 24 different correlations.

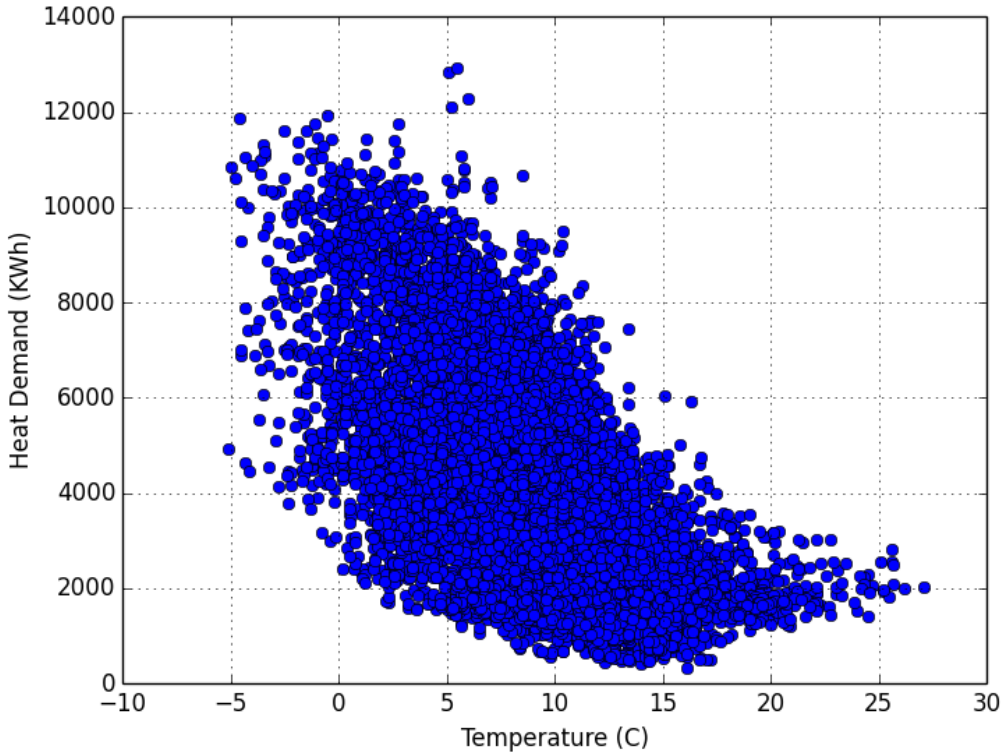

Figure A-B1 *2012 data*

B3) Results

B3-1) Optimum fitting functions

Firstly, the optimum combination of dependent variables will be examined. As mentioned earlier, one of the dependent variables will always be the temperature at the specific time step, while the independent variable will be the heat demand at the specific time step, i.e. the predicted heat demand. The other dependent variable will be either the temperature or the heat demand on various previous time steps. In our case, the time step is one hour. The previous time steps studied are one, five and twenty-four hours earlier in order to capture possible different influences of the building envelope. The second case was a random choice between the two extremes of one and twenty-four hours. The results can be seen in Table A-B1 for 3 different possible correlations, 1^{st}-2^{nd} and 3^{rd} polynomial. It should be mentioned that both dependent variables were risen in the same force. The exponential and logarithmic correlations were also tested, but the produced results were much worse, so for sake of simplicity they are not shown in this paper. It should be noted that these results refer to the 2012 data.

By observing Table A-B1, it is clear that the best combination of dependent variables is the temperature of the current time step and the heat demand of the previous time step. It seems that the influence of the heat demand one hour earlier is very important for the current heat demand. This makes clear the effect of the building envelope or the heat capacity of the building in this kind of problems and this is something very under-estimated in previous works. Therefore, the correlation that will be examined will be of the following kind:

$$HD = f(T, HD_{-1}) \quad \text{(A-B4)}$$

Where:

HD_{-1} = Heat demand of the previous time step (kWh)

Although the results show that the optimum kind of correlation is a 3rd polynomial, this was researched further by rising each of the variables in different forces. The results can be seen in Table A-B2.

Table A-B1 *Values of R^2 (%) for different dependent variables and three different correlations (the subscripts in the variables denote the number of previous time steps to which the variable refers)*

Dependent Variables	**Correlations**		
	1st Polynomial	2nd Polynomial	3rd Polynomial
$\boldsymbol{T}$	39.74	39.94	40.82
$\boldsymbol{T, T_{-1}}$	41.77	42.18	94.47
$\boldsymbol{T, T_{-5}}$	47.83	48.4	48.82
$\boldsymbol{T, T_{-24}}$	40.61	41.13	42.02
$\boldsymbol{T, HD_{-1}}$	98.95	97.08	99.12
$\boldsymbol{T, HD_{-5}}$	31.67	93.76	97.69
$\boldsymbol{T, HD_{-24}}$	93.2	96.71	98.28

Table A-B2 *Values of R^2 (%) for different possible polynomial correlations*

		Force of $\boldsymbol{HD_{-1}}$		
		1	2	3
Force of $\boldsymbol{T}$	1	98.95	99.01	97.87
	2	98.69	97.08	99.03
	3	98.89	98.83	99.12

In the above table, it can be seen that there is a general, although not necessary, trend of an increasing value of R^2 when the forces of the two dependent variables increase. But, this increase is considered not to be that big to make it worth to make the fitting function more complex by adopting the maximum forces of the dependent variables. So, it is decided to select as the fitting function the case in which the forces of T and HD_{-1} are 1 and 2, respectively. Therefore, the final fitting function will be the following:

$$HD = A + B \cdot T + C \cdot HD_{-1} + D \cdot T \cdot HD_{-1} + E \cdot HD_{-1}^2 \quad \text{(A-B5)}$$

B3-2) Calculation of the correlations

Equation A-B5 is the fitting function that will be used in the rest of this study. In this section, the correlations will be calculated based on the 2012 data. The fitting was carried out for the different temporal splittings explained in section B2. It should be mentioned that it was not worth to combine different temporal splittings, e.g. different seasons and different hours at the same time as this did not improve the results. All the results are shown in Table A-B3.

A first major observation is that in the majority of the cases the fitting achieves very high correlation factors. More specifically, the values of R^2 are usually higher than 98% and even 99%. Even in the case where all the data are used, the value of R^2 is almost 99%. In the case of different seasons, it is observed that in general the correlation factors improve, apart from the case of October-December when the R^2 worsens a bit. When the data are separated in working and non-working days, it can be seen that in the case of the working days the correlation worsens, while in the case of the non-working days the correlation improves. Finally, when the data are splitted in different hours, it is seen that in most of the cases the value of R^2 is more than 99% and reaches also its highest value amongst the cases which is 99.76%. But, there are four cases (05:00 to 08:00) in which the value of R^2 is considerably lower compared to the other cases.

Table A-B3 Results of the fitting function's coefficients and values of R^2 for the 2012 data

	A	B	C	D	E	R^2 (%)
All 2012 Data	107	2.541	1.052	-0.00815	-9.178E-6	99.01
Different Seasons						
Jan-Mar	566.2	-35.36	0.9667	-0.0005676	-5.352E-6	99.43
Apr-Jun	-17.64	17.78	1.213	-0.01678	-2.839E-5	99.26
Jul-Sep	-220.8	26.92	1.26	-0.0212	-2.961E-5	99.54
Oct-Dec	-191.1	37.77	1.11	-0.01286	-1.312E-5	98.91
Working and non-working days						
Working days	156.5	-1.283	1.1	-0.009378	-1.442E-5	97.76
Non-working days	88.56	4.61	1.052	-0.009619	-1.016E-5	99.51
Different hours						
00:00	584.2	-39.95	0.542	-0.0008695	7.413E-5	98.11
01:00	106.6	-6.292	0.9948	0.0007628	-6.95E-6	98.06
02:00	-54.73	27.37	1.65	-0.03702	-1.061E-4	98.46
03:00	-243.2	28.85	1.6	-0.04386	-8.178E-5	98.42
04:00	-350.2	79.02	1.76	-0.04061	-0.0001198	98.67
05:00	2584	-214.4	0.682	0.02774	-2.71E-6	73.45
06:00	-4917	284.8	3.248	-0.0505	-1.84E-4	74.24
07:00	7541	-411.4	-0.08956	0.0176	3.778E-5	85.33
08:00	-2690	126.1	1.873	-0.03144	-5.888E-5	77.21
09:00	312.6	-6.856	1.109	-0.01791	-1.846E-5	99.4
10:00	-1091	75.39	1.335	-0.02302	-3.072E-5	99.6
11:00	-478.1	20.28	1.23	-0.009561	-2.343E-5	99.71
12:00	-176.6	12.54	1.219	-0.01212	-2.281E-5	99.75
13:00	-246.4	14.18	1.052	-0.004202	-4.456E-6	99.76
14:00	-8.53	2.746	1.083	-0.008493	-8.593E-6	99.69
15:00	802.8	-39.42	0.8157	0.004971	1.539E-5	99.6
16:00	440.9	-16.93	1.023	-0.004324	-2.819E-6	99.78
17:00	211.8	-12.69	1.015	0.002753	-6.097E-6	99.7
18:00	-608	34.1	1.072	-0.0007737	-1.208E-5	99.58
19:00	-505.4	4.053	1.612	-0.01559	-5.984E-5	99.62
20:00	1542	-66.28	0.4024	0.01536	4.064E-5	99.71
21:00	1336	-64.15	0.7566	-0.002604	-6.915E-6	99.66
22:00	1451	-72.05	0.5347	0.005745	7.179E-6	99.61
23:00	-377.8	42.49	1.25	-0.04078	-7.2E-5	99.12

An interesting observation in Table A-B3 is that the coefficient C (see eq.A-B5), which is the coefficient of the heat demand of the previous time-step, usually has a value which is very close to 1. This indicates the very high influence of the heat demand of the previous time-step on the current heat demand justifying further our prior selection. It might also not be coincidental that the cases of lower R^2 have a value of C relatively further to 1 compared to the other cases.

In general, it can be stated that the proposed simple two-dimensional correlation is very powerful achieving high correlation factors. There is also a trend of the correlation factor improving when the data are splitted with the cases of different seasons and different hours to show the best improvement. On the other hand, it is somehow risky to state that fact since the correlation factor are already quite high. Furthermore, it is shown by previous works that a specific correlation in some specific data might achieve high correlation factors, but this does not guarantee a good prediction of other data with the same correlation. Therefore, it is of utmost importance to check the fitting of these correlations with the 2013 data. This is studied in detail in the next section.

B3-3) Checking the correlations with the 2013 data

As explained previously, in this section the correlation functions calculated in section B3-2 will now be tested against the 2013 data. The available data for 2013 are for the first five months of the year, so the correlations of July-September and October-December seasons will not be checked. The results of the testing are shown in Table A-B4.

It is observed that the values of R^2 in this case are much lower than in the initial fitting of the 2012 data. This shows that although a fitting function can fit very well some specific data, then when this function is tested to predict other data then it might not work so well. There can be many reasons why this occurs. First of all, the heat demand as well as the weather conditions are, in reality, stochastic phenomena, and, therefore, any discrepancies can happen. Secondly, the heat demand might have changed because of external reasons, such as additional loads. In the studied case, there is no knowledge if this happened or not. Thirdly, the heat demand depends a lot on the human factor, and although an effort was done to capture this, it can never be totally captured. Especially, in a case like the studied one, where there are buildings managed by the University, the human factor is very changeable and unpredictable.

Table A-B4 *Testing the fitting function against the 2013 data*

	R^2 (%)
All 2013 data	9.91
Different seasons	
January-March	18.18
April-June	23.18
Working and non-working days	
Working days	37.64
Non-working days	37.90
Different hours	
00:00	74.74
01:00	72.07
02:00	59.94
03:00	51.35
04:00	53.08
05:00	24.24
06:00	21.89
07:00	-27.34
08:00	45.57
09:00	64.93
10:00	61.42
11:00	59.99
12:00	63.12
13:00	63.42
14:00	65.24
15:00	66.91
16:00	63.08
17:00	50.12
18:00	44.01
19:00	51.87
20:00	50.74
21:00	36.06
22:00	60.25
23:00	62.78

For example, in our case the heating is free for the consumers, so it might be turned on for more time than is really needed resulting in higher heat demand. These are the basic reasons for this disagreement which demonstrates in the best way the stochastic nature of the problem and the great attention that should be paid in the engineering applications which involve the prediction of these phenomena. Simple assumptions for the heat demand or adopting values of the previous years can be very misleading for future prediction.

In Table A-B4, it can also be seen that now there is a clear distinction between the values of R^2 in each case, while in the case of 2012 data all the cases showed almost the same values of R^2. More specifically, the case of different hours seems to have the best prediction of all the cases with most of the values of R^2 being between 50% and 70%. There is also a negative value of R^2 which shows that the fitting in this case is very bad. Furthermore, some of the values are worse compared to the other cases, but, in general, this case seems to be the best choice.

B4) Conclusion

Some important conclusions can be drawn by the previous analysis. These are summarised as:

- A simple polynomial two-dimensional model produces correlations with very high correlation factors. It is shown that a simple model can predict the heat demand very satisfactorily.
- The main novelty of this paper is that it was shown that the heat demand in a specific time-step is highly affected by the heat demand in the previous time-step, proving the big effect of the heat capacity of the building. Therefore, one of the dependent variables of the studied correlation is the heat demand in the previous time step.
- High correlation factors are achieved when the studied function is fitted in the 2012 data, but when the produced functions are tested against new data (2013 data), the correlation factors are much lower. This shows that any simplified assumptions, such as that the heat demand will follow the same pattern each year or season, can be very misleading. If the heat demand can be predicted very well one year, it is not necessary that it can be predicted well the next year with the same predicting functions. Therefore, it is necessary to adopt demand side management techniques that can make the heat demand more predictable.

- The correlations improve a lot when multiple correlations are carried out and not a single correlation in all the data. It seems that the splitting of the data into different hours across the day is the best option.
- This study was carried out with simple correlations in order to make the above very useful conclusions. By taking into account these observations into more sophisticated models, the prediction of the heat demand can be much more accurate and the discrepancies between the expected and the observed heat demand can be much smoother.

Appendix C

Calculation of the cost of the storage tanks

As mentioned in section 5.2.1, the capital cost of the storage tanks includes the cost of their materials as well as other costs (mainly for civil and fabrication costs). The calculation of the material costs has been extensively analysed in the aforementioned section. In this Appendix, a compact analysis of the other costs of the tanks as well as the assumptions that were used for their calculation will be provided.

Firstly as a basis for these calculations, an e-mail received by Dr Richard Coulton of SiltBuster was used. This e-mail is shown in the following figure.

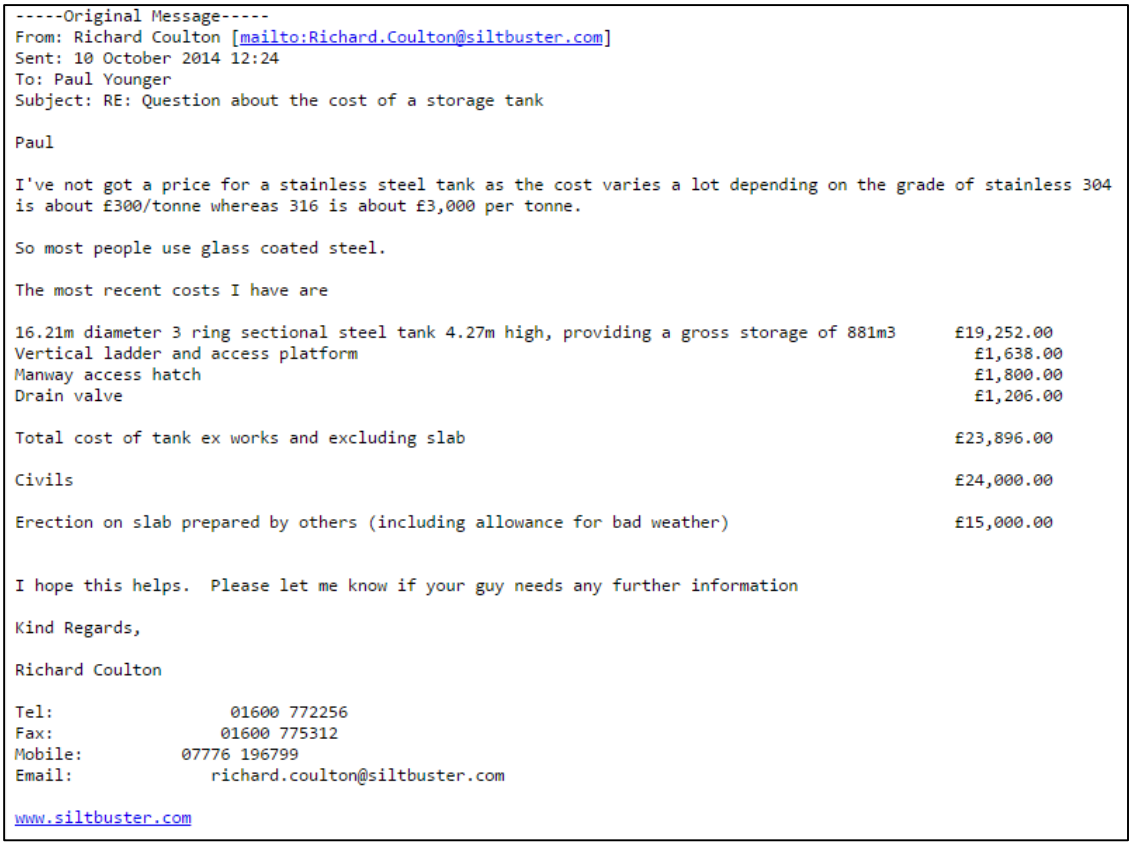

-----Original Message-----
From: Richard Coulton [mailto:Richard.Coulton@siltbuster.com]
Sent: 10 October 2014 12:24
To: Paul Younger
Subject: RE: Question about the cost of a storage tank

Paul

I've not got a price for a stainless steel tank as the cost varies a lot depending on the grade of stainless 304 is about £300/tonne whereas 316 is about £3,000 per tonne.

So most people use glass coated steel.

The most recent costs I have are

16.21m diameter 3 ring sectional steel tank 4.27m high, providing a gross storage of 881m3	£19,252.00
Vertical ladder and access platform	£1,638.00
Manway access hatch	£1,800.00
Drain valve	£1,206.00
Total cost of tank ex works and excluding slab	£23,896.00
Civils	£24,000.00
Erection on slab prepared by others (including allowance for bad weather)	£15,000.00

I hope this helps. Please let me know if your guy needs any further information

Kind Regards,

Richard Coulton

Tel: 01600 772256
Fax: 01600 775312
Mobile: 07776 196799
Email: richard.coulton@siltbuster.com

www.siltbuster.com

Figure A-C1 *Informative e-mail by Dr Richard Coulton on the cost of storage tanks*

Since the material costs have already been calculated, their corresponding value (£19252) will not be used. The other costs provided will be used as reference costs together with the dimensions of the specific tank referred in the e-mail. Furthermore for the other costs, the following assumptions are made:

- The cost of the vertical ladder and access platform will be proportional to the height of the storage tank.
- The costs of the manway access hatch and the drain valve will be the same as those provided in the e-mail as these are not considered to be significantly

affected by the dimensions of the tank. Furthermore, these costs are low compared to the others, so any error on their calculation will be negligible from an engineering point of view.

- The civils costs as well as the erection on slab are assumed to be proportional to the volume of the tank.

Therefore, by taking into account these assumptions as well as the costs and the dimensions provided in the e-mail, the other costs of the storage tanks are calculated by the following equations:

$$CC_{ST,VLAP} = 1638 \cdot \frac{H_{ST}}{4.27} \quad \text{(A-C1)}$$

$$CC_{ST,MAH} = 1800 \quad \text{(A-C2)}$$

$$CC_{ST,DV} = 1206 \quad \text{(A-C3)}$$

$$CC_{ST,CV} = 24000 \cdot \frac{V_{ST}}{881} \quad \text{(A-C4)}$$

$$CC_{ST,EOS} = 15000 \cdot \frac{V_{ST}}{881} \quad \text{(A-C5)}$$

Where:

$CC_{ST,VLAP}$, $CC_{ST,MAH}$, $CC_{ST,DV}$, $CC_{ST,CV}$, $CC_{ST,EOS}$ = Capital costs (£) of the vertical ladder and access platform, manway access hatch, drain valve, civils and erection on slab of the storage tank, respectively

H_{ST} = Height of the storage tank (m)

V_{ST} = Volume of the storage tank (m^3)

It should be pointed out that this analysis is valid both for the hot and cold water storage tank. For this reason, no distinction is made between them in the specific nomenclature. So, the other costs of the storage tank (last term in Eq. 5.7) is calculated as the summary of the previous costs.

$$\sum CC_i = CC_{ST,VLAP} + CC_{ST,MAH} + CC_{ST,DV} + CC_{ST,CV} + CC_{ST,EOS} \quad \text{(A-C6)}$$

Appendix D

Historic electricity and gas prices for non-domestic users in the U.K.

In this Appendix, the historic prices of electricity and gas for non-domestic users in the U.K. is provided. These prices were used for the economic analysis in Chapter 5. More details can be found in the corresponding sections. It should be mentioned that in the initial Tables the prices of two cases were included, those excluding and those including the climate change levy. In our case, the prices of excluding the climate change levy were used and these will be presented. This was the case as in the whole economic analysis the carbon taxes were taken into account, which is a similar fee to the climate change levy, so it was considered unrealistic to take both into account.

It is reiterated that these prices were found in the website of the U.K. government, and more specifically in footnote 3 of this thesis. Eventually, the historic prices are shown in the following two Tables.

Table A-D1 *Historic electricity and gas prices for non-domestic users in the U.K. (2004-2008)*

Fuel	**Size of consumer**		**2004**	**2005**	**2006**	**2007**	**2008**
Electricity	Very Small		5.99868	6.65641	8.1594	9.53619	10.38
	Small		4.96118	5.80569	7.00163	7.83446	8.76619
	Small/ Medium		3.89101	5.25304	6.86618	7.18867	8.00499
	Medium		3.48191	4.61012	6.17056	6.45378	7.36318
	Large		3.35952	4.31205	5.95282	6.07369	7.13955
	Very Large		3.00337	3.95494	5.1339	5.93764	7.352
	Extra Large					5.14735	6.39219
	Average		3.871	4.865	6.36533	6.8549	7.93467
Gas	Very Small		1.43839	1.81891	2.34869	2.69117	3.15057
	Small		1.30341	1.7569	2.27324	2.3273	2.54902
	Medium		1.16352	1.63492	2.09182	1.86639	2.23064
	Large		1.00303	1.45311	1.92842	1.57328	2.13589
	Very Large		0.95189	1.43117	1.57359	1.24863	2.03733
	Average		1.17626	1.61122	2.03476	1.87738	2.36792

Table A-D2 *Historic electricity and gas prices for non-domestic users in the U.K. (2009-2013)*

Fuel	**Size of consumer**		**2009**	**2010**	**2011**	**2012**	**2013**
Electricity	Very Small		11.874	12.0114	11.7892	12.2511	12.6687
	Small		10.039	9.71556	9.8104	10.3273	10.8689
	Small/ Medium		9.13605	8.16026	8.39764	9.07946	9.67907
	Medium		8.23734	7.21272	7.57437	8.24836	8.88201
	Large		8.07661	6.67545	7.15391	8.11991	8.93879
	Very Large		7.99791	6.53817	6.94866	7.70888	8.7342
	Extra Large		7.06512	6.60028	6.94392	7.95584	8.41807
	Average		9.05696	8.24591	8.2819	8.94259	9.5204
Gas	Very Small		3.52427	3.14098	3.30481	3.94295	4.099
	Small		2.53324	2.28657	2.47039	2.90064	3.1207
	Medium		2.209	1.84209	2.13813	2.56372	2.88442
	Large		1.9872	1.71926	2.07199	2.3539	2.5652
	Very Large		1.50159	1.54443	2.01398	2.11426	2.26374
	Average		2.3244	2.03664	2.30447	2.74995	2.96931

REFERENCES

Afram, A., and Janabi-Sharifi, F., 2015. Black-box modelling of residential HVAC system and comparison of gray-box and black-box modelling methods. Energy and Buildings, 94: 121-149.

Aksoy, F., Yabanova, I., and Bayrakceken, H., 2011. Estimation of dynamic viscosities of vegetable oils using artificial neural networks. Indian Journal of Chemical Technology, 18: 227-233.

Arslan, O., and Kose, R., 2010. Exergoeconomic optimization of integrated geothermal system in Simav, Kutahya. Energy Conversion and Management, 51: 663-676.

Arslan, O., Ozgur, M.A., Kose, R., and Tugcu, A., 2009. Exergoeconomic evaluation on the optimum heating circuit system of Simav geothermal district heating system. Energy and Buildings, 41: 1325-1333.

Arteconi, A., Hewitt, N.J., and Polonara, F., 2012. State of the art of thermal storage for demand side management. Applied Energy, 93: 371-389.

Atkinson, D.J., and Huxtable, D.D., 1984. Geothermal district heating for Reno, Nevada, U.S.A. Geothermics, 13: 265-279.

Baker, M., 2009. The Basics of API 650. Presented in the 2009 Aboveground Storage Tank Management Conference and Trade Show, 11 September 2009, Houston Texas, U.S.A. Unpaginated, available online at "http://docslide.us/documents/the-basics-of-api-650.html", last accessed on 16/02/2015, 52pp.

Banks, D., 2012. Thermogeology: ground-source heating and cooling. Wiley Blackwell (Second Edition), Chichester, 526pp.

Barelli, L., Bidini, G., and Pinchi, E.M., 2006. Implementation of a cogenerative district heating system: Optimization of a simulation model for the thermal power demand. Energy and Buildings, 38: 1434-1442.

Bellache, O., Bouyousfi, B., and Ait-Messaoudene, N., 2000. Design and study of a geothermal district heating system at Hammam-Righa (Algeria). In: Sayigh A.A.M.

(Editor). Proceedings of the 6th World Renewable Energy Congress. Brighton, United Kingdom, July 2000, pp.: 305-309.

Bjornsson, S., 2010. Geothermal development and research in Iceland. National Energy Authority of Iceland, Reykjavik, Iceland, 40pp.

Bloomquist, R.G., 2003. Geothermal space heating. Geothermics, 32: 513-526.

Bloomquist, G., O'Brien, R.G., and Strunge, S., 2004. Improving the operations and economic performance of the Zakopane, Poland geothermal district heating system through modelling. Proceedings of International Geothermal Days 2004. Zakopane, Poland, 13 -17 September 2004, pp.: 238-244.

Bohm, B., 2000. On transient heat losses from buried district heating pipes. International Journal of Energy Research, 24: 1311-1334.

Bosman, M.G.C., Bakker, V., Molderink, A., Hurink, J.L., and Smit, G.J.M., 2012. Planning the production of a fleet of domestic combined heat and power generators. European Journal of Operational Research, 216: 140-151.

British Standards Institution, 2002. European Standard: Seamless and welded steel tubes. Dimensions and masses per unit length. BS EN 10220:2002. BSI Group, London, 9pp.

Brown, B., 2006. Klamath Falls geothermal district heating system at 25 years. Geothermal Resources Council Transactions, 30: 185-190.

Campos Celador, A., Odriozola, M., and Sala, J.M., 2011. Implications of the modelling of stratified hot water storage tanks in the simulation of CHP plants. Energy Conversion and Management, 52: 3018-3026.

Cassito, L., 1990. District heating systems in Europe. A review. Resources, Conservation and Recycling, 4: 271-281.

Catalina, T., Iordache, V., and Caracaleanu, B., 2013. Multiple regression model for fast prediction of the heating energy demand. Energy and Buildings, 57: 302-312.

Chan, C.W., Ling-Chin, J., and Roskilly, A.P., 2013. A review of chemical heat pumps, thermodynamic cycles and thermal energy storage technologies for low grade heat utilisation. Applied Thermal Engineering, 50: 1257-1273.

Chuanshan, D., 1997. Thermal analysis of indirect geothermal district heating systems. Geothermics, 26: 351-364.

Coskun, C., 2010. A novel approach to degree-hour calculation: Indoor and outdoor reference temperature based degree hour calculation. Energy, 35: 2455-2460.

Coskun, C., Oktay, Z., and Dincer, I., 2009. New energy and exergy parameters for geothermal district heating systems. Applied Thermal Engineering, 29: 2235-2242.

Coskun, C., Oktay, Z., and Dincer, I., 2012. Performance assessment of a novel hybrid district energy system. Applied Thermal Engineering, 48: 268-274.

Dalla Rosa, A., and Christensen, J.E., 2011. Low-energy district heating in energy-efficient building areas. Energy, 36: 6890-6899.

Dalla Rosa, A., Boulter, R., Church, K., and Svendsen, S., 2012. District heating (DH) network design and operation toward a system-wide methodology for optimizing renewable energy solutions (SMORES) in Canada: A case study. Energy: 45: 960-974.

Dagdas, A., 2007. Heat exchanger optimization for geothermal district heating systems: A fuel saving approach. Renewable Energy, 32: 1020-1032.

DECC, 2014. Annual Energy Statement 2014. Department of Energy & Climate Change, U.K. Government, London, 72pp.

DECC, 2015. Energy Trends. Department of Energy & Climate Change, U.K. Government, London, 92pp.

Di Pippo, R., 2007. Geothermal power plants. Principles, applications, case studies and environmental impact. Butterworth-Heinemann (Second Edition), Oxford, 493pp.

Dincer, I., and Rosen, M.A., 2011. Thermal energy storage: Systems and applications. Wiley Blackwell (Second Edition), pp.: 51-82.

Difs, K., Danestig, M., and Trygg, L., 2009. Increased use of district heating in industrial processes- Impacts on heat load duration. Applied Energy, 86: 2327-2334.

Dlugosz, P., 2003. Podhale (South Poland) geothermal district heating system. Geothermics, 32: 527-533.

Dotzauer, E., 2002. Simple model for prediction of loads in district-heating systems. Applied Energy, 73: 277-284.

Dotzauer, E., 2003. Experiences in mid-term planning of district heating systems. Energy, 28: 1545-1555.

Dounis, A., 2010. Artificial intelligence for energy conservation in buildings. Advances in Building Energy Research, 4: 267-299.

Erdogmus, B., Toksoy, M., Ozerdem, B., and Aksoy, N., 2006. Economic assessment of geothermal district heating systems: A case study of Balcova-Narlidere, Turkey. Energy and Buildings, 38: 1053-1059.

European Parliament and Council. Directive 2010/31/EU of the European Parliament and of the Council of 19 May 2010 on the energy performance of buildings. Official Journal of the European Union 2010, L153: 13-15.

Gabrielaitiene, I., Bohm, B., and Sunden, B., 2007. Modelling temperature dynamics of a district heating system in Naestved, Denmark- A case study. Energy Conversion and Management, 48: 78-86.

Garcia-Mari, E., Gasque, M., Gutierrez-Colomer, R.P., Ibanez, F., and Gonzalez-Altozano, P., 2013. A new inlet device that enhances thermal stratification during charging in a hot water storage tank. Applied Thermal Engineering, 61: 663-669.

Gelegenis, J., 2005. Rapid estimation of geothermal coverage by district-heating systems. Applied Energy, 80: 401-426.

Gelegenis, J., 2009. A simplified quadratic expression for the approximate estimation of heating degree-days to any base temperature. Applied Energy, 86: 1986-1994.

GeoDH Project, 2012. Newsletter Issue 2, April 2013. Geothermal District Heating project (GEODH). European Geothermal Energy Council (EGEC), Brussels, 4pp. Available online at 'http://geodh.eu/wp-content/uploads/2013/04/GeoDH-Newsletter-Issue-2.pdf', last accessed on 17/07/2013.

Ghaddar, N.K., 1994. Stratified storage tank influence on performance of solar water heating system tested in Beirut. Renewable Energy, 4: 911-925.

Gonnet, G., 2002. *Brent's Method (Golden Section Search in one dimension).* Available: http://linneus20.ethz.ch:8080/1_5_2.html. Last accessed 24th July 2014.

Grohnheit, P.E., and Mortensen, B.O.G., 2003. Competition in the market for space heating. District heating as the infrastructure for competition among fuels and technologies. Energy Policy, 31: 817-826.

Guo, J., Wu, J., and Wang, R., 2011. A new approach to energy consumption prediction of domestic heat pump water heater based on grey system theory. Energy and Buildings, 43: 1273-1279.

Gustafsson, S.I., and Ronnqvist, M., 2008. Optimal heating of large blocks of flats. Energy and Buildings, 40: 1699-1708.

Gustavsson, L., 1994a. District heating systems and energy conservation- Part I. Energy, 19: 81-91.

Gustavsson, L., 1994b. District heating systems and energy conservation- Part II. Energy, 19: 93-102.

Haeseldonckx, D., Peeters, L., Helsen, L., and D'haeseleer, W., 2007. The impact of thermal storage on the operational behavior of residential CHP facilities and the overall CO_2 emissions. Renewable and Sustainable Energy Reviews, 11: 1227-1243.

Hammond, G.P., and Stapleton, A.J., 2001. Exergy analysis of the United Kingdom energy system. Proceedings of the Institution of Mechanical Engineers, Part A: Journal of Power and Energy, vol.: 215, pp.: 141-162.

Han, Y.M., Wang, R.Z., and Dai, Y.J., 2009. Thermal stratification within the tank. Renewable and Sustainable Energy Reviews, 13: 1014-1026.

Harrison, R., 1987. Design and performance of direct heat exchange geothermal district heating schemes. Geothermics, 16: 197-211.

Harrison, R., 1994. The design and economics of European geothermal heating installations. Geothermics, 23: 61-71.

Hederman, W.F., and Cohen, L.A., 1981. Economics of geothermal direct heat applications. Geothermal Resources Council Transactions, 5: 647-650.

Heller, A.J., 2002. Heat-load modelling for large systems. Applied Energy, 72: 371-387.

Henning, D., 1997. MODEST- An energy system optimization model applicable to local utilities and countries. Energy, 22: 1135-1150.

Hepbasli, A., 2010. A review on energetic, exergetic and exergoeconomic aspects of geothermal district heating systems (GDHSs). Energy Conversion and Management, 51: 2041-2061.

Hepbasli, A., and Canakci, C., 2003. Geothermal district heating applications in Turkey: a case study of Izmir-Balcova. Energy Conversion and Management, 44: 1285-1301.

Iacobescu, F., and Badescu, V., 2011. Metamorphoses of cogeneration-based district heating in Romania: A case study. Energy Policy, 39: 269-280.

Jialing, Z., and Wei, Z., 2003. Design and utilization of plate heat exchangers in geothermal district heating systems. Geothermal Resources Council Transactions, 27: 97-100.

Jonasson, T., and Thordarson, S., 2007. Geothermal district heating in Iceland: Its development and benefits. Presented in the 26th Nordic History Congress. Reykjavik, Iceland, 8-12 August 2007. Unpaginated, available online at 'http://www.samorka.is/doc/1714', last accessed on 16/07/2013, 24pp.

Jordan, U., and Furbo, S., 2005. Thermal stratification in small solar domestic storage tanks caused by draw-offs. Solar Energy, 78: 291-30.

Kakatsios, X.K., 2006. Αρχές μεταφοράς θερμότητας και μάζας (Heat and mass transfer principles. Symeon, Athens, 656pp. (In Greek).

Kalogirou, S., 2006. Artificial neural networks in energy applications in buildings. International Journal of Low Carbon Technologies, 1: 201-216.

Kanoglu, M., 2002. Exergy analysis of a dual-level binary geothermal power plant. Geothermics, 31: 709-724.

Kanoglu, M., and Cengel, Y.A., 1999. Economic evaluation of geothermal power generation, heating, and cooling. Energy, 24: 501-509.

Karytsas, C., Mendrinos, D., and Goldbrunner, J., 2003. Low enthalpy geothermal energy utilisation schemes for greenhouse and district heating at Traianoupolis Evros, Greece. Geothermics, 32: 69-78.

Kecebas, A., 2011. Performance and thermo-economic assessments of geothermal district heating system: A case study in Afyon, Turkey. Renewable Energy, 36: 77-83.

Kecebas, A., 2013. Energetic, exergetic, economic and environmental evaluations of geothermal district heating systems: An application. Energy Conversion and Management, 65: 546-556.

Kecebas, A., and Yabanova, I., 2012. Thermal monitoring and optimization of geothermal district heating systems using artificial neural network: A case study. Energy and Buildings, 50: 339-346.

Kecebas, A., Kayfeci, M., and Gedik, E., 2011. Performance investigation of the Afyon geothermal district heating system for building applications: Exergy analysis. Applied Thermal Engineering, 31: 1229-1237.

Kecebas, A., Yabanova, I., and Yumurtaci, M., 2012. Artificial neural network modelling of geothermal district heating system thought exergy analysis. Energy Conversion and Management, 64: 206-212.

Kelly, S., and Pollitt, M., 2010. An assessment of the present and future opportunities for combined heat and power with district heating (CHP-DH) in the United Kingdom. Energy Policy, 38: 6936-6945.

Kenjo, L., Inard, C., and Caccavelli, D., 2007. Experimental and numerical study of thermal stratification in a mantle tank of a solar domestic hot water system. Applied Thermal Engineering, 27: 1986-1995.

Kostowski, W., and Skorek, J., 2005. Thermodynamic and economic analysis of heat storage application in co-generation systems. International Journal of Operational Research, 29: 177-188.

Krajacic, G., Duic, N., Tsikalakis, A., Zoulias, M., Caralis, G., Panteri, E., and Carvalho, M.D.G., 2011. Feed-in tariffs for promotion of energy storage technologies. Energy Policy, 39: 1410-1425.

Krarti, M., 2003. An overview of artificial intelligence-based methods for building energy systems. Journal of Solar Energy Engineering, 125: 331-342.

Krause, A., Tsatsaronis, G., and Sauthoff, M., 1999. On the cost optimization of a district heating facility using a steam-injected gas turbine cycle. Energy Conversion and Management, 40: 1617-1626.

Kreider, J., Claridge, D., Curtiss, P., Dodier, R., Haberl, J., and Krarti, M., 1995. Building energy use prediction and system identification using recurrent neural networks. Journal of Solar Energy Engineering, 117: 161-166.

Kristmannsdottir, H., and Bjornsson, A., 2012. Direct use of boiling saline water in the Oxafjordur heating system in NE Iceland- Production problems and solution. Geothermal Resources Council Transactions, 36: 241-246.

Lauenburg, P., Johansson, P.O., and Wollerstrand, J., 2010. District heating in case of power failure. Applied Energy, 87: 1176-1186.

Lee, K.C., 2001. Classification of geothermal resources by exergy. Geothermics, 30: 431-442.

Li, Y., Fu, L., Zhang, S., and Zhao, X., 2011. A new type of district heating system based on distributed absorption heat pumps. Energy, 36, 4570-4576.

Lindenberger, D., Bruckner, T., Groscurth, H.M., and Kummel, R., 2000. Optimization of solar district heating systems: seasonal storage, heat pump and cogeneration. Energy, 25: 591-608.

Little, N.H., and Bissell, R.R., 1980. Boise geothermal district heating system- Technical design. Geothermal Resources Council Transactions, 4: 585-588.

Loftsdottir, A.S., and Thorarinsdottir, R.I., 2006. Energy in Iceland. Historical perspective, present status, future outlook. Ministries of Industry and Commerce, Iceland Government (Second Edition), 44pp.

Lund, J.W., and Lienau, P.J., 2009. Geothermal district heating. In: Popovski, K., Vranovska, A., and Popovska V.A. (Editors). Proceedings of the International Conference on National Development of Geothermal Energy Use and International Course/EGEC Business Seminar on Organization of Successful Development of a Geothermal Project, Slovakia 2009. Unpaginated, available at 'https://pangea.stanford.edu/ERE/pdf/IGAstandard/ISS/2009Slovakia/II.1.LUND.pdf', last accessed on 31/10/2012, 18pp.

Lund, H., Hvelplund, F., Kass, I., Dukalskis, E., and Blumberga, D., 1999. District heating and market economy in Latvia. Energy, 24: 549-559.

Lund, J.W., Freeston, D.H., and Boyd, T.L., 2005. Direct application of geothermal energy: 2005 worldwide review. Geothermics, 34: 691-727.

Lunis, B.C., 1985. Geothermal district heating -basics to success. Geothermal Resources Council Transactions, 9: 33-37.

Ma, Z., Li, H., Sun, Q., Wang, C., Yan, A., and Starfelt, F., 2014. Statistical analysis of energy consumption patterns on the heat demand of buildings in district heating systems. Energy and Buildings, 85: 464-472.

Milanovic, P., Jacimovic, B., and Genic, S., 2004. The influence of heat exchanger performances on the design of indirect geothermal heating system. Energy and Buildings, 36: 9-14.

Moller, B., and Lund, H., 2010. Conversion of individual natural gas to district heating: Geographical studies of supply costs and consequences for the Danish energy system. Applied Energy, 87: 1846-1857.

Myhren, J.A., and Holberg, S., 2007. Energy savings and thermal comfort with ventilation radiators – a dynamic heating and ventilation system, Paper No.1510, 9th REHVA World Congress-Clima 2007, 10–14 June, Helsinki, Finland

Myhren, J.A., and Holberg, S., 2008. Flow patterns and thermal comfort in a room with panel, floor and wall heating. Energy and Buildings, 40: 524-536.

Nicol, A., 2009. Absorption cooling. Technical investigation of absorption cooling for Northern Ireland. Report prepared for Invest Northern Ireland. PO Reference: PO607024. Unpaginated, available at 'http://www.investni.com/absorption_cooling_technical_investigation_for_northern_ireland_17-may-2009-v2_draft.pdf', last accessed on 14/03/2013, 102pp.

Nielsen, H.A., and Madsen, H., 2006. Modelling the heat consumption in district heating systems using a grey-box approach. Energy and Buildings: 38: 63-71.

Noro, M., and Lazzarin, R., 2006. Local or district heating by natural gas: Which is better from energetic, environmental and economic point of views? Applied Thermal Engineering, 26: 244-250.

Oktay, Z., Coskun, C., and Dincer, I., 2008. Energetic and exergetic performance investigation of the Bigadic geothermal district heating system in Turkey. Energy and Buildings, 40: 702-709.

Ostergaard, P.A., and Lund, H., 2011. A renewable energy system in Frederikshavn using low-temperature geothermal energy for district heating. Applied Energy, 88: 479-487.

Ozgener, L., 2012. Coefficient of performance (COP) analysis of geothermal district heating systems (GDHSs): Salihli GDHS case study. Renewable and Sustainable Energy Reviews, 16: 1330-1334.

Ozgener, L., and Ozgener, O., 2009. Monitoring of energy exergy efficiencies and exergoeconomic parameters of geothermal district heating systems (GDHSs). Applied Energy, 86: 1704-1711.

Ozgener, L., Hepbasli, A., and Dincer, I., 2005a. Energy and exergy analysis of geothermal district heating systems: an application. Building and Environment, 40: 1309-1322.

Ozgener, L., Hepbasli, A., and Dincer, I., 2005b. Energy and exergy analysis of the Gonen geothermal district heating system, Turkey. Geothermics, 34: 632-645.

Ozgener, L., Hepbasli, A., Dincer, I., and Rosen, M.A., 2005c. Exergoeconomic modelling of geothermal district heating systems for building applications. Proceedings of the Ninth International IBPSA (International Building Performance Simulation Association) Conference. Montreal, Canada, 15-18 August 2005, pp.: 907-913.

Ozgener, L., Hepbasli, A., and Dincer, I., 2006a. Effect of reference state on the performance of energy and exergy evaluation of geothermal district heating systems: Balcova example. Building and Environment, 41: 699-709.

Ozgener, L., Hepbasli, A., and Dincer, I., 2006b. Performance investigation of two geothermal district heating systems for building applications: Energy analysis. Energy and Buildings, 38: 286-292.

Ozgener, L., Hepbasli, A., and Dincer I., 2007a. A key review of performance improvement aspects of geothermal district heating systems and applications. Renewable and Sustainable Energy Reviews, 11: 1675-1697.

Ozgener, L., Hepbasli, A., Dincer, I., and Rosen, M.A., 2007b. Exergoeconomic analysis of geothermal district heating systems: A case study. Applied Thermal Engineering, 27: 1303-1310.

Ozgener, L., Hepbasli, A., and Dincer, I., 2007c. Exergy analysis of two geothermal district heating systems for building applications. Energy Conversion and Management, 48: 1185-1192.

Ozisik, N.M., 1985. Heat Transfer. A basic approach. McGraw-Hill International Editions, New York, 780pp.

Pagliarini, G., and Rainieri, S., 2010. Modelling of a thermal energy storage system coupled with combined heat and power generation for the heating requirements of a University Campus. Applied Thermal Engineering, 30: 1255-1261.

Papantonis, D., 2006. Μικρά υδροηλεκτρικά έργα (Small hydroelectric plants). Symeon, Athens (In Greek).

Parri, R., 2007. Energy efficiency analysis of district heating using geothermal fluids. In: Sayigh, A.A.M. (Editor). Proceedings of the European Geothermal Congress 2007. Unterhaching, Germany, 30 May-1 June 2007. Unpaginated, available online at 'http://www.geothermal-energy.org/pdf/IGAstandard/EGC/2007/133.pdf?', last accessed on 28/01/2013, 6pp.

Persson, U., and Werner, S., 2011. Heat distribution and the future competitiveness of district heating. Applied Energy, 88: 568-576.

Pinson, P., Nielsen, T.S., Nielsen, H.Aa., Poulsen, N.K., and Madsen, H., 2009. Temperature prediction at critical points in district heating systems. European Journal of Operational Research, 194: 163-176.

Popescu, D., Ungureanu, F., and Serban, E., 2008. Simulation of consumption in district heating systems. Environmental problems and development: Proceedings of the 1st WSEAS International Conference on Urban Rehabilitation and Sustainability (URES '08), Bucharest, Romania, 7-9 November 2008, pp.: 50-55.

Popescu, D., Ungureanu, F., and Hernandez-Guerrero, A., 2009. Simulation models for the analysis of space heat consumption of buildings. Energy, 34: 1447-1453.

Popovski, K., Gnjezda, G., Niederbacher, P., and Naunov, J., 2000. Optimization of the geothermal district heating system "GEOTERMA"-Kocani, Macedonia. Proceedings of the 6th World Renewable Energy Congress, pp.: 310-313.

Python Software Foundation, 2016. Python Programming Language. Available online at "https://www.python.org/", last accessed on 16/02/2016.

Rezaie, B., and Rosen, M.A., 2012. District heating and cooling: Review of technology and potential enhancements. Applied Energy, 93: 2-10.

Richter, S., Hilbert, L.R., and Thorarinsdottir, R.I., 2006. On-line corrosion in geothermal district heating systems. I. General corrosion rates. Corrosion Science, 48: 1770-1778.

Rosada, J., 1988. Characteristics of district heating- Advantages and disadvantages. Energy and Buildings, 12: 163-171.

Rybach, L., 2003. Geothermal energy: Sustainability and the environment. Geothermics, 32: 463-470.

Rybach, L., 2014. Geothermal power growth 1995-2013- A comparison with other renewables. Energies, 7: 4802-4812.

Sahin, A.S., and Yazici, H., 2012. Thermodynamic evaluation of the Afyon geothermal district heating system by using neural network and neuro-fuzzy. Journal of Volcanology and Geothermal Research, 233-234: 65-71.

Schoenau, G., and Kehrig, R., 1990. A method for calculating degree-days to any base temperature. Energy and Buildings, 14: 299-302.

Shamshirband, S., Petkovic, D., Enayatifar, R., Abdullah, A.H., Markovic, D., Lee, M., and Ahmad, R., 2015. Heat load prediction in district heating systems with adaptive neuro-fuzzy method. Renewable and Sustainable Energy Reviews, 48: 760-767.

Simsek, S., 2001. An overview of geothermal developments in Turkey. Proceedings of ITIT Symposium on Geothermal In Asia, 28 February-1 March, Tokyo, Japan, pp.: 17-23.

Sommer, C.R., Kuby, M.J., and Bloomquist, G., 2003. The spatial economics of geothermal district energy in a small, low-density town: a case study of Mammoth Lakes, California. Geothermics, 32: 3-19.

Steins, C., and Zarrouk, S.J., 2012. Assessment of the geothermal space heating system at Rotorua hospital, New Zealand. Energy Conversion and Management, 55: 60-70.

Stoecker, W.F., 1989. Design of Thermal Systems. McGraw Hill (Third Edition), New York, 528pp.

Szita, G., 2010. High efficient cascaded use of geothermal energy in reality. Proceedings of the World Geothermal Congress 2010. Bali, Indonesia, 25-29 April 2010. Unpaginated, available at 'http://www.geothermal-energy.org/pdf/IGAstandard/WGC/2010/3423.pdf?', last accessed on 21/02/2013, 4pp.

Thorsteinsson, H.H., and Tester, J.W., 2010. Barriers and enablers to geothermal district heating system development in the United States. Energy Policy, 38: 803-813.

Torchio, M.F., Genon, G., Poggio, A., and Poggio, M., 2009. Merging of energy and environmental analyses for district heating systems. Energy, 34: 220-227.

Underwood, C., 2014. On the design and response of domestic ground-source heat pumps in the U.K. Energies, 7: 4532-4553.

Verda, V., and Colella, F., 2011. Primary energy savings through thermal storage in district heating networks. Energy, 36: 4278-4286.

Verda, V., Baccino, G., Sciacovelli, A., and Russo, S.L., 2012. Impact of district heating and groundwater heat pump systems on the primary energy needs in urban areas. Applied Thermal Engineering, 40: 18-26.

Vorum, M., and Petterson, C., 1981. A feasibility analysis of geothermal district heating for Lakeview, Oregon. Geothermal Resources Council Transactions, 5: 575-578.

Weber, C., and Shah, N., 2011. Optimisation based design of a district energy system for an eco-town in the United Kingdom. Energy, 36: 1292-1308.

Yao, R., and Steemers, K., 2005. A method of formulating energy load profile for domestic buildings in the UK. Energy and Buildings, 37: 663-671.

Yetemen, O., and Yalcin, T., 2009. Climatic parameters and evaluation of energy consumption of the Afyon geothermal district heating system, Afyon, Turkey. Renewable Energy, 34: 706-710.

Yildirim, N., Gokcen, G., and Toksoy, M., 2005. Low temperature geothermal district heating system design. Case study: IZTECH campus, Izmir, Turkey. Proceedings of the World Geothermal Congress 2005. Antalya, Turkey, 24-29 April 2005. Unpaginated, available at 'http://www.geothermal-energy.org/pdf/IGAstandard/WGC/2005/1431.pdf?', last accessed on 22/01/2013, 6pp.

Younger, P.L., 2015. Geothermal energy: Delivering on the global potential. Energies, 8: 11737-11754.

Yuksel, B, Aslan, A., and Akyol, T., 2012. Investigation of seasonal variations in the energy and exergy performance of the Gonen geothermal district heating system. Applied Thermal Engineering, 36: 39-50.

Zgoda, R., 1986. The Warsaw district heating system. Tunnelling and Underground Space Technology, 1: 5-6.

Zhao, H., and Magoules, F., 2012. A review on the prediction of building energy consumption. Renewable and Sustainable Energy Reviews, 16: 3586-3592.

Zhou, Q., Wang, S., Xu, X., and Xiao, F., 2008. A grey-box model of next-day building thermal load prediction for energy efficient control. International Journal of Energy Research, 32: 1418-1431.